Title

Extracellular electron transfer capabilities of lactic acid bacteria

Author

Stevens, Eric

Publication Date

2022

Peer reviewed|Thesis/dissertation

Extracellular electron transfer capabilities of lactic acid bacteria

By

Eric T. Stevens

DISSERTATION

Submitted in partial satisfaction of the requirements for the degree of

DOCTOR OF PHILOSOPHY

in

Microbiology

in the

OFFICE OF GRADUATE STUDIES

of the

UNIVERSITY OF CALIFORNIA

DAVIS

Approved:

Dr. Maria L. Marco, Chair

Dr. Andreas Baumler

Dr. Shota Atsumi

Committee in Charge

2022

DISSERTATION ABSTRACT

Extracellular electron transfer (EET) is a bioelectrochemical pathway in which microorganisms reduce electron acceptors in their environment. Through EET, microorganisms can enhance energy conservation and balance intracellular redox homeostasis while simultaneously reducing their extracellular environment. Outside of these direct impacts EET-capable microbial metabolism, the broader effects of EET in conducive environments remain underexplored outside of applications for microbial fuel cells. Chapter 1 of this dissertation focuses on the EET capabilities of bacteria found in diverse plant- and animal-associated niches, including the plant rhizosphere, animal mucosal surfaces, and during the fermentation of plant and animal foods. Ecological impacts of EET metabolism are explored, including the modulation of metal uptake by plants, the growth and proliferation of pathogenic bacteria in mucosal niches, and the increasing environmental acidification and reduction potential during food fermentations.

Food fermentations are of particular interest regarding EET due to the impact of lactic acid bacteria (LAB), a diverse group of Gram-positive organisms characterized by their production of lactic acid during fermentation. LAB are found in diverse environmental, plant, mammal, and insect-associated microbiomes, and used in the fermentation of hundreds of foods and beverages. In Chapter 2, the EET is identified and explored in *Lactiplantibacillus plantarum*, a model organism for studying LAB. We characterized *L. plantarum* EET through the reduction of extracellular, insoluble ferrihydrite (iron(III) oxyhydroxide) and the generation of current with a graphite anode. The genetic conservation of the *L. plantarum* flavin-mediated EET (FLEET) locus was identified in other LAB and led to the discovery that LAB EET required Ndh2 (a type-II NADH dehydrogenase) and conditionally required PplA (a membrane-associated flavin-binding reductase) for iron reduction or current generation. The metabolic impacts of EET were

also quantified and these data showed that *L. plantarum* had a shorter lag phase, greater cell abundance and viability, greater intracellular ATP and NAD^+/NADH under EET-conducive conditions. Furthermore, *L. plantarum* EET was demonstrated during the fermentation of kale juice and increased environmental acidification.

With the physiological impacts of EET on *L. plantarum* characterized, we turned towards exploring the role of quinones, an indispensable class of electron shuttles used by all bacteria for EET. In Chapter 3, the specificity of quinones and their physiological and ecological impacts on *L. plantarum* EET was explored. *L. plantarum* growth with DHNA led to membrane-associated menaquinone production but was not sufficient to stimulate EET in the absence of an exogenous DHNA. Instead, co-exposure of *L. plantarum* to DHNA during growth and EET significantly increased iron reduction at both high and low, environmentally relevant concentrations. DHNA and other quinones inhibited *L. plantarum* growth via hydrogen peroxide production and induced expression of oxidative stress response genes and redox-associated amino acid metabolism and transport. However, co-exposure of DHNA and ferric iron, a terminal electron acceptor, reversed these effects and partially restored *L. plantarum* growth. Other purified, naphthoquinone-based compounds, as well as spent cell-free growth medium from the LAB *Lactococcus lactis* and *Leuconostoc mesenteroides* was also sufficient in stimulated *L. plantarum* EET. Furthermore, we confirmed quinone cross-feeding *in situ* by showing that *L. plantarum* in co-culture with these LAB results in enhanced iron reduction and accelerated environmental acidification.

Taken together the results of this dissertation highlight a novel metabolic pathway present in *L. plantarum* and other LAB and explores both the physiological and ecological impacts of EET on niches inhabited by EET-capable LAB. These findings inform the use of LAB during the

fermentation of foods and beverages, during which successful outcomes as well as modulating flavor profiles may be achievable using EET.

ACKNOWLEDGEMENTS

I would first like to express my deepest gratitude to my committee members who helped shape this dissertation and myself as a scientist. My success would not have been possible without my research advisor, Dr. Maria Marco, whose extensive experience and advice helped shape my research projects from the very beginning. Likewise, the support and insightful suggestions from Dr. Andreas Baumler and Dr. Shota Atsumi were instrumental in guiding this research to its completion. I am extremely grateful to the past and present Marco Lab members who provided both invaluable experimental assistance and emotional support over the past five years. Together, we have supported one another through the roughest patches in life, summitted the highest points of scientific achievement, and made lifelong friendships. I am indebted to my salsa family, Los Puerquitos Peligrosos, with whom I have created countless memories with during graduate school. Their encouragement and belief in my capabilities bolstered me through some of the longest nights of research or dancing until The Davis Graduate closed. I am also indebted to my biological family, especially Rod and Teresa, for their unwavering support, love, and reassurance that one day, this dissertation would be complete. Lastly, I want to express my sincerest appreciation for my best friend and partner, Jennifer. I am forever grateful for your love and patience over the course of my graduate career. With new and exciting adventures just on the horizon, I am thrilled that I get to experience them with you by my side.

Table of Contents

Chapter 1. Microbial extracellular electron transfer capabilities in animal and plant ecosystems

Eric Stevens and Maria Marco*

Department of Food Science & Technology, University of California, Davis, CA, USA.

* Corresponding author:

Maria Marco

One Shields Avenue

University of California

Davis, CA 95656

Email: mmarco@ucdavis.edu

Keywords: EET, direct electron transfer, mediated electron transfer, oxidation/reduction, rhizosphere, fermentation, human microbiome

This work will be submitted as a shortened, perspective piece to *Trends in Microbiology*.

Abstract

Extracellular electron transfer (EET) is a bioelectrochemical process demonstrated by bacteria found in host-associated environments, including plant and animal ecosystems, and in fermenting plant and animal foods. In the plant rhizosphere, electron acceptors support the growth of electroactive bacteria which may influence iron and heavy metal uptake by plants. In animal microbiomes, EET reduces diet-derived iron in the guts of soil-dwelling organisms and supports the growth and colonization of pathogens in the mammalian oral cavity, intestine, and lungs. During the fermentation of plant materials and bovine milk, certain lactic acid bacteria use EET to increase growth and environmental acidification, as well as decrease environmental oxidation-reduction potential (ORP). EET is thus an important metabolic pathway for microorganisms which has implications for ecosystem function, microbial interactions with host tissues, as well as biotechnological applications.

Introduction

Electron flow directs the lives of all organisms (Zerfaß et al., 2019). Oxidative and reductive reactions, collectively referred to as "redox reactions," control the thousands of biochemical reactions required for energy conservation, cell growth, and stress response (Shimizu, 2013; Trachootham et al., 2008). Organisms that have greater flexibility with intracellular redox-maintenance pathways can adapt to a wider range of extracellular redox environments. One example of this is exoelectrogenic bacteria (Logan et al., 2019). These microorganisms can directly couple intracellular redox reactions with the reduction of extracellular electron acceptors through a process known as extracellular electron transfer (EET) (Kracke et al., 2015). Electron transfer from exoelectrogens can occur through either direct

electron transfer (DET) or mediated (indirect) electron transfer (MET) (Lovley and Holmes, 2022). DET requires physical contact with environmental electron acceptors (Shi et al., 2016), and includes the use of microbial "nanowires" or conductive pili (Feliciano et al., 2015; Gorby et al., 2006). MET systems require an electron shuttle (e.g., flavins, quinones, phenazines, etc.) to transfer electrons from cells to terminal electron acceptors (Glasser et al., 2017). By using EET, exoelectrogens can maintain the balance of intracellular redox couples (such as NAD^+/NADH or FAD/$FADH_2$) and conserve energy by exporting electrons derived from energy harvesting pathways to terminal electron acceptors in their environment (Huang et al., 2018).

Thus far, most studies on EET-capable microorganisms, and specifically bacteria, have focused on *Shewanella oneidensis* and *Geobacter sulfurreducens*, Gram-negative, soil-dwelling bacteria in the Proteobacteria phylum (Shi et al., 2016). The capacity for these bacteria produce electricity in microbial fuel cells (MFCs) has received significant interest (Deng et al., 2012; Heydorn et al., 2020; Kato, 2015; Ucar et al., 2017). However, it is now evident that EET metabolism is not limited to a few bacterial species, but is pervasive among diverse microorganisms in all three domains of life including yeasts, such as *Saccharomyces cerevisiae* and *Candida melibiosica*, and archaea like *Pyrococcus furiosus* and *Geoglobus ahangari* (Logan et al., 2019). These electroactive microorganisms reside in diverse habitats, ranging from extreme thermal or acidic environments to mesophilic aquatic, terrestrial, and host-associated sites (Koch and Harnisch, 2016; Logan et al., 2019). The phylogenetics and metabolic pathways of EET-capable microbes have been discussed in several recent reviews (Koch and Harnisch, 2016; Logan et al., 2019; Lovley and Holmes, 2022; Shi et al., 2016). This review emphasizes the diversity and activities of EET-capable microorganisms associated with the tissues of plant and animal microbiomes. We emphasize the interactions of these organisms with biotic and

abiotic factors in their respective environments, their ecological impacts, and the potential for using EET metabolism to benefit plant and human health.

EET in the rhizosphere

Microorganisms colonize above- and below-ground plant tissues including leaves, stems, flowers, fruits, vegetables, and roots (Leveau, 2018). Thus far, EET-capable bacteria have only been isolated from the rhizosphere, or the narrow zone of soil that is influenced by root secretions (Kabutey et al., 2019) (**Figure 1** and **Table 1**). General evidence of electroactive microbes in the rhizosphere stems, in part, from the finding that electricity generation from the rhizosphere is tied to root exudation of carbon sources from plant metabolism (Kaku et al., 2008). Several trials have also succeeded in harnessing electrical current from the rhizosphere of various plants using electrodes (Kouzuma et al., 2014). Unlike other sites on plants, the rhizosphere may be particularly suited for EET because of the abundance of humic acids (HA). HAs, a heterogenous group of redox-active organic molecules which make up over 60% of all soil organic content (Trevisan et al., 2010), can serve as electron shuttles to reduce soil-associated iron (Fe^{3+}) and manganese (Mn^{4+}) through MET (Asli and Neumann, 2010; Benz et al., 1998; Rengel, 2015). Iron availability, influenced by its redox state, is of particular importance due to its impact on both plant and microbial growth (Lurthy et al., 2020). For example, iron(II) is far more bioavailable than iron(III), and the activity of dissimilatory iron-reducing bacteria in the rhizosphere was associated with increased iron uptake by plants and greater plant growth (Robin et al., 2008; Valencia-Cantero et al., 2007).

Several genera recognized to posses EET metabolic pathways have been found in the rhizosphere. *Geobacter,* a bacterial genus with known EET capacities, has been identified in the

rhizospheres of rice paddies (Holmes et al., 2017; Kouzuma et al., 2013; Lu et al., 2019; Schamphelaire et al., 2010), reed mannagrass (Timmers et al., 2012), and other wetland plants (Weiss et al., 2004) at relative abundances ranging from 0.3 to 3% total bacteria. Several reports have demonstrated *Geobacter* species capable of reducing 9,10-Anthraquinone-2,7-disulphonic acid (AQDS), a soil HA-analogue, which resulted in increased iron reduction and *Geobacter* growth (Chen et al., 2016; Komlos and Jaffé, 2004; Voordeckers et al., 2010). The addition of 10^8-10^9 CFU/mL *G. metallireducens* to the rhizosphere of common cattail (*Typha latifolia*) coincided with a 2-fold increase in iron(III) reduction at those sites compared to the bulk soil (Weiss et al., 2004). Increased iron reduction was also found closer to the roots of *Phragmites australis* and *Spartina alterniflora* where *Geobacter* was more abundant, compared to the surrounding bulk soil (Liu et al., 2019; Luo et al., 2018).

Geobacter species can also donate electrons to other rhizosphere microbes such as methanogenic archaea (methanogens) through direct interspecies electron transfer (DIET) (Kato and Igarashi, 2018). Methanogens are abundant colonizers of the rhizospheres of freshwater marshes and rice paddies (Lee et al., 2015; Lin et al., 2017), and can range from 37% to 88% of all archaea present in those sites (Lee et al., 2015, 2014). Methanogenic archaea reduce carbon dioxide to methane with an electron donor present (primarily H_2) (Rowe et al., 2019). However, several studies have shown that *Geobacter* is capable of supplying these electrons for archaeal methanogenesis, and that DIET promotes syntrophic growth for both groups of microorganisms (Igarashi et al., 2020; Kato and Igarashi, 2018; S. Zheng et al., 2020). In rice paddy soils amended with nano-Fe_3O_4 and anthraquinone-2-sulfonate (AQS), another HA-analogue, an increased production of methane was associated with higher abundances of *Geobacteraceae* and *Methanosarcinaceae* (Li et al., 2015). However, when nonconductive, silica-coated nano-Fe_3O_4

was used instead, less methane production and growth of *Geobacteraceae* occurred. Likewise, another study found that only methanogens previously shown to perform DIET (*Methanotrix* spp. and *Methanosarcina* spp.) were most abundant in rice paddy soils (Holmes et al., 2017). This coincided with increased transcription of archaeal genes associated with methane production and *Geobacter* pilin genes involved in DET. These findings suggest that DIET between *Geobacter* and methanogenic archaea may contribute to the significant methane production from rice paddy soils.

The cable bacteria comprise a group of multicellular, filamentous, and EET-active microbes in *Desulfobulbaceae* family (Trojan et al., 2016). First identified in marine sediments (Pfeffer et al., 2012), these microorganisms are termed cable bacteria because they were shown to conduct long-range DET up to centimeters in length, potentially through conductive periplasmic fibers (Meysman et al., 2015). Cable bacteria have been identified in the rhizospheres of numerous aquatic plants at concentrations ranging from 0.01% to over 10% total bacteria (Scholz et al., 2021). Electrical potential profiling is used to measure the electroactivity of cable bacteria, and in one study, cable bacteria attached to the roots of *Littorella uniflora* were shown to generate an electric field up to centimeters in length (Scholz et al., 2019). EET allows cable bacteria to conserve energy by coupling oxidation of sulfides beyond the rhizosphere to the reduction of oxygen released from root hairs (Müller et al., 2020; Scholz et al., 2019). EET from cable bacteria may also influence plant health, as concurrent environmental acidification from sulfide oxidation changes the redox state of metals like iron or arsenic and affects their uptake by plants (Scholz et al., 2021; Wagner et al., 2020).

Comamonas is another genus of exoelectrogenic, rhizosphere-associated bacteria (Yu et al., 2015). These bacteria have been found in the rhizospheres of rice paddies (Lu et al., 2006),

Capsicum annuum (Zhang et al., 2019), and *Zea mays* (Yang et al., 2017) at approximately 1% of the total bacteria. Although *in situ* characterization of *Comamonas* EET in the rhizosphere has yet to be shown, instances of *Comamonas* EET in other environments may suggest potential activity in the rhizosphere. For example, *Comamonas koreensis* strain CY01 was shown to reduce both iron(III) and AQDS under laboratory conditions, and this activity coincided with degradation of the herbicide 2,4-dichlorophenoxyacetic acid (2,4-D) (Wang et al., 2009; Wu et al., 2009). *Comamonas* and *Comamonadaceae* can also be enriched when electrodes are placed in the rhizosphere to create a rhizosphere-MFC (Kouzuma et al., 2013; Timmers et al., 2012).

Lastly, *Clostridium* is one more bacterial genus in rhizosphere associated with EET metabolism. *Clostridium* comprises ~2% of the rhizosphere microbiome of tropical seagrass (X. Zhang et al., 2020), ~3% in two mangrove tree species (Gomes et al., 2014), and ~6% in the cucumber rhizosphere (Jia et al., 2018). Like with *Geobacter*, relative abundance of *Clostridium* was found to be higher in the rhizosphere of rice plants when compared to the surrounding bulk soil (Dai et al., 2020). The greater abundance of *Clostridium* also coincided with increased dissolved arsenic and iron in this rhizosphere. Clostridia like *Clostridium acetobutylicum* (Finch et al., 2011; List et al., 2019), *Clostridium butyricum* (Park et al., 2001), *Clostridium beijerinckii* (Dobbin et al., 1999), and yet classified species (Bhushan et al., 2006; Langner and Inskeep, 2000) are known to reduce iron or arsenic (As^{5+}), as well as AQDS and other rhizosphere HAs. Like with cable bacteria, clostridia EET not only promotes growth (Bhushan et al., 2006), but may also influence plant health by modulating the bioavailability of metals like iron and arsenic (Dai et al., 2020).

EET in the animal microbiome

Animals and humans harbor diverse microbiomes, with different microorganisms colonizing each mucosal site. The human body for example, contains trillions of microorganisms (Sender et al., 2016) and microbial composition differs between bodily sites under influences from both genetic and environmental factors (Blekhman et al., 2015). EET electron acceptors, such as redox-active metals acquired from diet or environmental sources, are also associated with host cells (Kalinowski et al., 2016; Kozlowski et al., 2007) and frequently contact mucosal surfaces (Bhattacharyya et al., 2014; Kesarwala et al., 2016). Coincidentally, EET-capable bacteria have been identified microbiomes of animals like termites, mice, and humans (**Figure 2** and **Table 2**), and specifically, within the mucosal niches of the oral cavity, gut, and lungs.

Oral cavity

The oral cavity has the second-most diverse microbiome on the human body and contains complex biofilm communities on the teeth, tongue, and other oral surfaces (Caselli et al., 2020; Hall et al., 2017). Filamentous, electroactive bacterial structures were first reported in the extracellular biofilm matrix of necrotic bone samples from human patients with bisphosphonate-related osteonecrosis of the jaw (BRONJ) (Wanger et al., 2013). The conductivity and resistivity of the bacterial nanowires are similar to those found in *S. oneidensis* (Gorby et al., 2006), and this activity was hypothesized to accelerate the destruction of bone tissue (Wanger et al., 2013). Electroactive bacterial biofilms were also found on titanium dental implants, and these biofilms were determined to be responsible for greater biocorrosion under EET-conducive conditions (Pozhitkov et al., 2015). Corrosion of dental implants can lead to peri-implantitis and result in soft tissue inflammation, and in more serious cases, bone loss and implant failure (Persson et al.,

2001). 16S rRNA sequencing of the biofilm microbial communities under EET-conducive conditions showed enrichment of EET-capable bacterial genera including *Enterococcus*, *Lactobacillus*, and *Geobacillus* (Gurumurthy et al., 2019; Pozhitkov et al., 2015). Thus, the growth of electroactive microorganisms on these oral implants may lead to implant corrosion and potentially peri-implantitis.

Electroactivity has been identified in several oral pathogens. For example, *Streptococcus mutans*, the primary cause of dental carries (Forssten et al., 2010), was shown to perform EET through current production (Naradasu et al., 2020a). This activity promoted electrode attachment, facilitated cellular energy production, as was associated with cell surface-localized, redox-active enzymes, as determined by differential pulse voltammetry. *S. mutans* is commonly found in peri-implantitis biofilms (Laosuwan et al., 2018) and two studies have identified *S. mutans* as capable of growth on, and corrosion of titanium implant screws (Meza-Siccha et al., 2019) and aluminum/copper dental alloys (Zavanelli et al., 2015). The *Streptococcus* genus was also associated with corrosive titanium implant biofilms under EET-conducive conditions (Pozhitkov et al., 2015). Given this evidence, it is possible that *S. mutans* uses EET for enhanced growth on dental implants, leading to the acceleration of implant corrosion.

EET has been demonstrated for other oral pathogens associated with peri-implantitis. Similar to *S. mutans*, *Aggregatibacter actinomycetemcomitans* was able to directly attach to an electrode for EET and contained redox-active proteins with transition metal centers in the outer membrane (Naradasu et al., 2020b). Electroactivity and electrode attachment was also observed for *Porphyromonas gingivalis* in the same study, but redox-active surface proteins were not found. Both *A. actinomycetemcomitans* (Freire et al., 2011) and *P. gingivalis* can establish biofilms on titanium implant screws (Meza-Siccha et al., 2019). The same may also be true for

Corynebacterium matruchotii and *Capnocytophaga ochracea*, two other electroactive oral pathogens associated with peri-implantitis (Jakobi et al., 2015; Zheng et al., 2015). *C. ochracea* was shown to use soluble electron shuttles like menadione (Vitamin K3) and riboflavin for robust current generation (S. Zhang et al., 2020a), while *C. matruchotii* was hypothesized to adsorb redox-active mediators onto the cell surface for electron transfer (Naradasu et al., 2020c). Taken together, these oral pathogens may use EET like *S. mutants* for enhanced growth on, and corrosion of redox-active dental implants.

Intestine/Gut

The intestine harbors a diverse microbiota with both cross-sectional and longitudinal heterogeneity (Miller et al., 2021). This heterogeneity is in part driven by the presence of electron donors and electron acceptors from diet-derived or host-derived sources (Miller et al., 2021). Ferric iron is one such electron acceptor in the gut, and potential evidence of iron-reducing gut microbes was observed in the soil-feeding termites *Cubitermes orthognatus* and *Cubitermes umbratus* (Kappler and Brune, 2002). Specifically, the reduction iron(III) and humic acids occurred in the midgut and hindgut, and a similar result was later seen in the dampwood termite *Zootermopsis nevadensis* gut (Vu et al., 2004). Gut suspensions from *Z. nevadensis* could also reduce iron(III) *in vitro*, as well as a *Clostridium* sp. and a *Desulfovibrio* sp. isolated from these suspensions. While the direct impact of gut-associated iron reduction on termite health it not yet known, the re-oxidation of iron(II) to iron(III) could generate ROS for degrading lignin like some terrestrial fungi (Kirk and Farrell, 1987).

Outside of termites, other soil-dwelling organisms have been shown to harbor iron-reducing bacteria. Reduction of humic acids and iron(III) was observed in the midgut, hindgut,

and feces of scarab beetle (*Pachnoda ephippiata*) larvae (Hobbie et al., 2012). Gut suspensions could similarly reduce iron(III) *in vitro*, and a *Bacillus* sp. isolated from these suspensions could reduce iron(III) in the presence of AQDS and fulvic acids derived from humus. A similar result was achieved with gut contents from the earthworm *Pheretima guillelmi* (Zhou et al., 2019). 16S rRNA sequencing of the microbial communities in these gut contents revealed the presence of dissimilatory iron(III)-reducing genera including *Pseudomonas*, *Bacillus*, and *Clostridium*. The reduction of iron by these soil-dwelling organisms may have larger implications for iron cycling in the environment, but further understanding is needed to quantify the effects of gut iron reduction on these hosts themselves.

The mammalian intestine also harbors EET-capable microorganisms. Exoelectrogenic activity in the mammalian intestinal microbiota was first demonstrated in mice (Ericsson et al., 2015). Current production from the microbiota differed between mice purchased from different vendors, and reverse transcription-PCR performed on the intestinal contents from electroactive microbiota revealed significant upregulation of two extracellular iron oxide respiratory *c*-type cytochromes (*omcA* and *mtrC*) associated with EET (Ericsson et al., 2015). Transmission electron microscopy and 16S rRNA PCR specific for segmented filamentous bacteria (*Candidatus* Arthromitus or SFB) detected these microorganisms only in mice with electroactive microbiota. Microbiota transfer from mice with electroactive microbiota to mice lacking electroactive microbiota through ileal scrape and gavage transferred current generating capabilities to the recipient mice microbiota. Moreover, the presence of electroactivity may have implications on the mammalian immune system. Transfer of electroactive microbiota resulted in greater recruitment of T and B cells towards to the gut (Ericsson et al., 2015). These findings are consistent with observations that both of these cell types undergo electrotaxis (Li et al., 2011).

Besides the association between current production and SFB, *Faecalibacterium prausnitzii* was shown to be current-producing as well (Khan et al., 2012a, 2012b). *F. prausnitzii* is a butyrate-producing member of the gut microbiome (Khan et al., 2012a). This microorganism is also strongly associated with promoting gut health by reducing intestinal mucosal inflammation and promoting intestinal barrier function (Lopez-Siles et al., 2017). One strain of *F. prausnitzii* (DSM 17677) was able to use flavins for MET to survive under ambient conditions, mitigate oxidative stress, and generate an electrical current (Khan et al., 2012a, 2012b; Prévoteau et al., 2015). Because *F. prausnitzii* is a strict anaerobe (Prévoteau et al., 2015) and oxygen acts as a scavenger for electrons during EET (Lu et al., 2017), *F. praunitzii* may use EET to reduce oxygen while adherent to the gut mucosa for improved ecological fitness (Khan et al., 2012b). Thus, EET metabolism of this probiotic gut microorganism may have direct implications on promoting host intestinal health.

Other intestinal commensals and probiotics have also shown EET capabilities. From the mouse intestinal bacterial collection (miBC), *Clostridium cochlearium* DSM 29358, *Limosilactobacillus reuteri* DSM 28673, and *Staphylococcus xylosus* DSM 28566 could produce an electrical current (Schwab et al., 2019). *C. cochlearium* DSM 29358 produced the most current out of all tested strains and cyclic voltammetry revealed that a soluble redox-mediator was responsible for facilitating EET. In comparison, current from *L. reuteri* and *S. xylosus* was ten-fold lower, and only *L. reuteri* cell-free supernatant produced a minor redox-related signal during cyclic voltammetry. We have also showed that the probiotic strains *Lacticaseibacillus rhamnosus* GG (Segers and Lebeer, 2014) and *L. plantarum* NCIMB8826 (Yin et al., 2017) could perform EET through iron(III) reduction and/or current generation (Tejedor-Sanz et al., 2021). Some of these taxa, including members of the Lactobacillus-genus complex (J. Zheng et

al., 2020) and *Clostridium* were found to be associated with the electroactive gut microbiota from conventionally-raised mice, rats, and Guinea pigs (Wang et al., 2019). Whether EET capabilities of these microorganisms results in improved ecological fitness, and subsequently the promotion of host intestinal health, remains to be characterized though.

Conversely, host health may be negatively affected by pathogenic, EET-capable microorganisms. For example, the food-borne pathogen *L. monocytogenes* can perform EET through current generation or iron(III) reduction, and this activity supported intracellular NAD^+ regeneration and anaerobic growth under laboratory conditions (Light et al., 2018). Survival of an EET-null mutant (*ndh2*::tn) was also impaired in colonizing the mouse digestive tract versus the wild-type strain. These results coincide with findings in *E. faecalis*, a prominent gut commensal (Franz et al., 2011) and potential opportunistic pathogen (Keogh et al., 2018). *E. faecalis* was shown to reduce iron(III) (Hederstedt et al., 2020; Tejedor-Sanz et al., 2021), generate current (Hederstedt et al., 2020; Pankratova et al., 2019; Tahernia et al., 2020), and possess several genetic homologues to the flavin-mediated EET (FLEET) system in *L. monocytogenes* (Light et al., 2018). The reduction of iron by *E. faecalis* coincided with increased biofilm depth and a slight (yet not significant) increase in ATP *in vitro* (Keogh et al., 2018). Disruption of a putative FLEET genes, including *ndh3* (encoding a type-II NADH dehydrogenase) or *menB* (encoding a demethylmenaquinone biosynthase) in *E. faecalis* strain OG1RF resulted in decreased biofilm depth *in vitro* and reduced cecal and colonic colonization in a mouse GI infection model compared to the wild-type strain (Lam et al., 2019). These data suggest that *L. monocytogenes*, *E. faecalis*, and potentially other EET-capable, intestinal pathogens like *Staphylococcus aureus* and *Streptococcus agalactiae* (Tahernia et al., 2020) may use EET for improved ecological fitness and colonization to the detriment of host health.

Lungs

The lung is a relatively nutrient poor environment compared to the oral cavity or gastrointestinal tract, yet still supports a dynamic microbiome affected by oxygen availability (O'Dwyer et al., 2016) and the presence of redox-active metals (Healy et al., 2021). In particular, the availability of metals like iron play a significant role in host-pathogen interactions in the lungs (Healy et al., 2021). *Pseudomonas aeruginosa*, a pathogen associated with persistent lung infections in cystic fibrosis (CF) patients, can acquire bioavailable iron in the lungs through phenazine-mediated EET (Wang et al., 2011). Phenazines are a class of small, redox-active compounds produced and secreted by *P. aeruginosa* (Schiessl et al., 2019) which can act as electron shuttles for MET (Yong et al., 2014, 2011). Phenazine-1-carboxylic acid was shown to reduce extracellular (and host protein-bound) iron(III) to iron(II), and this activity was associated with greater biofilm production in a wild-type *P. aeruginosa* strain versus a phenazine-null mutant (Wang et al., 2011). Iron reduction and acquisition through phenazine-EET may contribute to *P. aeruginosa* persistence during infection as sputum from CF patients contain elevated levels of iron (Reid et al., 2007). Other ecological advantages for *P. aeruginosa* phenazine-EET have been described as well. Phenazine-EET promoted *P. aeruginosa* survival under anaerobic conditions (Glasser et al., 2014; Wang et al., 2010) which can exist in CF patient lungs (Tunney et al., 2008). Phenazine-EET by *P. aeruginosa* also promotes intracellular redox homeostasis via NAD^+ regeneration, and this redox balance was associated with both *P. aeruginosa* biofilm morphology (Dietrich et al., 2013) and resistance to the clinical antibiotic ciprofloxacin (Schiessl et al., 2019). In summary, this evidence shows that phenazine-EET by *P.*

aeruginosa not only supports growth and survival, but potential recalcitrance to antibiotic treatment during lung infection of CF patients as well.

EET in plant and animal food fermentations

Further evidence of EET-capable microorganisms in host-associated microbiomes comes from the study of fermented foods. Fermented foods are foods and beverages made as result of intentional microbial growth and enzymatic conversion of food components (Marco, 2020). Most fermentations rely on the microorganisms present on the plant or animal food ingredients. Moreover, the consumption of these foods, and the microorganisms they can contain, are increasingly understood to benefit human health (Şanlier et al., 2019). A primary connection between plant and animal microbiomes, fermented foods, and health is with lactic acid bacteria (LAB). These bacteria, which are comprised of numerous phylogenetically and functionally diverse species in the Firmicutes phylum (Yu et al., 2020), are essential for the production of over 3500 foods, beverages, and silage (Tamang et al., 2016). There is also growing evidence of EET capabilities amongst LAB (**Figure 1** and **Table 3**) which may influence the outcome of these food and beverage fermentations.

We recently showed that *Lactiplantibacillus plantarum* could perform EET during food fermentations (Tejedor-Sanz et al., 2021). Specifically, we found that *L. plantarum* produced a robust current when fermenting kale juice in the presence of a polarized anode and with the additional supplementation of the exogenous quinone DHNA (1,4-dihydroxy-2-naphthoic acid). Under these conditions, *L. plantarum* also acidified the kale juice medium to a greater degree through an increase in fermentative flux via lactic and acetic acid production (Tejedor-Sanz et al., 2021). This activity suggests that EET-conducive conditions during food fermentations may

benefit *L. plantarum* and other LAB by resulting in a rapid acidification of the extracellular environment and inhibition of acid-sensitive, competing microorganisms (Gao et al., 2019). Kale leaf tissues (and other cruciferous vegetables) may also be an EET-conducive food matrix, as they contain several electron donor carbohydrates like simple sugars (e.g., glucose, fructose, and sucrose) and sugar alcohols (e.g., mannitol and sorbitol) (Thavarajah et al., 2016), as well as redox-active metals like iron and manganese which can act as electron acceptors for EET (Kim et al., 2017).

EET metabolism in *L. plantarum* was also associated with a lower oxidation-reduction potential (ORP) of laboratory culture medium during fermentation. ORP, which is defined as the ratio of oxidative to reductive compounds in a given environment (Killeen et al., 2018), is an important variable during food fermentations. A low ORP is believed to inhibit the growth of spoilage organisms (Brasca et al., 2007; Olsen and Pérez-Díaz, 2009) and improve flavor development in cheese (Morandi et al., 2016). Given the association of ORP reduction with EET capabilities in *L. plantarum*, evidence of EET among other LAB in food fermentations may be indicated by reductions in matrix ORP as well. For example, numerous studies have reported that the ORP of milk declines during the production of fermented dairy products by LAB, and that these ORP reduction kinetics are strain-specific (Abraham et al., 2013; Brasca et al., 2007; Cachon et al., 2002; Jeanson et al., 2009; Morandi et al., 2016). Reductions in milk ORP are not only due to the consumption and elimination of O_2 (Larsen et al., 2015), but also through the reduction of other compounds in the milk matrix including thiols (Brasca et al., 2007) and amino acids (Kieronczyk et al., 2006). Milk also contains oxidized metals (Tachon et al., 2010) and electron shuttles like riboflavin (Vitamin B2) and quinones (Daniel and Norris, 1944; Walther et al., 2013) which may be utilized by EET-capable LAB.

Lactococcus lactis, an LAB commonly used in dairy fermentations (Cavanagh et al., 2015), has been shown in several reports to perform EET through current generation (Freguia et al., 2009; Masuda et al., 2010; Tejedor-Sanz et al., 2021). Disruption or deletion of genes in *L. lactis* associated with menaquinone biosynthesis inhibited EET by preventing the reduction of colorimetric, redox-active salts on milk agar (Michelon et al., 2013; Tachon et al., 2009). Additionally, this reduced EET activity was associated with lower growth rate, higher ORP, and higher pH during milk fermentation (Tachon et al., 2010). Hence, *L. lactis* may use EET metabolism during the fermentation of milk for enhanced growth and environmental acidification. Several other predicted or demonstrated EET-capable LAB used in milk fermentations, including strains of *E. faecalis*, *Enterococcus durans*, *Enterococcus faecium*, *L. plantarum*, *Lacticaseibacillus casei*, and *Lacticaseibacillus paracasei*, could consistently reduce milk ORP during fermentation as well (Brasca et al., 2007; Morandi et al., 2016; Tejedor-Sanz et al., 2021). The capacity to lower milk ORP is not shared by all LAB though, including strains of *Pediococcus pentosaceus*, *Lactobacillus helveticus*, *Lactobacillus delbrueckii subsp. bulgaricus*, and *Streptococcus thermophilus* (Brasca et al., 2007; Cachon et al., 2002), which we previously determined to be deficient in EET activity or genes from the putative FLEET locus (Tejedor-Sanz et al., 2021). However, other studies have reported that strains of *L. bulgaricus* (Carrasco et al., 2005) and *S. thermophilus* (Alwazeer et al., 2020; Morandi et al., 2016) could generate negative ORP during milk fermentation, which may signal that that milk ORP reduction by these LAB occurs through the reduction of other milk matrix components.

Aside from vegetable and dairy fermentations, there are other plant- and animal-based fermentation matrixes which may be influenced by EET-capable LAB. Sourdough fermentations are one such environment where flavins and quinones are present in the dough or are produced

by bacteria (Capozzi et al., 2011; Rizzello et al., 2013). Fumarate, a recently identified electron acceptor for EET (Light et al., 2019), is also present (Lotong et al., 2000). Isolates of EET-capable LAB species including *L. plantarum* (Landis et al., 2021), *L. lactis* (Passerini et al., 2013), and *E. faecium* (Tan et al., 2013) have been found in the sourdough microbiome. Additionally, when used as the sole inoculated organism, both *L. plantarum* strain TMW 1.460 (Capuani et al., 2012) and *E. faecalis* strain TMW 2.630 (Capuani et al., 2013) were able to greatly reduce ORP during sourdough fermentation. Wine is another potential EET-conducive environment rich in redox-active compounds like iron and copper, along with quinones and flavins (Andrés-Lacueva et al., 1998; Waterhouse et al., 2016). In particular, iron(II) and iron(III) complexes dominate wine ORP during fermentation (Killeen et al., 2018). Several EET-capable LAB like *L. plantarum* (Virdis et al., 2021), *L. casei* (Virdis et al., 2021), *Lactiplantibacillus pentosus* (Nisiotou et al., 2015), and *L. rhamnosus* (Henríquez-Aedo et al., 2016) have either been isolated from wine fermentations, or purposefully added to wine for malolactic fermentation. Lastly, meats are rich in metals like iron, copper, and manganese (Alturiqi and Albedair, 2012; Macho-González et al., 2020), and are commonly fermented with lactic acid bacteria to prevent lipid oxidation, improve shelf life, and prevent the growth of pathogenic microorganisms (Neffe-Skocińska et al., 2020; Neffe-Skocińska et al., 2016). Two studies which monitored the fermentation of pork loins found that ORP significantly decreased when inoculated with a starter culture of *L. rhamnosus* LOCK900 (Kęska et al., 2020; Neffe-Skocińska et al., 2020).

Applications of EET in host-associated habitats

Several lines of evidence suggest EET capabilities promote an ecological advantage for microorganisms inhabiting plant- and animal-associated environments. EET activity may also have direct effects on host health and the environment. Thus, the presence of electroactive bacteria in these plant and animal niches may be informative for several biotechnological applications of EET. In the rhizosphere, methanogenic archaea from rice paddies produce 11% of the world's anthropogenic methane (CH_4) emissions (Jiang et al., 2019). DIET between *Geobacter* and methanogens promotes methane production (Rotaru et al., 2014), and thus inhibition of DIET between *Geobacter* species and methanogens in the rice rhizosphere could reduce these emissions. Interruption of DIET in rice paddies could be achieved through the addition of soil amendments which promote oxygenation (Han et al., 2016; Jiang et al., 2019) as oxygen acts as an electron scavenger during EET (Lu et al., 2017). Alternatively, a recent study showed that one-time administration of an enriched cable bacteria culture (*Ca.* Electronema sp. GS) to rice-vegetated soils resulted in the oxidation of hydrogen sulfide and a two- to seven-fold reduction of methane emissions (Scholz et al., 2020).

Another potential application of EET in the rhizosphere is altering the bioavailability of redox-active metals for plant health. One study found that administering 10^8 CFU/mL of dissimilatory iron-reducing bacteria led to improved growth and iron uptake in common bean plants (Valencia-Cantero et al., 2007). Iron bioavailability in the rhizosphere is low, especially in alkaline soils where iron predominately exists as iron(III) (Hsieh and Waters, 2016). Thus, administering EET-capable bacteria to these soils may improve iron uptake and growth of other plants. Conversely, EET-capable microorganisms could also be used to inhibit plant uptake of heavy metal contaminants. Heavy metals such as copper and cobalt are phytotoxic above certain

concentrations and can result in oxidative stress if assimilated by plants (Panda and Choudhury, 2005). *G. sulfurreducens* as well as a species of *Clostridium* have been shown to reduce these metals and remove them from aqueous solution through biomineralization (Dulay et al., 2020; Hofacker et al., 2015; Kimber et al., 2020). Other heavy metals like technetium and chromium can also be reduced by *Geobacter* spp. (Shi et al., 2016). Hence, *in situ* reduction of these heavy metals in the rhizosphere and inhibition of plant uptake could be possible through administration of EET-capable, metal-reducing bacteria in contaminated rhizosphere soils.

For human hosts, therapies aimed at inhibiting EET in human microbiomes may prevent the growth of pathogenic, EET-capable microorganisms. Titanium dental implants perform better for osseointegration than other materials, but their redox activity may promote the growth of electroactive pathogens like *S. mutans* and lead to accelerated corrosion and peri-implantitis (Pozhitkov et al., 2015). Nonconductive materials such as ceramics (Saini et al., 2015) could be incorporated into or coated onto titanium implants to dampen electrical conductivity. Sequestration of redox-active compounds or electron shuttles could be another method of inhibiting growth of electroactive pathogens. A recent study of the chronic kidney disease drug AST-120 found that this compound adsorbs several phenazines produced by *P. aeruginosa* and improves the survival of A-594 human lung epithelial cells treated with *P. aeruginosa* supernatants (Hirakawa et al., 2021). Use of similar compounds to adsorb phenazines may improve clinical outcomes for CF patients with recurring *P. aeruginosa* infections. Lastly, controlling iron availability in the intestine could limit its availability as an electron acceptor and inhibit proliferation of EET-capable pathogens associated with iron overload like *L. monocytogenes* and *E. faecalis* (Finlayson-Trick et al., 2020).

There are also uses of EET that may benefit the production of fermented plant and animal foods. Our findings of *L. plantarum* EET during kale juice fermentation showed that the relative production of flavor-imparting metabolites such as lactate and acetate (Chen et al., 2017) as well as environmental acidification was directly affected by EET-conducive or non-conducive conditions (Tejedor-Sanz et al., 2021). We also showed that ORP reduction, a factor which influences flavor development (Killeen et al., 2018; Morandi et al., 2016) and prevents the growth of spoilage organisms (Morandi et al., 2016; Olsen and Pérez-Díaz, 2009), occurred through EET as well (Tejedor-Sanz et al., 2021). The use of polarized electrodes to drive fermentation, a process defined as electro-fermentation (Moscoviz et al., 2016), could be employed with EET-capable LAB such as *L. plantarum* to influence the flavor profile of fermented foods or beverages. Similarly, promoting ORP reduction and acidification through EET during LAB fermentations could further prevent the growth of competitive or spoilage microorganisms.

Conclusions

Bacterial EET metabolism has been identified in several environments including the rhizosphere, animal mucosal niches, and fermented foods and beverages. Ecologically, EET provides several benefits for capable bacteria such as improved energy conservation or host colonization, enhanced growth of microorganisms to conduct direct electron exchange with, or the potential inhibition of competitors through acidification or ORP reduction. In a broader view, EET may play a significant role in agriculture, food production industries, and human health. Thus, further characterization of the mechanistic and ecological underpinnings of EET in these environments should be explored to better assess the impacts of EET.

References

Abraham, S., Cachon, R., Jeanson, S., Ebel, B., Michelon, D., Aubert, C., Rojas, C., Feron, G., Beuvier, E., Gervais, P., De Coninck, J., 2013. A procedure for reproducible measurement of redox potential (Eh) in dairy processes. Dairy Sci. Technol. 93, 675–690. https://doi.org/10.1007/s13594-013-0134-5

Alturiqi, A.S., Albedair, L.A., 2012. Evaluation of some heavy metals in certain fish, meat and meat products in Saudi Arabian markets. Egypt. J. Aquat. Res. 38, 45–49. https://doi.org/10.1016/j.ejar.2012.08.003

Alwazeer, D., Bulut, M., Tunçtürk, Y., 2020. Fortification of milk with plant extracts modifies the acidification and reducing capacities of yoghurt bacteria. Int. J. Dairy Technol. 73, 117–125. https://doi.org/10.1111/1471-0307.12643

Andrés-Lacueva, C., Mattivi, F., Tonon, D., 1998. Determination of riboflavin, flavin mononucleotide and flavin–adenine dinucleotide in wine and other beverages by high-performance liquid chromatography with fluorescence detection. J. Chromatogr. A 823, 355–363. https://doi.org/10.1016/S0021-9673(98)00585-8

Asli, S., Neumann, P.M., 2010. Rhizosphere humic acid interacts with root cell walls to reduce hydraulic conductivity and plant development. Plant Soil 336, 313–322. https://doi.org/10.1007/s11104-010-0483-2

Benz, M., Schink, B., Brune, A., 1998. Humic Acid Reduction by Propionibacterium freudenreichii and Other Fermenting Bacteria. Appl. Environ. Microbiol. 64, 4507–4512.

Bhattacharyya, A., Chattopadhyay, R., Mitra, S., Crowe, S.E., 2014. Oxidative Stress: An Essential Factor in the Pathogenesis of Gastrointestinal Mucosal Diseases. Physiol. Rev. 94, 329–354. https://doi.org/10.1152/physrev.00040.2012

Bhushan, B., Halasz, A., Hawari, J., 2006. Effect of iron(III), humic acids and anthraquinone-2,6-disulfonate on biodegradation of cyclic nitramines by Clostridium sp. EDB2. J. Appl. Microbiol. 100, 555–563. https://doi.org/10.1111/j.1365-2672.2005.02819.x

Blekhman, R., Goodrich, J.K., Huang, K., Sun, Q., Bukowski, R., Bell, J.T., Spector, T.D., Keinan, A., Ley, R.E., Gevers, D., Clark, A.G., 2015. Host genetic variation impacts microbiome composition across human body sites. Genome Biol. 16, 191. https://doi.org/10.1186/s13059-015-0759-1

Bosire, E.M., Blank, L.M., Rosenbaum, M.A., 2016. Strain- and Substrate-Dependent Redox Mediator and Electricity Production by Pseudomonas aeruginosa. Appl. Environ. Microbiol. 82, 5026–5038. https://doi.org/10.1128/AEM.01342-16

Bosire, E.M., Rosenbaum, M.A., 2017. Electrochemical Potential Influences Phenazine Production, Electron Transfer and Consequently Electric Current Generation by Pseudomonas aeruginosa. Front. Microbiol. 8. https://doi.org/10.3389/fmicb.2017.00892

Brasca, M., Morandi, S., Lodi, R., Tamburini, A., 2007. Redox potential to discriminate among species of lactic acid bacteria. J. Appl. Microbiol. 103, 1516–1524. https://doi.org/10.1111/j.1365-2672.2007.03392.x

Bulat, T., Topcu, A., 2019. The effect of oxidation-reduction potential on the characteristics of UF white cheese produced using single strains of Lactococcus lactis. LWT 109, 296–304. https://doi.org/10.1016/j.lwt.2019.04.025

Cachon, R., Jeanson, S., Aldarf, M., Divies, C., 2002. Characterisation of lactic starters based on acidification and reduction activities. Le Lait 82, 281–288. https://doi.org/10.1051/lait:2002010

Capozzi, V., Menga, V., Digesù, A.M., De Vita, P., van Sinderen, D., Cattivelli, L., Fares, C., Spano, G., 2011. Biotechnological Production of Vitamin B2-Enriched Bread and Pasta. J. Agric. Food Chem. 59, 8013–8020. https://doi.org/10.1021/jf201519h

Capuani, A., Behr, J., Vogel, R.F., 2013. Influence of lactic acid bacteria on redox status and on proteolytic activity of buckwheat (Fagopyrum esculentum Moench) sourdoughs. Int. J. Food Microbiol. 165, 148–155. https://doi.org/10.1016/j.ijfoodmicro.2013.04.020

Capuani, A., Behr, J., Vogel, R.F., 2012. Influence of lactic acid bacteria on the oxidation–reduction potential of buckwheat (Fagopyrum esculentum Moench) sourdoughs. Eur. Food Res. Technol. 235, 1063–1069. https://doi.org/10.1007/s00217-012-1834-4

Capuani, A., Werner, S., Behr, J., Vogel, R.F., 2014. Effect of controlled extracellular oxidation-reduction potential on microbial metabolism and proteolysis in buckwheat sourdough. Eur. Food Res. Technol. 238, 425–434.

Carrasco, M.S., Scarinci, H.E., Simonetta, A.C., 2005. Associative growth of lactic acid bacteria for cheese starters : Acidifying and proteolytic activities and redox potential development.

Caselli, E., Fabbri, C., D'Accolti, M., Soffritti, I., Bassi, C., Mazzacane, S., Franchi, M., 2020. Defining the oral microbiome by whole-genome sequencing and resistome analysis: the complexity of the healthy picture. BMC Microbiol. 20, 120. https://doi.org/10.1186/s12866-020-01801-y

Cavanagh, D., Fitzgerald, G.F., McAuliffe, O., 2015. From field to fermentation: The origins of Lactococcus lactis and its domestication to the dairy environment. Food Microbiol. 47, 45–61. https://doi.org/10.1016/j.fm.2014.11.001

Chen, C., Zhao, S., Hao, G., Yu, H., Tian, H., Zhao, G., 2017. Role of lactic acid bacteria on the yogurt flavour: A review. Int. J. Food Prop. 20, S316–S330. https://doi.org/10.1080/10942912.2017.1295988

Chen, M., Tong, H., Liu, C., Chen, D., Li, F., Qiao, J., 2016. A humic substance analogue AQDS stimulates Geobacter sp. abundance and enhances pentachlorophenol transformation in a paddy soil. Chemosphere 160, 141–148. https://doi.org/10.1016/j.chemosphere.2016.06.061

Dai, J., Tang, Z., Jiang, N., Kopittke, P.M., Zhao, F.-J., Wang, P., 2020. Increased arsenic mobilization in the rice rhizosphere is mediated by iron-reducing bacteria. Environ. Pollut. 263, 114561. https://doi.org/10.1016/j.envpol.2020.114561

Daniel, L., Norris, L.C., 1944. Riboflavin Content of Milk and Milk Products. Food Res. 9, 312–18.

Deng, H., Chen, Z., Zhao, F., 2012. Energy from Plants and Microorganisms: Progress in Plant–Microbial Fuel Cells. ChemSusChem 5, 1006–1011. https://doi.org/10.1002/cssc.201100257

Dietrich, L.E.P., Okegbe, C., Price-Whelan, A., Sakhtah, H., Hunter, R.C., Newman, D.K., 2013. Bacterial Community Morphogenesis Is Intimately Linked to the Intracellular Redox State. J. Bacteriol. 195, 1371–1380. https://doi.org/10.1128/JB.02273-12

Dobbin, P.S., Carter, J.P., García-Salamanca San Juan, C., von Hobe, M., Powell, A.K., Richardson, D.J., 1999. Dissimilatory Fe(III) reduction by Clostridium beijerinckii isolated from freshwater sediment using Fe(III) maltol enrichment. FEMS Microbiol. Lett. 176, 131–138. https://doi.org/10.1111/j.1574-6968.1999.tb13653.x

Dulay, H., Tabares, M., Kashefi, K., Reguera, G., 2020. Cobalt Resistance via Detoxification and Mineralization in the Iron-Reducing Bacterium Geobacter sulfurreducens. Front. Microbiol. 11, 2992. https://doi.org/10.3389/fmicb.2020.600463

Ericsson, A.C., Davis, D.J., Franklin, C.L., Hagan, C.E., 2015. Exoelectrogenic capacity of host microbiota predicts lymphocyte recruitment to the gut. Physiol. Genomics 47, 243–252. https://doi.org/10.1152/physiolgenomics.00010.2015

Feliciano, G.T., Steidl, R.J., Reguera, G., 2015. Structural and functional insights into the conductive pili of Geobacter sulfurreducens revealed in molecular dynamics simulations. Phys. Chem. Chem. Phys. 17, 22217–22226. https://doi.org/10.1039/C5CP03432A

Finch, A.S., Mackie, T.D., Sund, C.J., Sumner, J.J., 2011. Metabolite analysis of Clostridium acetobutylicum: Fermentation in a microbial fuel cell. Bioresour. Technol., Special Issue: Biofuels - II: Algal Biofuels and Microbial Fuel Cells 102, 312–315. https://doi.org/10.1016/j.biortech.2010.06.149

Finlayson-Trick, E.C., Fischer, J.A., Goldfarb, D.M., Karakochuk, C.D., 2020. The Effects of Iron Supplementation and Fortification on the Gut Microbiota: A Review. Gastrointest. Disord. 2, 327–340. https://doi.org/10.3390/gidisord2040030

Forssten, S.D., Björklund, M., Ouwehand, A.C., 2010. Streptococcus mutans, Caries and Simulation Models. Nutrients 2, 290–298. https://doi.org/10.3390/nu2030290

Franz, C.M.A.P., Huch, M., Abriouel, H., Holzapfel, W., Gálvez, A., 2011. Enterococci as probiotics and their implications in food safety. Int. J. Food Microbiol. 151, 125–140. https://doi.org/10.1016/j.ijfoodmicro.2011.08.014

Freguia, S., Masuda, M., Tsujimura, S., Kano, K., 2009. Lactococcus lactis catalyses electricity generation at microbial fuel cell anodes via excretion of a soluble quinone. Bioelectrochemistry, Advanced design of electron-transfer pathways across biomolecular interfaces, Dedicated to Professor Lo Gorton 76, 14–18. https://doi.org/10.1016/j.bioelechem.2009.04.001

Freire, M.O., Sedghizadeh, P.P., Schaudinn, C., Gorur, A., Downey, J.S., Choi, J.-H., Chen, W., Kook, J.-K., Chen, C., Goodman, S.D., Zadeh, H.H., 2011. Development of an Animal Model for Aggregatibacter Actinomycetemcomitans Biofilm-Mediated Oral Osteolytic Infection: A Preliminary Study. J. Periodontol. 82, 778–789. https://doi.org/10.1902/jop.2010.100263

Gao, Z., Daliri, E.B.-M., Wang, J., Liu, D., Chen, S., Ye, X., Ding, T., 2019. Inhibitory Effect of Lactic Acid Bacteria on Foodborne Pathogens: A Review. J. Food Prot. 82, 441–453. https://doi.org/10.4315/0362-028X.JFP-18-303

Glasser, N.R., Kern, S.E., Newman, D.K., 2014. Phenazine redox cycling enhances anaerobic survival in Pseudomonas aeruginosa by facilitating generation of ATP and a proton-motive force. Mol. Microbiol. 92, 399–412. https://doi.org/10.1111/mmi.12566

Glasser, N.R., Saunders, S.H., Newman, D.K., 2017. The Colorful World of Extracellular Electron Shuttles. Annu. Rev. Microbiol. 71, 731–751. https://doi.org/10.1146/annurev-micro-090816-093913

Gomes, N.C.M., Cleary, D.F.R., Pires, A.C.C., Almeida, A., Cunha, A., Mendonça-Hagler, L.C.S., Smalla, K., 2014. Assessing variation in bacterial composition between the rhizospheres of two mangrove tree species. Estuar. Coast. Shelf Sci. 139, 40–45. https://doi.org/10.1016/j.ecss.2013.12.022

Gorby, Y.A., Yanina, S., McLean, J.S., Rosso, K.M., Moyles, D., Dohnalkova, A., Beveridge, T.J., Chang, I.S., Kim, B.H., Kim, K.S., Culley, D.E., Reed, S.B., Romine, M.F.,

Saffarini, D.A., Hill, E.A., Shi, L., Elias, D.A., Kennedy, D.W., Pinchuk, G., Watanabe, K., Ishii, S., Logan, B., Nealson, K.H., Fredrickson, J.K., 2006. Electrically conductive bacterial nanowires produced by Shewanella oneidensis strain MR-1 and other microorganisms. Proc. Natl. Acad. Sci. 103, 11358–11363. https://doi.org/10.1073/pnas.0604517103

Gurumurthy, D.M., Bharagava, R.N., Kumar, A., Singh, B., Ashfaq, M., Saratale, G.D., Mulla, S.I., 2019. EPS bound flavins driven mediated electron transfer in thermophilic Geobacillus sp. Microbiol. Res. 229, 126324. https://doi.org/10.1016/j.micres.2019.126324

Hall, M.W., Singh, N., Ng, K.F., Lam, D.K., Goldberg, M.B., Tenenbaum, H.C., Neufeld, J.D., G. Beiko, R., Senadheera, D.B., 2017. Inter-personal diversity and temporal dynamics of dental, tongue, and salivary microbiota in the healthy oral cavity. Npj Biofilms Microbiomes 3, 1–7. https://doi.org/10.1038/s41522-016-0011-0

Han, X., Sun, X., Wang, C., Wu, M., Dong, D., Zhong, T., Thies, J.E., Wu, W., 2016. Mitigating methane emission from paddy soil with rice-straw biochar amendment under projected climate change. Sci. Rep. 6, 24731. https://doi.org/10.1038/srep24731

Healy, C., Munoz-Wolf, N., Strydom, J., Faherty, L., Williams, N.C., Kenny, S., Donnelly, S.C., Cloonan, S.M., 2021. Nutritional immunity: the impact of metals on lung immune cells and the airway microbiome during chronic respiratory disease. Respir. Res. 22, 133. https://doi.org/10.1186/s12931-021-01722-y

Hederstedt, L., Gorton, L., Pankratova, G., 2020. Two Routes for Extracellular Electron Transfer in Enterococcus faecalis. J. Bacteriol. 202. https://doi.org/10.1128/JB.00725-19

Henríquez-Aedo, K., Durán, D., Garcia, A., Hengst, M.B., Aranda, M., 2016. Identification of biogenic amines-producing lactic acid bacteria isolated from spontaneous malolactic fermentation of chilean red wines. LWT - Food Sci. Technol. 68, 183–189. https://doi.org/10.1016/j.lwt.2015.12.003

Heydorn, R.L., Engel, C., Krull, R., Dohnt, K., 2020. Strategies for the Targeted Improvement of Anodic Electron Transfer in Microbial Fuel Cells. ChemBioEng Rev. 7, 4–17. https://doi.org/10.1002/cben.201900023

Hirakawa, H., Takita, A., Uchida, M., Kaneko, Y., Kakishima, Y., Tanimoto, K., Kamitani, W., Tomita, H., 2021. Adsorption of Phenazines Produced by Pseudomonas aeruginosa Using AST-120 Decreases Pyocyanin-Associated Cytotoxicity. Antibiotics 10, 434. https://doi.org/10.3390/antibiotics10040434

Hobbie, S.N., Li, X., Basen, M., Stingl, U., Brune, A., 2012. Humic substance-mediated Fe(III) reduction by a fermenting Bacillus strain from the alkaline gut of a humus-feeding scarab beetle larva. Syst. Appl. Microbiol. 35, 226–232. https://doi.org/10.1016/j.syapm.2012.03.003

Hofacker, A.F., Behrens, S., Voegelin, A., Kaegi, R., Lösekann-Behrens, T., Kappler, A., Kretzschmar, R., 2015. Clostridium Species as Metallic Copper-Forming Bacteria in Soil under Reducing Conditions. Geomicrobiol. J. 32, 130–139. https://doi.org/10.1080/01490451.2014.933287

Holmes, D.E., Shrestha, P.M., Walker, D.J.F., Dang, Y., Nevin, K.P., Woodard, T.L., Lovley, D.R., 2017. Metatranscriptomic Evidence for Direct Interspecies Electron Transfer between Geobacter and Methanothrix Species in Methanogenic Rice Paddy Soils. Appl. Environ. Microbiol. 83. https://doi.org/10.1128/AEM.00223-17

Hsieh, E.-J., Waters, B.M., 2016. Alkaline stress and iron deficiency regulate iron uptake and riboflavin synthesis gene expression differently in root and leaf tissue: implications for iron deficiency chlorosis. J. Exp. Bot. 67, 5671–5685. https://doi.org/10.1093/jxb/erw328

Huang, L., Tang, J., Chen, M., Liu, X., Zhou, S., 2018. Two Modes of Riboflavin-Mediated Extracellular Electron Transfer in Geobacter uraniireducens. Front. Microbiol. 9. https://doi.org/10.3389/fmicb.2018.02886

Igarashi, K., Miyako, E., Kato, S., 2020. Direct Interspecies Electron Transfer Mediated by Graphene Oxide-Based Materials. Front. Microbiol. 10, 3068. https://doi.org/10.3389/fmicb.2019.03068

Islam, F.S., Pederick, R.L., Gault, A.G., Adams, L.K., Polya, D.A., Charnock, J.M., Lloyd, J.R., 2005. Interactions between the Fe(III)-Reducing Bacterium Geobacter sulfurreducens and Arsenate, and Capture of the Metalloid by Biogenic Fe(II). Appl. Environ. Microbiol. 71, 8642–8648. https://doi.org/10.1128/AEM.71.12.8642-8648.2005

Jakobi, M.L., Stumpp, S.N., Stiesch, M., Eberhard, J., Heuer, W., 2015. The Peri-Implant and Periodontal Microbiota in Patients with and without Clinical Signs of Inflammation. Dent. J. 3, 24–42. https://doi.org/10.3390/dj3020024

Jeanson, S., Hilgert, N., Coquillard, M.-O., Seukpanya, C., Faiveley, M., Neveu, P., Abraham, C., Georgescu, V., Fourcassié, P., Beuvier, E., 2009. Milk acidification by Lactococcus lactis is improved by decreasing the level of dissolved oxygen rather than decreasing redox potential in the milk prior to inoculation. Int. J. Food Microbiol., 15th Meeting of the Club des Bactéries Lactiques 131, 75–81. https://doi.org/10.1016/j.ijfoodmicro.2008.09.020

Jia, H.T., Chen, S.C., Yang, S.Y., Shen, Y.H., Qiao, P.L., Wu, F.Z., Zhou, X.G., 2018. Effects of vanillin on cucumber rhizosphere bacterial community. Allelopathy J. 44, 191–200.

Jiang, Y., Qian, H., Huang, S., Zhang, X., Wang, L., Zhang, L., Shen, M., Xiao, X., Chen, F., Zhang, H., Lu, C., Li, C., Zhang, J., Deng, A., Groenigen, K.J. van, Zhang, W., 2019. Acclimation of methane emissions from rice paddy fields to straw addition. Sci. Adv. 5, eaau9038. https://doi.org/10.1126/sciadv.aau9038

Kabutey, F.T., Zhao, Q., Wei, L., Ding, J., Antwi, P., Quashie, F.K., Wang, W., 2019. An overview of plant microbial fuel cells (PMFCs): Configurations and applications. Renew. Sustain. Energy Rev. 110, 402–414. https://doi.org/10.1016/j.rser.2019.05.016

Kaku, N., Yonezawa, N., Kodama, Y., Watanabe, K., 2008. Plant/microbe cooperation for electricity generation in a rice paddy field. Appl. Microbiol. Biotechnol. 79, 43–49. https://doi.org/10.1007/s00253-008-1410-9

Kalinowski, D.S., Stefani, C., Toyokuni, S., Ganz, T., Anderson, G.J., Subramaniam, N.V., Trinder, D., Olynyk, J.K., Chua, A., Jansson, P.J., Sahni, S., Lane, D.J.R., Merlot, A.M., Kovacevic, Z., Huang, M.L.H., Lee, C.S., Richardson, D.R., 2016. Redox cycling metals: Pedaling their roles in metabolism and their use in the development of novel therapeutics. Biochim. Biophys. Acta BBA - Mol. Cell Res. 1863, 727–748. https://doi.org/10.1016/j.bbamcr.2016.01.026

Kappler, A., Brune, A., 2002. Dynamics of redox potential and changes in redox state of iron and humic acids during gut passage in soil-feeding termites (Cubitermes spp.). Soil Biol. Biochem. 34, 221–227. https://doi.org/10.1016/S0038-0717(01)00176-6

Kato, S., 2015. Biotechnological Aspects of Microbial Extracellular Electron Transfer. Microbes Environ. 30, 133–139. https://doi.org/10.1264/jsme2.ME15028

Kato, S., Igarashi, K., 2018. Enhancement of methanogenesis by electric syntrophy with biogenic iron-sulfide minerals. MicrobiologyOpen 8. https://doi.org/10.1002/mbo3.647
Keogh, D., Lam, L.N., Doyle, L.E., Matysik, A., Pavagadhi, S., Umashankar, S., Low, P.M., Dale, J.L., Song, Y., Ng, S.P., Boothroyd, C.B., Dunny, G.M., Swarup, S., Williams, R.B.H., Marsili, E., Kline, K.A., 2018. Extracellular Electron Transfer Powers Enterococcus faecalis Biofilm Metabolism. mBio 9, e00626-17. https://doi.org/10.1128/mBio.00626-17
Kesarwala, A.H., Krishna, M.C., Mitchell, J.B., 2016. Oxidative Stress in Oral Diseases. Oral Dis. 22, 9–18. https://doi.org/10.1111/odi.12300
Kęska, P., Stadnik, J., Wójciak, K.M., Neffe-Skocińska, K., 2020. Physico-chemical and proteolytic changes during cold storage of dry-cured pork loins with probiotic strains of LAB. Int. J. Food Sci. Technol. 55, 1069–1079. https://doi.org/10.1111/ijfs.14252
Khan, M.T., Browne, W.R., van Dijl, J.M., Harmsen, H.J.M., 2012a. How Can Faecalibacterium prausnitzii Employ Riboflavin for Extracellular Electron Transfer? Antioxid. Redox Signal. 17, 1433–1440. https://doi.org/10.1089/ars.2012.4701
Khan, M.T., Duncan, S.H., Stams, A.J.M., van Dijl, J.M., Flint, H.J., Harmsen, H.J.M., 2012b. The gut anaerobe Faecalibacterium prausnitzii uses an extracellular electron shuttle to grow at oxic–anoxic interphases. ISME J. 6, 1578–1585. https://doi.org/10.1038/ismej.2012.5
Kieronczyk, A., Cachon, R., Feron, G., Yvon, M., 2006. Addition of oxidizing or reducing agents to the reaction medium influences amino acid conversion to aroma compounds by Lactococcus lactis. J. Appl. Microbiol. 101, 1114–1122. https://doi.org/10.1111/j.1365-2672.2006.02999.x
Killeen, D.J., Boulton, R., Knoesen, A., 2018. Advanced Monitoring and Control of Redox Potential in Wine Fermentation. Am. J. Enol. Vitic. 69, 394–399. https://doi.org/10.5344/ajev.2018.17063
Kim, M.J., Chiu, Y.-C., Ku, K.-M., 2017. Glucosinolates, Carotenoids, and Vitamins E and K Variation from Selected Kale and Collard Cultivars [WWW Document]. J. Food Qual. https://doi.org/10.1155/2017/5123572
Kimber, R.L., Bagshaw, H., Smith, K., Buchanan, D.M., Coker, V.S., Cavet, J.S., Lloyd, J.R., 2020. Biomineralization of Cu2S Nanoparticles by Geobacter sulfurreducens. Appl. Environ. Microbiol. 86, e00967-20. https://doi.org/10.1128/AEM.00967-20
Kirk, T.K., Farrell, R.L., 1987. Enzymatic “combustion”: the microbial degradation of lignin. Annu. Rev. Microbiol. 41, 465–505. https://doi.org/10.1146/annurev.mi.41.100187.002341
Koch, C., Harnisch, F., 2016. Is there a Specific Ecological Niche for Electroactive Microorganisms? ChemElectroChem 3, 1282–1295. https://doi.org/10.1002/celc.201600079
Komlos, J., Jaffé, P.R., 2004. Effect of Iron Bioavailability on Dissolved Hydrogen Concentrations During Microbial Iron Reduction. Biodegradation 15, 315–325. https://doi.org/10.1023/B:BIOD.0000042187.31072.60
Kouzuma, A., Kaku, N., Watanabe, K., 2014. Microbial electricity generation in rice paddy fields: recent advances and perspectives in rhizosphere microbial fuel cells. Appl. Microbiol. Biotechnol. 98, 9521–9526. https://doi.org/10.1007/s00253-014-6138-0
Kouzuma, A., Kasai, T., Nakagawa, G., Yamamuro, A., Abe, T., Watanabe, K., 2013. Comparative Metagenomics of Anode-Associated Microbiomes Developed in Rice

Paddy-Field Microbial Fuel Cells. PLoS ONE 8. https://doi.org/10.1371/journal.pone.0077443
Kozlowski, H., Brown, D.R., Valensin, G., 2007. Metallochemistry of Neurodegeneration: Biological, Chemical and Genetic Aspects. Royal Society of Chemistry.
Kracke, F., Vassilev, I., Krömer, J.O., 2015. Microbial electron transport and energy conservation – the foundation for optimizing bioelectrochemical systems. Front. Microbiol. 6. https://doi.org/10.3389/fmicb.2015.00575
Lam, L.N., Wong, J.J., Matysik, A., Paxman, J.J., Chong, K.K.L., Low, P.M., Chua, Z.S., Heras, B., Marsili, E., Kline, K.A., 2019. Sortase-assembled pili promote extracellular electron transfer and iron acquisition in Enterococcus faecalis biofilm. bioRxiv 601666. https://doi.org/10.1101/601666
Landis, E.A., Oliverio, A.M., McKenney, E.A., Nichols, L.M., Kfoury, N., Biango-Daniels, M., Shell, L.K., Madden, A.A., Shapiro, L., Sakunala, S., Drake, K., Robbat, A., Booker, M., Dunn, R.R., Fierer, N., Wolfe, B.E., 2021. The diversity and function of sourdough starter microbiomes. eLife 10, e61644. https://doi.org/10.7554/eLife.61644
Langner, H.W., Inskeep, W.P., 2000. Microbial Reduction of Arsenate in the Presence of Ferrihydrite. Environ. Sci. Technol. 34, 3131–3136. https://doi.org/10.1021/es991414z
Laosuwan, K., Epasinghe, D.J., Wu, Z., Leung, W.K., Green, D.W., Jung, H.S., 2018. Comparison of biofilm formation and migration of Streptococcus mutans on tooth roots and titanium miniscrews. Clin. Exp. Dent. Res. 4, 40–47. https://doi.org/10.1002/cre2.101
Larsen, N., Werner, B.B., Vogensen, F.K., Jespersen, L., 2015. Effect of dissolved oxygen on redox potential and milk acidification by lactic acid bacteria isolated from a DL-starter culture. J. Dairy Sci. 98, 1640–1651. https://doi.org/10.3168/jds.2014-8971
Lee, H.J., Jeong, S.E., Kim, P.J., Madsen, E.L., Jeon, C.O., 2015. High resolution depth distribution of Bacteria, Archaea, methanotrophs, and methanogens in the bulk and rhizosphere soils of a flooded rice paddy. Front. Microbiol. 6. https://doi.org/10.3389/fmicb.2015.00639
Lee, H.J., Kim, S.Y., Kim, P.J., Madsen, E.L., Jeon, C.O., 2014. Methane emission and dynamics of methanotrophic and methanogenic communities in a flooded rice field ecosystem. FEMS Microbiol. Ecol. 88, 195–212. https://doi.org/10.1111/1574-6941.12282
Leveau, J.H.J., 2018. Microbial Communities in the Phyllosphere, in: Annual Plant Reviews Online. American Cancer Society, pp. 334–367. https://doi.org/10.1002/9781119312994.apr0239
Li, H., Chang, J., Liu, P., Fu, L., Ding, D., Lu, Y., 2015. Direct interspecies electron transfer accelerates syntrophic oxidation of butyrate in paddy soil enrichments. Environ. Microbiol. 17, 1533–1547. https://doi.org/10.1111/1462-2920.12576
Li, J., Nandagopal, S., Wu, D., Romanuik, S.F., Paul, K., Thomson, D.J., Lin, F., 2011. Activated T lymphocytes migrate toward the cathode of DC electric fields in microfluidic devices. Lab. Chip 11, 1298–1304. https://doi.org/10.1039/C0LC00371A
Light, S.H., Méheust, R., Ferrell, J.L., Cho, J., Deng, D., Agostoni, M., Iavarone, A.T., Banfield, J.F., D'Orazio, S.E.F., Portnoy, D.A., 2019. Extracellular electron transfer powers flavinylated extracellular reductases in Gram-positive bacteria. Proc. Natl. Acad. Sci. 116, 26892–26899. https://doi.org/10.1073/pnas.1915678116

Light, S.H., Su, L., Rivera-Lugo, R., Cornejo, J.A., Louie, A., Iavarone, A.T., Ajo-Franklin, C.M., Portnoy, D.A., 2018. A flavin-based extracellular electron transfer mechanism in diverse Gram-positive bacteria. Nature 562, 140. https://doi.org/10.1038/s41586-018-0498-z

Lin, Y., Liu, D., Yuan, J., Ye, G., Ding, W., 2017. Methanogenic Community Was Stable in Two Contrasting Freshwater Marshes Exposed to Elevated Atmospheric CO2. Front. Microbiol. 8. https://doi.org/10.3389/fmicb.2017.00932

List, C., Hosseini, Z., Meibom, K.L., Hatzimanikatis, V., Bernier-Latmani, R., 2019. Impact of iron reduction on the metabolism of Clostridium acetobutylicum. Environ. Microbiol. 21, 3548–3563. https://doi.org/10.1111/1462-2920.14640

Liu, Y., Luo, M., Ye, R., Huang, J., Xiao, L., Hu, Q., Zhu, A., Tong, C., 2019. Impacts of the rhizosphere effect and plant species on organic carbon mineralization rates and pathways, and bacterial community composition in a tidal marsh. FEMS Microbiol. Ecol. 95. https://doi.org/10.1093/femsec/fiz120

Logan, B.E., Rossi, R., Ragab, A., Saikaly, P.E., 2019. Electroactive microorganisms in bioelectrochemical systems. Nat. Rev. Microbiol. 17, 307–319. https://doi.org/10.1038/s41579-019-0173-x

Lopez-Siles, M., Duncan, S.H., Garcia-Gil, L.J., Martinez-Medina, M., 2017. Faecalibacterium prausnitzii : from microbiology to diagnostics and prognostics. ISME J. 11, 841–852. https://doi.org/10.1038/ismej.2016.176

Lotong, V., Iv, E.C., Chambers, D.H., 2000. Determination of the Sensory Attributes of Wheat Sourdough Bread. J. Sens. Stud. 15, 309–326. https://doi.org/10.1111/j.1745-459X.2000.tb00273.x

Lovley, D.R., Giovannoni, S.J., White, D.C., Champine, J.E., Phillips, E.J.P., Gorby, Y.A., Goodwin, S., 1993. Geobacter metallireducens gen. nov. sp. nov., a microorganism capable of coupling the complete oxidation of organic compounds to the reduction of iron and other metals. Arch. Microbiol. 159, 336–344. https://doi.org/10.1007/BF00290916

Lovley, D.R., Holmes, D.E., 2022. Electromicrobiology: the ecophysiology of phylogenetically diverse electroactive microorganisms. Nat. Rev. Microbiol. 20, 5–19. https://doi.org/10.1038/s41579-021-00597-6

Lu, M., Chan, S., Babanova, S., Bretschger, O., 2017. Effect of oxygen on the per-cell extracellular electron transfer rate of Shewanella oneidensis MR-1 explored in bioelectrochemical systems. Biotechnol. Bioeng. 114, 96–105. https://doi.org/10.1002/bit.26046

Lu, Y., Liu, L., Wu, S., Zhong, W., Xu, Y., Deng, H., 2019. Electricity generation from paddy soil for powering an electronic timer and an analysis of active exoelectrogenic bacteria. AMB Express 9, 57. https://doi.org/10.1186/s13568-019-0781-x

Lu, Y., Rosencrantz, D., Liesack, W., Conrad, R., 2006. Structure and activity of bacterial community inhabiting rice roots and the rhizosphere. Environ. Microbiol. 8, 1351–1360. https://doi.org/10.1111/j.1462-2920.2006.01028.x

Luo, M., Liu, Y., Huang, J., Xiao, L., Zhu, W., Duan, X., Tong, C., 2018. Rhizosphere processes induce changes in dissimilatory iron reduction in a tidal marsh soil: a rhizobox study. Plant Soil 433, 83–100. https://doi.org/10.1007/s11104-018-3827-y

Lurthy, T., Cantat, C., Jeudy, C., Declerck, P., Gallardo, K., Barraud, C., Leroy, F., Ourry, A., Lemanceau, P., Salon, C., Mazurier, S., 2020. Impact of Bacterial Siderophores on Iron

Status and Ionome in Pea. Front. Plant Sci. 11, 730. https://doi.org/10.3389/fpls.2020.00730
Macho-González, A., Garcimartín, A., López-Oliva, M.E., Bastida, S., Benedí, J., Ros, G., Nieto, G., Sánchez-Muniz, F.J., 2020. Can Meat and Meat-Products Induce Oxidative Stress? Antioxidants 9, 638. https://doi.org/10.3390/antiox9070638
Marco, M.L., 2020. Defining how microorganisms benefit human health. Microb. Biotechnol. n/a. https://doi.org/10.1111/1751-7915.13685
Masuda, M., Freguia, S., Wang, Y.-F., Tsujimura, S., Kano, K., 2010. Flavins contained in yeast extract are exploited for anodic electron transfer by Lactococcus lactis. Bioelectrochemistry 78, 173–175. https://doi.org/10.1016/j.bioelechem.2009.08.004
Mehta, T., Coppi, M.V., Childers, S.E., Lovley, D.R., 2005. Outer Membrane c-Type Cytochromes Required for Fe(III) and Mn(IV) Oxide Reduction in Geobacter sulfurreducens. Appl. Environ. Microbiol. 71, 8634–8641. https://doi.org/10.1128/AEM.71.12.8634-8641.2005
Meysman, F.J.R., Risgaard-Petersen, N., Malkin, S.Y., Nielsen, L.P., 2015. The geochemical fingerprint of microbial long-distance electron transport in the seafloor. Geochim. Cosmochim. Acta 152, 122–142. https://doi.org/10.1016/j.gca.2014.12.014
Meza-Siccha, A.S., Aguilar-Luis, M.A., Silva-Caso, W., Mazulis, F., Barragan-Salazar, C., del Valle-Mendoza, J., 2019. In Vitro Evaluation of Bacterial Adhesion and Bacterial Viability of Streptococcus mutans, Streptococcus sanguinis, and Porphyromonas gingivalis on the Abutment Surface of Titanium and Zirconium Dental Implants. Int. J. Dent. 2019. https://doi.org/10.1155/2019/4292976
Michelon, D., Tachon, S., Ebel, B., De Coninck, J., Feron, G., Gervais, P., Yvon, M., Cachon, R., 2013. Screening of lactic acid bacteria for reducing power using a tetrazolium salt reduction method on milk agar. J. Biosci. Bioeng. 115, 229–232. https://doi.org/10.1016/j.jbiosc.2012.09.010
Miller, B.M., Liou, M.J., Lee, J.-Y., Bäumler, A.J., 2021. The longitudinal and cross-sectional heterogeneity of the intestinal microbiota. Curr. Opin. Microbiol. 63, 221–230. https://doi.org/10.1016/j.mib.2021.08.004
Morandi, S., Silvetti, T., Tamburini, A., Brasca, M., 2016. Changes in oxidation-reduction potential during milk fermentation by wild lactic acid bacteria. J. Dairy Res. 83, 387–394. https://doi.org/10.1017/S0022029916000339
Moscoviz, R., Toledo-Alarcón, J., Trably, E., Bernet, N., 2016. Electro-Fermentation: How To Drive Fermentation Using Electrochemical Systems. Trends Biotechnol. 34, 856–865. https://doi.org/10.1016/j.tibtech.2016.04.009
Müller, H., Marozava, S., Probst, A.J., Meckenstock, R.U., 2020. Groundwater cable bacteria conserve energy by sulfur disproportionation. ISME J. 14, 623–634. https://doi.org/10.1038/s41396-019-0554-1
Naradasu, D., Guionet, A., Miran, W., Okamoto, A., 2020a. Microbial current production from Streptococcus mutans correlates with biofilm metabolic activity. Biosens. Bioelectron. 162, 112236. https://doi.org/10.1016/j.bios.2020.112236
Naradasu, D., Guionet, A., Okinaga, T., Nishihara, T., Okamoto, A., 2020b. Electrochemical Characterization of Current-Producing Human Oral Pathogens by Whole-Cell Electrochemistry. ChemElectroChem. https://doi.org/10.1002/celc.202000117

Naradasu, D., Miran, W., Okamoto, A., 2020c. Metabolic Current Production by an Oral Biofilm Pathogen Corynebacterium matruchotii. Molecules 25, 3141. https://doi.org/10.3390/molecules25143141

Naradasu, D., Miran, W., Sakamoto, M., Okamoto, A., 2019. Isolation and Characterization of Human Gut Bacteria Capable of Extracellular Electron Transport by Electrochemical Techniques. Front. Microbiol. 9. https://doi.org/10.3389/fmicb.2018.03267

Neffe-Skocińska, K., Okoń, A., Zielińska, D., Szymański, P., Sionek, B., Kołożyn-Krajewska, D., 2020. The Possibility of Using the Probiotic Starter Culture Lacticaseibacillus rhamnosus LOCK900 in Dry Fermented Pork Loins and Sausages Produced Under Industrial Conditions. Appl. Sci. 10, 4311. https://doi.org/10.3390/app10124311

Neffe-Skocińska, K., Wójciak, K., Zielińska, D., 2016. Probiotic Microorganisms in Dry Fermented Meat Products, Probiotics and Prebiotics in Human Nutrition and Health. IntechOpen. https://doi.org/10.5772/64090

Nisiotou, A.A., Dourou, D., Filippousi, M.-E., Diamantea, E., Fragkoulis, P., Tassou, C., Banilas, G., 2015. Genetic and Technological Characterisation of Vineyard- and Winery-Associated Lactic Acid Bacteria. BioMed Res. Int. 2015, e508254. https://doi.org/10.1155/2015/508254

O'Dwyer, D.N., Dickson, R.P., Moore, B.B., 2016. The Lung Microbiome, Immunity and the Pathogenesis of Chronic Lung Disease. J. Immunol. Baltim. Md 1950 196, 4839–4847. https://doi.org/10.4049/jimmunol.1600279

Olsen, M.J., Pérez-Díaz, I.M., 2009. Influence of Microbial Growth on the Redox Potential of Fermented Cucumbers. J. Food Sci. 74, M149–M153. https://doi.org/10.1111/j.1750-3841.2009.01121.x

Panda, S.K., Choudhury, S., 2005. Chromium stress in plants. Braz. J. Plant Physiol. 17, 95–102. https://doi.org/10.1590/S1677-04202005000100008

Pankratova, G., Hederstedt, L., Gorton, L., 2019. Extracellular electron transfer features of Gram-positive bacteria. Anal. Chim. Acta 1076, 32–47. https://doi.org/10.1016/j.aca.2019.05.007

Pankratova, G., Leech, D., Gorton, L., Hederstedt, L., 2018. Extracellular Electron Transfer by the Gram-Positive Bacterium Enterococcus faecalis. Biochemistry 57, 4597–4603. https://doi.org/10.1021/acs.biochem.8b00600

Park, H.S., Kim, B.H., Kim, H.S., Kim, H.J., Kim, G.T., Kim, M., Chang, I.S., Park, Y.K., Chang, H.I., 2001. A Novel Electrochemically Active and Fe(III)-reducing Bacterium Phylogenetically Related to Clostridium butyricum Isolated from a Microbial Fuel Cell. Anaerobe 7, 297–306. https://doi.org/10.1006/anae.2001.0399

Passerini, D., Coddeville, M., Le Bourgeois, P., Loubière, P., Ritzenthaler, P., Fontagné-Faucher, C., Daveran-Mingot, M.-L., Cocaign-Bousquet, M., 2013. The Carbohydrate Metabolism Signature of Lactococcus lactis Strain A12 Reveals Its Sourdough Ecosystem Origin. Appl. Environ. Microbiol. 79, 5844–5852. https://doi.org/10.1128/AEM.01560-13

Persson, L.G., Berglundh, T., Lindhe, J., Sennerby, L., 2001. Re-osseointegration after treatment of peri-implantitis at different implant surfaces. An experimental study in the dog. Clin. Oral Implants Res. 12, 595–603. https://doi.org/10.1034/j.1600-0501.2001.120607.x

Pfeffer, C., Larsen, S., Song, J., Dong, M., Besenbacher, F., Meyer, R.L., Kjeldsen, K.U., Schreiber, L., Gorby, Y.A., El-Naggar, M.Y., Leung, K.M., Schramm, A., Risgaard-Petersen, N., Nielsen, L.P., 2012. Filamentous bacteria transport electrons over centimetre distances. Nature 491, 218–221. https://doi.org/10.1038/nature11586

Pozhitkov, A.E., Daubert, D., Donimirski, A.B., Goodgion, D., Vagin, M.Y., Leroux, B.G., Hunter, C.M., Flemmig, T.F., Noble, P.A., Bryers, J.D., 2015. Interruption of Electrical Conductivity of Titanium Dental Implants Suggests a Path Towards Elimination Of Corrosion. PLOS ONE 10, e0140393. https://doi.org/10.1371/journal.pone.0140393

Prévoteau, A., Geirnaert, A., Arends, J.B.A., Lannebère, S., Van de Wiele, T., Rabaey, K., 2015. Hydrodynamic chronoamperometry for probing kinetics of anaerobic microbial metabolism – case study of Faecalibacterium prausnitzii. Sci. Rep. 5, 11484. https://doi.org/10.1038/srep11484

Reid, D.W., Carroll, V., O'May, C., Champion, A., Kirov, S.M., 2007. Increased airway iron as a potential factor in the persistence of Pseudomonas aeruginosa infection in cystic fibrosis. Eur. Respir. J. 30, 286–292. https://doi.org/10.1183/09031936.00154006

Rengel, Z., 2015. Availability of Mn, Zn and Fe in the rhizosphere. J. Soil Sci. Plant Nutr. 15, 397–409. https://doi.org/10.4067/S0718-95162015005000036

Rizzello, C.G., Mueller, T., Coda, R., Reipsch, F., Nionelli, L., Curiel, J.A., Gobbetti, M., 2013. Synthesis of 2-methoxy benzoquinone and 2,6-dimethoxybenzoquinone by selected lactic acid bacteria during sourdough fermentation of wheat germ. Microb. Cell Factories 12, 105. https://doi.org/10.1186/1475-2859-12-105

Robin, A., Vansuyt, G., Hinsinger, P., Meyer, J.M., Briat, J.F., Lemanceau, P., 2008. Chapter 4 Iron Dynamics in the Rhizosphere: Consequences for Plant Health and Nutrition, in: Advances in Agronomy. Academic Press, pp. 183–225. https://doi.org/10.1016/S0065-2113(08)00404-5

Rotaru, A.-E., Malla Shrestha, P., Liu, F., Shrestha, M., Shrestha, D., Embree, M., Zengler, K., Wardman, C., P. Nevin, K., R. Lovley, D., 2014. A new model for electron flow during anaerobic digestion: direct interspecies electron transfer to Methanosaeta for the reduction of carbon dioxide to methane. Energy Environ. Sci. 7, 408–415. https://doi.org/10.1039/C3EE42189A

Rowe, A.R., Xu, S., Gardel, E., Bose, A., Girguis, P., Amend, J.P., El-Naggar, M.Y., 2019. Methane-Linked Mechanisms of Electron Uptake from Cathodes by Methanosarcina barkeri. mBio 10. https://doi.org/10.1128/mBio.02448-18

Saini, M., Singh, Y., Arora, P., Arora, V., Jain, K., 2015. Implant biomaterials: A comprehensive review. World J. Clin. Cases WJCC 3, 52–57. https://doi.org/10.12998/wjcc.v3.i1.52

Şanlier, N., Gökcen, B.B., Sezgin, A.C., 2019. Health benefits of fermented foods. Crit. Rev. Food Sci. Nutr. 59, 506–527. https://doi.org/10.1080/10408398.2017.1383355

Schamphelaire, L.D., Cabezas, A., Marzorati, M., Friedrich, M.W., Boon, N., Verstraete, W., 2010. Microbial Community Analysis of Anodes from Sediment Microbial Fuel Cells Powered by Rhizodeposits of Living Rice Plants. Appl. Environ. Microbiol. 76, 2002–2008. https://doi.org/10.1128/AEM.02432-09

Schiessl, K.T., Hu, F., Jo, J., Nazia, S.Z., Wang, B., Price-Whelan, A., Min, W., Dietrich, L.E.P., 2019. Phenazine production promotes antibiotic tolerance and metabolic heterogeneity in Pseudomonas aeruginosa biofilms. Nat. Commun. 10, 1–10. https://doi.org/10.1038/s41467-019-08733-w

Scholz, V.V., Martin, B.C., Meyer, R., Schramm, A., Fraser, M.W., Nielsen, L.P., Kendrick, G.A., Risgaard-Petersen, N., Burdorf, L.D.W., Marshall, I.P.G., 2021. Cable bacteria at oxygen-releasing roots of aquatic plants: a widespread and diverse plant–microbe association. New Phytol. 232, 2138–2151. https://doi.org/10.1111/nph.17415

Scholz, V.V., Meckenstock, R.U., Nielsen, L.P., Risgaard-Petersen, N., 2020. Cable bacteria reduce methane emissions from rice-vegetated soils. Nat. Commun. 11, 1878. https://doi.org/10.1038/s41467-020-15812-w

Scholz, V.V., Müller, H., Koren, K., Nielsen, L.P., Meckenstock, R.U., 2019. The rhizosphere of aquatic plants is a habitat for cable bacteria. FEMS Microbiol. Ecol. 95. https://doi.org/10.1093/femsec/fiz062

Schwab, L., Rago, L., Koch, C., Harnisch, F., 2019. Identification of Clostridium cochlearium as an electroactive microorganism from the mouse gut microbiome. Bioelectrochemistry 130, 107334. https://doi.org/10.1016/j.bioelechem.2019.107334

Segers, M.E., Lebeer, S., 2014. Towards a better understanding of Lactobacillus rhamnosus GG - host interactions. Microb. Cell Factories 13, S7. https://doi.org/10.1186/1475-2859-13-S1-S7

Sender, R., Fuchs, S., Milo, R., 2016. Revised Estimates for the Number of Human and Bacteria Cells in the Body. PLoS Biol. 14. https://doi.org/10.1371/journal.pbio.1002533

Shi, L., Dong, H., Reguera, G., Beyenal, H., Lu, A., Liu, J., Yu, H.-Q., Fredrickson, J.K., 2016. Extracellular electron transfer mechanisms between microorganisms and minerals. Nat. Rev. Microbiol. 14, 651–662. https://doi.org/10.1038/nrmicro.2016.93

Shimizu, K., 2013. Metabolic Regulation of a Bacterial Cell System with Emphasis on Escherichia coli Metabolism [WWW Document]. ISRN Biochem. https://doi.org/10.1155/2013/645983

Tachon, S., Brandsma, J.B., Yvon, M., 2010. NoxE NADH Oxidase and the Electron Transport Chain Are Responsible for the Ability of Lactococcus lactis To Decrease the Redox Potential of Milk. Appl. Environ. Microbiol. 76, 1311–1319. https://doi.org/10.1128/AEM.02120-09

Tachon, S., Michelon, D., Chambellon, E., Cantonnet, M., Mezange, C., Henno, L., Cachon, R., Yvon, M., 2009. Experimental conditions affect the site of tetrazolium violet reduction in the electron transport chain of Lactococcus lactis. Microbiol. Read. Engl. 155, 2941–2948. https://doi.org/10.1099/mic.0.029678-0

Tahernia, M., Plotkin-Kaye, E., Mohammadifar, M., Gao, Y., Oefelein, M.R., Cook, L.C., Choi, S., 2020. Characterization of Electrogenic Gut Bacteria. ACS Omega 5, 29439–29446. https://doi.org/10.1021/acsomega.0c04362

Tamang, J.P., Shin, D.-H., Jung, S.-J., Chae, S.-W., 2016. Functional Properties of Microorganisms in Fermented Foods. Front. Microbiol. 7. https://doi.org/10.3389/fmicb.2016.00578

Tan, Q., Xu, H., Aguilar, Z.P., Peng, S., Dong, S., Wang, B., Li, P., Chen, T., Xu, F., Wei, H., 2013. Safety Assessment and Probiotic Evaluation of Enterococcus Faecium YF5 Isolated from Sourdough. J. Food Sci. 78, M587–M593. https://doi.org/10.1111/1750-3841.12079

Tejedor-Sanz, S., Stevens, E.T., Finnegan, P., Nelson, J., Knoessen, A., Light, S.H., Ajo-Franklin, C.M., Marco, M.L., 2021. Extracellular electron transfer increases fermentation in lactic acid bacteria via a hybrid metabolism. bioRxiv 2021.05.26.445846. https://doi.org/10.1101/2021.05.26.445846

Thavarajah, D., Thavarajah, P., Abare, A., Basnagala, S., Lacher, C., Smith, P., Combs, G.F., 2016. Mineral micronutrient and prebiotic carbohydrate profiles of USA-grown kale (Brassica oleracea L. var. acephala). J. Food Compos. Anal. 52, 9–15. https://doi.org/10.1016/j.jfca.2016.07.003

Timmers, R.A., Rothballer, M., Strik, D.P.B.T.B., Engel, M., Schulz, S., Schloter, M., Hartmann, A., Hamelers, B., Buisman, C., 2012. Microbial community structure elucidates performance of Glyceria maxima plant microbial fuel cell. Appl. Microbiol. Biotechnol. 94, 537–548. https://doi.org/10.1007/s00253-012-3894-6

Trachootham, D., Lu, W., Ogasawara, M.A., Valle, N.R.-D., Huang, P., 2008. Redox Regulation of Cell Survival. Antioxid. Redox Signal. 10, 1343–1374. https://doi.org/10.1089/ars.2007.1957

Trevisan, S., Francioso, O., Quaggiotti, S., Nardi, S., 2010. Humic substances biological activity at the plant-soil interface. Plant Signal. Behav. 5, 635–643.

Trojan, D., Schreiber, L., Bjerg, J.T., Bøggild, A., Yang, T., Kjeldsen, K.U., Schramm, A., 2016. A taxonomic framework for cable bacteria and proposal of the candidate genera Electrothrix and Electronema. Syst. Appl. Microbiol. 39, 297–306. https://doi.org/10.1016/j.syapm.2016.05.006

Tunney, M.M., Field, T.R., Moriarty, T.F., Patrick, S., Doering, G., Muhlebach, M.S., Wolfgang, M.C., Boucher, R., Gilpin, D.F., McDowell, A., Elborn, J.S., 2008. Detection of Anaerobic Bacteria in High Numbers in Sputum from Patients with Cystic Fibrosis. Am. J. Respir. Crit. Care Med. 177, 995–1001. https://doi.org/10.1164/rccm.200708-1151OC

Ucar, D., Zhang, Y., Angelidaki, I., 2017. An Overview of Electron Acceptors in Microbial Fuel Cells. Front. Microbiol. 8. https://doi.org/10.3389/fmicb.2017.00643

Valencia-Cantero, E., Hernández-Calderón, E., Velázquez-Becerra, C., López-Meza, J.E., Alfaro-Cuevas, R., López-Bucio, J., 2007. Role of dissimilatory fermentative iron-reducing bacteria in Fe uptake by common bean (Phaseolus vulgaris L.) plants grown in alkaline soil. Plant Soil 1–2, 263–273. https://doi.org/10.1007/s11104-007-9191-y

Virdis, C., Sumby, K., Bartowsky, E., Jiranek, V., 2021. Lactic Acid Bacteria in Wine: Technological Advances and Evaluation of Their Functional Role. Front. Microbiol. 11, 3192. https://doi.org/10.3389/fmicb.2020.612118

Voordeckers, J.W., Kim, B.-C., Izallalen, M., Lovley, D.R., 2010. Role of Geobacter sulfurreducens Outer Surface c-Type Cytochromes in Reduction of Soil Humic Acid and Anthraquinone-2,6-Disulfonate. Appl. Environ. Microbiol. 76, 2371–2375. https://doi.org/10.1128/AEM.02250-09

Vu, A.T., Nguyen, N.C., Leadbetter, J.R., 2004. Iron reduction in the metal-rich guts of wood-feeding termites. Geobiology 2, 239–247. https://doi.org/10.1111/j.1472-4677.2004.00038.x

Wagner, S., Hoefer, C., Puschenreiter, M., Wenzel, W.W., Oburger, E., Hann, S., Robinson, B., Kretzschmar, R., Santner, J., 2020. Arsenic redox transformations and cycling in the rhizosphere of Pteris vittata and Pteris quadriaurita. Environ. Exp. Bot. 177, 104122. https://doi.org/10.1016/j.envexpbot.2020.104122

Walther, B., Karl, J.P., Booth, S.L., Boyaval, P., 2013. Menaquinones, Bacteria, and the Food Supply: The Relevance of Dairy and Fermented Food Products to Vitamin K Requirements123. Adv. Nutr. 4, 463–473. https://doi.org/10.3945/an.113.003855

Wang, W., Du, Y., Yang, S., Du, X., Li, M., Lin, B., Zhou, J., Lin, L., Song, Y., Li, J., Zuo, X., Yang, C., 2019. Bacterial Extracellular Electron Transfer Occurs in Mammalian Gut. Anal. Chem. 91, 12138–12141. https://doi.org/10.1021/acs.analchem.9b03176

Wang, Y., Kern, S.E., Newman, D.K., 2010. Endogenous Phenazine Antibiotics Promote Anaerobic Survival of Pseudomonas aeruginosa via Extracellular Electron Transfer. J. Bacteriol. 192, 365–369. https://doi.org/10.1128/JB.01188-09

Wang, Y., Wilks, J.C., Danhorn, T., Ramos, I., Croal, L., Newman, D.K., 2011. Phenazine-1-Carboxylic Acid Promotes Bacterial Biofilm Development via Ferrous Iron Acquisition. J. Bacteriol. 193, 3606–3617. https://doi.org/10.1128/JB.00396-11

Wang, Y., Wu, C., Wang, X., Zhou, S., 2009. The role of humic substances in the anaerobic reductive dechlorination of 2,4-dichlorophenoxyacetic acid by Comamonas koreensis strain CY01. J. Hazard. Mater. 164, 941–947. https://doi.org/10.1016/j.jhazmat.2008.08.097

Wanger, G., Gorby, Y., El-Naggar, M.Y., Yuzvinsky, T.D., Schaudinn, C., Gorur, A., Sedghizadeh, P.P., 2013. Electrically conductive bacterial nanowires in bisphosphonate-related osteonecrosis of the jaw biofilms. Oral Surg. Oral Med. Oral Pathol. Oral Radiol. 115, 71–78. https://doi.org/10.1016/j.oooo.2012.08.446

Waterhouse, A.L., Sacks, G.L., Jeffery, D.W., 2016. Wine Oxidation, in: Understanding Wine Chemistry. John Wiley & Sons, Ltd, pp. 278–293. https://doi.org/10.1002/9781118730720.ch24

Weiss, J.V., Emerson, D., Megonigal, J.P., 2004. Geochemical control of microbial Fe(III) reduction potential in wetlands: comparison of the rhizosphere to non-rhizosphere soil. FEMS Microbiol. Ecol. 48, 89–100. https://doi.org/10.1016/j.femsec.2003.12.014

Wu, C.-Y., Zhuang, L., Zhou, S.-G., Li, F.-B., Li, X.-M., 2009. Fe(III)-enhanced anaerobic transformation of 2,4-dichlorophenoxyacetic acid by an iron-reducing bacterium Comamonas koreensis CY01. FEMS Microbiol. Ecol. 71, 106–113. https://doi.org/10.1111/j.1574-6941.2009.00796.x

Yang, Y., Wang, N., Guo, X., Zhang, Y., Ye, B., 2017. Comparative analysis of bacterial community structure in the rhizosphere of maize by high-throughput pyrosequencing. PLoS ONE 12. https://doi.org/10.1371/journal.pone.0178425

Yin, X., Heeney, D., Srisengfa, Y., Golomb, B., Griffey, S., Marco, M., 2017. Bacteriocin biosynthesis contributes to the anti-inflammatory capacities of probiotic Lactobacillus plantarum. Benef. Microbes 9, 333–344. https://doi.org/10.3920/BM2017.0096

Yong, X.-Y., Shi, D.-Y., Chen, Y.-L., Jiao, F., Lin, X., Zhou, J., Wang, S.-Y., Yong, Y.-C., Sun, Y.-M., OuYang, P.-K., Zheng, T., 2014. Enhancement of bioelectricity generation by manipulation of the electron shuttles synthesis pathway in microbial fuel cells. Bioresour. Technol. 152, 220–224. https://doi.org/10.1016/j.biortech.2013.10.086

Yong, Y.-C., Yu, Y.-Y., Li, C.-M., Zhong, J.-J., Song, H., 2011. Bioelectricity enhancement via overexpression of quorum sensing system in Pseudomonas aeruginosa-inoculated microbial fuel cells. Biosens. Bioelectron. 30, 87–92. https://doi.org/10.1016/j.bios.2011.08.032

Yu, A.O., Leveau, J.H.J., Marco, M.L., 2020. Abundance, diversity and plant-specific adaptations of plant-associated lactic acid bacteria. Environ. Microbiol. Rep. 12, 16–29. https://doi.org/10.1111/1758-2229.12794

Yu, Y., Wu, Y., Cao, B., Gao, Y.-G., Yan, X., 2015. Adjustable bidirectional extracellular electron transfer between Comamonas testosteroni biofilms and electrode via distinct electron mediators. Electrochem. Commun. 59, 43–47. https://doi.org/10.1016/j.elecom.2015.07.007

Zacharoff, L.A., Morrone, D.J., Bond, D.R., 2017. Geobacter sulfurreducens Extracellular Multiheme Cytochrome PgcA Facilitates Respiration to Fe(III) Oxides But Not Electrodes. Front. Microbiol. 8. https://doi.org/10.3389/fmicb.2017.02481

Zavanelli, A.C., Zavanelli, R.A., Mazaro, J.V.Q., Falcón-Antenucci, R.M., 2015. Streptococcus mutans adhesion and releasing of metallic ions in dental alloys. Braz. J. Oral Sci. 14, 36–40. https://doi.org/10.1590/1677-3225v14n1a08

Zerfaß, C., Asally, M., Soyer, O.S., 2019. Interrogating metabolism as an electron flow system. Curr. Opin. Syst. Biol., • Systems biology of model organisms • Systems ecology and evolution 13, 59–67. https://doi.org/10.1016/j.coisb.2018.10.001

Zhang, L.-N., Wang, D.-C., Hu, Q., Dai, X.-Q., Xie, Y.-S., Li, Q., Liu, H.-M., Guo, J.-H., 2019. Consortium of Plant Growth-Promoting Rhizobacteria Strains Suppresses Sweet Pepper Disease by Altering the Rhizosphere Microbiota. Front. Microbiol. 10, 1668. https://doi.org/10.3389/fmicb.2019.01668

Zhang, S., Miran, W., Naradasu, D., Guo, S., Okamoto, A., 2020a. A Human Pathogen Capnocytophaga Ochracea Exhibits Current Producing Capability. Electrochemistry 88, 224–229. https://doi.org/10.5796/electrochemistry.20-00021

Zhang, S., Miran, W., Naradasu, D., Guo, S., Okamoto, A., 2020b. A Human Pathogen Capnocytophaga Ochracea Exhibits Current Producing Capability. Electrochemistry advpub. https://doi.org/10.5796/electrochemistry.20-00021

Zhang, X., Zhao, C., Yu, S., Jiang, Z., Liu, S., Wu, Y., Huang, X., 2020. Rhizosphere Microbial Community Structure Is Selected by Habitat but Not Plant Species in Two Tropical Seagrass Beds. Front. Microbiol. 11, 161. https://doi.org/10.3389/fmicb.2020.00161

Zheng, H., Xu, L., Wang, Z., Li, L., Zhang, J., Zhang, Q., Chen, T., Lin, J., Chen, F., 2015. Subgingival microbiome in patients with healthy and ailing dental implants. Sci. Rep. 5. https://doi.org/10.1038/srep10948

Zheng, J., Wittouck, S., Salvetti, E., Franz, C.M.A.P., Harris, H.M.B., Mattarelli, P., O'Toole, P.W., Pot, B., Vandamme, P., Walter, J., Watanabe, K., Wuyts, S., Felis, G.E., Gänzle, M.G., Lebeer, S., 2020. A taxonomic note on the genus Lactobacillus: Description of 23 novel genera, emended description of the genus Lactobacillus Beijerinck 1901, and union of Lactobacillaceae and Leuconostocaceae. Int. J. Syst. Evol. Microbiol. https://doi.org/10.1099/ijsem.0.004107

Zheng, S., Liu, F., Wang, B., Zhang, Y., Lovley, D.R., 2020. Methanobacterium Capable of Direct Interspecies Electron Transfer. Environ. Sci. Technol. 54, 15347–15354. https://doi.org/10.1021/acs.est.0c05525

Zhou, G.-W., Yang, X.-R., Sun, A.-Q., Li, H., Lassen, S.B., Zheng, B.-X., Zhu, Y.-G., 2019. Mobile Incubator for Iron(III) Reduction in the Gut of the Soil-Feeding Earthworm Pheretima guillelmi and Interaction with Denitrification. Environ. Sci. Technol. 53, 4215–4223. https://doi.org/10.1021/acs.est.8b06187

Zhou, S., Yang, G., Lu, Q., Wu, M. 2014, 2014. Geobacter soli sp. nov., a dissimilatory Fe(III)-reducing bacterium isolated from forest soil. Int. J. Syst. Evol. Microbiol. 64, 3786–3791. https://doi.org/10.1099/ijs.0.066662-0

Tables

Table 1. EET activity from rhizosphere-associated bacteria

Organism	Strain	Environment / Electron acceptors	Experimental outcome	References
Clostridium acetobutylicum	ATCC 824	Clostridium growth medium w/ anode	Electrical potential generated (0.14 V)	(Finch et al., 2011)
Clostridium acetobutylicum	ATCC 824	Clostridium growth medium w/ Fe(III) and AQDS or riboflavin	Reduction of Fe(III); greater iron reduction when exogenous AQDS or riboflavin was supplemented	(List et al., 2019)
Clostridium beijerinckii		Lake sediment w/ Fe(III)	Reduction of Fe(III)	(Dobbin et al., 1999)
Clostridium butyricum	EG3	HEPES buffer w/ Fe(III)	Reduction of Fe(III)	(Park et al., 2001)
Clostridium sp.		Copper-contaminated soil w/ artificial floodwater	Reduction of Cu(II) to Cu(0)	(Hofacker et al., 2015)
Clostridium sp. CN8		Minimal salts medium w/ As(V)	Reduction of As(V) to As(III)	(Langner and Inskeep, 2000)
Clostridium sp. EDB2		M1 medium w/ Fe(III), humic acids, or AQDS	Reduction of Fe(III), humic acids, and AQDS	(Bhushan et al., 2006)
Comamonas koreensis	CY01	LB w/ 2,4-D and AQDS, Mineral salts medium w/ Fe(III)	Reduction of AQDS; reduction of Fe(III)	(Wang et al., 2009)
Comamonas koreensis	CY01	Mineral salts medium w/ Fe(III)	Reduction of Fe(III)	(Wu et al., 2009)
Cable bacteria (*Desulfobulbaceae*)		*Littorella uniflora* rhizosphere	Electrical potential generation (EP_{max}: 5.25 mV); greater electrical potential further from root surface and deeper into sediment column	(Scholz et al., 2019)
Cable bacteria (*Desulfobulbaceae*)		Freshwater mineral medium with ferrihydrite	Concurrent reduction of Fe(III) to Fe(II) with thiosulfate oxidation	(Müller et al., 2020)
Geobacter metallireducens	DSM7210	IEP-T Medium w/ graphene oxides and	Direct electron transfer from *G. metallireducens* to *M. bakeri* with concurrent methane production	(Igarashi et al., 2020)

		Methanosarcina barkeri		
Geobacter metallireducens	GS-15	Mineral medium w/ Fe(III) or Mn(IV)	Reduction of Fe(III) and Mn(IV)	(Lovley et al., 1993)
Geobacter metallireducens	GS-15	DSM 120 Medium w/ *Methanobacterium* strain YSL	Direct electron transfer from *G. metallireducens* to *M. bakeri* with concurrent methane production	(S. Zheng et al., 2020)
Geobacter metallireducens		Simulated wetland rhizosphere	Reduction of Fe(III); greater reduction of Fe(III) from rhizosphere than bulk soil or when AQDS was added	(Weiss et al., 2004)
Geobacter metallireducens		Fresh water medium w/ *Methanosaeta spp.*	Direct electron transfer from *G. metallireducens* to *Methanosaeta harundinacea* with concurrent methane production No methane produced from *M. harundinacea* coculture with *pilA* deficient *G. metallireducens*	(Rotaru et al., 2014)
Geobacter soli	GSS01	Mineral salts medium w/Fe(III), Mn(IV), or AQDS	Reduction of Fe(III), Mn(IV), and AQDS	(Zhou et al., 2014)
Geobacter sulfurreducens		Soil w/ basal medium and AQDS	Reduction of soil Fe(III)	(Komlos and Jaffé, 2004)
Geobacter sulfurreducens	ATCC 51573	MOPS w/ Cu(II)	Biomineralization and reduction of $CuSO_4$ or $CuCl_2$ to Cu_2S	(Kimber et al., 2020)
Geobacter sulfurreducens	ATCC 51573	Freshwater medium w/ Fe(III) and As(V)	Formation of reduced Fe(II) biominerals and reduction of As(V) from aqueous solution	(Islam et al., 2005)
Geobacter sulfurreducens	DL1	Mn(IV) oxide medium w/ Fe(III) or AQDS	Less Fe(III) reduction by *omcE*, *omcS*, and *omcT* deletion mutants; almost equal Fe(III) reduction amongst all strains with AQDS supplementation Less Mn(IV) reduction by *omcE* and *omcS* deletion mutants	(Mehta et al., 2005)
Geobacter sulfurreducens	DL6	Osmotically balanced solution w/ humic acids	Less AQDS or humic acid standard from single or compound deletion mutants of *omcB, omcE, omcS, omcT, or omcZ*	(Voordeckers et al., 2010)
Geobacter sulfurreducens	PCA	NB medium w/ anode or Fe(III)	Less Fe(III) oxide reduction from *pgcA* deletion mutant; same Fe(III) citrate reduction and current generation from *pgcA* and wild-type (I_{max}: 200 $\mu A/cm^2$)	(Zacharoff et al., 2017)
Geobacter sulfurreducens	PCA	DB medium w/ Co(II)	Biomineralization and reduction of Co(II) to Co(0)	(Dulay et al., 2020)

Abbreviations: 2,4-D – (2,4-Dichlorophenoxyacetic acid; AQDS - anthraquinone 2,6-disulfonate; EP_{max} – maximum electrical potential; I_{max} – maximum current; LB – Lauria-bertani medium; omcB/E/S/T/Z – outer membrane cytochrome; pgcA – extracellular multiheme cytochrome; pilA – electrically conductive pili structural protein; "::tn" – transposon insertion mutant strain

Table 2. EET activity from animal host-associated bacteria

Organism	Strain	Environment / Electron acceptors	Experimental outcome	References
Aggregatibacter actinomycetemcomitans	Y4	Minimal defined medium w/ anode	Current generation from lactate (I_{max}: 70 nA/cm^2) and glucose (I_{max}: 25 nA/cm^2) as electron donors; detection of secreted redox mediators and redox-active cell-surface proteins	(Naradasu et al., 2020b)
Bacillus sp.	PeC11	Mineral medium with ferrihydrite and AQDS or fulvic acids	Reduction of (III); increased iron reduction w/ AQDS or fulvic acids	(Hobbie et al., 2012)
Capnocytophaga ochracea	ATCC 27872	DSMZ 340 medium w/ anode	Positive correlation between cell density and current generation (I_{max}: 75 nA/cm^2); >10-fold increase in current w/ riboflavin or menadione	(S. Zhang et al., 2020b)
Clostridium cochlearium	DSM 29358	Firmicutes minimal medium w/ anode	I_{max}: 0.53 $\pm$ 0.02 mA/cm^2; detection of secreted redox mediators	(Schwab et al., 2019)
Clostridium sp.	ZIRB-1	4YACo medium with Fe(III) hydroxide	Reduction of Fe(III)	(Vu et al., 2004)
Corynebacterium matruchotii	TCC 14266	Minimal defined medium w/ anode	Current generation (I_{max}: 50 nA/cm^2); detection of secreted redox mediators	(Naradasu et al., 2020c)
Desulfovibrio sp.		4YACo medium with Fe(III) hydroxide	Reduction of Fe(III)	(Vu et al., 2004)
Enterococcus avium (predicted)	Gut-S1	Minimal defined medium w/ anode	Current generation from acetate (I_{max}: 80 nA/cm^2) and glucose (I_{max}: 120 nA/cm^2) as electron donors	(Naradasu et al., 2019)
Enterococcus faecalis	ATCC 19433	Todd-Hewitt broth w/ anode	P_{max}: 17 μW/cm^2	(Tahernia et al., 2020)
Enterococcus faecalis	ATCC 29219	PBS w/ DHNA and Fe(III)	Reduction of Fe(III)	(Tejedor-Sanz et al., 2021)
Enterococcus faecalis	OG1RF	TSB w/ $FeCl_3$ and anode	Current collected (100 mQ) in the presence of $FeCl_3$; less current collected (40 mQ) from *ldh1*::tn	(Keogh et al., 2018)

Enterococcus faecalis	OG1RF	PBS w/ anode	Current generated w/ OsRP-coated anode (I_{max}: 20 $\mu A/cm^2$); potassium ferricyanide (I_{max}: 28 $\mu A/cm^2$), and menadione sodium bisulfite (I_{max}: 40 $\mu A/cm^2$) No current from (DMK-null mutant) strain WY84 unless w/ menadione sodium bisulfite (I_{max}: 31 $\mu A/cm^2$)	(Pankratova et al., 2018)
Enterococcus faecalis	OG1RF	TSB w/ ferric ammonium sulfate, potassium ferricyanide, or anode	Less ferric ammonium sulfate reduction from strain WY84 (DMK-null mutant), or *ndh3*::tn, *eetA*::tn, and *pplA*::tn Less ferricyanide reduction from WY84, *ndh3*::tn and *eetA*::tn; greater ferricyanide reduction from *pplA*::tn With OsRP-coated anode; I_{max}: 38 $\mu A/cm^2$ from OG1RF; less current from *pplA*::tn (I_{max}: 35 $\mu A/cm^2$), *ndh3*::tn (I_{max}: 24 $\mu A/cm^2$); no current from WY84 With graphite electrode and ferricyanide; I_{max}: 42 $\mu A/cm^2$ from OG1RF; more current from *pplA*::tn (I_{max}: 63 $\mu A/cm^2$); no current from *ndh3*::tn or WY84	(Hederstedt et al., 2020)
Enterococcus faecium	ATCC 8459	PBS w/ DHNA and Fe(III)	Reduction of Fe(III)	(Tejedor-Sanz et al., 2021)
Faecalibacterium prausnitzii	DSM 17677	PBS w/ DTNB	Greater reduction of DTNB or current generation (I_{max}: 6 mA) with riboflavin	(Khan et al., 2012b)
Faecalibacterium prausnitzii	DSM 17677	PBS w/ anode	Positive correlation between current generation and riboflavin concentration (I_{max}: 650 µA with 300 µM riboflavin)	(Khan et al., 2012a)
Faecalibacterium prausnitzii	DSM 17677	Salt solution w/ riboflavin and anode	Positive correlation between current generation and riboflavin concentration (I_{max}: 145 µA with 13.8 µM riboflavin)	(Prévoteau et al., 2015)

Klebsiella pneumoniae (predicted)	Gut-S2	Minimal defined medium w/ anode	Current generation from lactate (I_{max}: 30 nA/cm^2) and glucose (I_{max}: 125 nA/cm^2) as electron donors; detection of secreted redox mediator	(Naradasu et al., 2019)
Lacticaseibacillus rhamnosus	GG	PBS w/ DHNA and Fe(III)	Reduction of Fe(III)	(Tejedor-Sanz et al., 2021)
Limosilactobacillus reuteri	DSM 28673	Firmicutes minimal medium w/ anode	I_{max}: 0.05 $\pm$ 0.02 mA/cm^2	(Schwab et al., 2019)
Listeria monocytogenes	10403S	Chemically defined medium w/ fumarate	Fumarate to succinate; no reduction of fumarate from *frdA* deletion mutant	(Light et al., 2019)
Listeria monocytogenes	10403S	Listeria synthetic medium w/ ferric ammonium citrate or anode	Fe(III) reduction (30 μM/min) and current generation (I_{max}: 22 μA/cm^2); significantly less Fe(III) reduction or current from transposon insertions of FLEET locus genes	(Light et al., 2018)
Porphyromonas gingivalis	W83	Minimal defined medium w/ anode	Current generation from glucose (I_{max}: 20 nA/cm^2) as electron donor; detection of redox-active cell-surface proteins	(Naradasu et al., 2020b)
Pseudomonas aeruginosa	CGMCC 1.860	LB w/ anode	Wild-type; I_{max}: 2 μA/cm^2 *rhlI* and *rhlR* overexpression; I_{max}: 6 μA/cm^2	(Yong et al., 2011)
Pseudomonas aeruginosa	PA14	AB medium w/ anode	Greater phenazine-1-carboxylic acid production at higher applied voltages; I_{max}: 24 μA/cm^2 at 0.2 V	(Bosire and Rosenbaum, 2017)
Pseudomonas aeruginosa	PA14 Δ*phz*	MOPS culture medium w/ anode	No current generated in absence of PYO; with PYO: 0.8 μA	(Wang et al., 2010)
Pseudomonas aeruginosa	PA14, KRP1, PAO1	AB medium w/ anode	Current production: KRP1 (I_{max}: 19 μA/cm^2) > PA14 (I_{max}: 17 μA/cm^2) > PAO1 (I_{max}: 4 μA/cm^2)	(Bosire et al., 2016)
Pseudomonas aeruginosa	PAO1	LB w/ anode	Wild-type; I_{max}: 500 μA/cm^2 *phzM* deletion mutant; I_{max}: 200 μA/cm^2	(Yong et al., 2014)
Staphylococcus auerus	ATCC 6538	Todd-Hewitt broth w/ anode	Wild-type; P_{max}: 25 μW/cm^2 *sirABC*::tn; P_{max}: 10 μW/cm^2 *sstBCDA*::tn; P_{max}: 40 10 μW/cm^2	(Tahernia et al., 2020)
Staphylococcus xylosus	DSM 28566	Firmicutes minimal medium w/ anode	I_{max}: 0.04 $\pm$ 0.01 mA/cm^2	(Schwab et al., 2019)
Streptococcus agalactiae	A909	Todd-Hewitt broth w/ anode	P_{max}: 14 μW/cm^2	(Tahernia et al., 2020)

Streptococcus mutans	UA159	Minimal defined medium w/ anode	Greater current generation from cells pre-grown in low pH (I_{max}: 50 nA/cm^2) versus neutral pH (I_{max}: 20 nA/cm^2); detection of redox-active cell-surface proteins	(Naradasu et al., 2020a)

Abbreviations: AQDS - anthraquinone 2,6-disulfonate; DHNA – 1,4 dihydroxy-2-napthoic acid; DMK – demethylmenaquinone; DTNB; 5,5'-dithiobis-(2-nitrobenzoate); eetA – electron carrying protein; I_{max} – maximum current; LB – Luria-Bertani broth; ldh1 – lactate dehydrogenase; MOPS – morpholinepropanesulfonic acid; ndh2/3 – NADH dehydrogenase; OsRP – [Os(2,2′-bipyridine)2-poly(N-vinylimidazole)10Cl]$2^{+/+}$; PBS – phosphate-buffered saline; phz – phenazine biosynthesis operon; P_{max} – maximum power output; pplA – flavin-binding ferric reductase; PYO – pyocyanin; rhlR/rhlI – quorum-sensing genes; sirABC – iron ABC transporter system; sstBCDA – iron ABC transporter system; TSB – tryptone soy broth; "::tn" – transposon insertion mutant strain

Table 3. EET-related activity from lactic acid bacteria used in food fermentations

Organism	Strain	Environment / Electron acceptors	Experimental outcome	References
Enterococcus durans	156, 175, 219, 222, M4A, VS258, VS263, VS266, VS268, VS269	Skim milk	Negative Eh_{min} for all strains; Avg. -120.5 $\pm$ 29.0 mV	(Brasca et al., 2007)
Enterococcus durans	Unspecified (66 strains)	1% fat milk	Negative Eh_{min} for all strains; Avg. -152.32 $\pm$ 56.15	(Morandi et al., 2016)
Enterococcus faecalis	195, 238, BK2, QK, AA4, Mora13, FK2, TO1, S13, VS368	Skim milk	Negative Eh_{min} for all strains; Avg. -221.1 $\pm$ 13.4 mV	(Brasca et al., 2007)
Enterococcus faecalis	Unspecified (193 strains)	1% fat milk	Negative Eh_{min} for all strains; Avg. -237.31 $\pm$ 30.22	(Morandi et al., 2016)
Enterococcus faecalis	TMW 2.630	Sourdough	Eh_{min}: -50 mV	(Capuani et al., 2013)
Enterococcus faecium	62, 132, 67, 184, 180, FK5, FK6, FK7, 131, 174	Skim milk	Negative Eh_{min} for all strains; Avg. -137.7 $\pm$ 31.3 mV	(Brasca et al., 2007)
Enterococcus faecium	Unspecified (193 strains)	1% fat milk	Negative Eh_{min} for almost all strains; Avg. -123.73 $\pm$ 51.06	(Morandi et al., 2016)
Lacticaseibacillus casei	BL23	PBS w/ DHNA and Fe(III)	Reduction of Fe(III)	(Tejedor-Sanz et al., 2021)

Lacticaseibacillus paracasei subsp. paracasei	VS377, B10B, B1B, B2B, B3B, BB3, M5, JR1, JR2, JR3	Skim milk	Negative Eh_{min} for all strains; Avg. -169.1 $\pm$ 13.8 mV	(Brasca et al., 2007)
Lactiplantibacillus pentosus	BGM48	PBS w/ DHNA and Fe(III)	Reduction of Fe(III)	(Tejedor-Sanz et al., 2021)
Lactiplantibacillus plantarum	VS370, VSD1, BB2, H7, M38	Skim milk	Negative Eh_{min} for all strains; Avg. -153.8 $\pm$ 18.2 mV	(Brasca et al., 2007)
Lactiplantibacillus plantarum	WCFS1	Whole milk agar w/ tetrazolium salts	Reduction of TTC, TV, and BT under N_2 only	(Michelon et al., 2013)
Lactiplantibacillus plantarum	NCIMB8826, ATCC 202195, AJ11, 8.1, NCIMB700965, B1.3	PBS w/ DHNA and Fe(III)	Reduction of Fe(III) from all strains (NCIMB8826 > ATCC 202195 = AJ11 = B1.3) except 8.1 and NCIMB700965	(Tejedor-Sanz et al., 2021)
Lactiplantibacillus plantarum	NCIMB8826	Mannitol-MRS or kale juice medium w/ DHNA and anode	Current generation in mannitol-MRS (I_{max}: 120 $\mu A/cm^2$) and kale juice medium (38 $\mu A/cm^2$)	(Tejedor-Sanz et al., 2021)
Lactiplantibacillus plantarum	TMW 1.460	Sourdough	$Eh7_{start}$: 344.5 $\pm$ 6.4 mV $Eh7_{min}$: 30.9 $\pm$ 13.1 mV $Eh7_{end}$: 89.2 $\pm$ 4.0 mV	(Capuani et al., 2012)
Lactobacillus delbrueckii subsp. bulgaricus	C, F, CM 43	Skim milk	Negative Eh_{min} for all strains; C < CM 43 < F	(Carrasco et al., 2005)
Lactobacillus delbrueckii subsp. bulgaricus	Unspecified	Skim milk w/ plant extracts	Negative $Eh_{coagulation}$ with all plant extracts tested	(Alwazeer et al., 2020)
Lactococcus lactis	Unspecified (133 strains)	1% fat milk	Negative Eh_{min} for all strains; Avg. −219.05 $\pm$ 22.44 mV	(Morandi et al., 2016)
Lactococcus lactis	KF147, IL1403	Minimal medium w/ anode	Current generation by KF147 and IL1403; I_{max}: 500 $\mu A/cm^2$	(Tejedor-Sanz et al., 2021)
Lactococcus lactis subsp. lactis	SRTA2001, SRTA2004, SRTA2056, SL01, SL03, SL04	Skim milk	Negative Eh^a_{min}	(Cachon et al., 2002)
Lactococcus lactis subsp. lactis	LOD4, LOD6, VS179, VS180, A24, AA1, L2, L6, ST84A, ST85	Skim milk	Negative Eh_{min} for all strains; Avg. -162.3 $\pm$ 32.9 mV	(Brasca et al., 2007)

Lactococcus lactis subsp. lactis	SRTA2004, SRTA2001, SRTA2056, DGCC7290	Skim milk (sparged w/ different gases)	Negative Eh_{final} (-100 to -200 mV) for all strains in all conditions	(Jeanson et al., 2009)
Lactococcus lactis subsp. lactis	SL03	Skim milk	Negative Eh_{final}; 114 $\pm$ 6 mV	(Abraham et al., 2013)
Lactococcus lactis subsp. lactis	CM41	Ultrafiltered white cheese	Negative Eh (approx. -290 mV) throughout cheese ripening	(Bulat and Topcu, 2019)
Lactococcus lactis subsp. lactis bv. diacetylactis	SD17, SD18	Skim milk	Negative Eh^{a}_{min}	(Cachon et al., 2002)
Lactococcus lactis subsp. lactis bv. diacetylactis	SRTA2116	Skim milk (sparged w/ different gases)	Negative Eh_{final} (-100 to -200 mV)	(Jeanson et al., 2009)
Lactococcus lactis subsp. lactis bv. diacetylactis	DSM 4366, CHCC D1, CHCC D2, CHCC D3	Full fat milk (sparged w/ different gases)	Normal $O_2^{initial}$; negative Eh_{final} for DSM 4366 < CHCC D2; positive Eh_{final} for CHCC D1 = CHCC D3 Low $O_2^{initial}$; negative Eh_{final} for DSM 4366 = CHCC D2; positive Eh_{final} for CHCC D1 = CHCC D3	(Larsen et al., 2015)
Leuconostoc mesenteroides subsp. cremoris	DSM 20346, CHCC M1	Full fat milk (sparged w/ different gases)	Normal $O_2^{initial}$; negative Eh_{final} for both strains; CHCC M1 < DSM 20346 Low $O_2^{initial}$; negative Eh_{final} for both strains; DSM 20346 = CHCC M1	(Larsen et al., 2015)
Levilactobacillus brevis	BCRC 12945	Skim milk	Negative Eh_{final}; -84 $\pm$ 4 mV	(Abraham et al., 2013)
Levilactobacillus spicheri	TIL46	Whole milk agar w/ tetrazolium salts	WT strain; reduction of TTC and TV (under air/N_2); reduction of BT (under N_2 only) Δ*menC*; reduction of BT, TTC, and TV under N_2 only	(Michelon et al., 2013)
Levilactobacillus spicheri	DSM 20069, CHCC 01, CHCC 02	Full fat milk (sparged w/ different gases)	Normal $O_2^{initial}$; negative Eh_{final} for all strains; DSM 20069 = CHCC 01 = CHCC 02 Low $O_2^{initial}$; negative Eh_{final} for all strains; DSM 20069 = CHCC 01 = CHCC 02	(Larsen et al., 2015)

Levilactobacillus spicheri	UD459	Ultrafiltered white cheese	Negative Eh (-300 mV) throughout cheese ripening	(Bulat and Topcu, 2019)
Streptococcus thermophilus	CH3-3, CH3-4, CL5	Skim milk	Negative Eh_{min} for all strains; CL5 < CH3-4 < CH3-3	(Carrasco et al., 2005)
Streptococcus thermophilus	VS365A, VS373, VS375, LOD8, LOD10, LOD11, LOD12, O2A, O5A, ST78B	Skim milk	Positive Eh_{min} for all strains except O2A and O5A; Avg. 7.9 $\pm$ 12.3 mV	(Brasca et al., 2007)
Streptococcus thermophilus	Unspecified (124 strains)	1% fat milk	Negative Eh_{min} for almost strains; Avg. -81.12 $\pm$ 32.67	(Morandi et al., 2016)
Streptococcus thermophilus	Unspecified	Skim milk w/ plant extracts	Negative $Eh_{coagulation}$ with all plant extracts tested	(Alwazeer et al., 2020)

Abbreviations: ahpF – NADH oxidase; BT – tetrazolium blue chloride; DHNA – 1,4 dihydroxy-2-napthoic acid; Eh7 – redox potential adjusted to pH 7; $Eh_{coagulation}$ – redox potential at pH 4.6; Eh_{final} – final redox potential, Eh_{min} – minimum redox potential; Eh^{a}_{min} – minimum redox potential at maximum acidification rate; ldh – lactate dehydrogenase; MRS – de Mann, Rogosa and Sharpe medium; noxAB – NADH dehydrogenase; noxE – NADH oxidase; menC – menaquinone biosynthase; PBS – phosphate-buffered saline; TTC – 2,3,5-triphenytetrazolium chloride; TV – tetrazolium violet; WT – wild-type

Figures

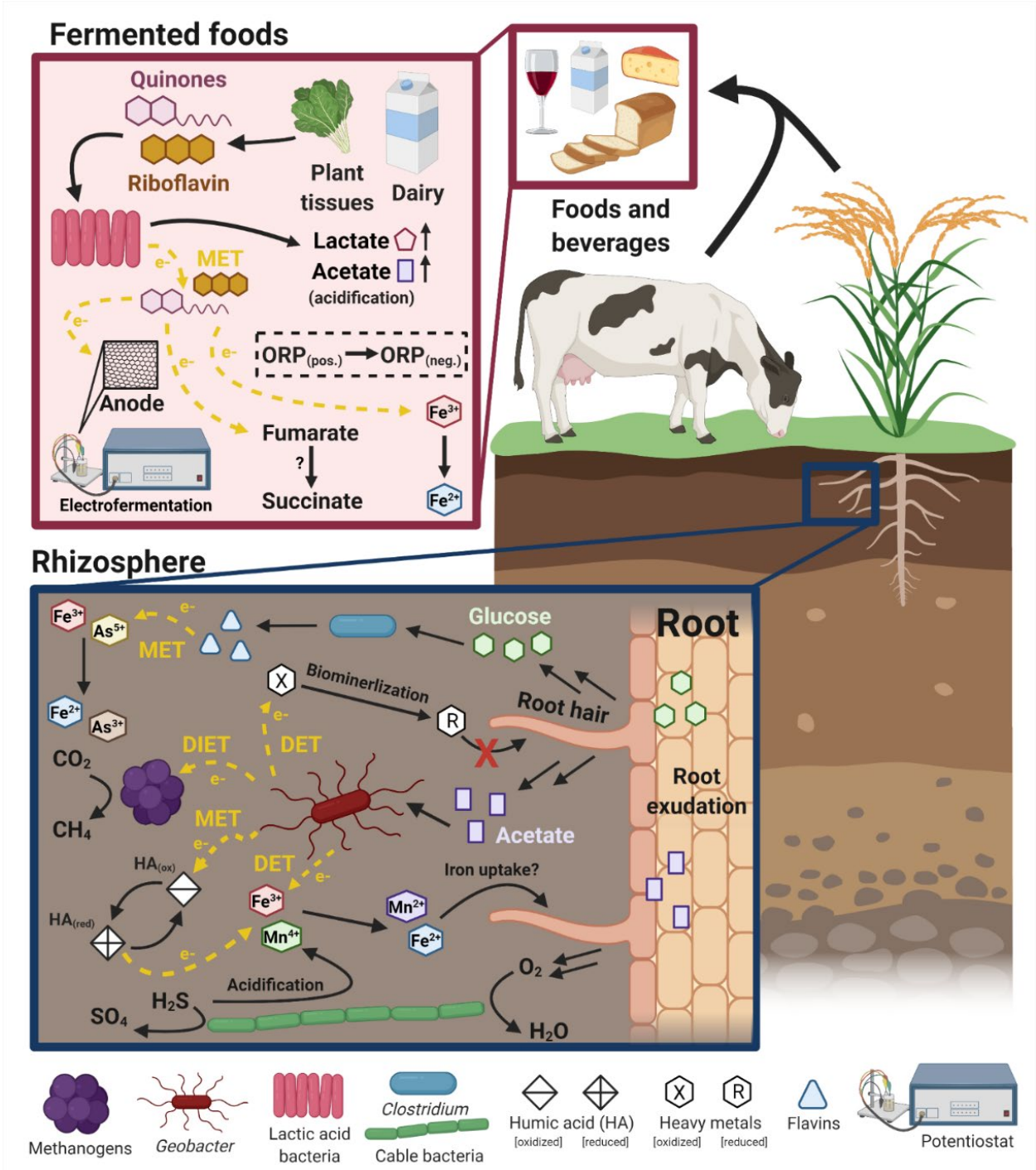

Figure 1. Summary of EET activity present in the plant rhizosphere and fermented foods. (Top) Foods such as cruciferous vegetables and dairy products are sources of flavins and quinones which LAB can utilize as electron acceptors for MET. These electron acceptors include iron, fumarate (putatively), or an anode during electrofermentation. This metabolism is believed to increase LAB production of organic acids like lactate and acetate, as well as decrease

environmental oxidation-reduction potential (ORP). (Bottom) Exudation of carbon compounds from roots provides electron sources for metal-reducing bacteria such as *Geobacter* spp. and Clostridia. These bacteria can use DET or MET to reduce electron acceptors such as humic acids, iron, or manganese. The biomineralization of heavy metals through EET reduces their uptake by plants and prevents oxidative stress. In addition, *Geobacter* can give and/or receive electrons from other rhizosphere microoganisms like methanogenic archaea.

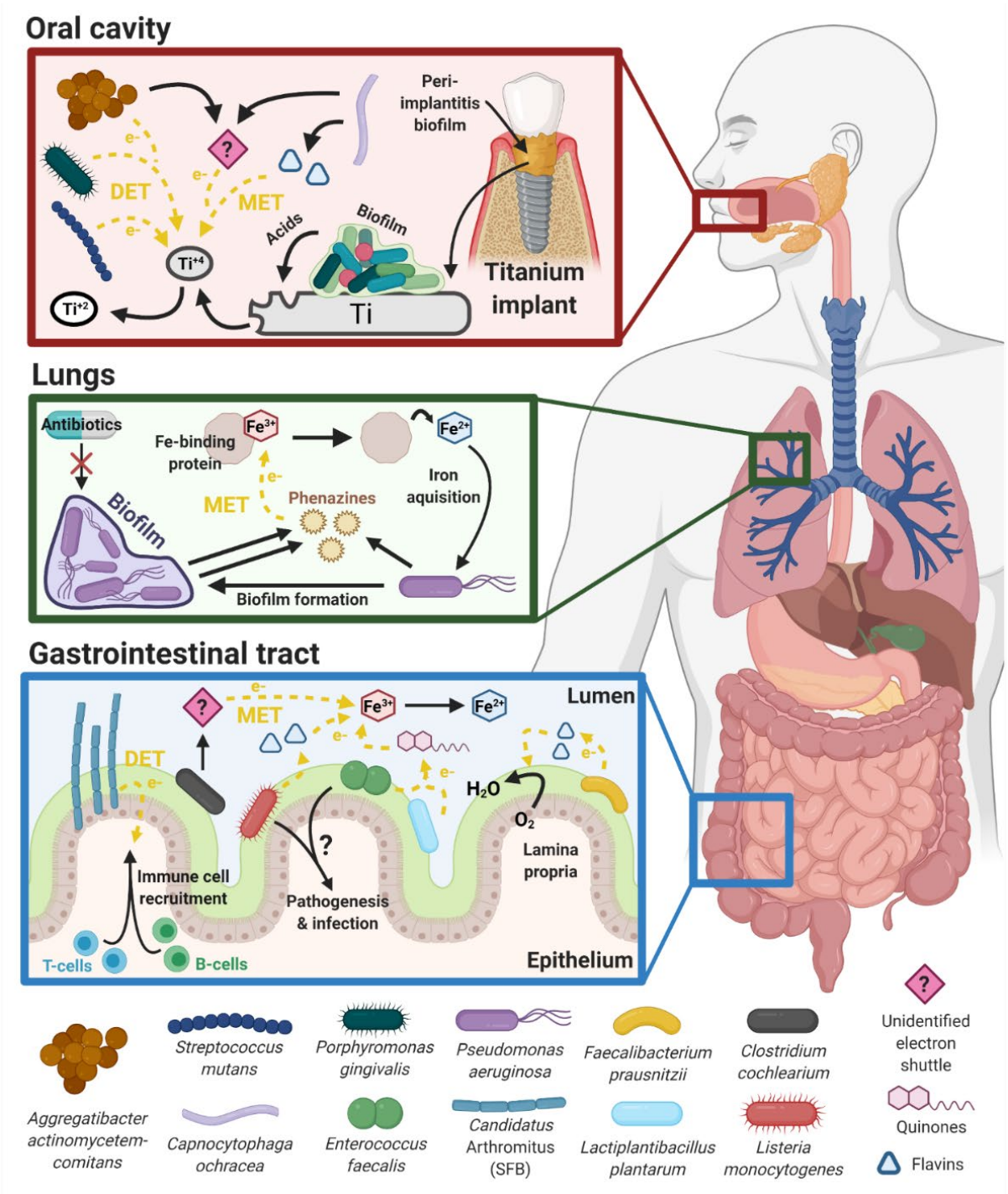

Figure 2. Summary of EET activity within several animal host mucosal sites.
(Top) Titanium dental implants develop biofilms which release titanium ions through acid corrosion. Electroactive bacteria can subsequently reduce titanium ions through DET or MET with flavins or yet-identified electron shuttles. The proliferation of electroactive bacteria is believed to further accelerate implant corrosion. (Middle) *Pseudomonas aeruginosa* performs phenazine-MET in the lungs to sequester host protein-bound iron and form biofilms. Biofilms also rely on phenazine-MET for redox balancing and to promote resistance against antibiotics. (Bottom) Putative DET by Segmented Filamentous Bacteria (SFB) in the intestine stimulates host immune cell recruitment while probiotic bacterial species such as *Lactiplantibacillus plantarum* and *Faecalibacterium prausnitzii* use flavins and/or quinones in MET. Conversely, intestinal pathogens can use these same electron shuttles for MET which promotes infection.

Chapter 2. Extracellular electron transfer increases fermentation in lactic acid bacteria via a hybrid metabolism

Sara Tejedor-Sanz[1,2,*], Eric T. Stevens[3,*], Siliang Li[1] , Peter Finnegan[3], James Nelson[4], Andre Knoessen[4], Samuel H. Light[5], Caroline M. Ajo-Franklin[1,2,†], and Maria L. Marco[3,†]

[1]Department of Biosciences, Rice University, Houston, United States;

[2]Biological Nanostructures Facility, The Molecular Foundry, Lawrence Berkeley National Laboratory, Berkeley, United States;

[3]Department of Food Science & Technology, University of California-Davis, Davis, United States

[4]Department of Electrical and Computer Engineering, University of California-Davis, Davis, United States

[5]Department of Microbiology, University of Chicago, Chicago, United States

*These authors contributed equally.

[†]For correspondence: cajo-franklin@rice.edu, mmarco@ucdavis.edu

This manuscript is published in eLife.

https://doi.org/10.7554/eLife.70684

Abstract

Energy conservation in microorganisms is classically categorized into respiration and fermentation, however recent work shows some species can use mixed or alternative bioenergetic strategies. We explored the use of extracellular electron transfer for energy conservation in diverse lactic acid bacteria (LAB), microorganisms that mainly rely on fermentative metabolism and are important in food fermentations. The LAB *Lactiplantibacillus plantarum* uses extracellular electron transfer to increase its NAD^+/NADH ratio, generate more ATP through substrate-level phosphorylation, and accumulate biomass more rapidly. This novel, hybrid metabolism is dependent on a type-II NADH dehydrogenase (Ndh2) and conditionally requires a flavin-binding extracellular lipoprotein (PplA) under laboratory conditions. It confers increased fermentation product yield, metabolic flux, and environmental acidification in laboratory media and during kale juice fermentation. The discovery of a single pathway that simultaneously blends features of fermentation and respiration in a primarily fermentative microorganism expands our knowledge of energy conservation and provides immediate biotechnology applications.

introduction

The ways in which microorganisms extract energy to maintain cellular functions are directly linked to their environment, including the availability of nutrients and cooperative or antagonistic interactions with other organisms (Haruta and Kanno, 2015). Microorganisms must also maintain redox homeostasis by responding to oxidative and reductive changes inside and outside the cell (Sporer *et al.*, 2017). Ultimately, microorganisms that can effectively generate cellular energy while also managing redox requirements will maintain higher growth and survival rates, and therefore exhibit greater ecological fitness.

All organisms possess mechanisms to conserve energy, that is, to convert light or chemical energy into cellular energy in the form of ATP (Russell and Cook, 1995). During respiration, microorganisms rely on either oxygen (aerobic respiration) or other exogenous substrates (anaerobic respiration) as terminal electron acceptors. Some microorganisms, most notably *Geobacter* spp., can anaerobically respire using electron acceptors outside the cell, such as iron (III) oxides or an electrode (Renslow *et al*., 2013; Richter *et al*., 2012). This process is called extracellular electron transfer (EET). Regardless of the identity of the electron acceptor, ATP synthesis during respiration occurs via oxidative phosphorylation (Kim and Gadd, 2019). In oxidative phosphorylation, electrons from electron carriers are transported by an electron transport chain, which creates a proton motive force (PMF) for ATP generation. Under anaerobic conditions, some cells can also conserve energy using fermentation. In fermentation, microorganisms use internally supplied electron acceptors, and ATP is generated mainly through substrate-level phosphorylation (Kim and Gadd, 2019). In substrate level phosphorylation, ATP is generated in the cytoplasm by transfer of phosphate from metabolic intermediates to ADP (Kim and Gadd, 2019).

Lactic acid bacteria (LAB) are a diverse group of aerotolerant, saccharolytic microorganisms in the Firmicutes phylum which use mainly use fermentation for energy conservation. LAB are essential for many food fermentations, including fermented milk and meats, fruits and vegetables, and grains (Tamang *et al.,* 2020). Strains of LAB are also used for industrial chemical production (Sauer *et al*., 2017) and as probiotics to benefit human and animal health (Vinderola *et al*., 2019). LAB are generally grouped by their differences in hexose metabolism (Salvetti *et al*., 2013). Some species perform homofermentation, reducing pyruvate to lactate as the sole metabolic end-product from glycolysis. Other LAB perform heterofermentation, producing lactate along with ethanol, acetate, and CO_2 by the phosphoketolase pathway. However, for redox balancing, homofermentative LAB can also shift to a mixed acid fermentation and heterofermentative LAB use alternative electron acceptors, like fructose or citrate (Hansen, 2018). Although some LAB can respire in the presence of heme and menaquinone, those bacteria are unable to synthesize heme and many are also auxotrophic for menaquinone (Pedersen *et al*., 2012). Even those species capable of respiration still use fermentation metabolism as the primary mechanism to conserve energy (Pedersen *et al*., 2012). Therefore, LAB growth rates and cell yields are constrained by access to electron acceptors used to maintain intracellular redox balance during substrate-level phosphorylation.

The bioenergetics of anaerobic bacteria have been tightly linked to oxidative phosphorylation for anaerobic respiration and substrate-level phosphorylation for fermentation. However, experimental evidence shows a concurrent use of oxidative phosphorylation and substrate-level phosphorylation. For instance, some yeasts perform respiro-fermentation to enhance ATP production (Pfeiffer and Morley, 2014). Another example is the electron bifurcating mechanism used by some fermentative microorganisms such as *Clostridium* spp.

(Herrmann *et al*., 2008; Li *et al*., 2008). Through that energy conservation strategy, cells can generate extra ATP through oxidative phosphorylation (Buckel and Thauer, 2013; Müller *et al*., 2018). Along with other examples that are not fully understood (Hunt *et al*, 2010; Kracke *et al*., 2018), these observations suggest metabolisms that combine aspects of fermentation and respiration may exist.

We recently discovered that *Listeria monocytogenes,* a facultative anaerobic pathogen known to rely on respiratory metabolism, uses EET to reduce Fe^{3+} or an anode through a flavin-based extracellular electron transfer pathway (Light *et al*., 2018). Use of this pathway allowed *L. monocytogenes* to maintain intracellular redox balance via NADH oxidation. This capacity was associated with the presence of a gene locus, called a flavin-based EET (FLEET) locus, that was identified in many Gram-positive species in the Firmicutes phylum, including LAB. Studies in individual species of LAB such as *Lactococcus lactis* (Freguia *et al*., 2009; Masuda *et al*., 2010), *Enterococcus faecalis* (Hederstedt *et al*., 2020; Keogh *et al*., 2018), and *Lactiplantibacillus pentosus* (Vilas Boas *et al*., 2015) show that they can perform EET with an anode endogenously, that is without addition of molecules foreign to their native niches. These observations are quite surprising because endogenous EET has been mainly associated with respiratory organisms, even though some of these organisms also possess fermentative-type metabolism (Glassier *et al*, 2014). Those observations also raise the question of whether the FLEET locus is functional in LAB and what, if any, role it plays in energy conservation and metabolism.

Here, we explored EET across LAB and studied the implications of this trait at a metabolic and energetic level in *Lactiplantibacillus plantarum*, a homofermentative LAB capable of mixed acid fermentation and which can respire in the presence of exogenous heme and menaquinone. *L. plantarum* is of particular interest as it is a generalist LAB species found in

insect, animal, and human digestive tracts and is essential for the production of many fermented foods (Behera *et al*., 2018; Duar *et al*., 2017). These findings have significance for the understanding of energy conservation strategies in primarily fermentative microorganisms and on lactic acid fermentations in food biotechnology.

Results

L. plantarum reduces extracellular electron acceptors

To determine whether *L. plantarum* can reduce extracellular electron acceptors, we first measured its ability to reduce insoluble ferrihydrite (iron (III) oxyhydroxide). Incubation of the model strain *L. plantarum* NCIMB8826 in the presence of ferrihydrite showed that this strain reduces Fe^{3+} to Fe^{2+} (**Figure 1A and Figure 1-figure supplement 1A).** Viable cells are required for iron reduction and this activity is dependent on the presence of exogenous quinone (DHNA, 1,4-dihydroxy-2-naphthoic acid) (**Figure 1A and Figure 1-figure supplement 1A-B**). The requirement for DHNA was hypothesized because DHNA is a precursor of demethylmenaquinone (DMK), a membrane electron shuttle utilized by *L. monocytogenes* for EET (Light *et al*., 2018), and *L. plantarum* lacks a complete DHNA biosynthetic pathway (Brooijmans *et al*., 2009). For full activity, an electron donor (such as mannitol or glucose) was required to be present (**Figure 1A and Figure 1-figure supplement 1A**). Like *L. monocytogenes* (Light *et al*., 2018), the addition of riboflavin during the iron reduction assay also increased Fe^{3+} reduction in a dose-dependent manner (**Figure 1-figure supplement 1C**). Thus, *L. plantarum* reduces insoluble iron in a manner similar to *L. monocytogenes*.

Next, we investigated whether the ability of *L. plantarum* to reduce insoluble iron was altered by growth media. *L. plantarum* was able to reduce iron after growth in either complete

(MRS) medium or chemically defined medium (CDM) (**Figure 1-figure supplement 1B**). Iron reduction was greater when mannitol, a sugar alcohol, rather than glucose, was provided as the sole carbon source in MRS (**Figure 1-figure supplement 1B**). However, reduction was highest when *L. plantarum* was incubated in mannitol-containing MRS (mMRS) with both DHNA and ferric ammonium citrate present (**Figure 1-figure supplement 1D**). The addition of riboflavin to the growth medium did not further increase iron reduction by *L. plantarum* (**Figure 1-figure supplement 1E**), potentially because riboflavin is already present in high quantities in MRS, a medium containing yeast extract (Tomé, 2021). Thus, *L. plantarum* was grown in mMRS supplemented with DHNA and iron before ferrihydrite reduction assays in all subsequent experiments.

L. plantarum EET activity was confirmed in a bioelectrochemical reactor by quantifying electron output as current (**Figure 1B**). *L. plantarum* reduced a carbon electrode (anode) polarized to +200 $mV_{Ag/AgCl}$ in the presence of both DHNA and an electron donor (mannitol) (**Figure 1C**). No current was observed in the absence of *L. plantarum* (**Figure 1- figure supplement 2A**), indicating that current production stems from a biological process. *L. plantarum* produced a maximum current of 129 ± 19 $\mu A/cm^2$ in mCDM (**Figure 1C**) and 225 ± 9 $\mu A/cm^2$ in mMRS (**Figure 1-figure supplement 2B**). Under EET conditions in mCDM, the *L. plantarum* biomass was 2.7 mg (dry cell mass). Assuming 50% of the dry cell mass was protein, the specific electron transfer rate was 57 µmol electrons/mg- protein/h and the current production was 1.5 mA/mg-protein. This value is lower than that reported for *Geobacter sulfurrenducens* (4-8 mA/mg-protein) (Marsili *et al*., 2010; Rose and Regan, 2015), the model species for direct EET, and higher than that of *Shewanella oneidensis* (0.67 mA/mg-protein) (Marsili *et al*., 2008), the model species for mediated EET. It should be noted that these species, unlike *L. plantarum*,

can synthesize riboflavin and quinones and do not require the addition of either for EET activity. Similar to our iron reduction experiments, EET to an anode occurred with different electron donors and growth media (**Figure 1-figure supplement 2B-C**), and current increased after supplementation of riboflavin when it was omitted from the growth medium (**Figure 1-figure supplement 2D**). Because of these differences, CDM was amended with mannitol and riboflavin in subsequent experiments.

DHNA is found in concentrations of 0.089 to 0.44 μg/mL in commercial fermented beverages (Eom *et al*., 2011), and under laboratory conditions, microbes can synthesize and secrete DHNA leading to concentrations of 0.37 to 48 μg/mL (Isawa *et al*., 2002; Furuichi *et al*., 2012; Kang *et al* 2015). To test whether EET in *L. plantarum* is relevant under these physiological concentrations, we probed whether *L. plantarum* can perform EET with a sub-physiological DHNA concentration of 0.01 μg/mL. Indeed, *L. plantarum* can reduce iron and produce significant current density (**Figure 1-figure supplement 3A-B**), although the magnitude of iron reduction and current was smaller than what was observed with 20 μg/mL. These results show that the concentrations of DHNA found in niches of *L. plantarum* can support EET and suggest the magnitude of EET will depend on the DHNA concentration.

Iron reduction in LAB is associated with the presence of *ndh2* and *pplA*

Because iron reduction by *L. monocytogenes* requires the genes in a 8.5 kb gene locus encoding a flavin-based EET (FLEET) pathway (Light *et al*., 2018), we looked for the presence of these genes in 1,788 complete LAB genomes deposited in NCBI. Homology searches identified the complete FLEET locus in 11 out of 38 genera including diverse LAB such as *Enterococcus* and *Lacticaseibacillus* (**Figure 2A**). The other LAB genera either lack multiple

FLEET pathway genes or, as was observed for all 68 strains of *Lactococcus*, contain all genes except for *pplA*, which is predicted to encode an extracellular flavin-binding reductase. Among the lactobacilli, genomes of 19 out of 94 species contain the entire FLEET system (**Figure 2-figure supplement 1**). The lactobacilli species with the entire FLEET system are homofermentative and are distributed between different phylogenetic groups (Zheng *et al*., 2020). These data show that the FLEET locus is conserved across LAB genera besides *L. plantarum*, including other homofermentative LAB species known to colonize host and food environments.

To determine whether LAB FLEET gene presence was associated with EET activity, a diverse collection of LAB strains were examined for their capacity to reduce ferrihydrite. The assay showed that isolates of *L. plantarum*, *Lactiplantibacillus pentosus, Lacticaseibacillus rhamnosus, Lacticaseibacillus casei, Enterococcus faecium*, and *Enterococcus faecalis* are capable of Fe^{3+} reduction (**Figure 2B**). The genomes of those species also contain a complete FLEET locus (**Figure 2A and Figure 2-figure supplement 1**). Conversely, strains of *Lactococcus lactis*, *Ligilactobacillus murinus*, *Levilactobacillus brevis*, *Pediococcus pentosaceus*, and *Streptococcus agalactiae* showed little to no iron reduction activity (**Figure 2B**). The presence of FLEET-associated genes varied between those species, but only strains of species found to contain both *ndh2,* a predicted membrane-bound, type-II NADH dehydrogenase, and *pplA* were able to reduce iron under the conditions tested.

L. plantarum NCIMB8826 exhibited the highest EET activity resulting in at least 2.5-fold greater Fe^{3+} reduction than the other *L. plantarum* strains (**Figure 2B**). Remarkably, however, the *L. plantarum* NCIMB8826 genome and the genomes of 138 other *L. plantarum* strains queried all harbored a complete FLEET locus including *ndh2* and *pplA* (**Figure 2-figure supplement 1**

and Figure 2-figure supplement 2A). Among those strains tested for the capacity to reduce Fe^{3+}, *L. plantarum* NCIMB700965 and 8.1 could not reduce Fe^{3+} but possessed all genes in the FLEET system. Closer examination of both strains by aligning their FLEET loci with NCIMB8826 revealed unique IS30-family transposons in the intergenic promoter regions spanning *ndh2* and *pplA* (**Figure 2-figure supplement 2A**). These genes were minimally expressed in *L. plantarum* NCIMB700965 and 8.1 in comparison to NCIMB8826 (**Figure 2-figure supplement 2B**). *ndh2* and *pplA* were also the only two genes in the FLEET pathway that were induced when *L. plantarum* NCIMB8826 was incubated in mMRS supplemented with DHNA and iron (**Figure 2C and Figure 1-figure supplement 1D**). Both *ndh2* and *pplA* were induced (~1.6-fold, $p \leq 0.05$) in MRS containing mannitol, DHNA, and ferric ammonium citrate (**Figure 2C**), but were not up-regulated when either DHNA or ferric ammonium citrate were omitted from the culture medium (**Figure 2-figure supplement 2C**). Taken together, these data show that widespread iron reduction in LAB is tightly associated with the presence and upregulation of *ndh2* and *pplA*, suggesting they are required for EET.

ndh2 is required and *pplA* is conditionally required for *L. plantarum* EET

In order to confirm the necessity of *ndh2* and *pplA* for EET in *L. plantarum*, we constructed *ndh2* and *ppA* deletion mutants of *L. plantarum* NCIMB8826. Both mutants were significantly impaired in their capacities to reduce ferrihydrite compared with the wild-type strain (**Figure 3A**). The *ndh2* and *pplA* deletion mutants also had different effects on the oxidation-reduction potential (ORP) of mMRS. ORP is defined as the ratio of all oxidative to reductive components in an environment (Killeen *et al*., 2018) and is an important environmental condition which influences the outcome of LAB fermentations such as flavor development in

cheese (Morandi *et al*., 2016) and the growth of spoilage microorganisms (Olsen and Pérez-Díaz, 2009). Expectedly for the *L. plantarum* EET phenotype, significant reductions in mMRS ORP only occurred during *L. plantarum* growth when DHNA was included in the culture medium (**Figure 3-figure supplement 1A**). Although ORP declined for all three strains in a manner consistent with other ORP-reducing enzymatic activities (for example the reduction of oxygen by NADH oxidase) (Tachon *et al*., 2010), wild-type *L. plantarum* resulted in greater reductions in ORP compared to either mutant in mMRS, and these differences were significant at most time points measured over a 12 h period (**Figure 3B**). The effects on ORP occurred in the absence of changes in growth rates, cell yields, and medium pH (**Figure 3-figure supplement 1A-D**). The ΔmV_{max} was reached during mid-exponential phase growth (approx. 5 h) (**Figure 3-figure supplement 1B**), and at that time, wild-type *L. plantarum* cells but not the Δ*ndh2* or Δ*pplA* strains were active in the ferrihydrite reduction assay (**Figure 3-figure supplement 1E**). This difference in ferrihydrite reduction activity similarly persisted in stationary phase cells (12 h) (**Figure 3-figure supplement 1F**). These observations show that *ndh2* and *pplA* contribute to the capacity of *L. plantarum* to reduce iron and have relevance to the ORP-dependent activities occurring during food fermentations (van Dijk *et al*., 2000).

Use of an anode as an external electron acceptor instead of ferrihydrite showed a similar, but not identical genetic dependency. *L. plantarum* Δ*ndh2* produced a significantly lower current density (**Figure 3C**) and a lower peak current (**Figure 3-figure supplement 2A**). Surprisingly, *L. plantarum* Δ*pplA* was able to produce the same amount of current as the wild-type strain, suggesting that the lipoprotein PplA is not essential and might not be involved in anode reduction through EET. This observation led us to investigate the anodic-EET ability of other LAB species lacking *pplA* like *Lactococcus lactis* (**Figure 3D**). DHNA was not provided to these

strains because they can synthesize demethylmenaquinone and other quinones (Rezaïki *et al*., 2008). Both *L. lactis* strain IL1403 and strain KF147 were capable of current generation, confirming that PplA is not essential for LAB to produce current. This is consistent with the finding that other extracellular reductases besides PplA are responsible for EET activity in Gram-positive bacteria (Light *et al*., 2019). Taken together these results show that EET activity is dependent upon the presence of the putative FLEET locus, and specifically *ndh2* and conditionally *pplA*.

L. plantarum increases energy conservation and balances intracellular redox state when performing EET

Building from studies in *E. faecalis* (Keogh *et al*., 2018), it has been suggested that EET improves growth by either enabling iron to be acquired as a macronutrient or by enhancing respiration (Jeuken *et al*., 2020). It is worth noting that several studies have shown that *L. plantarum* does not require iron to grow (Elli *et al*., 2000; Weinberg, 1997). To test whether EET allowed increased iron acquisition by *L. plantarum*, we measured intracellular iron by Inductively Coupled Plasma-Mass Spectrometry (ICP-MS). There was no significant difference in the amount of intracellular iron between *L. plantarum* growth in mMRS supplemented with DHNA and iron compared to growth in mMRS alone (**Figure 4-figure supplement 1A**). Moreover, deletion of *ndh2* did not significantly change the amount of intracellular iron (**Figure 4-figure supplement 1B**). ICP-MS showed that other redox-active metals used for EET, such as manganese and copper (Kouzuma *et al*., 2012; Fan *et al*., 2018) were also not affected (**Figure 4-figure supplement 1 and 2**). In contrast to studies in *E. faecalis* in which iron supplementation leads to intracellular accumulation of this metal (Keogh *et al*., 2018), these data show that *L.*

plantarum does not use EET to increase its acquisition of iron or other redox-active metals, suggesting EET may instead play a role in energy conservation.

We next sought to understand if EET impacts energy conservation in *L. plantarum* by comparing its growth and ATP levels in the presence of a polarized anode. The highest current density (i.e., greatest EET activity) produced by *L. plantarum* in mannitol CDM typically occurred within 24 h after inoculation into the bioreactor (**Figure 1C**). At this point, there was an approximately 4-fold higher dry cell weight and 2-fold higher numbers of viable cells compared to *L. plantarum* incubated in open circuit (OC) conditions (**Figure 4A-B**) Current density declined from its maximum value when *L. plantarum* cells performing EET were in exponential growth (**Figure 1C** and **Figure 4C**). By comparison, growth was not observed until two days later under OC conditions (**Figure 4C**). During peak current production, intracellular ATP levels were significantly higher (4.5-fold) under EET compared to OC conditions (**Figure 4D** and **Table 1**). These results strongly suggest faster ATP accumulation under EET conditions allowed *L. plantarum* to exit lag phase more rapidly. ATP levels were also greater in *L. plantarum* when in the presence of both mannitol and DHNA, compared to either mannitol or DHNA separately (**Figure 4D**). Thus, EET allows *L. plantarum* to initiate growth and accumulate ATP more rapidly, indicating that EET significantly increases energy conservation in *L. plantarum*.

Because fermentation, anaerobic respiration, and aerobic respiration are each associated with a different NAD^+/NADH ratio, energy conservation is linked to intracellular redox homeostasis (Holm *et al*., 2010). Therefore, we probed redox homeostasis in *L. plantarum* under EET conditions by measuring intracellular NAD^+/NADH at the point of maximum current density (**Figure 4E**). *L. plantarum* showed an 8-fold higher NAD^+/NADH ratio under EET conditions compared to OC (**Figure 4E**). This result was not limited to the presence of a

polarized anode as *L. plantarum* also contained a significantly higher NAD^+/NADH ratio when Fe^{3+} was available as a terminal electron acceptor (**Figure 4-figure supplement 3**). These NAD^+/NADH ratios are more similar to those found for in *E. coli* performing aerobic respiration (de Graef *et al*., 1999) or *G. sulfurreducens* performing anaerobic respiration than in LAB performing fermentation (Guo *et al*. 2017). Taken together, our data indicate that EET is involved in energy conservation, and the intracellular redox balance during EET mimics a respiratory rather than a fermentative process.

EET increases fermentative metabolism through substrate-level phosphorylation and reduction in extracellular pH

Metal-reducing bacteria use EET in anaerobic respiration (Richter *et al*., 2012; Shi *et al*., 2007). Ndh2 is considered an anaerobic respiratory protein, and *L. plantarum* can perform anaerobic respiration with exogenous menaquinone and heme using an electron transport chain (Brooijmans *et al*., 2009). This led us to hypothesize that those electron transport proteins could also be involved for EET to conserve energy as part of anaerobic respiration. To test this hypothesis, we examined whether any of the known electron transfer proteins needed for PMF generation in aerobic and anaerobic respiration are required for *L. plantarum* EET. Neither the addition of heme to restore bd-type cytochrome (*cydABCD*) used in aerobic respiration, nor deletion of the respiratory nitrate reductase (Δ*narGHJI*) significantly altered current production (**Figure 5-figure supplement 1A-B**). Because Ndh2 is a type-II NADH dehydrogenase which does not contribute to a proton gradient (Lin *et al*., 2008; Nakatani *et al*., 2020), these observations show that while EET does involve a respiratory protein, it does not involve any of the known PMF-generating electron transfer proteins in *L. plantarum*.

Respiration is also associated with the tricarboxylic acid (TCA) cycle. *L. plantarum*, like other LAB, does not possess an oxidative branch of the TCA cycle and only contains a reductive branch (Tsuji *et al*, 2013). To probe whether the reductive branch was active during EET, we also examined production of succinate, the terminal end-product of the reductive branch. EET did not increase the succinate concentration (**Figure 5-figure supplement 2**). Moreover, we did not detect any intermediates of the reductive branch of the TCA cycle, i.e. oxalacetate, malate, or fumarate. This indicates that EET did not cause additional metabolic flux through its TCA cycle. Thus, none of the known metabolic pathways or electron transport proteins associated with anaerobic respiration, besides Ndh2, are required for EET. These results suggest increased energy conservation during EET in *L. plantarum* is not through canonical anaerobic respiration.

An alternative hypothesis is that increased energy conservation under EET conditions is driven by changes in fermentation. *L. plantarum* uses glycolysis to convert mannitol to two molecules of pyruvate which is then converted mainly to lactate or ethanol via NADH-consuming steps, or acetate via an ATP-generating reaction using substrate-level phosphorylation (Dirar and Collins, 1972). Thus, shifting towards production of acetate from to lactate or ethanol production can increase ATP yield during fermentation. Additionally, NADH can be re-generated by oxidizing pyruvate to yield 2,3-butanediol, using acetoin as an intermediate. Fermentation in *L. plantarum* also decreases the pH of the surrounding media.

To probe changes in fermentation, we measured the concentrations of mannitol, acetate, lactate, ethanol, acetoin, 2,3-butanediol, formate, and pyruvate and the pH in *L. plantarum* cultures during OC and EET conditions. After four days, we accounted for ~80% and ~55% of the total carbon under EET and OC conditions (for all metabolite concentrations see **Supplement File 1**), giving us a quantitative view of metabolism under EET conditions.

Surprisingly, under EET conditions, the distribution of major end-fermentation products (acetate, lactate, and ethanol) did not change, but their yield per cell was 2.6-fold higher compared to OC conditions (**Figure 5A**). While we did not detect acetoin or 2,3-butanediol, formate was found at trace levels, and pyruvate was found at similar, low levels under EET and OC conditions (**Figure 5-figure supplement 2**). After accounting for mannitol consumption, we observed that EET allowed cells to produce ~1.75x more fermentation products per each mol of mannitol utilized ($Y_{fermentation}$, **Table 1**). The culture medium pH was also significantly lower than under OC (**Figure 5B**), a result which may indicate that EET conferred higher levels of acid stress on *L. plantarum*, and therefore, reductions in cell viability, despite EET leading to higher cell numbers overall (as measured by dry cell weight) (**Figure 4A-B**). A similar acidification of the medium was observed for Δ*pplA*, but not for Δ*ndh2*, when an anode was present as electron acceptor, indicating that *ndh2*-dependent EET is needed to decrease the pH (**Figure 3-figure supplement 2B**). When much lower, sub-physiological levels of DHNA were supplied (0.01 μg/mL), a smaller but significant decrease in the pH of the medium was also observed (**Figure 1-figure supplement 3C**). Overall, these results show that EET allows *L. plantarum* to ferment to ~1.75x greater extent and to acidify the medium to a greater extent as well.

We also observed that EET led to higher cellular metabolic fluxes, that is, higher changes in metabolites per cell per unit time. Although the final OD_{600nm} and dry cell weight were not significantly different (**Supplement file 1**), *L. plantarum* utilized mannitol and produced acetate and lactate more rapidly under EET conditions than OC conditions (**Figure 5C-F**). Cells performing EET were ~2-fold faster at consuming mannitol (**Figure 5C**) between days one and three. Mannitol consumption increased between day one and day two, approximately when the cells transitioned to higher current density (**Figure 3C**), suggesting that increased EET drove that

increased consumption. The overall rates of acetate and lactate production also increased 3.4 and 3.6 times (**Figure 5D-E**), respectively. Measurements of metabolites produced by Δ*pplA* and Δ*ndh2* strains confirmed that, like for current production to an anode, the EET-associated increased metabolic flux in *L. plantarum* requires the presence of Ndh2, but not PplA (**Figure 3-figure supplement 2C**). Overall, these data indicate that *ndh2*-dependent EET increases both the flux and final yield of fermentation in *L. plantarum.*

Because the production of acetate yields ATP, these results also suggested that the increase in ATP generation under EET conditions may be due to substrate-level phosphorylation. To probe whether EET-associated increase in fermentative flux could account for the changes in ATP generation, we calculated fermentation balances (**Table 1**). Our measurements account for 80% of the carbon under EET conditions (see **Supplement file 1**), leaving a maximum of ~20% systematic uncertainty in these calculations. The concentrations of fermentation products detected (**Supplement file 1**) were used to estimate the total ATP in the presence and absence of EET. The estimated ATP was 3-fold higher under EET conditions than OC conditions (**Table 1**), a result that is consistent with the ~2.5-fold higher accumulation of ATP measured at maximum current density (**Figure 4D**). Overall, this quantitative analysis shows that the vast majority of the increased energy conservation under EET conditions can be accounted for by an increase in fermentation yield and substrate-level phosphorylation.

EET shifts how *L. plantarum* uses electron acceptors and converts ATP into biomass

Thus far, our results provided an unusual picture of the energy metabolism of *L. plantarum* under EET conditions; while EET significantly shifted the intracellular redox state to a more respiratory-like balance, its increased ATP yield was mainly accounted for by an

increased fermentative yield. Another major difference in fermentation and anaerobic respiration is the use of the endogenous versus exogenous electron acceptors. To more deeply understand how *L. plantarum* uses organic molecules and the anode as electron acceptors when performing EET, the electron balances under EET and OC conditions were calculated (**Table 1 and Supplement file 1**). We estimated the NADH produced using two different methods (see **Supplement file 1** for methodology) and the NADH re-oxidized through the reduction of the anode (measured as current) and via substrate-level phosphorylation. This allowed us to obtain a global balance of the NAD^+/NADH ratio. Under OC conditions between 35-66% of the NADH produced from the oxidation of mannitol to pyruvate (a range is given using the two methods used) was re-oxidized to NAD^+ (5.5 mM NADH consumed, **Table 1**), qualitatively agreeing with the low NAD^+/NADH ratios measured (**Figure 4E**). In contrast, electron balance calculations showed that between 77-96% of the NADH produced under EET conditions was re-oxidized (17 mM NADH consumed, **Table 1**), a result that is consistent with the significantly higher NAD^+/NADH ratios measured (**Figure 4E**). Interestingly, these calculations estimate that 55-69% of the total NADH generated was oxidized through fermentation, while 21-28% of the NADH was oxidized using the electrode as a terminal electron acceptor (**Table 1**). Thus, *L. plantarum* growing under EET conditions achieves a more oxidized intracellular redox balance by more completely fermenting mannitol to lactate and ethanol and by using the electrode as a terminal electron acceptor (**Figure 5G**). These observations reinforce that the energy metabolism of *L. plantarum* under EET conditions utilizes elements of both fermentation and anaerobic respiration.

In rapidly dividing cells, energy conservation, a catabolic process, is associated with growth, an anabolic process. However, catabolism need not be coupled with anabolism (Russell

& Cook,1995). To determine how catabolic and anabolism are connected under EET conditions, the ATP requirements to grow biomass (Y_{ATP}) were estimated using the calculated ATP and the measured dry weight. Under OC conditions, the Y_{ATP} obtained (8.06 ± 0.8 g dw/mol ATP) for *L. plantarum* was similar to that observed previously (10.9 g-dw/mol ATP) (Dirar and Collins, 1972). Hence, without EET, the ATP generated from fermentation was converted into biomass nearly at the expected efficiency. In contrast, a significantly lower Y_{ATP} was reached for *L. plantarum* performing EET (3.07 ± 0.35 g dw/mol ATP) (**Table 1**). This observation indicates that under EET conditions, either more ATP is required to produce biomass or more ATP is utilized by other functions such as for PMF-generation and intracellular pH regulation (Russell and Cook, 1995). EET conditions also resulted in 79% more ATP per mol of fermented mannitol ($Y_{mannitol}$). Consequently, molar biomass yields (g-dw/mol-mannitol) under EET conditions were significantly lower (**Table 1**), in agreement with previous observations in respiratory electroactive species (Esteve-Núñez *et al*., 2005). These calculations show that when *L. plantarum* performs EET, anabolism and catabolism processes are differently coupled than under OC conditions. ATP is produced more efficiently, but this it is less efficiently utilized to make biomass. Overall, these results show an intriguing pattern of coupling between anabolism and catabolism, indicative of a novel energy metabolism in *L. plantarum* during EET.

EET is active in vegetable fermentations

Our results inspired us to explore whether EET could occur in a physiological niche of LAB such as fermented foods. LAB are necessary for the making of many fermented fruit and vegetable foods and the properties of those foods depend on the metabolic diversity of the LAB strains present (Gänzle, 2015). Plant tissues also contain a much wider variety of carbon

substrates and potential electron acceptors than the CDM used in our prior experiments. To study the physiological and biotechnological relevance of EET in food fermentations, kale juice was fermented using *L. plantarum* as a starter culture (**Figure 6A**). The fermentation of kale juice was measured under EET conditions (a polarized anode with or without DHNA), and an OC control (a nonpolarized anode with DHNA) was used to separate the role of DHNA and electron flow to the anode on the fermentation process. An additional bioreactor without cells, but with DHNA, was operated to identify any possible electrochemical-driven conversion of substrates. When *L. plantarum* was added to the prepared kale juice, approximately 10-fold more current was generated during EET conditions with DHNA (EET+DHNA) as compared to abiotic and biological non-EET promoting conditions (no DHNA) (**Figure 6B**). This current was comparable to the current generated in laboratory medium (**Figure 3C**), indicating that robust EET by LAB is possible in the complex physiological conditions of a food fermentation.

We next investigated the impact of EET on *L. plantarum* growth and metabolism in the kale juice fermentation. Significant changes in the pH and fermentation products were detected under EET conditions (**Figure 6C-D**). These differences occurred in the absence of significant changes in viable cell numbers (**Figure 6-figure supplement 1A**) at the time points measured. As previously observed using laboratory culture media, an approximately two-fold greater accumulation of total end-fermentation products per cell was obtained when cells interacted with an anode in the presence of DHNA (**Figure 6C**). In the kale juice fermentation, EET+DHNA conditions enhanced both lactate and acetate production per cell (**Figure 6E** and **Figure 6-figure supplement 1B**). Thus, when DHNA was provided, EET enhanced the overall yield of fermentation end-products and their production rates per cell, mimicking our observations in laboratory medium (**Figure 5C-D**). EET also led to a significantly higher acidification of the

kale juice compared to OC conditions, and the presence of DHNA dramatically enhanced this pH drop (**Figure 6D**). In general, when no DHNA was supplied but an anode was present as an electron acceptor, the fermentation process was very similar to OC conditions. This means in kale juice, a source of quinones is essential to support *L. plantarum* EET activity. Overall, these results show that EET under physiological conditions impacts cellular metabolism in *L. plantarum* by increasing metabolic flux which ultimately can affect the flavor profile of fermented foods (Chen *et al*., 2017).

Discussion

Increases in fermentation and energy conservation from EET have important bioenergetic implications for the mainly fermentative LAB. We showed that *L. plantarum* and other diverse LAB species perform EET if riboflavin and quinones are present. *L. plantarum* EET activity requires an NADH dehydrogenase (Ndh2) and conditionally requires an extracellular, flavin-binding reductase (PplA). EET in *L. plantarum* generates a high NAD^+/NADH ratio, increases fermentation yield and flux, shortens lag phase, and increases ATP production. Thus, EET in *L. plantarum* is a hybrid energy metabolism that contains metabolic features of fermentation, redox features of anaerobic respiration, and predominately uses substrate-level phosphorylation to conserve energy. This pathway is active in *L. plantarum* with physiologically relevant DHNA concentrations and in a food fermentation and results in an increased metabolic flux and acidification rate.

The combined EET fermentation hybrid metabolism is distinct from anaerobic respiration, fermentation, and other energy conservation strategies

When performing EET, the metabolism of *L. plantarum,* a primarily fermentative bacterial species, is fundamentally different from EET-driven, anaerobic respiration of metal-reducing bacteria. Although aspects of EET in *L. plantarum* and metal-reducing *Geobacter* spp. are similar, such as the upregulation of NADH dehydrogenase, the reduction rate of extracellular electron acceptors, and the high NAD^+/NADH ratio, other aspects of energy metabolism during EET in these two organisms are starkly different (see comparison in **Supplement file 2**). *Geobacter* spp. direct their metabolic flux through the TCA cycle, rely almost exclusively on extracellular electron acceptors to regenerate NADH, and produce ATP exclusively through oxidative phosphorylation. In contrast, *L. plantarum* regenerates a substantial fraction of its NADH by directing metabolic flux through fermentative pathways. Additionally, oxidative phosphorylation is not a major mechanism of energy conservation in *L. plantarum* during EET, as supported by three lines of evidence: the marginal metabolic flux through the reduced branch of TCA cycle, no involvement of known PMF-generating proteins, and that increased ATP levels can be accounted for by increased substrate-level phosphorylation. While additional data are required to eliminate the possibility that oxidative phosphorylation is occurring in *L. plantarum* during EET, we can qualitatively state that substrate-level phosphorylation is the major mechanism for ATP generation.

Comparing EET and respiratory metabolism in LAB also reveals substantial differences in these metabolisms (**Supplement file 2**). While both metabolisms require quinones, respiration also requires exogenous heme. Our findings and similar findings in *E. faecalis* (Pankratova *et al*., 2018) confirm that heme is not required for EET. Moreover, EET also differs from respiration in LAB because it occurs at the start of or prior to exponential phase growth, does not change the final cell density, and increases fermentation with no effect on the resultant proportions of

lactate, acetate, and ethanol (Duwat *et al*., 2001). Thus, EET in LAB diverges from respiration in metal-reducing bacteria or LAB in its metabolic pattern and energetic consequences. In addition, compared to other studies with different bacteria in which anodic-EET provokes a shift in fermentative metabolism upon the addition of artificial mediators (Vassilev *et al*, 2021; Emde and Schink, 1990), *L. plantarum* EET is active upon the presence of a mediator present in a complex food system.

This EET mechanism is also a novel energy conservation strategy compared to known fermentative metabolisms in LAB (comparison in **Supplement file 2**). *L. plantarum* and other LAB, reduce alternative intracellular electron acceptors like citrate, fructose, and phenolic acids, resulting in increased intracellular NAD^+/NADH ratios (Hansen, 2018). This metabolic activity is especially important for heterofermentative LAB in order to synthesize additional ATP through acetate kinase (Gänzle, 2015). Unlike these examples, however, the reduction of extracellular Fe^{3+} or an anode by EET requires a respiratory protein (Ndh2) and the shuttling of electrons outside of the cell. In addition, the reduction of the oxygen and organic compounds for cofactor regeneration by LAB leads to a metabolic shift towards acetate production and altered metabolic end-product ratios (Gänzle, 2015), which does not occur during EET. These differences show how the hybrid metabolism under EET conditions is distinct from other pathways that alleviate reduced intracellular conditions in LAB.

Previous studies have reported a simultaneous use of fermentation and electron transport elements, such as in the so-called respiro-fermentation in *Saccharomyces cerevisiae* (Blom *et al*., 2000). However, respiro-fermentation produces ATP and maintains intracellular redox balance through substrate-level phosphorylation and/or oxidative phosphorylation using separate pathways. Our data strongly suggests a single pathway is responsible for both ATP generation

and intracellular redox balance. This hybrid fermentation mode is also different from the electron bifurcating mechanism, in which the extra ATP generation is driven by the creation of a H^+ or Na^+ potential from the oxidation of a ferredoxin (Buckel and Thauer, 2013). Unlike in this example, EET in LAB does not involve PMF creating elements and EET drives ATP generation through substrate-level phosphorylation. Another poorly understood example of the use of substrate-level phosphorylation and electron transport chains to balance intracellular redox state is found in the non-fermentative bacterium *S. oneidensis*. Although this species is a respiratory bacterium, it relies predominately on substrate-level phosphorylation to grow anaerobically with the exogenous electron acceptor fumarate (Hunt *et al*., 2010). In this scenario, it is unclear if there are changes in intracellular redox state or metabolism in this species.

In contrast to and expanding upon these studies, our work elucidates a qualitatively and quantitatively different blending of fermentation and respiration in a primarily fermentative organism. *L. plantarum* EET-associated metabolism contains features of both fermentation (e.g., substrate-level phosphorylation, high fermentation product yields) and respiratory metabolisms (e.g., NAD^+/NADH ratios, NADH dehydrogenase required) (**Supplement file 2**). Quantitatively, this hybrid metabolism leads to an overall ~1.75x-more efficient and ~1.75x-faster energy conservation (increased $Y_{mannitol}$, mannitol flux), but an overall ~1.5-fold weaker coupling between anabolism and catabolism (lower Y_{ATP}). Additionally, the increased NAD^+/NADH ratio arises from using an ~2:1 ratio of endogenous to extracellular electron acceptors. Thus, to our knowledge, the hybrid strategy that *L. plantarum* uses to generate ATP performing EET constitutes a novel mode of energy conservation in a primarily fermentative microorganism.

Different mechanisms of EET appear to be widespread in LAB

Based on our observations and others, we propose that EET is widespread in LAB and occurs by different mechanisms. Besides *L. plantarum*, we showed that *L. lactis* is able to generate current despite lacking *pplA*. Current generation by *L. lactis* was observed previously, found to be riboflavin dependent, and resulted in a small metabolic shift (yet to be defined) in which the flux through NADH-oxidizing pathways was reduced and ATP generating pathways were increased (Freguia *et al*., 2009; Masuda *et al*., 2010). *L. lactis* can also perform EET by reduction of tetrazolium violet and this activity depends on the presence of both quinones and an NADH dehydrogenase (NoxAB) (Tachon *et al*., 2009). *E. faecalis* is another LAB that performs EET, and similar to *L. plantarum,* it requires quinones (Pankratova *et al*., 2018) and a type-II NADH dehydrogenase (Ndh3) (Hederstedt *et al*., 2020) for Fe^{3+} reduction. In contrast to this mechanistic similarity, *E. faecalis* performs EET using matrix-associated iron resulting in both increased final cell biomass and intracellular iron (Keogh *et al*. 2018). Moreover, unlike *L. plantarum* and *L. lactis*, the presence of PplA is not necessary for anode reduction or Fe^{3+} reduction (Hederstedt *et al*., 2020). The conditional need for PplA in EET may be explained by the different prior growth conditions used and/or related to the existence of different mechanisms and proteins depending on the redox potential of the extracellular electron acceptor. Other flavin-binding, extracellular reductases amongst Gram-positive organisms, such as FrdA (acting on fumarate) have been identified in *L. monocytogenes* and UrdA (acting on urocanate) in *Enterococcus rivorum* (Light *et al*., 2019). Thus, there may exist a yet unidentified extracellular reductase in *L. plantarum* and *L. lactis* required for anode reduction. Thus, our findings substantially expand the understanding of this capacity by elucidating a new pattern of metabolic changes associated with EET. It seems likely that these many mechanisms reflect the ability of

EET to alleviate constraints of intracellular redox balance in fermentative metabolism across LAB.

EET has important implications for ecology and biotechnology of LAB

Conservation of the FLEET locus among different LAB species supports the premise that this hybrid fermentation with EET provides an important metabolic strategy for these bacteria in their natural habitats. LAB with a complete FLEET locus are homofermentative, thus underscoring the distinct ways homofermentative and heterofermentative LAB have evolved for energy conservation (Salvetti *et al*., 2013). *L. plantarum* and other LAB with FLEET systems such as *L. casei* are genetically and metabolically diverse and grow in a variety of nutrient rich environments including dairy and plant foods and the digestive tract (Cai *et al*., 2009; Martino *et al*., 2016; Siezen *et al*., 2010). Those environments also are rich sources of sources of quinones, flavins, and extracellular electron acceptors such as iron (Cataldi *et al*., 2003; Fenn *et al*., 2017; Kim, 2017-9; Roughead and McCormick, 1990; Walther *et al*., 2013). Increased organic acid production and environmental acidification by LAB with this hybrid metabolism would provide an effective mechanism to inhibit competing microorganisms and confer a competitive advantage for growth. The increased ATP relative to biomass generation observed during growth on mannitol might also give sufficient readiness for using this energy later on to outcompete neighboring organisms (Russell and Cook, 1995). These effects of EET may be particularly important on plant tissues and intestinal environments, wherein LAB tend to be present in low numbers. Besides our observation that *L. plantarum* performs EET in kale juice, the FLEET pathway is important for intestinal colonization by both *L. monocytogenes* (Light *et al*., 2018)

and *E. faecalis* (Lam *et al*., 2019), and *L. plantarum* FLEET genes including *ndh2* and *pplA* were highly induced in the small intestine of rhesus macaques (Golomb *et al*., 2016).

The hybrid fermentation metabolism of LAB also has technological relevance. For many LAB food fermentations, acidification of the food matrix is required to prevent the growth of undesired microorganisms and result in a more consistent and reproducible product (Marco *et al.,* 2021). Starter cultures are frequently selected based on their capacity for rapid growth and acid production (Bintsis, 2018). In the presence of the anode, exposure of *L. plantarum* to EET conditions during kale juice fermentation increased the acidification rate. Thus, this shows that EET metabolism is active in complex nutritive environments such as kale leaf tissues that contain other potential electron acceptors besides the anode and diverse electron donors (glucose, fructose, sucrose) (Thavarajah *et al*., 2016). This example also shows how electro-fermentation, the technological process by which fermentation is modulated using electrodes, can be used to control food fermentations (Moscoviz *et al*., 2016; Schievano *et al*., 2016; Vassilev *et al*, 2021). Because *L. plantarum* also increased fermentation flux when the electrode was available as an electron sink, higher quantities of organic acid flavor compounds were formed. Therefore, by the manipulation of extracellular redox potential, electro-food fermentations may be used to control microbial growth. This would allow the creation of new or altered sensory profiles in fermented foods, such as through altered organic acid production and metabolism or synthesis of other compounds that alter food flavors, aromas, and textures.

Final Perspective

We expect that our study will improve the current understanding of energy conservation in primarily fermentative microorganisms and contribute to establishing the ecological relevance

of EET in lactic acid bacteria. This work will ultimately allow the use of EET to electronically modulate the flavor and textural profiles of fermented foods and expand the use of lactic acid bacteria in bioelectronics, biomedicine, and bioenergy (Moscoviz *et al*., 2016). The identification of the precise components and full bioenergetics involved in *L. plantarum* EET will be key to unravel physiological and ecological questions and to develop other biotechnological applications.

Materials and Methods

Strains and culture conditions

All strains and plasmids used in this study are listed in **Supplement file 3.** Standard laboratory culture medium was used for routine growth of bacteria as follows: *Lactiplantibacillus* spp., *Lacticaseibacillus* spp., *Levilactobacillus brevis*, *Ligilactobacillus murinus*, and *Pediococcus pentosaceus*, MRS (BD, Franklin Lakes, NJ, USA); *Lactococcus lactis* and *Streptococcus agalactiae*, M17 (BD) with 2% w/v glucose; *Enterococcus faecalis*, and *Enterococcus faecium*, BHI (BD); and *Escherichia coli*, LB (Teknova, Hollister, CA, USA). Bacterial strains were incubated without shaking except for *E. coli* (250 RPM) and at either 30 or 37 °C. Where indicated, strains were grown in filter-sterilized MRS (De MAN *et al*., 1960) lacking beef extract with either 110 mM glucose [gMRS] or 110 mM mannitol [mMRS], or a chemically defined minimal medium (**Supplement file 4**) with 125 mM glucose [gCDM] or 125 mM mannitol [mCDM] for 18 h (Aumiller *et al*., 2021). Riboflavin (1 mg/L) was routinely added to the CDM. When indicated, culture medium was supplemented with 20 μg/mL of the quinone 1,4-dihydroxy-2-naphthoic acid (DHNA) (Alfa Aesar, Haverhill, MA, USA), 1.25 mM ferric

ammonium citrate ($C_6H_8FeNO_7$) (1.25 mM) (VWR, Radnor, PA, USA), riboflavin (Sigma-Aldrich, St. Louis, MO, USA), or 5 µg/mL erythromycin (VWR).

DNA sequence analysis

The FLEET gene locus of *L. plantarum* NCIMB8826 was identified using NCBI basic local alignment search tool (BLAST) (McGinnis and Madden, 2004) using the *L. monocytogenes* 10403S FLEET genes (lmo2634 to lmo2641) as a reference. *L. plantarum* genes were annotated based on predicted functions within the FLEET system (Light *et al*., 2018). FLEET locus genes were identified in other LAB by examining 1,788 complete Lactobacillales genomes available at NCBI (downloaded 02/25/2021). A local BLAST (ver 2.10.1) database containing these genomes was queried using tBLASTx with NCIMB8826 FLEET genes a reference. A gene was considered to be present in the Lactobacillales strain genome if the Bit-score was $\geq$ 50 and the E-value was $\leq 10^{-3}$ (Pearson, 2013). Heatmaps showing the percentage of strains in Lactobacillales genera and the *Lactobacillus*-genus complex (Zheng *et al*., 2020) identified to contain individual FLEET genes were visualized using the R-studio package ggplot2 (Wickham, 2011) with clustering done through UPGMA. The FLEET loci of *L. plantarum* strain 8.1 and NCIMB700965 were aligned to the NCIMB8826 genome in MegAlign Pro (DNAstar Inc., Madison, WI, USA).

Insoluble iron reduction assays

Cells were collected by centrifugation at 10,000 g for 3 min, washed twice in phosphate-buffered saline (PBS), pH 7.2 (http://cshprotocols.cshlp.org), and adjusted to an optical density (OD) at 600 nm (OD_{600nm}) of 2 in the presence of 2.2 mM ferrihydrite (Schwertmann and Fischer, 1973;

Stookey, 1970) and 2 mM ferrozine (Sigma-Aldrich). Where indicated, 55 mM glucose or mannitol, 20 μg/mL DHNA, and riboflavin were added. After 3 h incubation at 30 °C, the cells were collected by centrifugation at 10,000 g for 5 min and the absorbance of the supernatant was measured at 562 nm with a Synergy 2 spectrophotometer (BioTek, Winooski, VT, USA). Quantities of ferrihydrite reduced were determined using a standard curve containing a 2-fold range of $FeSO_4$ (Sigma-Aldrich) (0.25 mM to 0.016 mM) and 2 mM ferrozine. The $FeSO_4$ was dissolved in 10 mM cysteine-HCl (RPI, Mount Prospect, IL, USA) to prevent environmental re-oxidation of Fe^{2+} to Fe^{3+} in the standard curve. For testing iron reduction activity of cells with a DHNA concentration of 0.01 μg/mL in the medium, iron(III) oxide nanoparticles <50 nm (Sigma-Aldrich) were used as insoluble iron form (**Figure 1 – figure supplement 3**).

L. plantarum mutant construction

L. plantarum NCIMB8826 *ndh2*, *pplA*, and *narGHIJ* deletion mutants were constructed by double-crossover homologous recombination with the suicide plasmid pRV300 (Leloup *et al*., 1997). For mutant construction, upstream and downstream flanking regions of these genes were amplified using the A/B and C/D primers, respectively, listed in **Supplement file 5**. Splicing-by-overlap extension (SOEing) PCR was used to combine PCR products as previously described (Heckman and Pease, 2007). PCR products were digested with restriction enzymes EcoRI, SacI, SacII, or SalI (New England Biolabs, Ipswich, MA, USA) for plasmid ligation and transformation into *E. coli* DH5α. The resulting plasmids were then introduced to *L. plantarum* NCIMB8826 by electroporation. Erythromycin-resistant mutants were selected and confirmed for plasmid integration by PCR (see **Supplement file 5** for primer sequences). Subsequently,

deletion mutants were identified by a loss of resistance to erythromycin, PCR (see **Supplement file 5** for primer sequences) confirmation, and DNA sequencing (http://dnaseq.ucdavis.edu).

Bioelectrochemical reactors (BES) construction, operation, and electrochemical techniques

L. plantarum NCIMB8826 strains were grown overnight (approx. 16-18 h) from glycerol stocks in MRS. Cells were harvested by centrifugation (5200 g, 12 min, 4 °C) and washed twice in PBS. When *L. plantarum* wild-type EET activity versus the Δ*ndh2* (MLES100) and Δ*pplA* (MLES101) deletion mutants was compared, cells were grown as described and the number of cells was normalized across the three strains prior to inoculation in the BES. The bioreactors consisted of double-chamber electrochemical cells (Adams & Chittenden, Berkeley, CA) (**Figure 1B**) with a cation exchange membrane (CMI-7000, Membranes International, Ringwood, NJ) that separated them. A 3-electrode configuration was used consisting of an Ag/AgCl sat KCl reference electrode (BASI, IN, USA), a titanium wire counter electrode, and a 6.35-mm-thick graphite felt working electrode (anode) of 4x4 cm (Alfa Aesar, MA, USA) with a piece of Ti wire threaded from bottom to top as a current collector and connection to the potentiostat. We used a Bio-Logic Science Instruments (TN, USA) potentiostat model VSP-300 for performing the electrochemical measurements (chronoamperometry). The bioreactors were sterilized by filling them with ddH_2O and autoclaving at 121 ºC for 30 min. The water was then removed and replaced with 150 mL of filter sterilized mMRS or mCDM media for the working electrode chamber, and 150 mL of M9 medium (6.78 g/L Na_2HPO_4, 3 g/L KH_2PO_4, 0.5 g/L NaCl, 1 g/L NH_4Cl) (BD) for the counter electrode chamber. Both media of the working electrode chamber were supplemented with 20 µg/mL DHNA or 0.01 µg/mL diluted 1:1 in DMSO:ddH_2O where appropriate. To test the role of *bd*-cytochrome, heme was added in a final

concentration of 10 μg/mL (diluted 1:1 in DMSO: ddH_2O). The medium in the working electrode chamber was continuously mixed with a magnetic stir bar and N_2 gas was purged to maintain anaerobic conditions for the course of the experiment. The applied potential to the working electrode was of +0.2 V versus Ag/AgCl (sat. KCl) (BASI, IN, USA). Reactors run under OC conditions were similarly assembled but kept at open circuit and used as control for non-current circulating conditions. Once the current stabilized, the electrochemical cells were inoculated to a final OD_{600} of 0.12-0.15 with the cell suspensions prepared in PBS. Current densities are reported as a function of the geometric surface area of the electrode (16 cm^2). The bioreactors were sampled by taking samples under sterilized conditions at different time points for subsequent analysis. The samples for organic acids analyses were centrifuged (15,228 g, 7 min) and the supernatant was separated for High-Performance Liquid Chromatography (HPLC) assessments. Samples for ATP and NAD^+/NADH analyses were flash frozen in a dry ice/ethanol bath.

Metabolite analysis

Organic acids, ethanol and sugar concentrations were measured by HPLC (Agilent, 1260 Infinity), using a standard analytical system (Shimadzu, Kyoto, Japan) equipped with an Aminex Organic Acid Analysis column (Bio-Rad, HPX-87H 300 x 7.8 mm) heated at 60 ºC. The eluent was 5 mM of sulfuric acid, used at a flow rate of 0.6 mL min^{-1}. We used a refractive index detector 1260 Infinity II RID. A five-point calibration curve based on peak area was generated and used to calculate concentrations in the unknown samples. The following standards were included in the HPLC measurements: acetate, formate, pyruvate, malate, lactate, succinate,

oxalacetate, fumarate, ethanol, acetoin, butanediol, mannitol, and glucose. No gaseous products were measured.

BES biomass growth determination

Bioreactors were shaken to remove the cells attached to the working electrode and afterwards sampled to measure viable cells (colony forming units (CFUs)) and total biomass (dry weight). Samples for CFU enumeration were collected under sterile conditions at the time of inoculation and at the time of approximately maximum current density. Samples were serially diluted (1:1000 to 1:1000000) in sterile PBS and plated on MRS for CFUs enumeration after overnight incubation at 30 ºC. Dry weight was determined using a 25 mL sample collected at approximately maximum current density. Cells were harvested by centrifugation (5250 g, 12 min, 4 ºC) and washed twice in 50 mL ddH_2O. Afterwards cells were resuspended in 1mL of ddH_2O and transferred to microfuge tubes (previously weighted). Cells were harvested by centrifugation (5250 g, 12 min, 4 ºC), and the tubes were then transferred to an evaporator to remove humidity. The microfuge tubes were then cooled in a desiccator for 30 min and the weight of each tube was measured to determine cell weight. The difference between the weight of each tube with the pellet and before containing it allowed us to determine the dry weight/mL.

RNA-seq library construction and transcriptome analysis

L. plantarum NCIMB8826 was grown in triplicate to exponential phase (OD_{600} 1.0) at 37 °C in mMRS with or without the supplementation of 20 μg/mL DHNA and 1.25 mM ferric ammonium citrate. Cells were collected by centrifugation at 10,000 g for 3 min at 4 °C, flash frozen in liquid N_2 and stored at -80 °C prior to RNA extraction as previously described (Golomb *et al*., 2016).

Briefly, frozen cell pellets were resuspended in cold acidic phenol:chloroform:isoamyl alcohol (pH 4.5) [125:24:1] (Invitrogen, Carlsbad, CA, USA) before transferring to 2 mL screw cap tubes containing buffer (200 mM NaCl, 20 mM EDTA), 20% SDS, and 300 mg 0.1 mm zirconia/silica beads. RNA was extracted by mechanical lysis with an MP Fastprep bead beater (MP Biomedicals, Santa Ana, CA, USA) at 6.5 m/s for 1 min. The tubes were centrifuged at 20,000 g at 4 °C for 3 min and the upper aqueous phase was transferred to a new tube. The aqueous phase was extracted twice with chloroform:isoamyl alcohol [24:1] (Fisher Scientific, Waltham, MA, USA), The aqueous phase was then transferred to a new tube for RNA ethanol precipitation (Green and Sambrook, 2020). RNA was then quantified on a Nanodrop 2000c (ThermoFisher), followed by double DNAse digestion with the Turbo DNA-free Kit (Invitrogen) according to the manufacturer's protocols. The quality of the remaining RNA was checked using a Bioanalyzer RNA 6000 Nano Kit (Agilent Technologies, Santa Clara, CA, USA) (all RIN values > 9) and then quantified with the Qubit 2.0 RNA HS Assay (Life Technologies, Carlsbad, CA, USA). For reverse-transcription PCR (RT-PCR), 800 ng RNA was converted to cDNA with the High Capacity cDNA Reverse Transcription Kit (Applied Biosystems, Foster City, CA, USA) according to the manufacturer's protocols. Quantitative RT-PCR was performed on a 7500 Fast Real-Time PCR System (Applied Biosystems) using the PowerUp SYBR Green Master Mix (ThermoFisher) and RT-PCR primers listed in **Supplement file 5**. The 2-ΔΔCt method was used for relative transcript quantification using *rpoB* as a control (Livak and Schmittgen, 2001).

For sequencing, ribosomal-RNA (rRNA) was depleted from 4 μg RNA using the RiboMinus Eukaryote Kit v2 with specific probes for prokaryotic rRNA (ThermoFisher) following the manufacturer's instructions. RNA was then fragmented to approximately 200 bp, converted to

cDNA, and barcoded using the NEBnext Ultra-directional RNA Library Kit for Illumina (New England Biolabs, Ipswitch, MA, USA) with NEBnext Multiplex Oligos for Illumina (Primer Set 1) (New England Biolabs) following the manufacturer's protocols. cDNA libraries containing pooled barcoded samples was run across two lanes of a HiSeq400 (Illumina, San Diego, CA, USA) on two separate runs for 150 bp paired-end reads (http://dnatech.genomecenter.ucdavis.edu/). An average of 36,468,428 raw paired-end reads per sample was collected (**Supplement file 6**). The DNA sequences were quality filtered for each of the 12 samples by first visualizing with FastQC (ver. 0.11.8) (Andrews and Others, 2010) to check for appropriate trimming lengths, followed by quality filtering with Trimmomatic (ver. 0.39) (Bolger *et al*., 2014). Remaining reads then were aligned to the NCIMB8826 chromosome and plasmids using Bowtie2 (ver. 2.3.5) in the [-sensitive] mode (Langmead and Salzberg, 2012). The resulting ".sam" files containing aligned reads from Bowtie2 were converted to ".bam" files with Samtools (ver 1.9) (Li *et al*., 2009) before counting aligned reads with FeatureCounts in the [--stranded=reverse] mode (ver. 1.6.4) (Liao *et al*., 2014). Reads aligning to noncoding sequences (e.g., rRNA, tRNA, trRNA, etc.) were excluded for subsequent analyses. Differential gene expression based on culture condition was determined with DESeq2 (Love *et al*., 2014) using the Wald test in the R-studio shiny app DEBrowser (ver 1.14.2) (Kucukural *et al*., 2019). Differential expression was considered significant with a False-discovery-rate (FDR)-adjusted p-value ≤ 0.05 and a Log_2 (fold-change) ≥ 0.5. Clusters of Orthologous Groups (COGs) were assigned to genes based on matches from the eggNOG (ver. 5.0) database (Huerta-Cepas *et al*., 2019).

Redox probe assays

Hamilton oxidation-reduction potential (ORP) probes (Hamilton Company, Reno, NV, USA) were inserted into air-tight Pyrex (Corning Inc., Corning, NY, USA) bottles containing mMRS supplemented with 20 μg/mL DHNA and/or 1.25 mM ferric ammonium citrate and incubated in a water bath at 37 °C. A custom cap for the Pyrex bottles was 3D printed with polylactic acid filament (2.85 mm diameter) such that the ORP probe threads into the cap and an o-ring seal can be used to provide an air-tight seal between the probe and the cap. The ORP was allowed to equilibrate over 40 min before *L. plantarum* NCIMB8826, Δ*ndh2* (MLES100), or Δ*pplA* (MLES101) were inoculated at an OD600 of 0.10. Two uninoculated controls were used to measure baseline ORP over time. The ORP data was collected via Modbus TCP/IP protocol (Stride Modbus Gateway, AutomationDirect, Cumming, GA, USA) into a database (OSIsoft, San Leandro, CA, USA) and analyzed in MATLAB (Mathworks, Nantick, MA, USA). pH was measured using a Mettler Toledo SevenEasy pH meter (Mettler Toledo, Columbus, OH, USA). Cells were collected at either 24 h or at the greatest ORP difference between the wild-type and mutant strains (ΔmV_{max}) by centrifugation at 10,000g for 3 min and used for ferrihydrite reduction analyses.

ATP and NAD^+/NADH quantification

Frozen cell pellets were suspended in PBS and lysed by mechanical agitation in a FastPrep 24 (MP Biomedicals) at 6.5 m/sec for 1 min. The cell lysates were then centrifuged at 20,000 g for 3 min at 4°C. ATP and NAD^+ and NADH in the supernatants were then quantified with the Molecular Probes ATP Quantification Kit (ThermoFisher) and the Promega NAD/NADH-Glo Kit (Promega, Madison, WI, USA), respectively according to the manufacturers' instructions.

Inductively Coupled Plasma-Mass Spectrometry (ICP-MS)

L. plantarum was inoculated in mMRS with or without 20 µg/mL DHNA and 1.25 mM ferric ammonium citrate at an OD_{600} of 0.10 for 3.5 h. Cells were then collected by centrifugation at 10,000 x g for 3 min and washed twice in PBS to remove cell surface-associated metals. Viable cell numbers were enumerated by plating serial dilutions on MRS laboratory culture medium and the resulting cell materials were digested by incubating at 95 ˚C for 45 minutes in a 60% concentrated trace metal grade HNO_3, allowed to cool, then diluted with MilliQ water to a final concentration of 6% HNO_3. The contents were quantified with internal standards with an Agilent 7500Ce ICP-MS (Agilent Technologies, Palo Alto, CA) for simultaneous determination of select metals (Na, Mg, Al, K, Ca, Cu, Zn, Ba, Mn, Fe) at the UC Davis Interdisciplinary Center for Plasma Mass Spectrometry (http://icpms.ucdavis.edu/).

Kale juice fermentation assay

Green organic kale purchased from a market (Whole Foods) was washed with tap water and air dried for 1 h as previously recommended (Kim, 2017-9). A total of 385 g of the leaves and stems were shredded with an electric food processor in 1 L ddH20. The kale juice was then diluted with 0.35 L ddH2O and autoclaved (121°C, 15 min). The juice was then centrifuged under sterile conditions at 8000 rpm for 20 min and the supernatant was collected. A rifampicin-resistant variant of *L. plantarum* NCIMB8826-R (Tachon *et al*., 2014) (grown for 19 h in MRS medium at 37 °C, 50 µg Rif/mL) was inoculated to an estimated final OD of approximately 0.05, and DHNA (20 µg/mL) was added where appropriate. Cells were collected and washed as previously described for the bioelectrochemical assays in mCDM. The anodic chambers of bioreactors assembled as previously described (anode of 4.3*6 cm) were filled with 125 mL of the

inoculated kale juice and incubated at 30°C purged with N_2. After 1 h, the anodes were polarized to 0.2 V versus Ag/AgCl (sat. KCl) (EET conditions) or kept at open circuit (OC, no EET). Viable cells were measured by plating 10-fold serial dilutions in MRS agar plates with 50 μg/mL of Rif.

Calculations

The total electrons harvested on the anode were estimated by integrating the area (charge) under the chronoamperometric curve (current response (A) over time (s)), which was corrected by subtracting the current baseline obtained before *L. plantarum* was added to the system. This obtained charge was then converted to mol of electrons using the Faraday constant (96,485.3 A*s/mol electrons).

Data accession numbers

L. plantarum RNA-seq data are available in the NCBI Sequence Read Archive (SRA) under BioProject accession no. PRJNA717240. A list of the completed Lactobacillales genomes used in the DNA sequence analysis is available in the Harvard Dataverse repository at https://doi.org/10.7910/DVN/IHKI0C. Source data can be found on eLife alongside the published article.

Acknowledgements

This work was supported by the National Science Foundation grant #1650042, Office of Naval Research grant 0001418IP00037 (CMAF), and the USDA National Institute of Agriculture Multi-State Project (W4122). Work at the Molecular Foundry was supported by the Office of

Science, Office of Basic Energy Sciences, of the U.S. Department of Energy under Contract No. DE-AC02-05CH11231. James Nelson was supported by the Rodgers University fellowship in Electrical and Computer Engineering.

References

Andrews S. 2010. FastQC: a quality control tool for high throughput sequence data. Available online at: http://www.bioinformatics.babraham.ac.uk/projects/fastqc

Aumiller K, Stevens E, Scheffler R, Güvener ZT, Tung E, Grimaldo AB, Carlson HK, Deutschbauer AM, Taga ME, Marco ML, Ludington WB. 2021. A chemically-defined growth medium to support *Lactobacillus – Acetobacter* community analysis. *bioRxiv*. doi:10.1101/2021.05.12.443930

Behera SS, Ray RC, Zdolec N. 2018. *Lactobacillus plantarum* with functional properties: an approach to increase safety and shelf-life of fermented foods. *Biomed Res Int* **2018**:9361614. doi:10.1155/2018/9361614

Bintsis T. 2018. Lactic acid bacteria as starter cultures: an update in their metabolism and genetics. *AIMS Microbiol* **4**:665–684. doi:10.3934/microbiol.2018.4.665

Blom J, De Mattos MJT, Grivell LA. 2000-5. Redirection of the respiro-fermentative flux distribution in *Saccharomyces cerevisiae* by overexpression of the transcription factor Hap4p. *Appl Environ Microbiol* **66**:1970–1973 doi: 10.1128/aem.66.5.1970-1973.2000

Bolger AM, Lohse M, Usadel B. 2014. Trimmomatic: a flexible trimmer for Illumina sequence data. *Bioinformatics* **30**:2114–2120. doi:10.1093/bioinformatics/btu170

Bolotin, A., Wincker, P., Mauger, S., Jaillon, O., Malarme, K., Weissenbach, J., Ehrlich, S.D., Sorokin, A., 2001. The complete genome sequence of the lactic acid bacterium *Lactococcus lactis* ssp. *lactis* IL1403. Genome Res. 11, 731–753. doi:10.1101/gr.169701

Brooijmans RJW, Vos WM de, Hugenholtz J. 2009. *Lactobacillus plantarum* WCFS1 electron transport chains. *Appl Environ Microbiol* **75**:3580–3585. doi:10.1128/AEM.00147-09

Brooijmans, R., Smit, B., Santos, F., van Riel, J., de Vos, W.M., Hugenholtz, J., 2009b. Heme and menaquinone induced electron transport in lactic acid bacteria. Microb. Cell Factories 8, 28. doi:10.1186/1475-2859-8-28

Buckel W, Thauer RK. 2013. Energy conservation via electron bifurcating ferredoxin reduction and proton/Na^+ translocating ferredoxin oxidation. *Biochimica et Biophysica Acta (BBA) - Bioenergetics* **1827**:94–113. doi:10.1016/j.bbabio.2012.07.002

Cai H, Thompson R, Budinich MF, Broadbent JR, Steele JL. 2009. Genome sequence and comparative genome analysis of *Lactobacillus casei*: insights into their niche-associated evolution. *Genome Biol Evol* **1**:239–257. doi:10.1093/gbe/evp019

Cataldi TRI, Nardiello D, Carrara V, Ciriello R, De Benedetto GE. 2003. Assessment of riboflavin and flavin content in common food samples by capillary electrophoresis with laser-induced fluorescence detection. *Food Chem* **82**:309–314. doi:10.1016/S0308-8146(02)00567-8

Chan, C.H., Levar, C.E., Jiménez-Otero, F., Bond, D.R., 2017. Genome scale mutational analysis of *Geobacter sulfurreducens* reveals distinct molecular mechanisms for respiration and

sensing of poised electrodes versus Fe(III) oxides. J. Bacteriol. 199. doi:10.1128/JB.00340-17
Chen C, Zhao S, Hao G, Yu H, Tian H, Zhao G. 2017. Role of lactic acid bacteria on the yogurt flavour: A review. *Int J Food Prop* **20**:S316–S330. doi:10.1080/10942912.2017.1295988
Dandekar, S., 2019. *Lactiplantibacillus plantarum* strain:NCIMB8826 (ID 527135) - BioProject - NCBI [WWW Document]. URL https://www.ncbi.nlm.nih.gov/bioproject/527135 (accessed 5.20.21).
Dantas J, Morgado L, Aklujkar M, Bruix M, Londer Y, Schiffer M, Pokkuluri PR, Salgueiro C. 2015. Rational engineering of *Geobacter sulfurreducens* electron transfer components: a foundation for building improved *Geobacter*-based bioelectrochemical technologies. Front Microbiol 6:752. doi:10.3389/fmicb.2015.00752
de Graef MR, Alexeeva S, Snoep JL, Teixeira de Mattos MJ. 1999. The steady-state internal redox state (NADH/NAD) reflects the external redox state and is correlated with catabolic adaptation in *Escherichia coli*. *J Bacteriol* **181**:2351–2357
De MAN JC, Rogosa M, Sharpe ME. 1960. A medium for the cultivation of lactobacilli. *J Appl Bacteriol* **23**:130–135. doi:10.1111/j.1365-2672.1960.tb00188.x
Dirar H, Collins EB. 1972. End-products, fermentation balances and molar growth yields of homofermentative lactobacilli. *J Gen Microbiol* **73**:233–238. doi:10.1099/00221287-73-2-233
Duar RM, Lin XB, Zheng J, Martino ME, Grenier T, Pérez-Muñoz ME, Leulier F, Gänzle M, Walter J. 2017. Lifestyles in transition: evolution and natural history of the genus *Lactobacillus*. *FEMS Microbiol Rev* **41**:S27–S48. doi:10.1093/femsre/fux030
Dumas C, Basseguy R, Bergel A. 2007. Electrochemical activity of *Geobacter sulfurreducens* biofilms on stainless steel anodes. *Electrochim Acta* **53**:5235–5241. doi:10.1016/j.electacta.2008.02.056
Duwat P, Sourice S, Cesselin B, Lamberet G, Vido K, Gaudu P, Le Loir Y, Violet F, Loubière P, Gruss A. 2001. Respiration capacity of the fermenting bacterium *Lactococcus lactis* and its positive effects on growth and survival. *J Bacteriol* **183**:4509–4516. doi:10.1128/JB.183.15.4509-4516.2001
Elli M, Zink R, Rytz A, Reniero R, Morelli L. 2000. Iron requirement of *Lactobacillus spp.* in completely chemically defined growth media. *J Appl Microbiol* **88**:695–703. doi:10.1046/j.1365-2672.2000.01013.x
Emde R, Schink B. 1990. Enhanced propionate formation by *Propionibacterium freudenreichii* subsp. freudenreichii in a three-electrode amperometric culture system. Appl Environ Microbiol. 56:2771-6. doi: 10.1128/aem.56.9.2771-2776.1990
Eom JE, Kwon SC, Moon GS. 2012. Detection of 1 4-dihydroxy-2-naphthoic acid from commercial Makgeolli products. Prev Nutr Food Sci 17:83. doi:10.3746/pnf.2015.20.1.78
Esteve-Núñez A, Rothermich M, Sharma M, Lovley D. 2005. Growth of *Geobacter sulfurreducens* under nutrient-limiting conditions in continuous culture. *Environ Microbiol* **7**:641–648. doi:10.1111/j.1462-2920.2005.00731.x
Fenn K, Strandwitz P, Stewart EJ, Dimise E, Rubin S, Gurubacharya S, Clardy J, Lewis K. 2017. Quinones are growth factors for the human gut microbiota. *Microbiome* **5**:161. doi:10.1186/s40168-017-0380-5
Freguia S, Masuda M, Tsujimura S, Kano K. 2009. *Lactococcus lactis* catalyses electricity generation at microbial fuel cell anodes via excretion of a soluble quinone. *Bioelectrochemistry* **76**:14–18. doi:10.1016/j.bioelechem.2009.04.001

Furuichi K, Hojo KI, Katakura Y, Ninomiya K, Shioya S. 2006. Aerobic culture of Propionibacterium freudenreichii ET-3 can increase production ratio of 1 4-dihydroxy-2-naphthoic acid to menaquinone. J Biosci Bioeng 101:464-470. doi:10.1263/jbb.101.464

Galushko, A.S., Schink, B., 2000. Oxidation of acetate through reactions of the citric acid cycle by *Geobacter sulfurreducens* in pure culture and in syntrophic coculture. Arch. Microbiol. 174, 314–321. doi:10.1007/s002030000208

Gänzle MG. 2015. Lactic metabolism revisited: metabolism of lactic acid bacteria in food fermentations and food spoilage. *Current Opinion in Food Science* **2**:106–117. doi:10.1016/j.cofs.2015.03.001

Glasser NR, Kern SE, Newman DK. 2014. Phenazine redox cycling enhances anaerobic survival in *Pseudomonas aeruginosa* by facilitating generation of ATP and a proton-motive force. Mol Microbiol. **92**:399-412. doi: 10.1111/mmi.12566.

Golomb BL, Hirao LA, Dandekar S, Marco ML. 2016. Gene expression of *Lactobacillus plantarum* and the commensal microbiota in the ileum of healthy and early SIV-infected rhesus macaques. *Sci Rep* **6**:24723. doi:10.1038/srep24723

Golomb, B.L., Morales, V., Jung, A., Yau, B., Boundy-Mills, K.L., Marco, M.L., 2013. Effects of pectinolytic yeast on the microbial composition and spoilage of olive fermentations. Food Microbiol. 33, 97–106. doi:10.1016/j.fm.2012.09.004

Green MR, Sambrook J. 2020. Precipitation of RNA with Ethanol. *Cold Spring Harb Protoc* **2020**:101717. doi:10.1101/pdb.prot101717

Guo, Y., Tian, X., Huang, R., Tao, X., Shah, N.P., Wei, H., Wan, C., 2017. A physiological comparative study of acid tolerance of *Lactobacillus plantarum* ZDY 2013 and L. plantarum ATCC 8014 at membrane and cytoplasm levels. Ann. Microbiol. 67, 669–677. doi:10.1007/s13213-017-1295-x

Hansen EB. 2018. Redox reactions in food fermentations. *Current Opinion in Food Science* **19**:98–103. doi:10.1016/j.cofs.2018.03.004

Haruta S, Kanno N. 2015. Survivability of microbes in natural environments and their ecological impacts. *Microbes Environ* **30**:123–125. doi:10.1264/jsme2.ME3002rh

Hatti-Kaul, R., Chen, L., Dishisha, T., Enshasy, H.E., 2018. Lactic acid bacteria: from starter cultures to producers of chemicals. *FEMS Microbiology Letters* 365. doi:10.1093/femsle/fny213

Heckman KL, Pease LR. 2007. Gene splicing and mutagenesis by PCR-driven overlap extension. *Nat Protoc* **2**:924–932. doi:10.1038/nprot.2007.132

Hederstedt L, Gorton L, Pankratova G. 2020. Two routes for extracellular electron transfer in *Enterococcus faecalis*. *J Bacteriol* **202**. doi:10.1128/JB.00725-19

Heeney, D.D., Marco, M.L., 2019. Complete genome sequence of the plantaricin-sensitive strain *Lactobacillus plantarum* NCIMB 700965. Microbiol. Resour. Announc. 8. doi:10.1128/MRA.01724-18

Herrmann G, Jayamani E, Mai G, Buckel W. 2008. Energy conservation via electron-transferring flavoprotein in anaerobic bacteria. *J Bacteriol* **190**:784–791. doi:10.1128/JB.01422-07

Holm AK, Blank LM, Oldiges M, Schmid A, Solem C, Jensen PR, Vemuri GN. 2010. Metabolic and transcriptional response to cofactor perturbations in *Escherichia coli*. *J Biol Chem* **285**:17498–17506. doi:10.1074/jbc.M109.095570

Holmes, D.E., Chaudhuri, S.K., Nevin, K.P., Mehta, T., Methé, B.A., Liu, A., Ward, J.E., Woodard, T.L., Webster, J., Lovley, D.R., 2006. Microarray and genetic analysis of

electron transfer to electrodes in *Geobacter sulfurreducens*. Environ. Microbiol. 8, 1805–1815. doi:10.1111/j.1462-2920.2006.01065.x

Huerta-Cepas J, Szklarczyk D, Heller D, Hernández-Plaza A, Forslund SK, Cook H, Mende DR, Letunic I, Rattei T, Jensen LJ, von Mering C, Bork P. 2019. eggNOG 5.0: a hierarchical, functionally and phylogenetically annotated orthology resource based on 5090 organisms and 2502 viruses. *Nucleic Acids Res* **47**:D309–D314. doi:10.1093/nar/gky1085

Hunt KA, Flynn JM, Naranjo B, Shikhare ID, Gralnick JA. 2010. Substrate-level phosphorylation is the primary source of energy conservation during anaerobic respiration of *Shewanella oneidensis* Strain MR-1. *J Bacteriol* **192**:3345–3351. doi:10.1128/JB.00090-10

Isawa K, HoJo K, Yoda N, Kamiyama T, Makino S, Saito M, Sugano H, Mizoguchi C, Kurama S, Shibasaki M, Endo N. 2002. Isolation and identification of a new bifidogenic growth stimulator produced by *Propionibacterium freudenreichii* ET-3. *Biosci Biotechnol Biochem* **66**:679-681. doi:10.1271/bbb.66.679

Jeuken LJC, Hards K, Nakatani Y. 2020. Extracellular electron transfer: respiratory or nutrient homeostasis? *J Bacteriol* **202**:4.

Johanson, A., Goel, A., Olsson, L., Franzén, C.J., 2020. Respiratory physiology of *Lactococcus lactis* in chemostat cultures and its effect on cellular robustness in frozen and freeze-dried starter cultures. Appl. Environ. Microbiol. 86. doi:10.1128/AEM.02785-19

Kang JE, Kim TJ, Moon GS. 2015. A novel *Lactobacillus casei* LP1 producing 1 4-dihydroxy-2-naphthoic acid a bifidogenic growth stimulator. *Prev Nutr Food Sci* **20**:78.
doi:10.3746/pnf.2015.20.1.78

Kankainen, M., Paulin, L., Tynkkynen, S., Ossowski, I. von, Reunanen, J., Partanen, P., Satokari, R., Vesterlund, S., Hendrickx, A.P.A., Lebeer, S., Keersmaecker, S.C.J.D., Vanderleyden, J., Hämäläinen, T., Laukkanen, S., Salovuori, N., Ritari, J., Alatalo, E., Korpela, R., Mattila-Sandholm, T., Lassig, A., Hatakka, K., Kinnunen, K.T., Karjalainen, H., Saxelin, M., Laakso, K., Surakka, A., Palva, A., Salusjärvi, T., Auvinen, P., Vos, W.M. de, 2009. Comparative genomic analysis of *Lactobacillus rhamnosus* GG reveals pili containing a human- mucus binding protein. Proc. Natl. Acad. Sci. 106, 17193–17198. doi:10.1073/pnas.0908876106

Keogh D, Lam LN, Doyle LE, Matysik A, Pavagadhi S, Umashankar S, Low PM, Dale JL, Song Y, Ng SP, Boothroyd CB, Dunny GM, Swarup S, Williams RBH, Marsili E, Kline KA. 2018. Extracellular electron transfer powers *Enterococcus faecalis* biofilm metabolism. *mBio* **9**. doi:10.1128/mBio.00626-17

Killeen DJ, Boulton R, Knoesen A. 2018. Advanced monitoring and control of redox potential in wine fermentation. *Am J Enol Vitic* **69**:394–399. https://doi.org/10.5344/ajev.2018.17063

Kim BH, Gadd GM. 2019. Prokaryotic metabolism and physiology. Cambridge University Press.

Kim SY. 2017-9. Production of fermented kale juices with *Lactobacillus* Strains and nutritional composition. *Prev Nutr Food Sci* **22**:231–236. doi:10.3746/pnf.2017.22.3.231

Kopit, L.M., Kim, E.B., Siezen, R.J., Harris, L.J., Marco, M.L., 2014. Safety of the surrogate microorganism *Enterococcus faecium* NRRL B-2354 for use in thermal process validation. Appl. Environ. Microbiol. 80, 1899–1909. doi:10.1128/AEM.03859-13

Kouzuma A, Hashimoto K, Watanabe K. 2012. Roles of siderophore in manganese-oxide reduction by *Shewanella oneidensis* MR-1. FEMS Microbiol Lett 326:91–98. doi:10.1111/j.1574-6968.2011.02444.x

Kouzuma A, Oba H, Tajima N, Hashimoto K, Watanabe K. 2014. Electrochemical selection and

characterization of a high current-generating *Shewanella oneidensis* mutant with altered cell-surface morphology and biofilm-related gene expression. *BMC Microbiol* **14**:190. doi:10.1186/1471-2180-14-190

Kracke F, Lai B, Yu S, Krömer JO. 2018. Balancing cellular redox metabolism in microbial electrosynthesis and electro fermentation – A chance for metabolic engineering. *Metab Eng* **45**:109–120. doi:10.1016/j.ymben.2017.12.003

Kucukural A, Yukselen O, Ozata DM, Moore MJ, Garber M. 2019. DEBrowser: interactive differential expression analysis and visualization tool for count data. *BMC Genomics* **20**:6. doi:10.1186/s12864-018-5362-x

Lam LN, Wong JJ, Matysik A, Paxman JJ, Chong KKL, Low PM, Chua ZS, Heras B, Marsili E, Kline KA. 2019. Sortase-assembled pili promote extracellular electron transfer and iron acquisition in *Enterococcus faecalis* biofilm. *Cold Spring Harbor Laboratory*. doi:10.1101/601666

Langmead B, Salzberg SL. 2012. Fast gapped-read alignment with Bowtie 2. *Nat Methods* **9**:357–359. doi:10.1038/nmeth.1923

Leloup L, Ehrlich SD, Zagorec M, Morel-Deville F. 1997. Single-crossover integration in the *Lactobacillus sake* chromosome and insertional inactivation of the ptsI and lacL genes. *Appl Environ Microbiol* **63**:2117–2123. doi: 10.1128/aem.63.6.2117-2123.1997

Li F, Hinderberger J, Seedorf H, Zhang J, Buckel W, Thauer RK. 2008. Coupled ferredoxin and crotonyl coenzyme a (coA) reduction with NADH catalyzed by the butyryl-coA dehydrogenase/Etf complex from *Clostridium kluyveri*. *J Bacteriol* **190**:843–850. doi:10.1128/JB.01417-07

Li H, Handsaker B, Wysoker A, Fennell T, Ruan J, Homer N, Marth G, Abecasis G, Durbin R, 1000 Genome Project Data Processing Subgroup. 2009. The sequence alignment/map format and SAMtools. *Bioinformatics* **25**:2078–2079. doi:10.1093/bioinformatics/btp352

Liao Y, Smyth GK, Shi W. 2014. featureCounts: an efficient general purpose program for assigning sequence reads to genomic features. *Bioinformatics* **30**:923–930. doi:10.1093/bioinformatics/btt656

Light SH, Méheust R, Ferrell JL, Cho J, Deng D, Agostoni M, Iavarone AT, Banfield JF, D'Orazio SEF, Portnoy DA. 2019. Extracellular electron transfer powers flavinylated extracellular reductases in Gram-positive bacteria. *Proc Natl Acad Sci U S A*. doi:10.1073/pnas.1915678116

Light SH, Su L, Rivera-Lugo R, Cornejo JA, Louie A, Iavarone AT, Ajo-Franklin CM, Portnoy DA. 2018. A flavin-based extracellular electron transfer mechanism in diverse Gram-positive bacteria. *Nature* **562**:140–144. doi:10.1038/s41586-018-0498-z

Lin SS, Kerscher S, Saleh A, Brandt U, Gross U, Bohne W. 2008. The *Toxoplasma gondii* type-II NADH dehydrogenase TgNDH2-I is inhibited by 1-hydroxy-2-alkyl-4(1H)quinolones. *Biochim Biophys Acta* **1777**:1455–1462. doi:10.1016/j.bbabio.2008.08.006

Livak KJ, Schmittgen TD. 2001. Analysis of relative gene expression data using real-time quantitative PCR and the 2(-Delta Delta C(T)) Method. *Methods* **25**:402–408. doi:10.1006/meth.2001.1262

Love MI, Huber W, Anders S. 2014. Moderated estimation of fold change and dispersion for RNA-seq data with DESeq2. *Genome Biol* **15**:550. doi:10.1186/s13059-014-0550-8

Mahadevan, R., Bond, D.R., Butler, J.E., Esteve-Nuñez, A., Coppi, M.V., Palsson, B.O., Schilling, C.H., Lovley, D.R., 2006. Characterization of metabolism in the Fe(III)-

reducing organism *Geobacter sulfurreducens* by constraint-based modeling. Appl. Environ. Microbiol. 72, 1558–1568. doi:10.1128/AEM.72.2.1558-1568.2006

Makarova, K., Slesarev, A., Wolf, Y., Sorokin, A., Mirkin, B., Koonin, E., Pavlov, A., Pavlova, N., Karamychev, V., Polouchine, N., Shakhova, V., Grigoriev, I., Lou, Y., Rohksar, D., Lucas, S., Huang, K., Goodstein, D.M., Hawkins, T., Plengvidhya, V., Welker, D., Hughes, J., Goh, Y., Benson, A., Baldwin, K., Lee, J.-H., Díaz-Muñiz, I., Dosti, B., Smeianov, V., Wechter, W., Barabote, R., Lorca, G., Altermann, E., Barrangou, R., Ganesan, B., Xie, Y., Rawsthorne, H., Tamir, D., Parker, C., Breidt, F., Broadbent, J., Hutkins, R., O'Sullivan, D., Steele, J., Unlu, G., Saier, M., Klaenhammer, T., Richardson, P., Kozyavkin, S., Weimer, B., Mills, D., 2006. Comparative genomics of the lactic acid bacteria. Proc. Natl. Acad. Sci. 103, 15611–15616. doi:10.1073/pnas.0607117103

Marco ML, Sanders ME, Gänzle M, Arrieta MC, Cotter PD, De Vuyst L, Hill C, Holzapfel W, Lebeer S, Merenstein D, Reid G, Wolfe BE, Hutkins R. 2021. The International Scientific Association for Probiotics and Prebiotics (ISAPP) consensus statement on fermented foods. *Nat Rev Gastroenterol Hepatol* **18**:196-208.

Marsili E, Baron DB, Shikhare ID, Coursolle D, Gralnick JA, Bond DR. 2008. *Shewanella* secretes flavins that mediate extracellular electron transfer. P*roc Natl Acad Sci U S A* **105**:3968–3973. doi:10.1073/pnas.0710525105

Marsili E, Sun J, Bond DR. 2010. Voltammetry and growth physiology of *Geobacter sulfurreducens* biofilms as a function of growth stage and imposed electrode potential. *Electroanalysis* **22**:865–874. doi:10.1002/elan.200800007

Martino ME, Bayjanov JR, Caffrey BE, Wels M, Joncour P, Hughes S, Gillet B, Kleerebezem M, van Hijum SAFT, Leulier F. 2016. Nomadic lifestyle of *Lactobacillus plantarum* revealed by comparative genomics of 54 strains isolated from different habitats. *Environ Microbiol* **18**:4974–4989. doi:10.1111/1462-2920.13455

Masuda M, Freguia S, Wang Y-F, Tsujimura S, Kano K. 2010. Flavins contained in yeast extract are exploited for anodic electron transfer by *Lactococcus lactis. Bioelectrochemistry* **78**:173–175. doi:10.1016/j.bioelechem.2009.08.004

Mazé, A., Boël, G., Zúñiga, M., Bourand, A., Loux, V., Yebra, M.J., Monedero, V., Correia, K., Jacques, N., Beaufils, S., Poncet, S., Joyet, P., Milohanic, E., Casarégola, S., Auffray, Y., Pérez-Martínez, G., Gibrat, J.-F., Zagorec, M., Francke, C., Hartke, A., Deutscher, J., 2010. Complete genome sequence of the probiotic *Lactobacillus casei* strain BL23. J. Bacteriol. 192, 2647–2648. doi:10.1128/JB.00076-10

McDonald, T.J., McDonald, J.S., 1976. Streptococci isolated from bovine intramammary infections. Am. J. Vet. Res. 37, 377–381.

McFeeters, R. F., Chen, K. H. 1986. Utilization of electron acceptors for anaerobic mannitol metabolism by *Lactobacillus plantarum*. Compounds which serve as electron acceptors. Food Microbiol, 3, 73-81. doi:10.1016/S0740-0020(86)80029-6

McGinnis S, Madden TL. 2004. BLAST: at the core of a powerful and diverse set of sequence analysis tools. *Nucleic Acids Res* **32**:W20-5. doi:10.1093/nar/gkh435

Minogue, T.D., Daligault, H.E., Davenport, K.W., Broomall, S.M., Bruce, D.C., Chain, P.S., Coyne, S.R., Chertkov, O., Freitas, T., Gibbons, H.S., Jaissle, J., Koroleva, G.I., Ladner, J.T., Palacios, G.F., Rosenzweig, C.N., Xu, Y., Johnson, S.L., 2014. Complete genome assembly of *Enterococcus faecalis* 29212, a laboratory reference strain. Genome Announc. 2. doi:10.1128/genomeA.00968-14

Morandi S, Silvetti T, Tamburini A, Brasca M. 2016. Changes in oxidation-reduction potential during milk fermentation by wild lactic acid bacteria. *J Dairy Res* **83**:387–394. doi:10.1017/S0022029916000339

Moscoviz R, Toledo-Alarcón J, Trably E, Bernet N. 2016. Electro-fermentation: how to drive fermentation using electrochemical systems. *Trends Biotechnol* **34**:856–865. doi:10.1016/j.tibtech.2016.04.009

Müller V, Chowdhury NP, Basen M. 2018. Electron bifurcation: a long-hidden energy-coupling mechanism. *Annu Rev Microbiol* **72**:331–353. doi:10.1146/annurev-micro-090816-093440

Nakatani Y, Shimaki Y, Dutta D, Muench SP, Ireton K, Cook GM, Jeuken LJC. 2020. Unprecedented properties of phenothiazines unraveled by a NDH-2 bioelectrochemical assay platform. *J Am Chem Soc* **142**:1311–1320. doi:10.1021/jacs.9b10254

Olsen MJ, Pérez-Díaz IM. 2009. Influence of microbial growth on the redox potential of fermented cucumbers. *J Food Sci* **74**:M149–M153. doi:10.1111/j.1750-3841.2009.01121.x

Pankratova G, Leech D, Gorton L, Hederstedt L. 2018. Extracellular electron transfer by the gram-positive bacterium *Enterococcus faecalis*. *Biochemistry* **57**:4597–4603. doi:10.1021/acs.biochem.8b00600

Pearson WR. 2013. An introduction to sequence similarity ("homology") searching. *Curr Protoc Bioinformatics* **Chapter 3**:Unit3.1. doi:10.1002/0471250953.bi0301s42

Pedersen MB, Gaudu P, Lechardeur D, Petit MA, Gruss A. 2012. Aerobic respiration metabolism in lactic acid bacteria and uses in biotechnology. *Annu Rev Food Sci Technol* **3**, 37–58. doi:10.1146/annurev-food-022811-101255

Pedersen, M.B., Garrigues, C., Tuphile, K., Brun, C., Vido, K., Bennedsen, M., Møllgaard, H., Gaudu, P., Gruss, A., 2008. Impact of aeration and heme-activated respiration on *Lactococcus lactis* gene expression: identification of a heme-responsive operon. J. Bacteriol. 190, 4903–4911. doi:10.1128/JB.00447-08

Pfeiffer T, Morley A. 2014. An evolutionary perspective on the Crabtree effect. *Front Mol Biosci* **1**:17. doi:10.3389/fmolb.2014.00017

Renslow RS, Babauta JT, Majors PD, Beyenal H. 2013. Diffusion in biofilms respiring on electrodes. *Energy Environ Sci* **6**:595–607. doi:10.1039/C2EE23394K

Rezaïki L, Lamberet G, Derré A, Gruss A, Gaudu P. 2008. *Lactococcus lactis* produces short-chain quinones that cross-feed Group B *Streptococcus* to activate respiration growth. *Mol Microbiol* **67**:947–957. doi:10.1111/j.1365-2958.2007.06083.x

Richter K, Schicklberger M, Gescher J. 2012. Dissimilatory reduction of extracellular electron acceptors in anaerobic respiration. *Appl Environ Microbiol* **78**:913–921. doi:10.1128/AEM.06803-11

Rose ND, Regan JM. 2015. Changes in phosphorylation of adenosine phosphate and redox state of nicotinamide-adenine dinucleotide (phosphate) in *Geobacter sulfurreducens* in response to electron acceptor and anode potential variation. *Bioelectrochemistry* **106**: 213–220. doi:10.1016/j.bioelechem.2015.03.003

Roughead ZK, McCormick DB. 1990. Qualitative and quantitative assessment of flavins in cow's milk. *J Nutr* **120**:382–388. doi:10.1093/jn/120.4.382

Russell JB, Cook GM. 1995. Energetics of bacterial growth: balance of anabolic and catabolic reactions. *Microbiol Rev* **59**:48–62.

Salvetti E, Fondi M, Fani R, Torriani S, Felis GE. 2013. Evolution of lactic acid bacteria in the

order Lactobacillales as depicted by analysis of glycolysis and pentose phosphate pathways. *Syst Appl Microbiol* **36**:291–305. doi:10.1016/j.syapm.2013.03.009
Sauer M, Russmayer H, Grabherr R, Peterbauer CK, Marx H. 2017. The efficient clade: lactic acid bacteria for industrial chemical production. *Trends Biotechnol* **35**:756–769. doi:10.1016/j.tibtech.2017.05.002
Schievano A, Pepé Sciarria T, Vanbroekhoven K, De Wever H, Puig S, Andersen SJ, Rabaey K, Pant D. 11 2016. Electro-fermentation - merging electrochemistry with fermentation in industrial applications. *Trends Biotechnol* **34**:866–878. doi:10.1016/j.tibtech.2016.04.007
Schwertmann U, Fischer WR. 1973. Natural "amorphous" ferric hydroxide. *Geoderma* **10**:237–247. doi:10.1016/0016-7061(73)90066-9
Shi L, Squier TC, Zachara JM, Fredrickson JK. 2007. Respiration of metal (hydr)oxides by *Shewanella* and *Geobacter*: a key role for multihaem c-type cytochromes. *Mol Microbiol* **65**:12–20. doi:10.1111/j.1365-2958.2007.05783.x
Shuler M.L., Kargi F. 2002. Bioprocess Engineering: Basic Concepts. Prentice Hall
Siezen, R.J., Bayjanov, J., Renckens, B., Wels, M., Hijum, S.A.F.T. van, Molenaar, D., Vlieg, J.E.T. van H., 2010. Complete genome sequence of *Lactococcus lactis* subsp. *lactis* KF147, a plant-associated lactic acid bacterium. J. Bacteriol. 192, 2649–2650. doi:10.1128/JB.00276-10
Siezen RJ, Tzeneva VA, Castioni A, Wels M, Phan HTK, Rademaker JLW, Starrenburg MJC, Kleerebezem M, Molenaar D, van Hylckama Vlieg JET. 2010. Phenotypic and genomic diversity of *Lactobacillus plantarum* strains isolated from various environmental niches. *Environ Microbiol* **12**:758–773. doi:10.1111/j.1462-2920.2009.02119.x
Sporer AJ, Kahl LJ, Price-Whelan A, Dietrich LEP. 2017. Redox-based regulation of bacterial development and behavior. *Annu Rev Biochem* **86**:777–797. doi:10.1146/annurev-biochem-061516-044453
Stookey LL. 1970. Ferrozine-a new spectrophotometric reagent for iron. *Anal Chem* **42**:779–781. doi:10.1021/ac60289a016
Tachon S, Lee B, Marco ML. 2014. Diet alters probiotic *Lactobacillus* persistence and function in the intestine. *Environ Microbiol* **16**:2915–2926. doi:10.1111/1462-2920.12297
Tachon, S, Brandsma, J.B., Yvon, M., 2010. NoxE NADH oxidase and the electron transport chain are responsible for the ability of *Lactococcus lactis* to decrease the redox potential of milk. *Appl. Environ. Microbiol* 76, 1311–1319. https://doi.org/10.1128/AEM.02120-09
Tachon S, Michelon D, Chambellon E, Cantonnet M, Mezange C, Henno L, Cachon R, Yvon M. 2009. Experimental conditions affect the site of tetrazolium violet reduction in the electron transport chain of *Lactococcus lactis*. *Microbiology* **155**:2941–2948. doi:10.1099/mic.0.029678-0
Tamang JP, Cotter P, Endo A, Han NS, Kort R, Liu SQ, Mayo B, Westerik N, Hutkins, R. 2020. Fermented foods in a global age: East meets West. *Compr Rev Food Sci Food Saf* **9**:184–217. doi: 10.1111/1541-4337.12520
Thavarajah D, Thavarajah P, Abare A, Basnagala S, Lacher C, Smith P, Combs GF. 2016. Mineral micronutrient and prebiotic carbohydrate profiles of USA-grown kale (*Brassica oleracea* L. var. *acephala*). *J Food Compost Anal* **52**:9–15. doi:10.1016/j.jfca.2016.07.003
Tomé D. 2021. Yeast extracts: nutritional and flavoring food ingredients. *ACS Food Sci Technol* **1**:487–494. doi:10.1021/acsfoodscitech.0c00131

Tsuji A, Okada S, Hols P, Satoh E. 2013. Metabolic engineering of *Lactobacillus plantarum* for succinic acid production through activation of the reductive branch of the tricarboxylic acid cycle. *Enzyme Microb Technol* **53**:97–103. doi:10.1016/j.enzmictec.2013.04.008

van Dijk C, Ebbenhorst-Selles T, Ruisch H, Stolle-Smits T, Schijvens E, van Deelen W, Boeriu C. 2000. Product and redox potential analysis of sauerkraut fermentation. *J Agric Food Chem* **48**:132–139. doi:10.1021/jf990720t

Vassilev I, Averesch NJ, Ledezma P, Kokko M. 2021. Anodic electro-fermentation: Empowering anaerobic production processes via anodic respiration. *Biotechnology Advances* **107728**. doi:10.1016/j.biotechadv.2021.107728

Vilas Boas J, Oliveira VB, Marcon LRC, Pinto DP, Simões M, Pinto AMFR. 2015. Effect of operating and design parameters on the performance of a microbial fuel cell with *Lactobacillus pentosus*. *Biochem Eng J*, 12th International Chemical and Biological Engineering Conference- Interfacing Bio- and Chemical Engineering **104**:34–40. doi:10.1016/j.bej.2015.05.009

Vinderola G, Ouwehand A, Salminen S, Wright A von. 2019. Lactic acid bacteria: microbiological and functional aspects. CRC Press.

Walther B, Karl JP, Booth SL, Boyaval P. 2013. Menaquinones, bacteria, and the food supply: the relevance of dairy and fermented food products to vitamin K requirements. *Adv Nutr* **4**:463–473. doi:10.3945/an.113.003855

Weinberg ED. 1997. The *Lactobacillus* anomaly: total iron abstinence. *Perspect Biol Med* **40**:578–583. doi:10.1353/pbm.1997.0072

Wickham H. 2011. ggplot2. *Wiley Interdiscip Rev Comput Stat* **3**:180–185. doi:10.1002/wics.147

Yi H, Nevin KP, Kim B-C, Franks AE, Klimes A, Tender LM, Lovley DR. 2009. Selection of a variant of *Geobacter sulfurreducens* with enhanced capacity for current production in microbial fuel cells. *Biosens Bioelectron* **24**:3498–3503. doi:10.1016/j.bios.2009.05.004

Zheng J, Wittouck S, Salvetti E, Franz CMAP, Harris HMB, Mattarelli P, O'Toole PW, Pot B, Vandamme P, Walter J, Watanabe K, Wuyts S, Felis GE, Gänzle MG, Lebeer S. 2020. A taxonomic note on the genus *Lactobacillus*: description of 23 novel genera, emended description of the genus *Lactobacillus Beijerinck 1901*, and union of Lactobacillaceae and Leuconostocaceae. *Int J Syst Evol Microbiol* **70**:2782–2858. doi:10.1099/ijsem.0.004

Tables

Table 1. Bioenergetic balances suggest energy conservation under EET conditions occurs via substrate-level phosphorylation. The reactors contained 20 μg/mL of DHNA and mannitol as the electron donor. Balances were calculated with data obtained by day 4 from Figure 5. See also **Supplement file 1**. SLP stands for substrate-level phosphorylation. $Y_{fermentation}$ refers to the total fermentation products obtained (see **Supplement file 1**) per mol of sugar consumed. $Y_{mannitol}$ is the ATP produced from the total fermentation products per mol of sugar consumed, and Y_{ATP} is the dry weight measured per mol of ATP produced from fermentation products.

	NADH consumed*	**Calculated ATP** (from metabolites)**	**Biomass yield**	**$Y_{fermentation}$**	**$Y_{mannitol}$**	**Y_{ATP}**
Units	mM	mM	g-dw/mol-mannitol	mmol product/mmol-mannitol	mol ATP/mol mannitol	g dw/mol ATP
EET	6.44 ± 0.48 via anode 16.69 ± 2.72 via SLP	16.6 ± 1.5	4.85 ± 0.33	1.53 ± 0.13	1.59 ± 0.13	3.09 ± 0.36
OC	5.51 ± 0.97 via SLP	5.7 ± 0.6	7.21 ± 1.41	0.87 ± 0.09	0.89 ± 0.09	8.06 ± 0.86

*Calculated based on production of 3 mol of NADH produced per mol of mannitol, 1 mol of NAD^+ per lactate, 2 mol of NAD^+ per ethanol, 2 mol of NAD^+ mol per succinate produced and 0.5 mmol of NAD^+ per mol of electrons harvested on the anode.
** Calculated based on production of 1 mol of ATP per lactate, 2 mol per acetate, 1 mol per ethanol, and 3 mol per succinate produced.

Figures

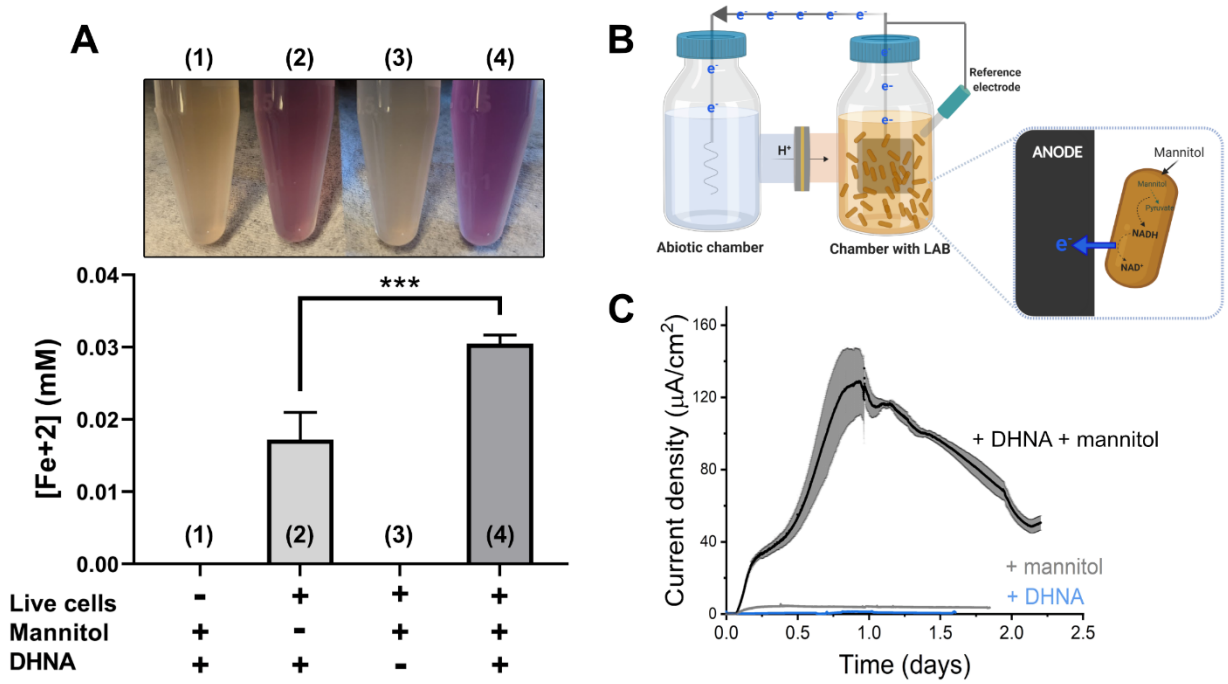

Figure 1. *L. plantarum* can reduce both Fe^{3+} and an anode through EET. (A) Reduction of Fe^{3+} (ferrihydrite) to Fe^{2+} by *L. plantarum* NCIMB8826 after growth in mMRS. The assays were performed in PBS supplemented with 20 µg/mL DHNA and/or 55 mM mannitol. Fe^{2+} was detected colorimetrically using 2 mM ferrozine. For *L. plantarum* inactivation, cells were incubated at 85 ℃ in PBS for 30 min prior to the assay. Significant differences were determined by one-way ANOVA with Tukey's post-hoc test (n = 3), *** $p \leq 0.001$. **(B)** Two-chambered electrochemical cell setup for measuring current generated by *L. plantarum*. **(C)** Current density production over time by *L. plantarum* in CDM supplemented with 20 µg/mL DHNA and/or 110 mM mannitol. The anode was polarized at $+0.2V_{Ag/AgCl}$. The avg ± stdev of three biological replicates is shown. See also Figure 1-figure supplement 1 and Figure 1-figure supplement 2 and related data in Figure 1 – Source data 1.

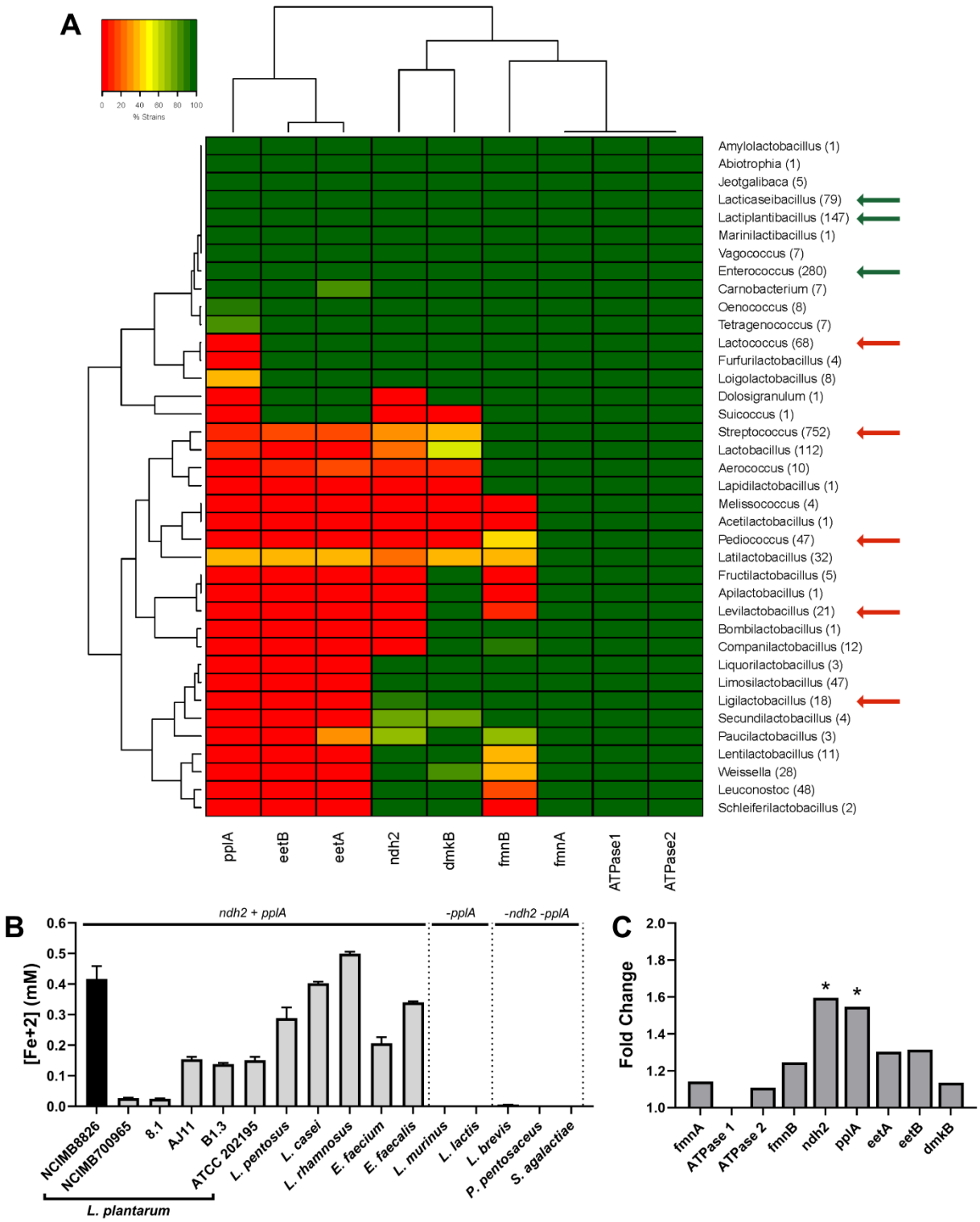
A
0 20 40 60 80 100
% Strains
Amylolactobacillus (1)
Abiotrophia (1)
Jeotgalibaca (5)
Lacticaseibacillus (79)
Lactiplantibacillus (147)
Marinilactibacillus (1)
Vagococcus (7)
Enterococcus (280)
Carnobacterium (7)
Oenococcus (8)
Tetragenococcus (7)
Lactococcus (68)
Furfurilactobacillus (4)
Loigolactobacillus (8)
Dolosigranulum (1)
Suicoccus (1)
Streptococcus (752)
Lactobacillus (112)
Aerococcus (10)
Lapidilactobacillus (1)
Melissococcus (4)
Acetilactobacillus (1)
Pediococcus (47)
Latilactobacillus (32)
Fructilactobacillus (5)
Apilactobacillus (1)
Levilactobacillus (21)
Bombilactobacillus (1)
Companilactobacillus (12)
Liquorilactobacillus (3)
Limosilactobacillus (47)
Ligilactobacillus (18)
Secundilactobacillus (4)
Paucilactobacillus (3)
Lentilactobacillus (11)
Weissella (28)
Leuconostoc (48)
Schleiferilactobacillus (2)
pplA
eetB
eetA
ndh2
dmkB
fmnB
fmnA
ATPase1
ATPase2
B
ndh2 + pplA
-pplA
-ndh2 -pplA
[Fe+2] (mM)
0.0
0.1
0.2
0.3
0.4
0.5
0.6
NCIMB8826
NCIMB700965
8.1
AJ11
B1.3
ATCC 202195
L. pentosus
L. casei
L. rhamnosus
E. faecium
E. faecalis
L. murinus
L. lactis
L. brevis
P. pentosaceus
S. agalactiae
L. plantarum
C
Fold Change
1.0
1.2
1.4
1.6
1.8
2.0
*
*
fmnA
ATPase 1
ATPase 2
fmnB
ndh2
pplA
eetA
eetB
dmkB

Figure 2. The FLEET genes *ndh2* and *pplA* are associated with iron reduction by LAB. (A) Heatmap showing the genera in the Lactobacillales order containing FLEET genes. Homology searches were conducted using tBLASTx for 1,788 complete LAB genomes in NCBI (downloaded 02/25/2021) against the *L. plantarum* NCIMB8826 FLEET locus. A match was considered positive with a Bit-score > 50 and an E-value of < 10^{-3}. Arrows designate genera tested for iron reduction activity; green = EET-active with Fe^{3+}, red = EET-inactive with Fe^{3+}. **(B)** Reduction of ferrihydrite in PBS with 20 μg/mL DHNA and 55 mM mannitol after growth in mMRS supplemented with 20 μg/mL DHNA and 1.25 mM ferric ammonium citrate. The avg ± stdev of three biological replicates per strain is shown. **(C)** Relative expression of NCIMB8826 FLEET locus genes in mMRS with 20 μg/mL DHNA and 1.25 mM ferric ammonium citrate compared to growth in mMRS. Significant differences in expression were determined by the Wald test (n = 3) with a Log_2 (fold change) > 0.5 and an FDR-adjusted p-value of < 0.05. See also Figure 2-figure supplement 1 and Figure 2-figure supplement 2 and related data in Figure 2–Source data 1.

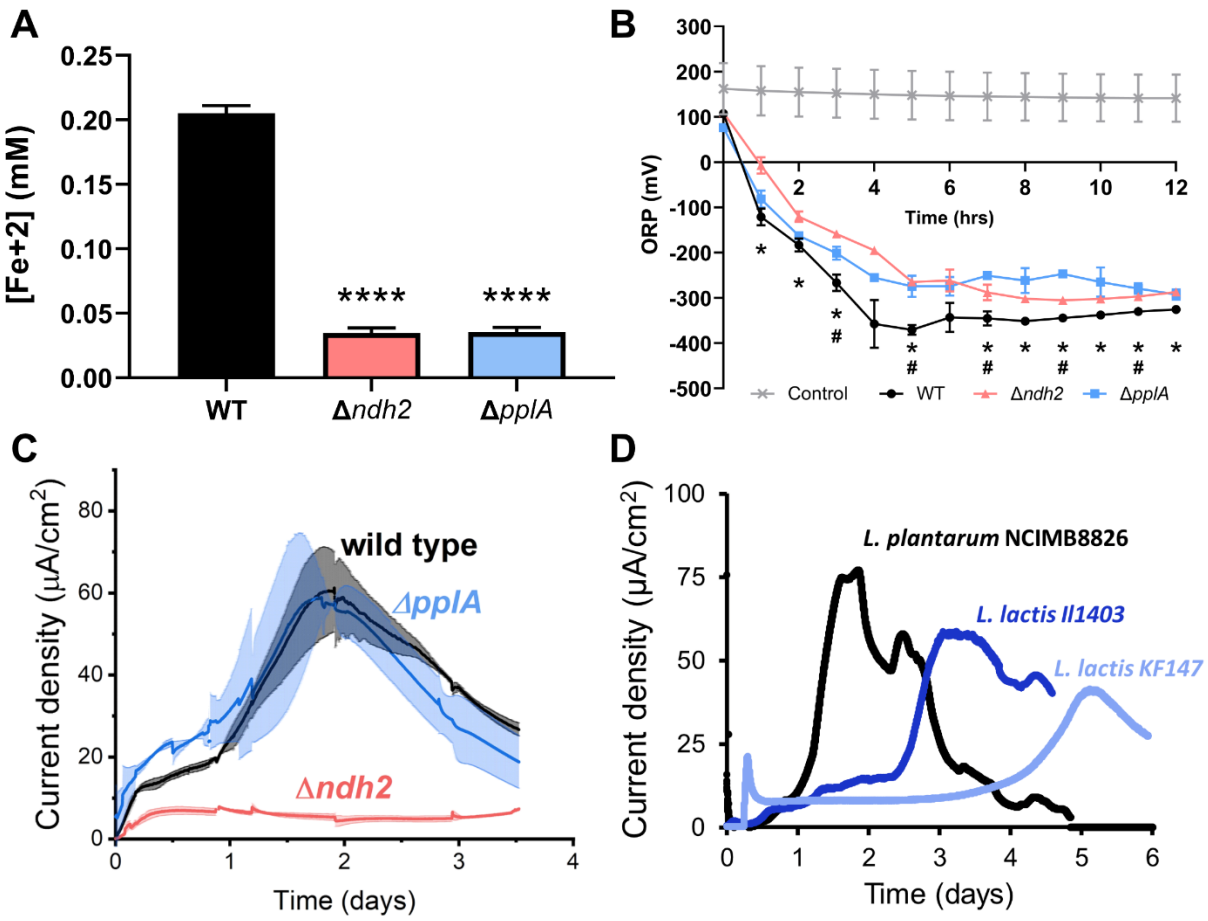

Figure 3. *L. plantarum* requires *ndh2* and conditionally *pplA* for EET. (A) Reduction of Fe^{3+} (ferrihydrite) to Fe^{2+} with wild-type *L. plantarum* or EET deletion mutants in the presence of 20 µg/mL DHNA and 55 mM mannitol after growth in mMRS supplemented with 20 µg/mL DHNA and 1.25 mM ferric ammonium citrate. Significant differences determined by one-way ANOVA with Dunnett's post-hoc test, **** $p \leq 0.0001$. **(B)** Redox potential of mMRS supplemented with 20 µg/mL DHNA and 1.25 mM ferric ammonium citrate after inoculation with wild-type *L. plantarum* or EET deletion mutants. Significant ORP differences between the wild-type and mutant strains determined by two-way RM ANOVA with Tukey's post-hoc test, * $p < 0.05$ (WT vs. Δ*ndh2*); # $p < 0.05$ (WT vs. Δ*pplA*). **(C)** Current density generated by wild-type *L. plantarum* and deletion mutants in mCDM supplemented with 20 µg/mL DHNA. The

avg ± stdev is shown. **(D)** Current density generated by *L. plantarum* and two *L. lactis* strains lacking *pplA* in mCDM. For *L. plantarum,* the mCDM was supplemented with 20 µg/mL DHNA. The data correspond to the average of two (D) or three (A to C) biological replicates per strain. See also Figure 3-figure supplement 1 and Figure 3-figure supplement 2 and related data in Figure 3– Source data 1.

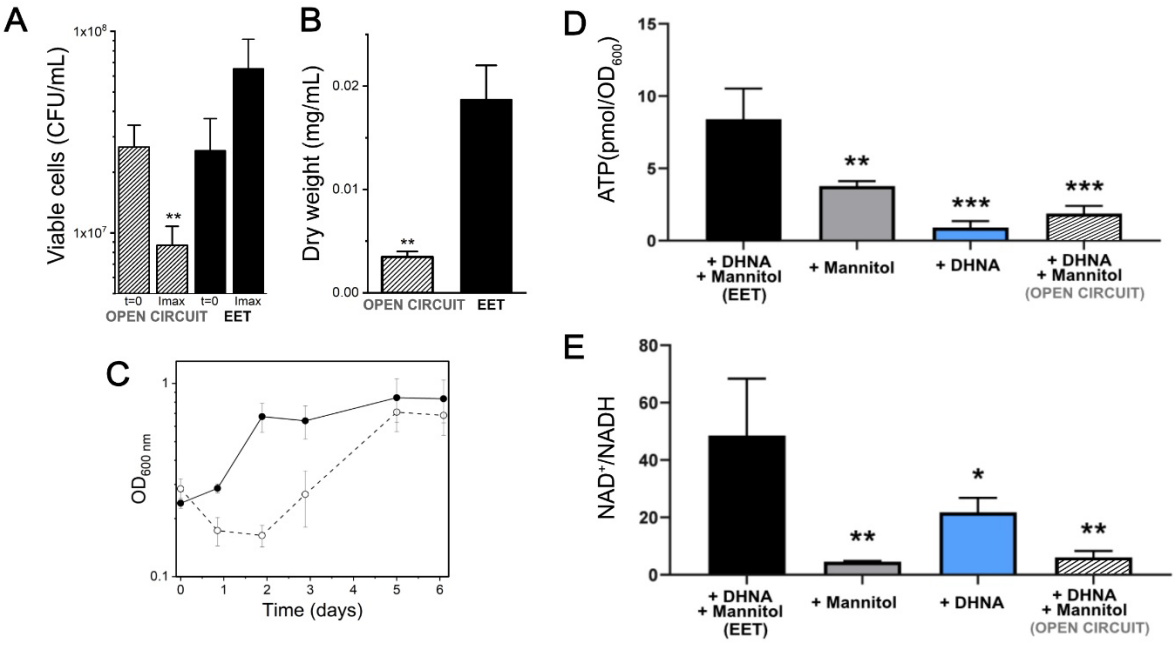

Figure 4. Growth, ATP, and redox balance of *L. plantarum* changes when an anode is provided as an extracellular electron acceptor. These measurements and the current density plot shown in Fig 1C are from the same experiment. **(A)** Viable cells and **(B)** dry weight at the point of maximum current density under current circulating conditions (EET) and at open circuit conditions (OC) at the same time point. **(C)** Change in cell numbers measured by OD_{600} over time in the bioreactors under EET (continuous line) and OC conditions (dotted lines). **(D)** ATP production per OD_{600} unit and **(E)** NAD^+/NADH ratios at the point of maximum current density.

The bioreactors were shaken vigorously to dislodge cells before sampling. The avg ± stdev of three biological replicates is shown. Significant differences were determined by one-way ANOVA with (**A and B**) Dunn-Sidak post-hoc test (n = 3) and **(D and E)** Dunnett's post-hoc test (n = 3), * $p < 0.05$; ** $p < 0.01$; *** $p < 0.001$; **** $p < 0.0001$. See also Figure 1-figure supplement 4 and Figure 4-figure supplement 3 and related data in Figure 4– Source data 1.

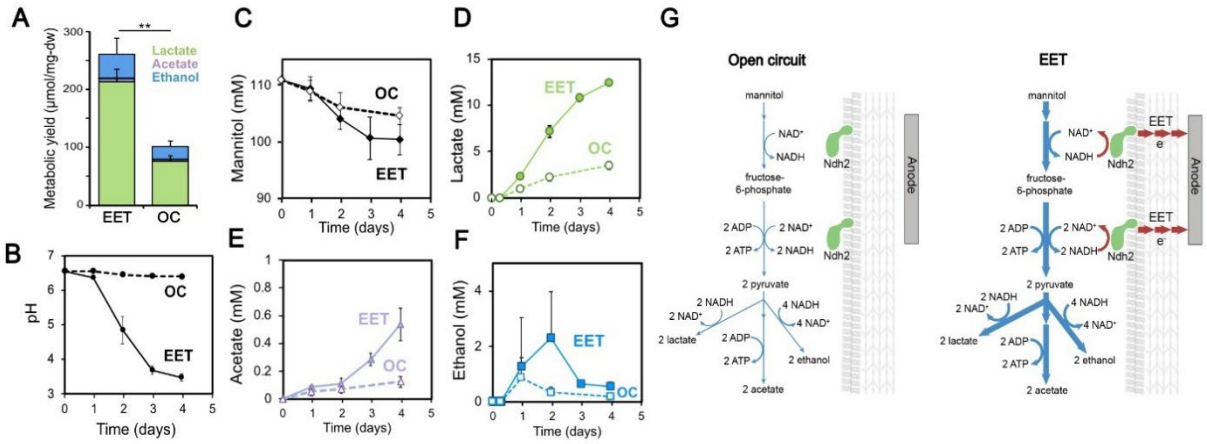

Figure 5. Fermentation fluxes are increased when an anode is provided as an extracellular electron acceptor. Results are from the same set of experiments as the current density plot shown in Fig 3C. **(A)** Metabolic yields of *L. plantarum* end-fermentation products under open circuit conditions (OC) and current circulating conditions (EET) in mCDM supplemented with 20 µg/mL DHNA. **(B)** pH measurements and **(C)** mannitol, **(D)** lactate, **(E)** acetate, and **(F)** ethanol concentrations over time under OC and EET conditions. **(G)** Schematic of proposed model for NADH regeneration during fermentation of mannitol in the presence of an anode as electron sink for *L. plantarum*. The avg ± stdev of three biological replicates is shown. Significant differences were determined by One-way ANOVA with Dunn-Sidak post-hoc (n = 3), ** $p \leq 0.01$. See also Figure 5-figure supplement 1 and Figure 5-figure supplement 2 and related data in Figure 5– Source data 1.

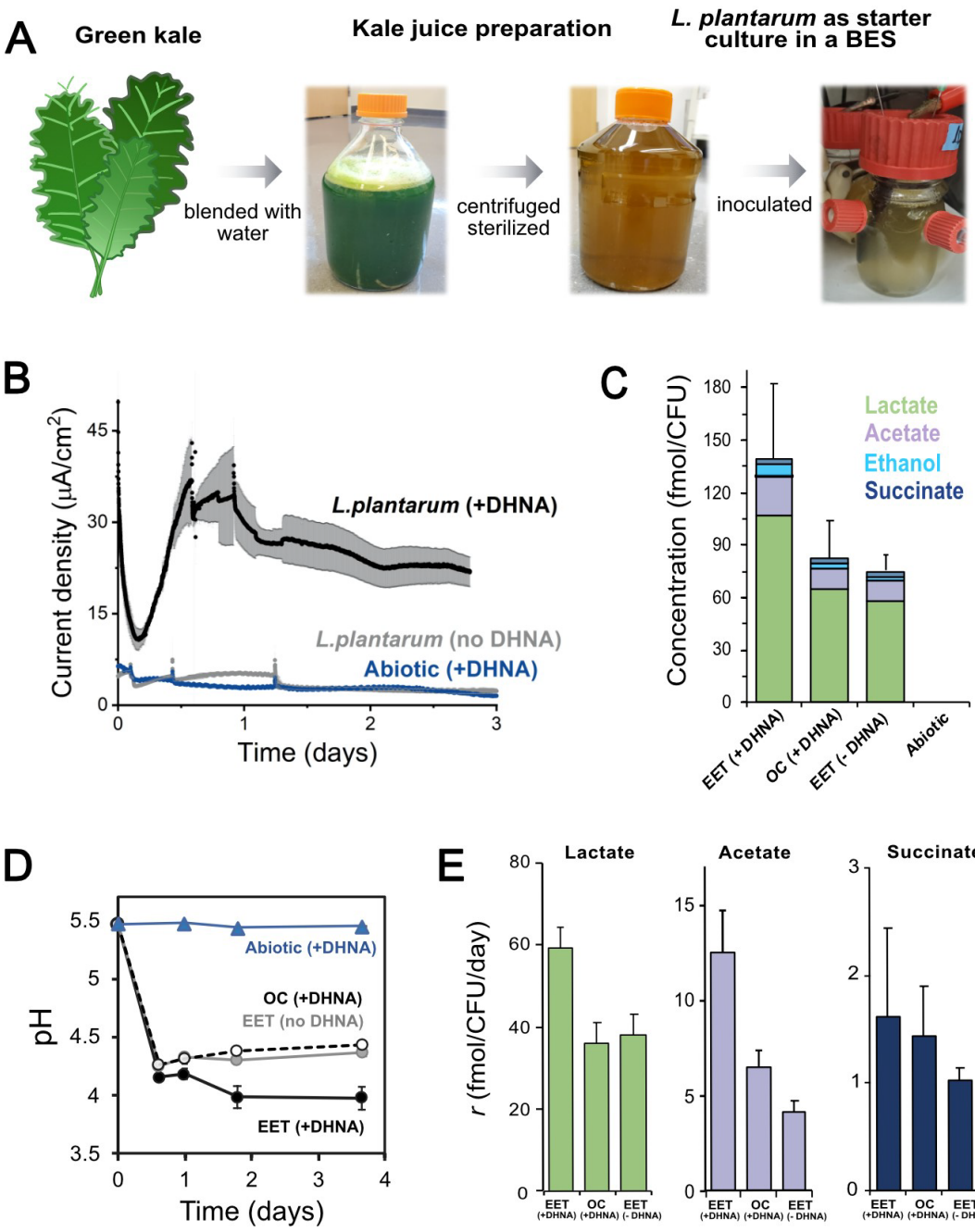

Figure 6. EET in a kale juice increases the production of fermentation end products. (A) Preparation of kale juice medium used for fermentation in bioelectrochemical reactors**. (B)** Current density production measured from kale juice medium over time in the presence of *L. plantarum* and 20 μg/mL DHNA, no DHNA, or under abiotic conditions with addition of 20

μg/mL DHNA. The anode polarization was maintained at 0.2 $V_{Ag/AgCl}$. **(C)** Normalized total quantities of the metabolites detected per cell (CFU_{max} used for calculations). **(D)** pH measurements over time under different conditions tested on a second set of kale juice fermentations performed under the same conditions. **(E)** Production rate per viable cell, *r*, of lactate, acetate, and succinate. The avg $\pm$ stdev of three biological replicates is shown. See also Figure 6-figure supplement 1 and related data in Figure 6– Source data 1.

Supplemental

Supplement file 1. Data used for calculating the bioenergetic balances.

	Mannitol consumed	Lactic acid	Acetic acid	Ethanol	Succinic acid	Pyruvic acid	Formic acid	Dry weight	Electrons to anode
	mM	mM	mM	mM	mM	mM	mM	g/L	mM
EET (anode)	10.05 ± 2.58	12.41 ± 0.33	0.55 ± 0.13	2.12 ± 1.38	0.021 ± 0.006	0.86 ± 0.16	0.07 ± 0.01	0.052 ± 0.04	12.87 ± 0.96
OCP	5.28±1.5	3.46 ± 0.4	0.12 ± 0.04	1.01 ± 0.49	0.01 ± 0.00	0.83 ± 0.15	0.09 ± 0.08	0.046 ± 0.009	-

The following standards were included in the HPLC measurements: acetate, formate, pyruvate, malate, lactate, succinate, oxalacetate, fumarate, ethanol, acetoin, butanediol, mannitol and glucose. No gaseous products were measured.
Carbon recovery-EET conditions (fermentation products+biomass): 79±5 %
Carbon recovery-OC conditions (fermentation products+biomass): 55±5 %
A 53% of the biomass was considered to be C, as previously reported (Shuler and Kargi, 2002)

Methods to calculations of NADH regeneration

The concentration of NADH regenerated is calculated as the difference between the NADH consumed and produced through EET and the formation of fermentation products. Calculating the concentration of NADH consumed is straightforward. We assume NADH is consumed as a result of both fermentative pathways associated with substrate-level phosphorylation and EET pathways. For the substrate-level phosphorylation pathways, we assume that 1 mol of lactate, ethanol, or succinate each consume 1, 2 or 2 mol of NADH, respectively. For EET pathways, the concentration of NADH consumed was calculated by first determining the moles of electrons harvested by the anode:

$$mol\ electrons = charge\ (A*s) *\ Faraday\ constant\ (96485\ \frac{mol\ e}{A*s})$$

Eqn 1

where

$$charge = current\ (A) * time\ (s) = current\ density\ (\frac{A}{cm^2}) *\ area\ anode\ (cm^2)\ *\ time\ (s)$$

Eqn 2

Then, the concentration of NADH regenerated was calculated using the volume of the reactor and the fact that 2 electrons are released in the oxidation of NADH to NAD^+ basis:

$$[NADH] = mol\ electrons * 2\ \frac{mole\ NADH}{mol\ electrons} * \frac{1}{0.15\ L\ reactor}$$

Eqn 3

Because the amount of mannitol consumed cannot be completely accounted for by biomass and fermentation products, there are two different assumptions that can be made to calculate the NADH produced. These two assumptions represent lower and upper bounds on the concentration of NADH regenerated. Using these bounds, we provide a range of NADH concentrations in Table 1.

Method 1: Establishing a lower bound of NADH regenerated

This method assumes that the production or consumption of NADH is only due to formation of fermentation products. Since 79% of the carbon in consumed mannitol was recovered in fermentation products and biomass under EET conditions, this method accounts for the majority of the NADH produced. However, this method does not account for any undetected metabolites and may underestimate the total NADH produced. Thus, we consider this calculation to be a lower bound on the amount of NADH regenerated.

This method uses the known stoichiometry of the fermentation pathways (McFeeters and Chen, 1986) to assume 1.5 mol of NADH is produced for each mole of lactate, acetate, ethanol, pyruvate, succinate and formate detected. Using this method, we estimate that 96% of the NADH is reoxidized under EET conditions. Of this fraction, 63% of the NADH is reoxidized by substrate-level phosphorylation and 27% by EET. In contrast, under OC condition, 69% of the NADH produced is reoxidized via substrate-level phosphorylation.

Method 2: Establishing an Upper Bound of NADH regenerated

This method assumes NADH production is directly related to disappearance of mannitol. Thus, this method overestimates this fraction since a proportion of this mannitol will be used for biomass synthesis and will not lead to NADH generation.

This method uses the known stoichiometry of mannitol oxidation to assume that 3 mol of NADH is produced for each mole of mannitol that is consumed. Calculations performed using this method estimate that 77% of the NADH is reoxidized under EET conditions. Of this fraction, 55% of the NADH is regenerated through substrate-level phosphorylation and 21% via EET. In contrast, 66% of the NADH produced is reoxidized via substrate-level phosphorylation under OC conditions.

Supplement file 2. Comparison of the energy metabolism discovered in this study with fermentation in LAB and anaerobic respiration in *Geobacter* spp.

	Homofermentation in LAB	Respiration in LAB	Anaerobic EET respiration in *Geobacter* spp.	Hybrid metabolism in LAB (this study)
Reduction of insoluble extracellular electron acceptor	No	No	Yes 4-8 mA/mg protein at peak (Marsili et al., 2010; Rose and Regan, 2015)	Both - soluble and insoluble 1.5 mA/mg- protein (at peak[a])
NADH:quinone oxidoreductase is required for reduction of electron acceptor	No (Tachon et al., 2010)	Ndh1 (R. Brooijmans et al., 2009b, 2009b)	Yes Ndh1 (proton pumping) (Chan et al., 2017)	Yes Ndh2 (non-proton pumping)
Electron acceptor transcriptionally upregulates NADH dehydrogenase	No (this study)	No [aerobic respiration] (Pedersen et al., 2008)	Yes (Holmes et al., 2006)	Yes (with DHNA)
NAD^+/NADH ratio	~1 for glucose (Guo et al., 2017, p. 201) ~5 for mannitol (this study)	Near-zero for lactose (Johanson et al., 2020)	10 (Fe^{3+}) 10-100 (anode) (Rose and Regan, 2015; Song et al., 2016)	260 (Fe^{3+}) 45 (anode)
Fraction of electrons on electron acceptor	40-98% pyruvate (Dirar and Collins, 1972)	33% (nitrate) (R. J. W. Brooijmans et al., 2009, p. 1)	75-90% anode (Speers and Reguera, 2012)	20% anode 48% pyruvate
Metabolic flux is primarily through	Fermentative pathway (Bintsis, 2018)	Mixed-acid fermentation (R. Brooijmans et al., 2009a)	TCA cycle (Galushko and Schink, 2000; Mahadevan et al., 2006)	Fermentative pathway - Mixed acid

ATP yield per substrate	~2-3 mol ATP/mol glucose for homolactic (Dirar and Collins, 1972) 0.75 mol ATP/mol mannitol (this study)	3.3-3.9 mol ATP/mol lactose (Johanson et al., 2020)	~1.5 mol ATP/mol substrate[b] (Mahadevan et al., 2006)	1.6 mol ATP/mol mannitol

[a] Calculated assuming that 50% of the dry cell weight is protein. [b] *G. sulfurreducens* uses acetate as its electron donor. Since acetate is a 2 carbon electron donor, ATP yield is expressed per mol of a 6 carbon substrate.

Supplement file 3. Strains and plasmids used in this study.

Strains	Isolation Source / Description	Reference
L. plantarum NCIMB8826	Human saliva	(Dandekar, 2019)
L. plantarum NCIMB8826-R	Rifampicin-resistant mutant of NCIMB8826	(Yin et al., 2018)
L. plantarum MLES100	Deletion mutant of NCIMB8826 lacking *ndh2*	This study
L. plantarum MLES101	Deletion mutant of NCIMB8826 lacking *pplA*	This study
L. plantarum MLEY100	Deletion mutant of NCIMB8826 lacking *narGHIJ*	This study
L. plantarum B1.3	Brown flour teff injera	(Yu et al., 2021)
L. plantarum AJ11	Fermented olives; commercial fermentation	(Yu et al., 2021)
L. plantarum 8.1	Wheat boza	(Yu et al., 2021)
L. plantarum ATCC 202195	Human stool	(Wright et al., 2020)
L. plantarum NCIMB700965	Cheese	(Heeney and Marco, 2019)
L. pentosus BGM48	Fermented olives	(Golomb et al., 2013)
L. casei BL23	Dairy products	(Mazé et al., 2010)
L. brevis ATCC 367	Silage	(Makarova et al., 2006)
L. lactis KF147	Mung bean sprouts	(Siezen et al., 2010)
L. lactis IL1403	Cheese	(Bolotin et al., 2001)
L. rhamnosus GG	Human intestine	(Kankainen et al., 2009)
L. murinus ASF361	Mice	(Wannemuehler et al., 2014)
E. faecalis ATCC 29212	Urine	(Minogue et al., 2014)
E. faecium ATCC 8459	Cheese	(Kopit et al., 2014)
P. pentosaceus ATCC 25745	Plants	(Makarova et al., 2006)
S. agalactiae ATCC 27956	Bovine udder infection	(McDonald and McDonald, 1976)
E. coli DH5α	*fhuA2 lac(del)U169 phoA glnV44 Φ80' lacZ(del) M15 gyrA96 recA1 relA1 endA1 thi−1 hsdR17,* amplification of cloning vector	(Taylor et al., 1993)
Plasmids		
pRV300	EryR AmpR, *E. coli* Ori pMB1, integrative vector	(Leloup et al., 1997)
pRV300:ndh2	pRV300 derivative used for deletion of *ndh2*	This study
pRV300:pplA	pRV300 derivative used for deletion of *pplA*	This study
pRV300:narG	pRV300 derivative used for deletion of *narG*	This study

Supplement file 4. Chemically defined medium.

CDM component [a]	Final concentration (g/L)
Buffers and salts	
MOPS (3-(N-morpholino)propanesulfonic acid)	8.371
K_2HPO_4	0.871
NH_4Cl	1.070
Na_2SO_4	1.420
Metals	
$MgCl_2 * 6H_2O$	0.203
$MnCl_2 * 4H_2O$	0.001
$FeSO_4 * 7H_2O$	0.014
Amino acids	
Casamino acids	3.000
Cysteine-HCl * H_2O	0.145
Tryptophan	0.050
Wolfe's Vitamins[b]	
Pyridoxine HCl	0.002
Thiamine HCl	0.001
Riboflavin	0.001
Nicotinic acid	0.001
Calcium D-(+)-pantothenate	0.001
p-Aminobenzoic acid	0.001
Thioctic acid (α-Lipoic acid)	0.001
Biotin	0.0004
Folic acid	0.0004
Vitamin B12	0.00002
Wolfe's Minerals[c]	
Nitrilotriacetic acid (NTA)	0.3
$MgSO_4 * 7H_2O$	0.6
$MnSO_4 * H_2O$	0.1
NaCl	0.2
$FeSO_4 * 7H_2O$	0.02
$CoCl_2 * 6H_2O$	0.02
$CaCl_2$	0.02
$ZnSO_4 * 7H_2O$	0.02
$CuSO_4 * 5H_2O$	0.002
$AlK(SO)_4 * 12H_2O$	0.002
H_2BO_3	0.002
$Na_2MoO_4 * 2H_2O$	0.002

[a] All solutions were prepared separately and sterile filtered through a 0.22 μm filter before combining. Glucose or mannitol was also supplemented at 22.520 g/L or 22.772 g/L, respectively.

[b] pH adjusted to 11 before sterile filtering.

[c] After NTA addition, pH adjusted to 8 before adding remaining components and sterile filtering.

Supplement file 5. Primers developed for this study.

Primer ID	Sequence[a]	Description	Use
ndh2-A	CCG**GAATTC**GGCGGACACATA CTTGGTC	Upstream of *ndh2*	Deletion construction (EcoRI cut site)
ndh2-B	*GAAGCAGCTCCAGCCTACAC*TCT CATTACGACGGTGTTAAAAC	Upstream of *ndh2*	Deletion construction (SOEing PCR overlap region)
ndh2-C	*GTGTAGGCTGGAGCTGCTTC*GCA TCGAGGTTTGAACGGAA	Downstream of *ndh2*	Deletion construction (SOEing PCR overlap region)
ndh2-D	GGG**GAGCTC**TGCCGTTCTTGTT CACTTGG	Downstream of *ndh2*	Deletion construction (SacI cut site)
ndh2-Check-F	TCGTGGCCTTAATTTCAACC	Upstream of *ndh2* deletion	Confirmation of gene deletion
ndh2-Check-R	CCGGCGTTTTGTAATTGTTCC	Downstream of *ndh2* deletion	Confirmation of gene deletion
pplA-A	TAAGCA**GAATTC**CCGTTCGGTA GCAACTTCAT	Upstream of *pplA*	Deletion construction (EcoRI cut site)
pplA-B	*GAAGCAGCTCCAGCCTACAC*TCC CACTCCTAACCTTTTTGT	Upstream of *pplA*	Deletion construction (SOEing PCR overlap region)
pplA-C	*GTGTAGGCTGGAGCTGCTTC*GCT GAGGGCCTTTTGTTTTT	Downstream of *pplA*	Deletion construction (SOEing PCR overlap region)
pplA-D	TAAGCA**GAGCTC**TTAAACGCC CCAGCTAACAC	Downstream of *pplA*	Deletion construction (SacI cut site)
pplA-Check-F	TTGCGTAAACACCAGCAAAC	Upstream of *pplA* deletion	Confirmation of gene deletion
pplA-Check-R	GCTGCTTTGATCATTGGGTA	Downstream of *pplA* deletion	Confirmation of gene deletion
narG-A	GCGAAA**GTCGAC**AAGCAGCCA GTCAGTAATAG	Upstream of *narG*	Deletion construction (SalI cut site)

narG-B	*GAAGCAGCTCCAGCCTACA*CTCA CCGATAAGACCTCCTTT	Upstream of *narG*	Deletion construction (SOEing PCR overlap region)
narG-C	*GAAGCAGCTCCAGCCTACA*GCAC AAATTGGGATGGTCTT	Downstream of *narG*	Deletion construction (SOEing PCR overlap region)
narG-D	GCGAAA**CCGCGG**CATCACGCT TATACATCGCC	Downstream of *narG*	Deletion construction (SacII cut site)
narG-Check-F	TACATTGCGTTAGGACCGAA	Upstream of *narG*	Confirmation of gene deletion
narG-Check-R	CCATAACCACCGACCATTTG	Downstream of *narG*	Confirmation of gene deletion
rpoB-F	CGATGACTCTAACCGTGC	*rpoB*	RT-PCR
rpoB-R	CAAGGCAATCCCTGAGTC	*rpoB*	RT-PCR
ndh2-F	CCGGCTGTCCAGATTAACGT	*ndh2*	RT-PCR
ndh2-R	CGAAGCAGCGCCGACTATTA	*ndh2*	RT-PCR
pplA-F	GCTCTGCCGCTACTGGTAAC	*pplA*	RT-PCR
pplA-R	TCGCACCAGTCACAACATCA	*pplA*	RT-PCR

[a] Restriction sites for enzymes are in bold, SOEing PCR overlap sequences are italicized.

Supplement file 6. Transcriptome read counts, alignment rate, and gene assignment rate.

Sample ID	Total paired reads	Paired reads passed quality filtering[a]	Reads passed quality control (%)	Reads aligned to *Lp*[b]	Alignment (%)	Assigned reads[c]	Read assignment rate (%)	rRNA/ tRNA/ncRNA Reads	Remaining reads for DE[d]	Remaining reads for DE[d] (%)
mMRS-1	3.91E+07	3.40E+07	86.8	3.38E+07	99.6	30287036	89.6	10670771	19616265	64.8
mMRS-2	3.96E+07	3.46E+07	87.2	3.44E+07	99.5	29762763	86.6	11736601	18026162	60.6
mMRS-3	3.43E+07	3.03E+07	88.4	3.02E+07	99.5	26518101	87.8	13822383	12695718	47.9
DHNA-1	4.13E+07	3.59E+07	87.0	3.57E+07	99.5	31800634	89.0	11364096	20436538	64.3
DHNA-2	3.83E+07	3.35E+07	87.5	3.33E+07	99.5	29672126	89.0	9933102	19739024	66.5
DHNA-3	3.99E+07	3.49E+07	87.5	3.47E+07	99.6	30954603	89.1	14806368	16148235	52.2
Iron-1	3.31E+07	2.88E+07	86.8	2.86E+07	99.4	25147375	87.9	7180253	17967122	71.4
Iron-2	2.47E+07	2.18E+07	88.2	2.16E+07	99.4	18943484	87.5	4976026	13967458	73.7
Iron-3	3.10E+07	2.67E+07	86.1	2.66E+07	99.7	23221100	87.4	7577947	15643153	67.4
Both-1	3.66E+07	3.03E+07	82.6	3.01E+07	99.6	26811334	88.9	12603853	14207481	53.0
Both-2	4.39E+07	3.86E+07	87.9	3.85E+07	99.7	34163533	88.8	16841230	17322303	50.7
Both-3	3.58E+07	3.11E+07	86.9	3.10E+07	99.7	27593814	89.0	14617870	12975944	47.0

[a] Paired-end reads filtered through Trimmomatic (ver. 0.39)
[b] Paired-end reads aligned to *L. plantarum* genome with Bowtie2 (ver. 2.3.5)
[c] Reads assigned to *L. plantarum* genes with FeatureCounts (ver. 1.6.4)
[d] Differential expression analyses done through DEseq2 on DEBrowser (ver. 1.14)

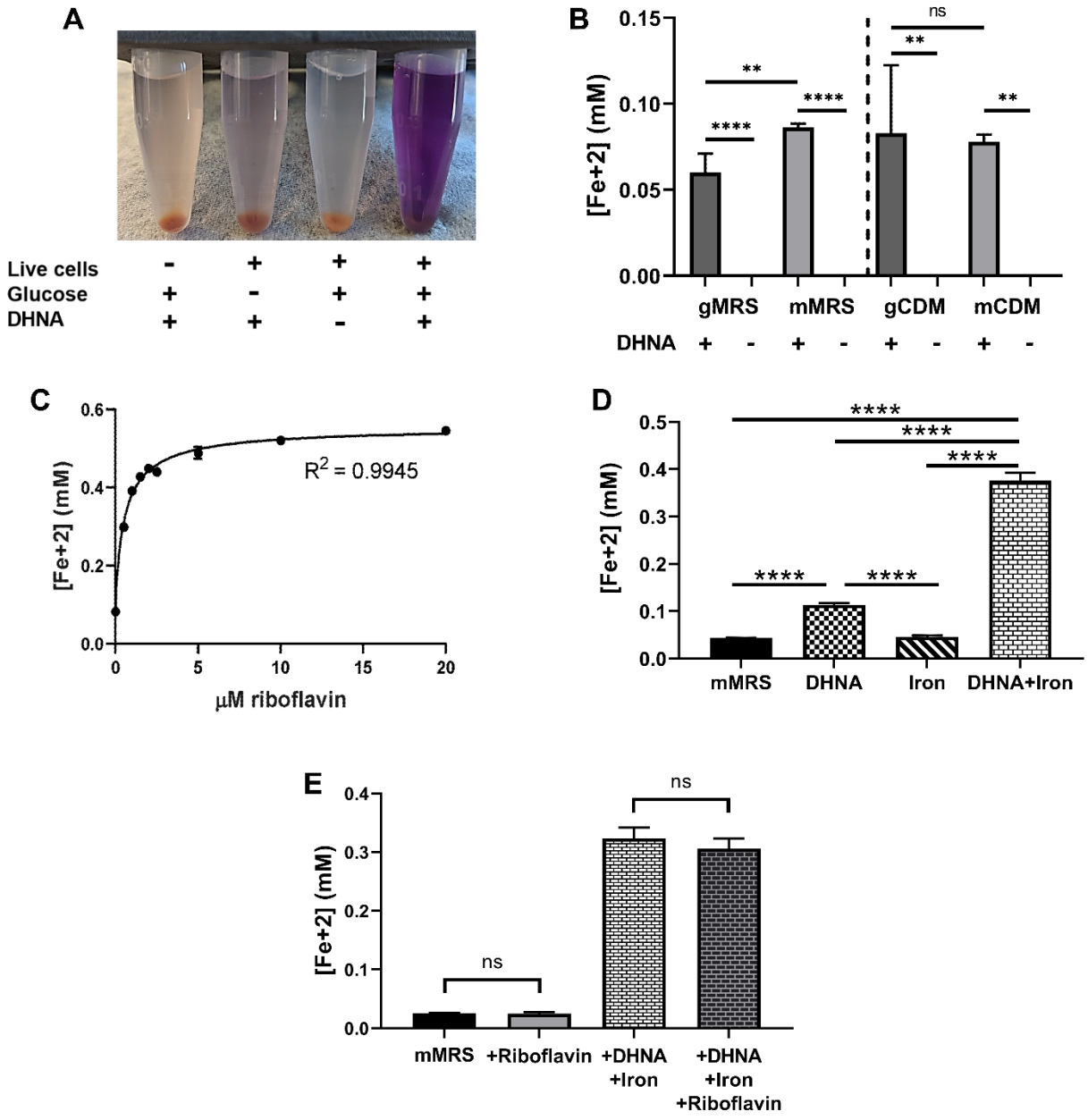

Figure 1-figure supplement 1. Iron reduction by *L. plantarum* is dependent upon DHNA, carbon source, and riboflavin. (A) Reduction of Fe^{3+} (ferrihydrite) to Fe^{2+} by *L. plantarum* NCIMB8826 after growth in MRS with glucose (gMRS). The assays were performed in PBS supplemented with 20 µg/mL DHNA and/or 55 mM glucose. For *L. plantarum* inactivation, cells were incubated at 85 ℃ in PBS for 30 min prior to the assay. **(B)** Reduction of ferrihydrite by *L.*

plantarum after growth in MRS with glucose (gMRS) or mannitol (mMRS) or CDM with glucose (gCDM) or mannitol (mCDM). The ferrihydrite reduction assays were performed in PBS supplemented with 20 µg/mL DHNA and the corresponding carbon source (55 mM glucose or mannitol). **(C)** Reduction of ferrihydrite by *L. plantarum* in the presence of 20 µg/mL DHNA, 55 mM mannitol, and increasing concentrations of riboflavin. **(D and E)** Reduction of ferrihydrite by *L. plantarum* after growth to mid-exponential phase in mMRS with or without the supplementation of 20 µg/mL DHNA, iron (1.25 mM ferric ammonium citrate), and/or 2.5 µM riboflavin. Significant differences in iron reduction were determined by one-way ANOVA with Tukey's post-hoc test (n = 3), ** $p \leq 0.01$; **** $p \leq 0.0001$. The avg $\pm$ stdev of three biological replicates is shown. See related data in Figure 1 Supplement 1 - Source Data 1.

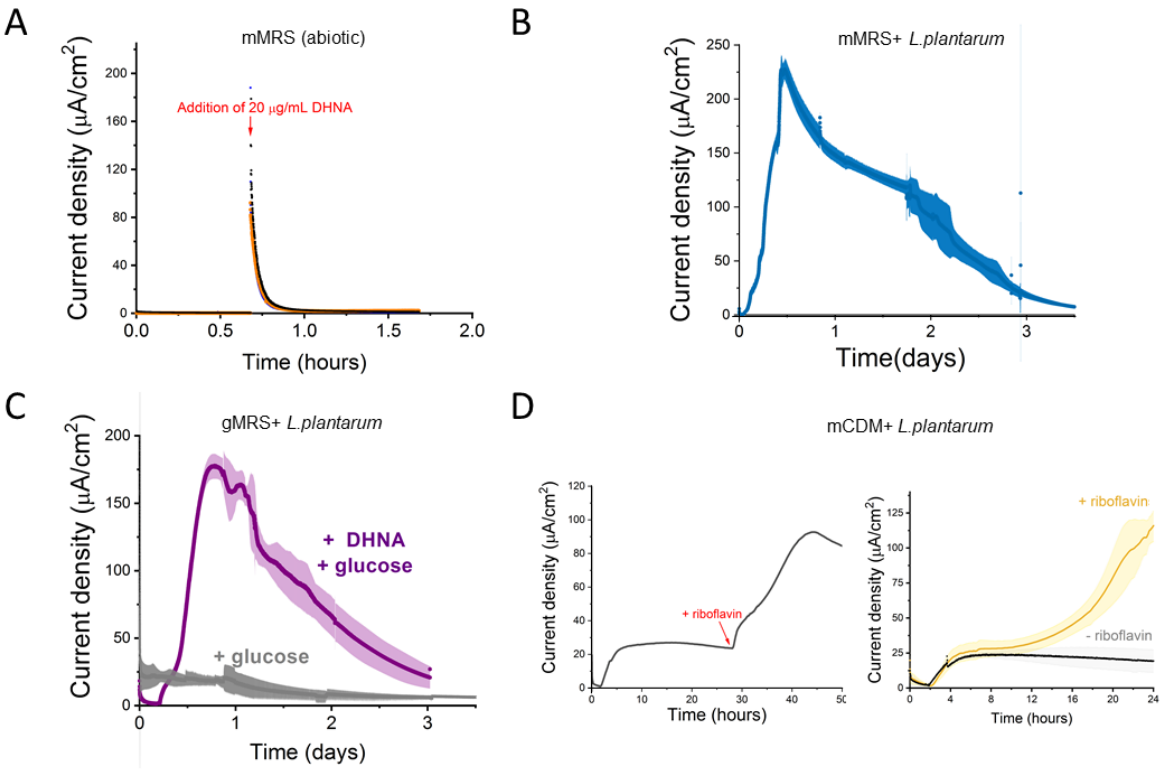

Figure 1–figure supplement 2. Current production by *L. plantarum* is a biotic process dependent on DHNA, carbon source, and riboflavin. (A) Abiotic current density response in bioelectrochemical reactors over time in mannitol-containing MRS (mMRS) upon DHNA (20 µg/mL) addition. Current density produced by *L. plantarum* in **(B)** mMRS with 20 µg/mL DHNA or **(C)** gMRS with 20 µg/mL DHNA. **(D)** Effect of riboflavin addition on current density production by *L. plantarum* in mannitol-containing CDM (mCDM) with 20 µg/mL DHNA. The avg ± stdev of three biological replicates is shown. See related data in Figure 1 Supplement 2 - Source Data 1.

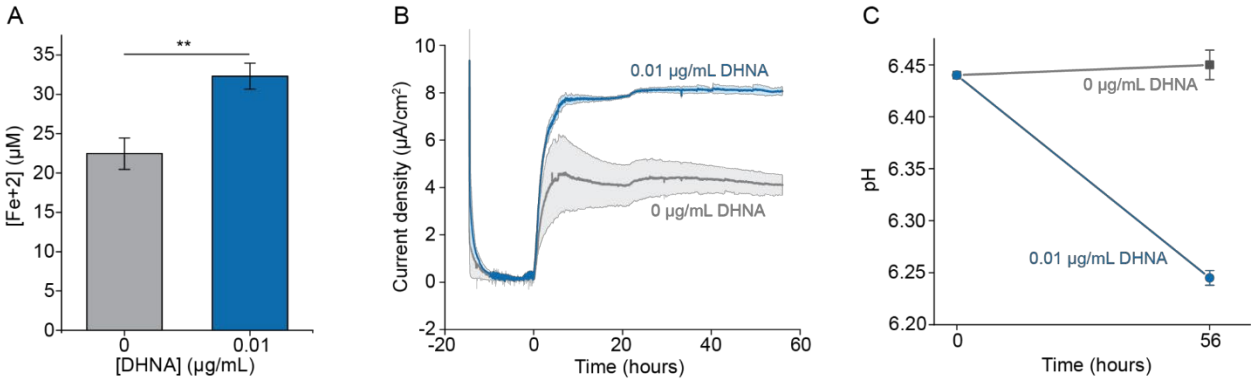

Figure 1–figure supplement 3. A sub-physiological concentration of DHNA stimulates EET in *L. plantarum*. Reduction of Fe^{3+} (iron III oxide nanoparticle, primarily γ-Fe_2O_3) to Fe^{2+} **(A)** and current production **(B)** by *L. plantarum* when 0.01 µg/mL DHNA was supplied. **(C)** pH measurements at 0 and 56 h for the experiment shown in **(B)**. The avg ± stdev is shown. Three replicates for **(A)** and two replicates for **(B)** and **(C)**. Significant differences were determined by two-tailed t-test, **$p \leq 0.01$. See related data in Figure 1 Supplement 13- Source Data 1.

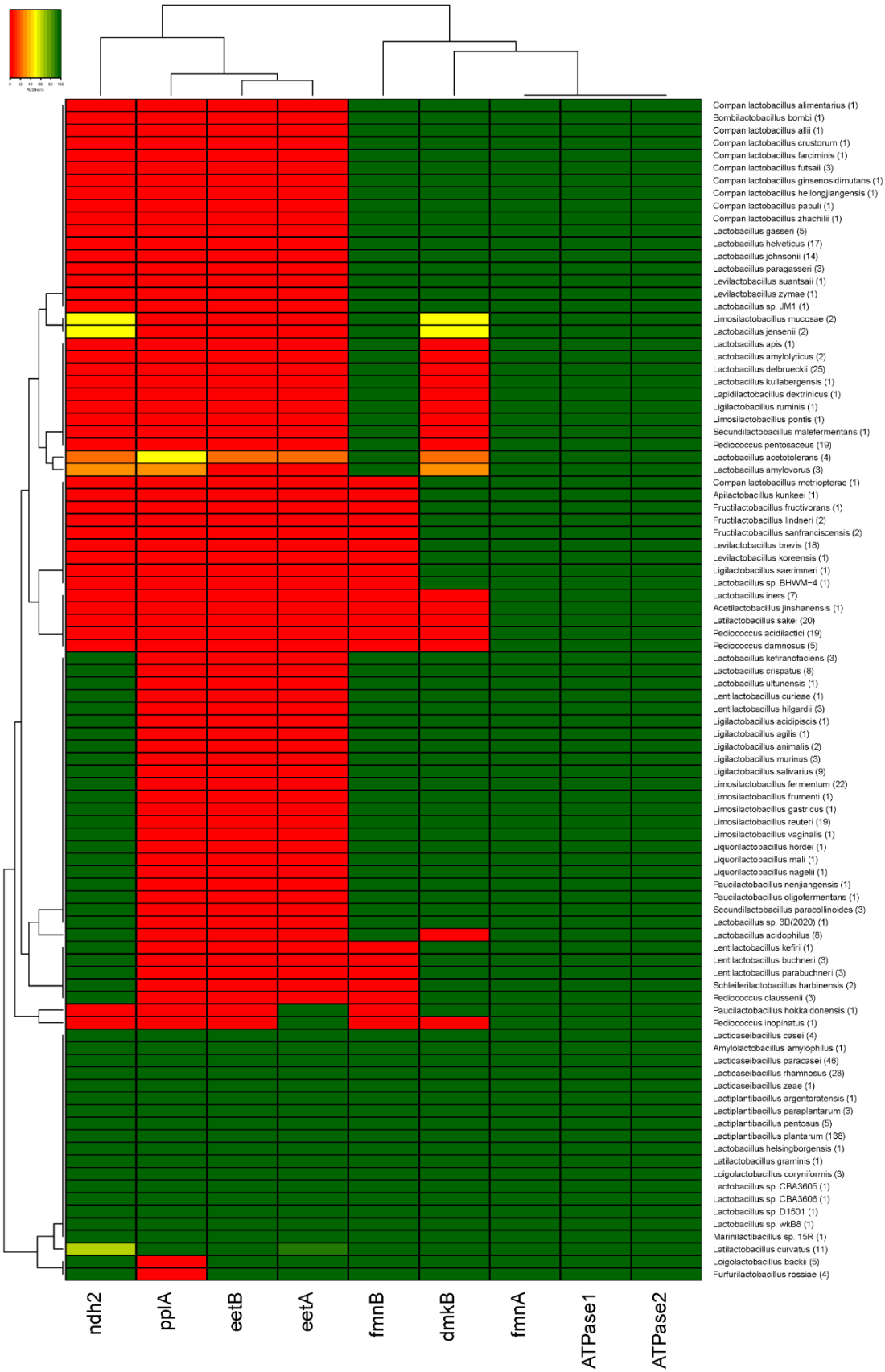
Companilactobacillus alimentarius (1)
Bombilactobacillus bombi (1)
Companilactobacillus allii (1)
Companilactobacillus crustorum (1)
Companilactobacillus farciminis (1)
Companilactobacillus futsaii (3)
Companilactobacillus ginsenosidimutans (1)
Companilactobacillus heilongjiangensis (1)
Companilactobacillus pabuli (1)
Companilactobacillus zhachili (1)
Lactobacillus gasseri (5)
Lactobacillus helveticus (17)
Lactobacillus johnsonii (14)
Lactobacillus paragasseri (3)
Levilactobacillus suantsaii (1)
Levilactobacillus zymae (1)
Lactobacillus sp. JM1 (1)
Limosilactobacillus mucosae (2)
Lactobacillus jensenii (2)
Lactobacillus apis (1)
Lactobacillus amylolyticus (2)
Lactobacillus delbrueckii (25)
Lactobacillus kullabergensis (1)
Lapidilactobacillus dextrinicus (1)
Ligilactobacillus ruminis (1)
Limosilactobacillus pontis (1)
Secundilactobacillus malefermentans (1)
Pediococcus pentosaceus (19)
Lactobacillus acetotolerans (4)
Lactobacillus amylovorus (3)
Companilactobacillus metriopterae (1)
Apilactobacillus kunkeei (1)
Fructilactobacillus fructivorans (1)
Fructilactobacillus lindneri (2)
Fructilactobacillus sanfranciscensis (2)
Levilactobacillus brevis (18)
Levilactobacillus koreensis (1)
Ligilactobacillus saerimneri (1)
Lactobacillus sp. BHWM-4 (1)
Lactobacillus iners (7)
Acetilactobacillus jinshanensis (1)
Latilactobacillus sakei (20)
Pediococcus acidilactici (19)
Pediococcus damnosus (5)
Lactobacillus kefiranofaciens (3)
Lactobacillus crispatus (8)
Lactobacillus ultunensis (1)
Lentilactobacillus curieae (1)
Lentilactobacillus hilgardii (3)
Ligilactobacillus acidipiscis (1)
Ligilactobacillus agilis (1)
Ligilactobacillus animalis (2)
Ligilactobacillus murinus (3)
Ligilactobacillus salivarius (9)
Limosilactobacillus fermentum (22)
Limosilactobacillus frumenti (1)
Limosilactobacillus gastricus (1)
Limosilactobacillus reuteri (19)
Limosilactobacillus vaginalis (1)
Liquorilactobacillus hordei (1)
Liquorilactobacillus mali (1)
Liquorilactobacillus nagelii (1)
Paucilactobacillus nenjiangensis (1)
Paucilactobacillus oligofermentans (1)
Secundilactobacillus paracollinoides (3)
Lactobacillus sp. 3B(2020) (1)
Lactobacillus acidophilus (8)
Lentilactobacillus kefiri (1)
Lentilactobacillus buchneri (3)
Lentilactobacillus parabuchneri (3)
Schleiferilactobacillus harbinensis (2)
Pediococcus claussenii (3)
Paucilactobacillus hokkaidonensis (1)
Pediococcus inopinatus (1)
Lacticaseibacillus casei (4)
Amylolactobacillus amylophilus (1)
Lacticaseibacillus paracasei (46)
Lacticaseibacillus rhamnosus (28)
Lacticaseibacillus zeae (1)
Lactiplantibacillus argentoratensis (1)
Lactiplantibacillus paraplantarum (3)
Lactiplantibacillus pentosus (5)
Lactiplantibacillus plantarum (138)
Lactobacillus helsingborgensis (1)
Latilactobacillus graminis (1)
Loigolactobacillus coryniformis (3)
Lactobacillus sp. CBA3605 (1)
Lactobacillus sp. CBA3606 (1)
Lactobacillus sp. D1501 (1)
Lactobacillus sp. wkB8 (1)
Marinilactibacillus sp. 15R (1)
Latilactobacillus curvatus (11)
Loigolactobacillus backii (5)
Furfurilactobacillus rossiae (4)
ndh2
pplA
eetB
eetA
fmnB
dmkB
fmnA
ATPase1
ATPase2

Figure 2–figure supplement 1. Conservation of FLEET locus genes among lactobacilli. Heatmap showing the bacteria in the Lactobacillus-genus complex containing genes in the FLEET locus. Homology searches were conducted using tBLASTx for 1,788 complete LAB genomes in NCBI (downloaded 02/25/2021) against the *L. plantarum* NCIMB8826 FLEET locus. A match was considered positive with a Bit-score > 50 and an E-value of < 10^{-3}. See related data in Figure 2 Supplement 1 - Source Data 1.

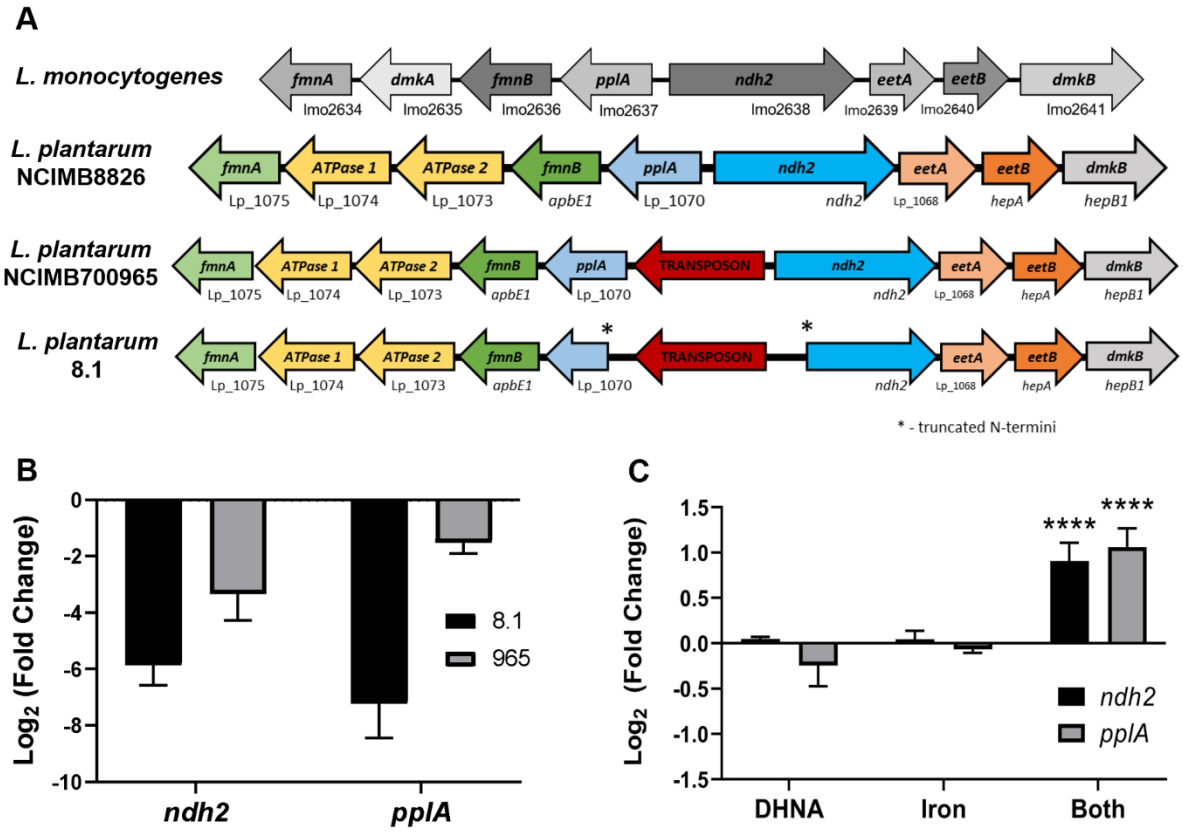

Figure 2–figure supplement 2. *ndh2* and *pplA* are required for iron reduction through EET. **(A)** Visualization of the FLEET locus in *L. monocytogenes* and three strains of *L. plantarum*. Genes are annotated based on predicted functions within the FLEET system. **(B)** Relative expression of *ndh2* and *pplA* in *L. plantarum* strains 8.1 and NCIMB700965 ("965") during

growth in MRS compared to *L. plantarum* NCIMB8826. The avg ± stdev of three biological replicates is shown. **(C)** Relative expression of *ndh2* and *pplA* in *L. plantarum* during growth in mMRS containing 20 µg/mL DHNA, iron (1.25 ferric ammonium citrate), or both (DHNA and iron), compared to during growth in mMRS. Significant differences determined through Two-way ANOVA with Sidak's post-hoc test (n = 3), **** $p \leq 0.0001$. See related data in Figure 2 Supplement 2 - Source Data 1.

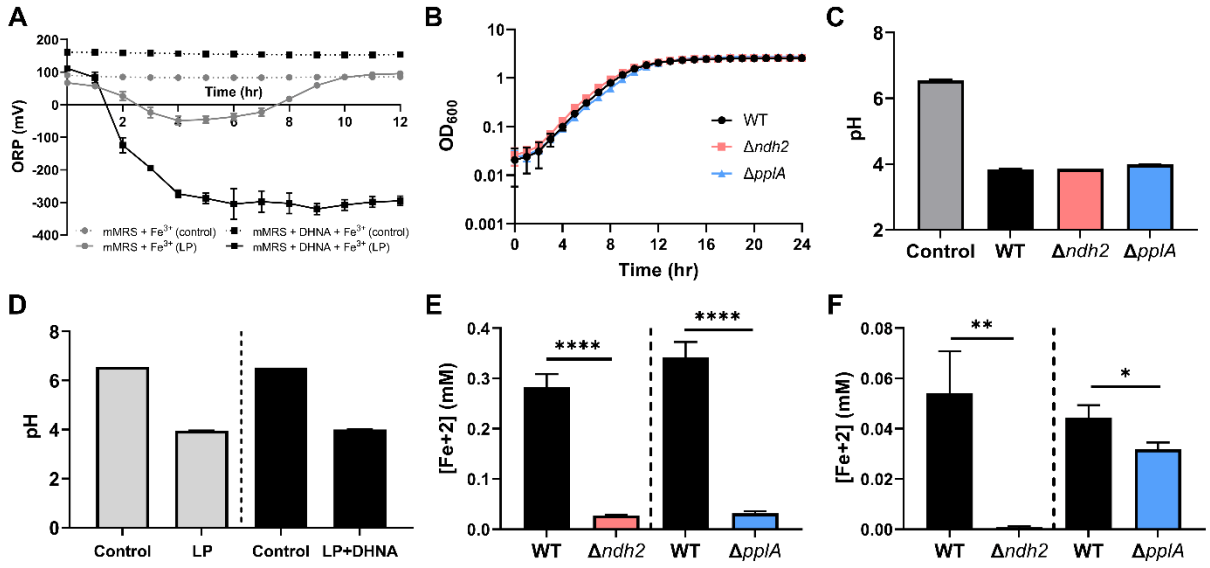

Figure 3–figure supplement 1. Impact of *ndh2* and *pplA* deletion on growth, iron reduction, current density, and metabolites production. (A) Redox potential of mMRS supplemented with 1.25 mM ferric ammonium citrate after inoculation with wild-type *L. plantarum*. Where indicated, 20 µg/mL DHNA was supplemented as well. **(B)** Growth of wild-type *L. plantarum*, Δ*ndh2*, or Δ*pplA* in mMRS supplemented with 20 µg/mL DHNA and 1.25 mM ferric ammonium citrate. **(C)** Final pH from **Fig 3B**. **(D)** Final pH from **Fig 3-S1A**. **(E and F)** Reduction of ferrihydrite by *L. plantarum* or FLEET deletion mutants from **Fig 3B** in the ferrihydrite reduction assay at **(E)** ΔmV_{max} (~ 5 h) or **(F)** stationary phase (12 h). Significant differences

determined through Two-tailed t-test (n = 3), * $p \leq 0.05$; ** $p \leq 0.01$; **** $p \leq 0.0001$. The avg ± stdev of three biological replicates is shown. See related data in Figure 3 Supplement 1 - Source Data 1.

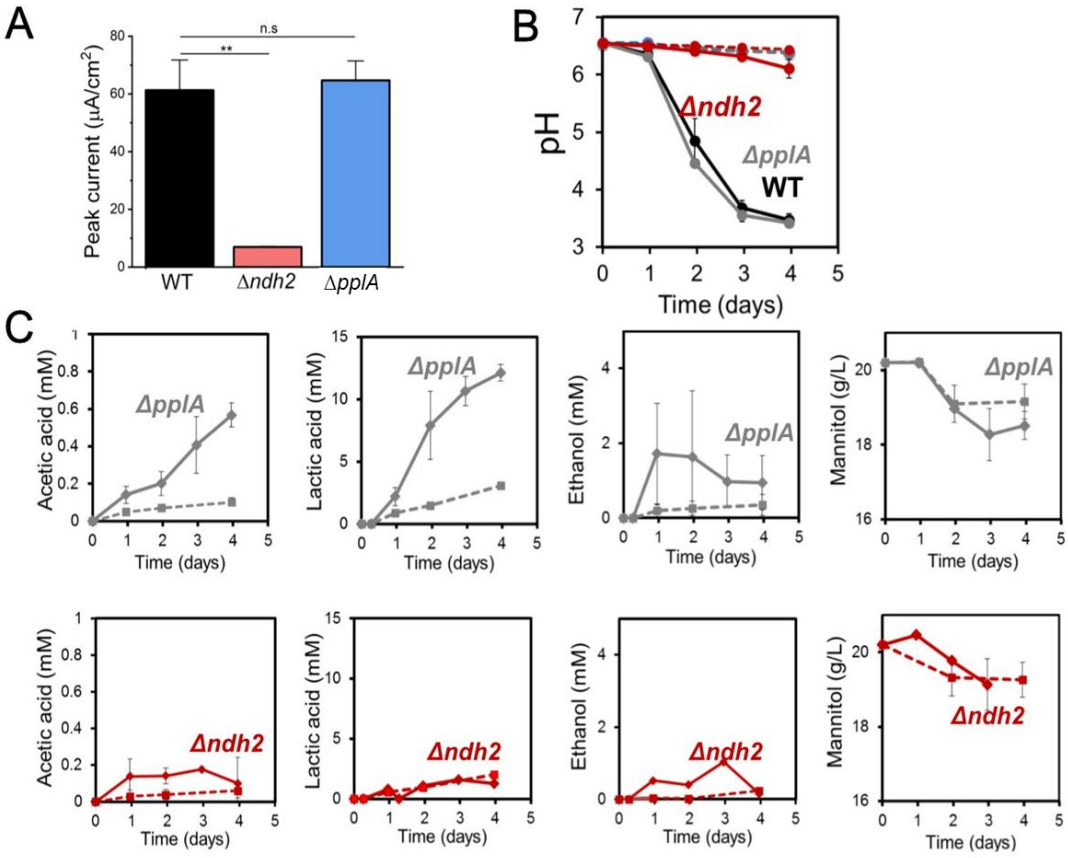

Figure 3–figure supplement 2. Impact of *ndh2* and *pplA* deletion on maximum current density, pH and metabolites production. (A) Peak current generated by wild-type *L. plantarum* or either the Δ*ndh2* or Δ*pplA* mutant from **Fig 3C**. **(B)** pH measurements and **(C)** metabolites produced in the bioelectrochemical reactors inoculated with wild-type *L. plantarum* or either the Δ*ndh2* or Δ*pplA* mutant from **Fig 3C**. Solid lines denote the presence of an anode polarized to +0.2V (vs Ag/AgCl sat. KCl) while dashed lines denote open circuit conditions. See related data in Figure 3 Supplement 2 - Source Data 1.

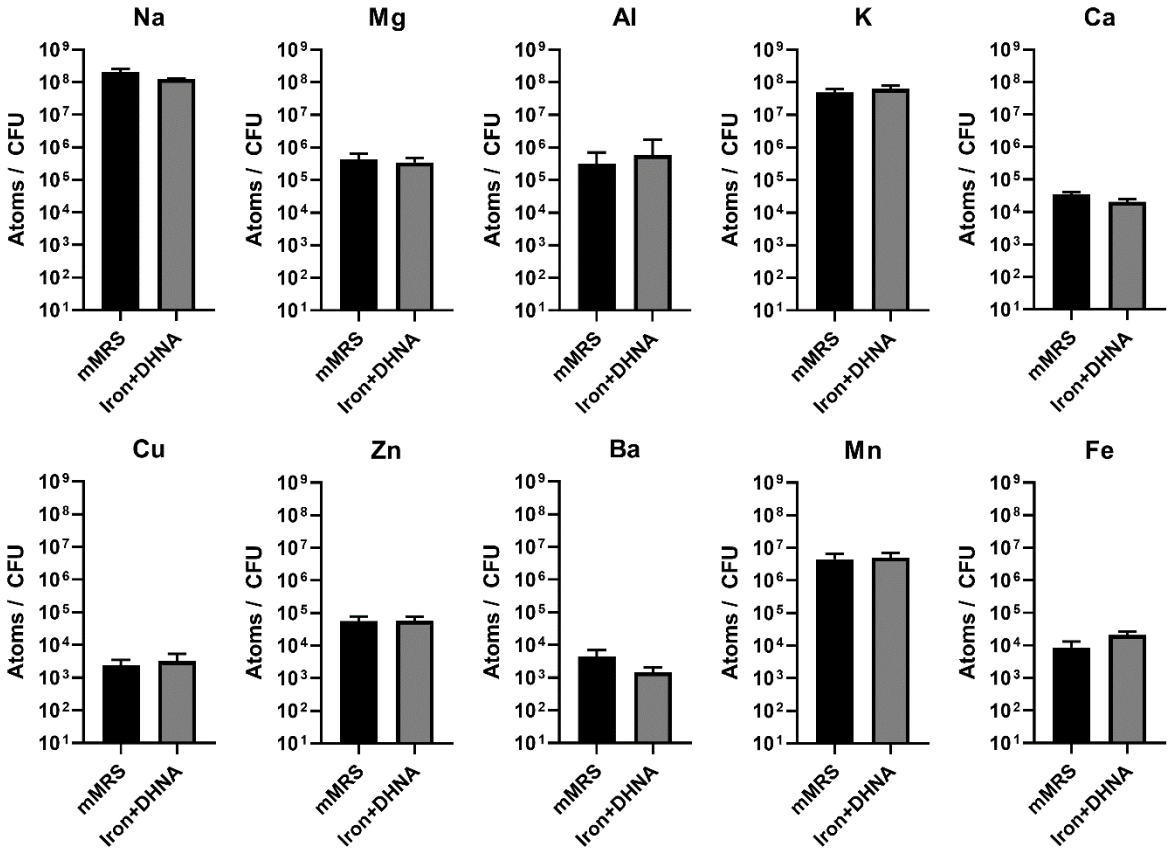

Figure 4 –figure supplement 1. Intracellular metal concentrations in *L. plantarum* are not affected by EET-conducive growth conditions. Inductively coupled plasma mass spectrometry (ICP-MS) quantification of intracellular metals in *L. plantarum* after growth for 18 h in mMRS or mMRS supplemented with 20 μg/mL DHNA and iron (1.25 mM ferric ammonium citrate). The avg ± stdev of three biological replicates is shown. See related data in Figure 4 Supplement 1 - Source Data 1.

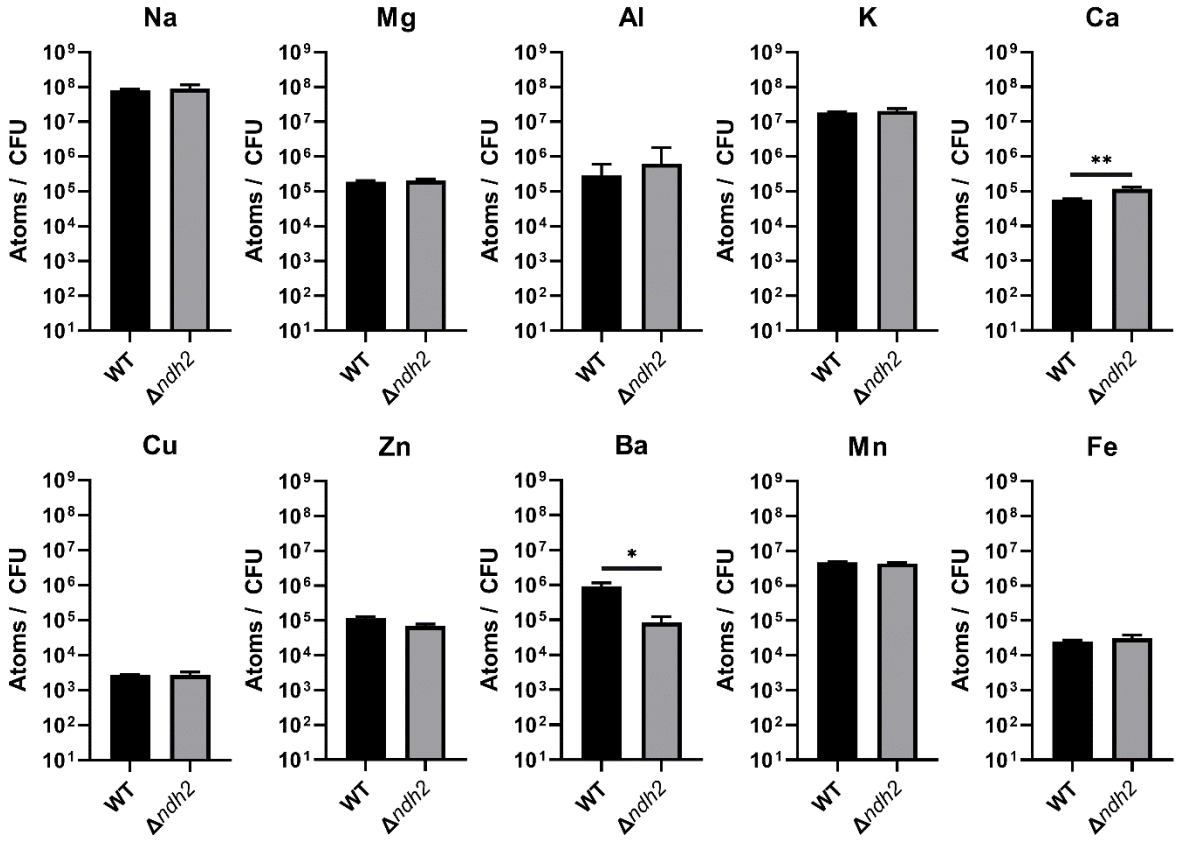

Figure 4 –figure supplement 2. Redox-active metal concentrations in *L. plantarum* are not affected by the presence of *ndh2*. Inductively coupled plasma mass spectrometry (ICP-MS) quantification of intracellular metals in wild-type *L. plantarum* and a *L. plantarum ndh2* deletion mutant after growth for 18 h in mMRS supplemented with 20 µg/mL DHNA and iron (1.25 mM ferric ammonium citrate). The avg ± stdev of three biological replicates is shown. Significant differences determined by One-way ANOVA with Dunnett's post-hoc test, * $p \leq 0.05$; ** $p \leq 0.01$. See related data in Figure 4 Supplement 2 - Source Data 1.

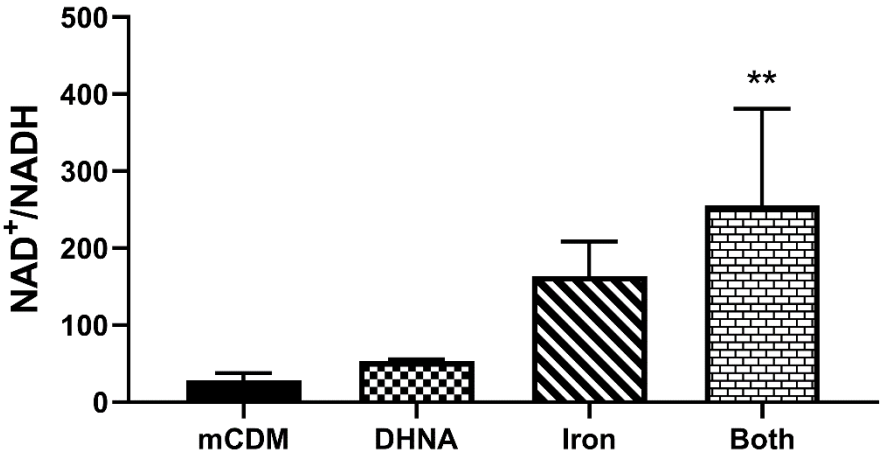

Figure 4–figure supplement 3. Use of Fe^{3+} as an electron acceptor allows *L. plantarum* to regenerate NAD^+. NAD^+/NADH ratios of *L. plantarum* grown to mid-exponential phase in mCDM with/without the supplementation of 20 µg/mL DHNA, iron (1.25 mM ferric ammonium citrate), or both. The avg ± stdev of three biological replicates is shown. Significant differences determined through One-way ANOVA with Dunnett's post-hoc test (n = 3), ** $p \leq 0.01$. See related data in Figure 4 Supplement 3 - Source Data 1.

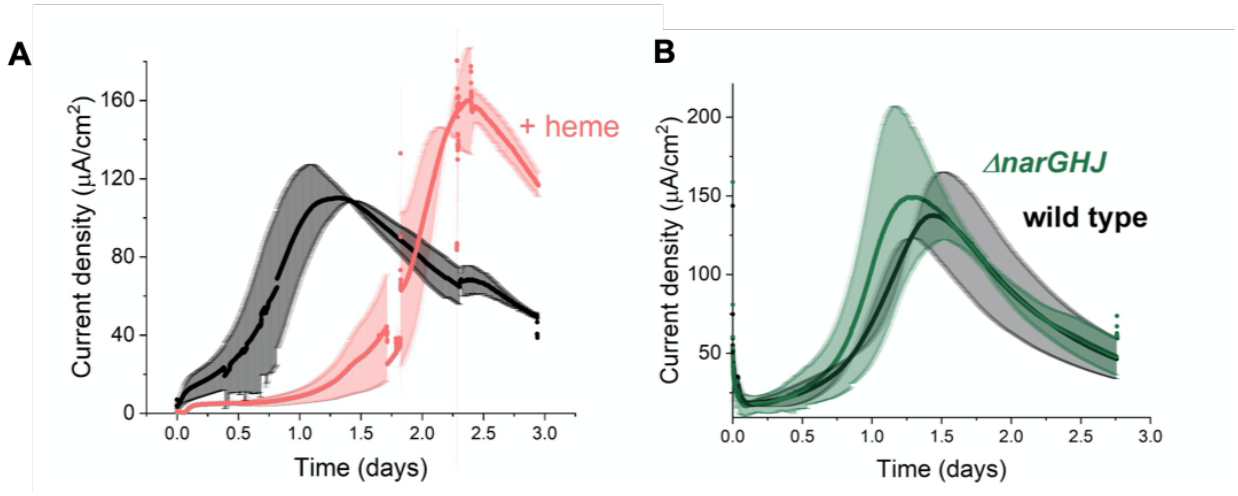

Figure 5–figure supplement 1. EET by *L. plantarum* is not dependent on aerobic or anaerobic respiration components. (A) Effect on *L. plantarum* current production with heme

addition to reconstitute the aerobic electron transport chain. **(B)** Effect on *L. plantarum* current production with the deletion of the nitrate reductase A. The anode was polarized to +0.2V (vs Ag/AgCl sat. KCl). The avg ± stdev of two biological replicates is shown. See related data in Figure 5 Supplement 1 - Source Data 1.

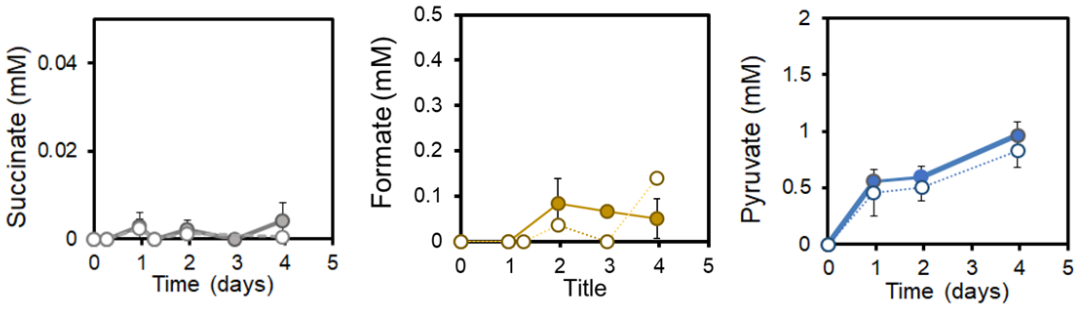

Figure 5–figure supplement 2. EET by *L. plantarum* does not involve TCA cycle metabolites. Succinate, formate and pyruvate produced under EET (solid line) and open-circuit (dashed line) conditions from **Fig 5**. The avg ± stdev of three biological replicates is shown. See related data in Figure 5 Supplement 2 - Source Data 1.

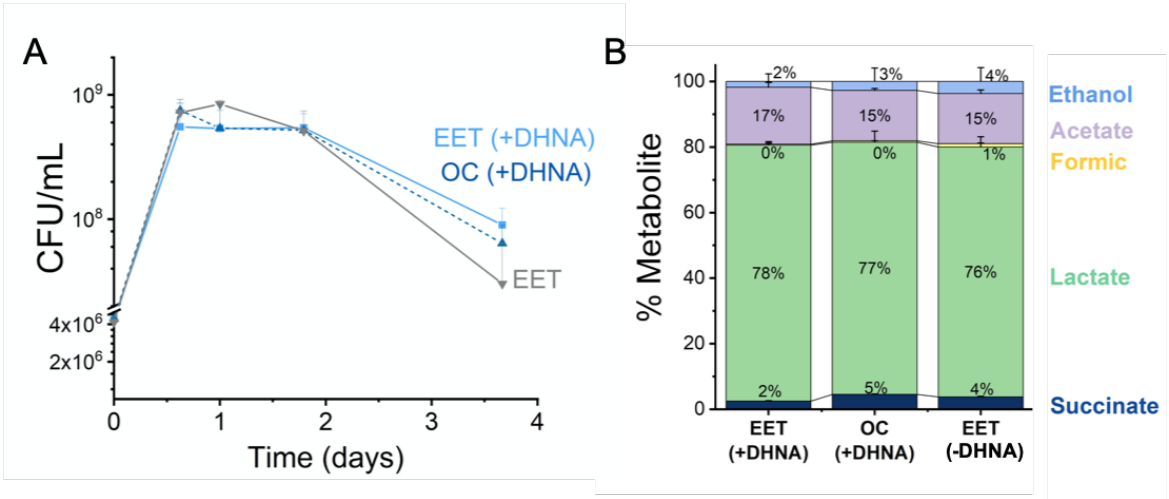

Figure 6–figure supplement 1. EET does not impact cell viability and distribution of metabolites in a kale fermentation. (A) Viable cells of *L. plantarum* NCIMB8826-R during the fermentation of kale juice in the presence of a polarized anode with/without DHNA, and under open circuit conditions with DHNA. **(B)** Distribution of metabolites after 2 days of kale juice fermentation. The anode polarization was maintained at +0.2 V (vs Ag/AgCl sat. KCl). The avg ± stdev of three biological replicates is shown. See related data in Figure 6 Supplement 1 - Source Data 1.

Chapter 3. *Lactiplantibacillus plantarum* is adapted for extracellular electron transfer using exogenous quinones

Eric T. Stevens[1], Alycia M. Rassumussen[1], Sara Tejedor-Sanz[2,3], Emily Mevers[4], Caroline M. Ajo-Franklin[2,3], and Maria L. Marco[3, †]

[1]Department of Food Science & Technology, University of California-Davis, Davis, United States

[2]Department of Biosciences, Rice University, Houston, United States

[3]Biological Nanostructures Facility, The Molecular Foundry, Lawrence Berkeley National Laboratory, Berkeley, United States

[4]Department of Chemistry, Virginia Polytechnic Institute and State University, Blacksburg, United States

[†]For correspondence: mmarco@ucdavis.edu

Abstract

Extracellular electron transfer (EET) is a metabolic process requiring quinones to respire using extracellular electron acceptors. The physiological relevance of this metabolism to EET-capable microorganisms which are unable to synthesize their own quinones remains to be determined. To address this question, we investigated the specificity and effects of quinones on *Lactiplantibacillus plantarum,* a quinone auxotroph able to perform a blended metabolism using fermentation and EET. Although *L. plantarum* requires exogenous quinones for EET-mediated reduction of extracellular ferrihydrite (iron(III) oxyhydroxide), this activity increased 5-fold when cells were grown with the quinone 1,4-dihydroxy-2-naphthoic acid (DHNA) and persisted at low DHNA concentrations. Yet, DHNA inhibited *L. plantarum* growth via abiotic hydrogen peroxide production and induced expression of redox stress-associated genes including glutathione reductase, thioredoxin reductase, and NADH peroxidase. These transcriptional effects were reversed by ferric iron which decreased hydrogen peroxide production and partially restored *L. plantarum* growth. The quinone 2-amino-3-carboxy-1,4-naphthoquinone (ACNQ) stimulated greater EET than DHNA, while the quinones 1,4-naphthoquinone and menadione stimulated EET but were not as effective as DHNA. Quinones secreted from the lactic acid bacteria (LAB) *Lactococcus lactis* and *Leuconostoc mesenteroides* also stimulated EET, and co-culturing *L. plantarum* with these LAB resulted in increased environmental acidification and *L. plantarum* cell numbers. These results have direct ecological implications in *L. plantarum* for adapting to quinone auxotrophy with quinone-producing LAB and has direct applications for food and beverage fermentations modulated by EET with *L. plantarum.*

Introduction

Oxidation-reduction (redox) reactions dictate the flow of electrons in all enzymatic reactions. Accordingly, these reactions are facilitated by an abundance of electron shuttling compounds used by bacteria to transport electrons within and outside of the cell (Glasser et al., 2017; Zerfaß et al., 2019). Quinones are one such class of diverse, redox-active molecules with similar functions in all three domains of life (Elling et al., 2016; Futuro et al., 2018). Quinones assist membrane electron transfer from dehydrogenases to oxidases during aerobic and anaerobic respiration (Nitzschke and Bettenbrock, 2018). In bacteria, ubiquinones and/or menaquinones are required for respiratory growth, and the presence of natural or synthetic menaquinone precursors (i.e., 1,4-dihydroxy-2-naphthoic acid (DHNA) and menadione) can stimulate growth of otherwise unculturable, gut-associated bacteria (Fenn et al., 2017). Yet, even low concentrations of these precursors, or other quinone derivatives such as 1,4-naphthoquinone and ubiqunone-1, can inhibit bacterial growth (Nagata et al., 2010; Schlievert et al., 2013). These antibacterial modes of action include competing with endogenous quinones to inhibit respiration (Nagata et al., 2010), or by abiotic generation of intracellular and extracellular reactive oxygen species (ROS) (Schlievert et al., 2013), resulting in cell membrane damage, DNA damage, and lipid peroxidation (Goel et al., 2020). Therefore, while redox-mediating quinones native to bacterial electron transport chains are beneficial to one species, exposure to other quinone forms present in the environment may be detrimental to the same species and highlights the complexity of bacterial-quinone relationships.

Besides their functions as cofactors in respiratory organisms and as antimicrobials, quinones are also necessary for extracellular electron transfer (EET), a metabolic process in which intracellular redox reactions are coupled to the reduction of extracellular electron

acceptors like redox-active metals or electrodes (Shi et al., 2016). Quinones are required to shuttle electrons between membrane-bound EET components, which in bacteria are either multi-heme, *c*-type cytochromes or membrane-associated flavoproteins (Lovley and Holmes, 2022). Quinones also serve as environmental electron shuttles, like flavins or phenazines (Glasser et al., 2017), to reduce long-range electron acceptors through EET (Voordeckers et al., 2010). We recently showed that *Lactiplantibacillus plantarum,* a species which lacks the capacity to synthesize both heme and quinones, performs flavoprotein-associated EET by a blended metabolism combining features of respiration and fermentation (Tejedor-Sanz et al., 2021). *L. plantarum* is a Gram-positive species in the Firmicutes phylum and member of the lactic acid bacteria (LAB) group of microorganisms defined by their production of lactic acid from fermentation metabolism and found in both food and intestinal environments (Martino et al., 2016). *L. plantarum* EET metabolism resulted in a shortened lag phase, increased fermentation flux through organic acid production, and greater environmental acidification (Tejedor-Sanz et al., 2021).

Remarkably, despite the advantages of EET metabolism for *L. plantarum,* this organism lacks the capacity to synthesize quinones (Brooijmans et al., 2009). The *L. plantarum* flavin-mediated EET (FLEET) pathway contains *dmkA* and *dmkB* encoding a 1,4-dihydroxy-2-naphthoate polyprenyltransferase and a heptaprenyl diphosphate synthase, respectively (Tejedor-Sanz et al., 2021). These genes are required for demethylmenaquinone (DMK) synthesis in *Listeria monocytogenes* (Light et al., 2018) and *Enterococcus faecalis* (Pankratova et al., 2018). However, *L. plantarum* lacks the other genes required for menaquinone biosynthesis (Watthanasakphuban et al., 2021). Instead, exogenous DHNA, a precursor of DMK, was shown to be sufficient for stimulating *L. plantarum* EET metabolism (Tejedor-Sanz et al., 2021).

DHNA was also associated with inducing *L. plantarum* EET activity; co-exposure of DHNA and soluble ferric ammonium citrate (FeAC) during growth resulted in significantly greater iron-reducing capabilities compared to exposure of either amendment alone. In addition, the combined exposure to DHNA and FeAC during growth significantly induced expression of two genes in the putative FLEET pathway, *ndh2* (encoding a type-II NADH dehydrogenase) and *pplA* (encoding a membrane-associated flavin-binding reductase).

Although exposure of *L. plantarum* to low concentrations of DHNA (10 ng/μL) was sufficient for *L. plantarum* to perform EET (Tejedor-Sanz et al., 2021), the effects of quinones (and their intermediates) on *L. plantarum*, as well as quinone ranges and requirements for *L. plantarum* to perform EET remained to be determined. This is important for understanding *L. plantarum* ecology, as this LAB inhabits food and intestinal niches which contain exogenous menaquinones and menaquinone precursors (Karl et al., 2017; Walther and Chollet, 2017). Herein, we measured *L. plantarum* EET after exposure to a range of DHNA concentrations during growth and EET. Exposure to DHNA and ferric iron, a terminal extracellular electron acceptor, were investigated for their impact on *L. plantarum* growth rate and gene expression. We measured *L. plantarum* EET and growth with a range of purified quinones, as well as secreted quinones from other LAB in spent growth media. Lastly, we showed how co-culture of *L. plantarum* with quinone-producing LAB affects *L. plantarum* EET, environmental acidification, and cell numbers. Our findings show how *L. plantarum* EET metabolism is adapted for exogenous environmental quinones and engages in quinone cross-feeding with environmentally-associated bacteria.

Results

L. plantarum relies on direct access to exogenous quinones for EET

We previously showed that reduction of insoluble ferrihydrite (iron(III) oxyhydroxide) and production of current in a bioelectrochemical reactor by our model strain *L. plantarum* NCIMB8826 is dependent on the presence of exogenous DHNA in the assay medium (Tejedor-Sanz et al., 2021). However, these results do not exclude the possibility that *L. plantarum* converts DHNA into a membrane-bound or secreted electron carrier. Therefore, *L. plantarum* was incubated in nutrient-replete laboratory culture medium (mMRS) containing 20 μg/mL DHNA, with or without soluble ferric ammonium citrate (FeAC), and analyzed for intracellular quinone contents. In the presence of DHNA, *L. plantarum* synthesized menaquinone-6 (MK-6) and menaquinone-7 (MK-7) in an approximate ratio of 13:1 (**Figure S1**). These findings show that although *L. plantarum* is not able to synthesize quinones *de novo*, it is able to convert DHNA to menaquinone species which may be needed for EET.

Next, we determined whether prior exposure to DHNA is sufficient for *L. plantarum* EET metabolism. To examine this, *L. plantarum* cells were collected and washed after growth in mMRS containing 20 μg/mL DHNA and then incubated with ferrihydrite to quantify iron reduction. Despite the prior exposure to DHNA, *L. plantarum* did not reduce ferrihydrite unless DHNA was also included in the assay medium (**Figure 1**). Similarly, while *L. plantarum* could generate current during growth with DHNA (**Figure S2A**), this activity stopped when *L. plantarum* was transferred to an electrochemical cell lacking an exogenous quinone source (**Figure S2B**). Growth in the presence of DHNA also did not result in the release of soluble redox-active mediators by *L. plantarum* according to cyclic voltammetry (**Figure S2C**).

Because *L. plantarum* is likely to grow in habitats which are also conducive for EET, we next incubated *L. plantarum* in mMRS containing 20 μg/mL DHNA and subsequently included the same quantity of DHNA in the ferrihydrite reduction assay. This combined exposure to DHNA resulted in a 5-fold increase compared to when only DHNA was included in the ferrihydrite reduction assay (**Figure 1**). The increased EET activity strongly suggests that *L. plantarum* uses endogenous quinones synthesized during growth to perform EET, but that even when intracellular menaquinones (MK-6 and MK-7) are present, exogenous quinones remain indispensable for *L. plantarum* EET.

Quinones and quinone intermediates are typically found in lower concentrations in *L. plantarum* food and intestinal environments in ranges between 0.089-6.44 μg/mL (Eom et al., 2012; Karl et al., 2017). To account for these low environmental concentrations, we also examined EET activity in response to a range of DHNA concentrations. Incubation of *L. plantarum* in DHNA in laboratory culture medium and the ferrihydrite reduction assay resulted in *L. plantarum* EET in DHNA concentrations less than 20 μg/mL (**Figure 2**). Similar levels of ferrihydrite reduction were found between 2.5 μg/mL and 5 μg/mL DNHA when the quinone was included in the mMRS growth medium. *L. plantarum* EET activity was stimulated even when it was exposed to very low levels of DHNA in mMRS (0.1 μg/mL DHNA) (**Figure S3**). These results show that robust reduction of extracellular electron acceptors by *L. plantarum* occurs at low concentrations of exogenous quinones when *L. plantarum* is grown in the presence of DHNA.

DHNA inhibits *L. plantarum* growth by inducing oxidative stress

Although the inclusion of DHNA in mMRS increased *L. plantarum* EET metabolism, we also observed that *L. plantarum* growth was inhibited under those conditions. In mMRS containing 20 μg/mL DHNA (mMRS+DHNA), the growth rate of *L. plantarum* reduced from 0.26 ± 0.01 (mMRS) to 0.18 ± 0.01 (mMRS+DHNA) ($p \leq 0.001$) (**Figure S4**). At higher concentrations of DHNA, the growth rate reduced exponentially and no increase in cell numbers was observed at 150 μg/mL. Inhibition was observed at DHNA concentrations as low as 5 μg/mL (0.22 ± 0.01) ($p \leq 0.05$). This effect of exogenous quinones was not limited to DHNA, as other menaquinone precursors and derivatives also inhibited *L. plantarum* growth (**Figure S5**). Menadione and 1,4-naphthoquinone were most toxic to *L. plantarum* and prevented growth above 50 μg/mL. ACNQ (2-amino-3-carboxy-1,4-naphthoquinone) was less toxic, with *L. plantarum* growth stopping at 100 μg/mL quinone.

To determine the cause of the DHNA-mediated growth inhibition, we examined the *L. plantarum* transcriptome during exponential phase in mMRS+DHNA. In the presence of DHNA, 925 *L. plantarum* genes were differentially expressed (452 genes up-regulated and 473 genes down-regulated) compared to *L. plantarum* grown in mMRS (**Table S2** and **Supplementary File 1**). *L. plantarum* expression of genes required for menaquinone biosynthesis, including *dmkA* (and similarly annotated genes lp_1135 and lp_1715) and *ubiE*, was not significantly induced in mMRS+DHNA (**Table S3**). Genes in the FLEET pathway were not induced, and specifically, *dmkB*, *pplA*, and *fmnB* (encoding a flavin-transferase lipoprotein) (Tejedor-Sanz et al., 2021) were ~1.4-fold downregulated on average. The growth rates of *L. plantarum* mutants deficient in *ndh2* or *pplA* required for EET were also similarly reduced in mMRS+DHNA (**Figure S6**). Therefore, the effect of DHNA was not due to activation of intracellular quinone biosynthesis or the FLEET locus.

Pathway analyses of the transcriptionally regulated genes showed that many genes known to be required for responding to oxidative stress (Feng and Wang, 2020) were induced in *L. plantarum* upon DHNA exposure (**Figure 3 and Table S3**). Genes coding for the synthesis of glutathione reductase (*gshR2*/*R3*/*R4*) were upregulated on average between 2 to 7-fold. *msrA2* and *msrB* encoding methionine-S-oxide reductase were induced between 5.0 and 5.5-fold and expression of *trxA2* (thioredoxin) and *trxB* (thioredoxin reductase) was increased, on average, 1.5-fold in mMRS+DHNA. Likewise, other genes associated with managing intracellular oxidative stress in *L. plantarum* were induced in mMRS+DHNA. These include NADH oxidase (*nox5*), NADH peroxidase (*npr2*), catalase (*kat*), and pyruvate oxidase (*pox3*) which were 1.6, 7.6, 3.4, and 3.3-fold upregulated, respectively (Bron et al., 2012).

Amino acid and lipid metabolism were also affected during *L. plantarum* growth in mMRS+DHNA. Genes coding for methionine synthesis (*metE* and *metH*), methionine transport (lp_1745), and chorismate biosynthesis (*aroD1* and *aroF*) were upregulated by an average of 3.1 to 5.8-fold under those conditions (**Table S3**). Methionine protects proteins from oxidative stress (Luo and Levine, 2009) and chorismate is a precursor compound to the membrane-associated antioxidant ubiquinol (Gerstle et al., 2012). Acetyl-CoA carboxylase (*accA2*, *accB2*, *accC2*, and *accD2*) and fatty acid biosynthesis (*fabD*, *fabF*, *fabG*, *fabH2*, *fabI*, and *fabZ1*) were increased on average between 2.1 to 2.6-fold in mMRS+DHNA. The induction of membrane biosynthesis pathways is consistent with responses to lipid peroxidation found in *E. coli* (Janßen and Steinbüchel, 2014). Lipid peroxidation can also occur from extracellular hydrogen peroxide (H_2O_2) generated by the reaction quinones with oxygen (Goel et al., 2020).

Because of the increased expression of oxidative stress response pathways, we measured hydrogen peroxide (H_2O_2) levels in the mMRS medium. Incubation of 20 μg/mL DHNA in

mMRS resulted in 41.90 mM ± 0.34 mM H_2O_2 (**Figure S7**). After *L. plantarum* incubation in mMRS+DHNA, a total of 29.92 mM ± 0.63 mM H_2O_2 was also detected. These quantities are approximately 7 to 10-fold higher than observed for mMRS (4.12 mM ± 0.03 mM). Taken together, these data show that DHNA inhibits *L. plantarum* growth via abiotic reactions resulting in reactive oxygen species in the extracellular environment.

Ferric iron alleviates DHNA-induced oxidative stress

L. plantarum performing EET will also require exogenous sources of terminal electron acceptors which may affect metabolism. To account for these electron acceptors, we also examined *L. plantarum* growth and gene expression in mMRS containing 1.25 mM FeAC and 20 μg/mL (DHNA+FeAC). *L. plantarum* growth in this environment reduces more ferrihydrite (0.2 mM Fe^{2+} ± 0.01 mM) (**Figure 2**) than growth with DHNA alone (0.14 mM Fe^{2+} ± 0.01 mM) (**Figure 1**). This is consistent with previous results, in which we also measured upregulated expression of the FLEET genes *ndh2* and *pplA* in mMRS+DHNA+FeAC (Tejedor-Sanz et al., 2021). Growth impairment caused by DHNA was partially alleviated when FeAC was also included in mMRS (**Figure 4**). The growth rate of *L. plantarum* in mMRS+DHNA+FeAC was 0.15 ± 0.011, a value significantly higher compared to mMRS+DHNA (0.09 ± 0.01) ($p = 0.002$), but significantly lower compared to mMRS (0.26 ± 0.01) ($p \leq 0.0001$). Although *L. plantarum* is able to use citrate as an electron acceptor to increase growth during mannitol metabolism (McFeeters and Chen, 1986), growth was not improved in mMRS+DHNA when 1.25 mM ammonium citrate was included. Thus, the improved growth rate of *L. plantarum* in the presence of DHNA was due to the ferric iron in the medium.

Although ferric iron is an important EET-inducing compound, it is also known oxidizing agent capable of generating ROS and acting as a redox partner with quinones (Jiang et al., 2015). In accordance with this, mMRS+DHNA+FeAC was found to contain H_2O_2 (30.25 mM ± 0.25 mM) (**Figure S7**). Incubation with *L. plantarum* resulted in a further 3-fold decrease in extracellular H_2O_2 (**Figure S7**). These reductions in H_2O_2 coincided with the significantly improved growth rate of *L. plantarum* in mMRS+DHNA+FeAC (**Figure 4**). The *L. plantarum* transcriptome also reflected less oxidative stress. Only 292 genes were differentially expressed (123 genes upregulated and 169 genes downregulated) in mMRS+DHNA+FeAC (**Table S2** and **Supplementary File 1**). Genes required for oxidative stress tolerance or redox-associated amino acid metabolism were either unaffected or were downregulated (**Table S3**).

Because the addition of 1.25 mM FeAC may have also impacted *L. plantarum*, we also examined the growth rate and transcriptomes of *L. plantarum* in mMRS with that amendment. Incubation in mMRS+FeAC resulted minimal changes in gene expression (35 genes upregulated and 72 genes downregulated). Despite increased capacity for iron uptake by *L. plantarum* under those conditions (Tejedor-Sanz et al., 2021), genes required for iron metabolism such as the ferrous iron uptake genes *feoAB*, iron-sulfur cluster assembly genes *sufBC*, and the iron-associated metal transport genes *mtsABC* were not differentially expressed compared to controls (**Table S3**). Only genes required for cell membrane biosynthesis were also upregulated in *L. plantarum* in mMRS containing DHNA and/or FeAC. Taken together, these data show that *L. plantarum* growth is negatively affected in the presence of exogenous quinones due to oxidative stress. The detrimental effects of DHNA are partially mitigated when ferric iron is also present.

L. plantarum EET is stimulated multiple quinones and by secreted compounds made by other LAB

Upon establishing that *L. plantarum* EET is active in the presence of low concentrations of exogenous quinones and the negative effects of quinones on *L. plantarum* growth can be mitigated in the presence of external electron acceptors, we next sought to investigate whether *L. plantarum* reduction of ferrihydrite is specific to DHNA or if other quinone species may be used. The capacity for *L. plantarum* to reduce ferrihydrite was quantified in the presence of menaquinones MK-4 and MK-7 and the menaquinone precursors or derivatives ACNQ, 1,4-naphthoquinone, menadione, hydroquinone, and phylloquinone. These compounds are found in plant and animal tissues (Beulens et al., 2010) and can be produced by other bacteria (Altwiley et al., 2021; Mevers et al., 2019; Widhalm and Rhodes, 2016). *L. plantarum* reduced ferrihydrite in the presence of ACNQ, 1,4-naphthoquinone, and menadione (**Figure 5**). ACNQ conferred the highest level of ferrihydrite reduction by *L. plantarum* with an IC_{50} of 4.70 μg/mL and a maximum iron reduction of 0.68 mM Fe^{2+}. This was significantly greater EET stimulation than with DHNA (IC_{50} = 223.4 μg/mL, 0.40 Fe^{2+} max). In contrast, neither 1,4-naphthoquinone (IC_{50} = 10.23 μg/mL, 0.05 Fe^{2+} max) and menadione (IC_{50} = 29.79 μg/mL, 0.05 Fe^{2+} max) were as effective as DHNA in stimulating iron reduction. Ferrihydrite was not reduced by *L. plantarum* in the presence of hydroquinone, menaquinone-4, menaquinone-7, or phylloquinone (data not shown) up to the maximum concentration tested (100 μg/mL). Notably, the level of ferrihydrite reduction (**Figure 5**) was not related to capacity of the quinone to inhibit *L. plantarum* growth (**Figure S5**). This is most likely due to *L. plantarum* being metabolically active, but not growing in the PBS-based ferrihydrite assay medium. These findings show that the *L. plantarum* quinone

requirements for EET are not limited to DHNA and that other environmental quinones are sufficient, providing a range of selectivity.

Other bacteria may by provide a source of quinones for *L. plantarum* in its natural habitats. *L. plantarum* is frequently found in high numbers with other LAB in food fermentations (Di Cagno et al., 2015). Some of these bacteria, such as *Lactococcus lactis* and *Leuconostoc mesenteroides*, are able to synthesize menaquinones (Morishita et al., 1999). These bacterial species also have the capacity to produce DHNA (Eom and Moon, 2015; Mevers et al., 2019). Therefore, to determine whether *L. plantarum* is able to perform EET by cross-feeding on quinones produced by other bacteria, we incubated *L. plantarum* in a cell-free supernatant (CFS) of gM17 laboratory culture medium collected after growth of *L. lactis* TIL46, a strain shown to produce menaquinones (Tachon et al., 2010). Incubation of *L. plantarum* cells in *L. lactis* TIL46 CFS was sufficient for ferrihydrite reduction (**Figure 6A**). Iron reduction was due to the production of quinones by *L. lactis* because this activity was not observed when *L. plantarum* was incubated in CFS from TIL999, a TIL46 *menC* deletion mutant lacking the capacity to synthesize any menaquinones (Tachon et al., 2009). Iron reduction was not specific to *L. lactis* because CFS collected from *Leuconostoc citreum* strain NRRL B-742 and *Leuconostoc mesenteroides* strain ATCC8293 after growth in a chemically defined culture medium (gCDM) also stimulated iron reduction (**Figure 6B**).

Co-culturing *L. plantarum* with quinone-producing LAB affects environmental acidification and growth

Because the CFS from quinone-producing LAB was sufficient for *L. plantarum* EET, we hypothesized that quinone cross-feeding in a co-culture environment would also simulate *L.*

plantarum iron reduction. *L. plantarum* was incubated in equal proportions with either *L. lactis* TIL46, *L. lactis* TIL999, or *L. mesenteroides* ATCC8293 in a chemically defined medium (gCDM) and 1.25 mM FeAC was used as a terminal electron acceptor to quantify EET activity *in situ* through colorimetric analysis. Within 24 h incubation of *L. plantarum* and *L. lactis* TIL46 in co-culture, significantly greater iron was reduced than when *L. plantarum* was grown separately or incubated with TIL999 (**Figure 6C**). Although there was spontaneous reduction of FeAC in acidified gCDM (**Figure S8**), this background level of iron reduction was minor and did not impact the significant increases in iron reduction when *L. plantarum* was present. As with *L. lactis* TIL46, co-cultures of *L. plantarum* and *L. mesenteroides* also simulated higher quantities of iron reduction than found for *L. plantarum* alone (**Figure 6D**). These findings show that environmental quinones secreted by other LAB can stimulate *L. plantarum* EET metabolism.

Stimulation of *L. plantarum* EET is associated with shorter lag phase, increased viable cell counts, and accelerated environmental acidification (Tejedor-Sanz et al., 2021). Because incubation of *L. plantarum* with quinone-producing LAB stimulated EET, we also quantified environmental acidification and growth under those co-culture conditions. Within 6 h of incubation, the co-culture of *L. plantaurm* and *L. lactis* TIL46 reached a lower pH (pH = 5.26) than the *L. plantarum* and TIL999 co-culture (pH = 6.16), as well as for either strain grown separate (**Figure 7A**). Likewise, incubation of *L. plantarum* and *L. mesenteroides* ATCC8293 led to greater acidification of the medium (pH = 5.27) within 8 h compared to either strain grown alone (**Figure 7B**). As found for *L. plantarum* previously (Tejedor-Sanz et al., 2021), EET metabolism was activated early in growth and by stationary phase (24 h incubation) the pH of all cultures was equal (pH = ~3.28) except for *L. mesenteroides* alone (pH = 4.18). These data show

that quinone-cross feeding from LAB to *L. plantarum* results in accelerated environmental acidification.

Besides increasing the acidification rate, *L. plantarum* growth was altered in co-culture with *L. lactis* and *L. mesenteroides.* When *L. lactis* was present, *L. plantarum* cell numbers were 2-fold higher after incubation for 24 h (**Figure 7C**). However, this increase was not significant nor was it dependent on menaquinone biosynthetic capacity because both TIL46 and TIL999 resulted in similar increases in *L. plantarum* cell quantities. By comparison, a greater effect was found when *L. plantarum* was incubated together with *L. mesenteroides.* Within 8 h, *L. plantarum* cell numbers increased 4-fold during incubation with *L. mesenteroides* relative to when grown alone ($p = 0.03$) (**Figure 7D**). Notably, the growth of *L. lactis* and *L. mesenteroides* was negatively affected by *L. plantarum*. *L. lactis* abundance in co-culture was slightly (but nonsignificantly) higher ($\geq$ 2-fold) at 6 h but decreased by 2-fold at 24 h (**Figure 7E**). A significant ($p = 0.04$), 10-fold decrease in *L. mesenteroides* abundance was also observed when grown in co-culture with *L. plantarum* at 24 h (**Figure 7F**). In summary, these results show that *L. lactis* and *L. mesenteroides* stimulate *L. plantarum* EET metabolism to result in consequences for their growth and acidification of their environments.

Discussion

Quinones are pervasive in foods and other microbial ecosystems. Microorganisms which have evolved to use these compounds to improve growth and metabolic processes are likely to have an ecological advantage. We showed that *L. plantarum* uses multiple exogenous quinones to stimulate EET for ferric iron reduction and that this activity is inducible when quinones are available during *L. plantarum* growth. *L. plantarum* overcomes the toxic effects of quinone

intermediates and EET increases when a terminal electron acceptor is also present in the growth medium. Increased cell numbers and medium acidification by *L. planarum* cross-feeding on quinones made by other LAB has important ecological implications in complex microbial ecosystems such as those found in food fermentations.

***L. plantarum* EET activity is inducible, but requires access to environmental quinones**

Quinones are an essential component for EET in bacteria which perform direct electron transfer (DET) and/or mediated electron transfer (MET) to environmental electron acceptors (Shi et al., 2016). These EET systems are best characterized in the Gram-negative microorganisms *Geobacter sulfurreducens* and *Shewanella oneidensis*. For DET, electrons derived from NADH are carried through the inner membrane to a series of *c*-type cytochromes or conductive membrane appendages (i.e., "nanowires") by menaquinones (Kracke et al., 2015). The reduction of long-range electron acceptors by these bacteria with quinones is also achievable. For example, both *G. sulfurreducens* and *S. oneidensis* can use anthraquinone-2,6-disulfonate, an analogue to environmental humic acids, for the reduction of metals and electrodes (Dantas et al., 2018; Meng et al., 2018). In addition, *S. oneidensis* can secrete its own electron-shuttling quinone (ACNQ) for MET (Mevers et al., 2019). Recent characterization of EET pathways in Gram-positive bacteria have also highlighted the importance of membrane-associated and/or secreted quinones for either DET through *c*-type cytochromes (e.g., *Thermincola potens*) or MET through membrane-bound flavoproteins (e.g., *L. monocytogenes* and *E. faecalis*) (Paquete, 2020).

Different from these bacteria, the Gram-positive *L. plantarum* can perform flavoprotein-associated EET, but lacks a complete menaquinone biosynthesis pathway (Brooijmans et al., 2009). Specifically, *L. plantarum* cannot biosynthesize DHNA, but possesses genes in the

FLEET pathway (*dmkA* and *dmkB*) to condense DHNA with an isoprenoid polymer to form demethylmenaquinone (DMK), the membrane electron carrier for *L. monocygenes* (Light et al., 2018) and *E. faecalis* (Hederstedt et al., 2020). However, quinone analysis of *L. plantarum* after growth with the DMK precursor DHNA yielded no DMK, but rather the presence of MK-6 and MK-7. *L. plantarum* possess the gene *ubiE* (also annotated as *menG*) to convert DMK to MK (Watthanasakphuban et al., 2021), and while the presence of these MKs was not enough to stimulate EET alone, co-exposure of *L. plantarum* to DHNA during growth and EET significantly induced iron reduction capabilities. Interestingly, MK is an aerobic respiratory quinone for *L. monocytogenes*, and disruption of *menG* had no effect on EET activity (Light et al., 2018). Thus, MK use by *L. plantarum* for promoting EET is a unique characteristic of this EET pathway compared to *L. monocytogenes* and *E. faecalis*.

The importance of quinones for *L. plantarum* EET is further emphasized by examining other electron shuttles used for EET. *L. monocytogenes* (Light et al., 2018), *E. faecalis* (Zhang et al., 2014), and *L. lactis* (Masuda et al., 2010) can utilize flavins for EET. *L. plantarum* is flavin auxotroph, but can use exogenous flavins in its environment for enhanced EET to ferric iron or an electrode (Tejedor-Sanz et al., 2021). In spite of this, *L. plantarum* EET is not measurable in the absence of exogenous quinones. Another class of electron shuttles used for EET is iron chelators, which bind and solubilize environmental iron for eventual cell-surface reduction (Lovley and Holmes, 2022). *L. plantarum* does not produce siderophores for binding iron, nor does the addition of exogenous iron chelators affect *L. plantarum* growth (Pandey et al., 1994).

L. plantarum and other LAB can be found in quinone-rich environments including plant and dairy foods (Damon et al., 2005; Walther et al., 2013), as well as the gastrointestinal tract (Fenn et al., 2017; Pessione, 2012). DHNA in particular can be found in fermented beverages

ranging from 0.089 to 0.440 μg/mL (Eom et al., 2012). It can also be secreted by other bacteria under laboratory conditions at concentrations ranging from 0.37 to 48 μg/mL (Furuichi et al., 2006; Isawa et al., 2002; Kang et al., 2015). We showed that supplementation of DHNA during *L. plantarum* growth and the subsequent ferrihydrite reduction assay results in significantly greater iron reduction at both high concentrations (200 μg/mL) down to physiologically relevant concentrations (100 ng/mL) of DHNA. Taken together, these findings illustrate a distinct use of membrane-associated and environmental quinones to induce *L. plantarum* EET metabolism at ecologically-relevant concentrations.

Exogenous quinones induce oxidative stress inhibiting L. plantarum growth

Quinones are associated with the abiotic production of hydrogen peroxide (Wendlandt and Stahl, 2016) which is inhibitory to LAB growth (Feng and Wang, 2020). In line with this, DHNA and other quinone species inhibited *L. plantarum* growth rates in a concentration-dependent manner, and DHNA induced abiotic hydrogen peroxide generation in mMRS. Although *L. plantarum* and other lactobacilli possess a heme-dependent catalase to reduce hydrogen peroxide (Zotta et al., 2017), this catalase is nonfunctional in *L. plantarum* (Zhai et al., 2020). Thus, *L. plantarum* relies on intracellular H_2O_2-detoxification pathways like NADH peroxidase and glutathione system to manage oxidative stress (Zotta et al., 2017).

An oxidative stress response from *L. plantarum* to hydrogen peroxide exposure was reflected in its transcriptome. Several genes associated with redox maintenance were upregulated with DHNA supplementation including glutathione reductase, NADH peroxidase, and thioredoxin reductase. A similar oxidative stress response was observed *L. plantaruim* CAUH2 in which mid-exponential phase cells were exposed to 5 mM H_2O_2 for 30 minutes (Zhai et al.,

2020). However, our transcriptome analysis reflects *L. plantarum* cells actively growing under oxidative stress conditions caused by DHNA and 6-fold higher levels of H_2O_2.

Furthermore, we discovered numerous genes coding for redox-associated amino acid metabolism that were also upregulated upon growth with DHNA. Hydrogen peroxide is known to readily react with amino acids and proteins causing oxidative damage (Finnegan et al., 2010). In support of this, we measured induction of *L. plantarum* protein repair pathways such as methionine sulfoxide reductase and thioredoxin reductase that essential for LAB under oxidative stress conditions (Feng and Wang, 2020). Oxidative stress has also been predicted to induce branched-chain amino acid (e.g., valine, isoleucine, and leucine) auxotrophy in *E. coli* due to the inactivation of iron-sulfur clusters used in their biosynthesis (Yang et al., 2019). Although *L. plantarum* is naturally auxotrophic for these amino acids (Teusink et al., 2005), branched chain amino acid transport genes were induced. Similarly, we observed upregulation in methionine transport and biosynthesis genes, a key antioxidant amino acid, and this finding is supported by increased methionine uptake by *Streptococcus suis* under hydrogen peroxide exposure (Zhang et al., 2012). In summary, these data illustrate a redox-stress centered response of *L. plantarum* to oxidative stress induced by quinone exposure during growth.

Extracellular ferric iron reduces oxidative stress

When FeAC was supplemented together with DHNA in mMRS, *L. plantarum* exhibited markedly less oxidative stress. *L. plantarum* growth rate partially, yet significantly recovered from inhibition caused by DHNA. Additionally, less abiotic, extracellular hydrogen peroxide was generated with ferric iron present. The use of iron-sulfur clusters for detoxifying ROS has been shown for *E. faecalis* and *Lacticaseibacillus casei* (Papadimitriou et al., 2016). However, *L.*

plantarum has no iron requirements for growth (Pandey et al., 1994), and we previously found that no significant increase in cell-associated iron was found in *L. plantarum* cells grown in mMRS with FeAC and DHNA (Tejedor-Sanz et al., 2021). Thus, iron uptake by *L. plantarum* was not related to the mitigation of oxidative stress caused by DHNA. FeAC contains citrate, a known scavenger of hydrogen peroxide and other ROS (Ryan et al., 2019). Citrate is also TCA cycle intermediate for *L. plantarum* which can act as an intracellular electron acceptor for LAB (Hansen, 2018). However, growth of *L. plantarum* with DHNA and ammonium citrate did not recover *L. plantarum* growth inhibition. These data suggest that extracellular ferric iron mitigates DHNA-induced oxidative stress.

Both our hydrogen peroxide measurements and transcriptome analysis support this model for oxidative stress mitigation. With FeAC present, significantly less abiotic hydrogen peroxide was generated in mMRS with DHNA. This result is surprising as ferric iron has been shown to catalyze ROS production in the presence of quinones (Lyngsie et al., 2018). In mMRS the complexing of iron with DHNA may perhaps make both compounds less available to react with molecular oxygen for hydrogen peroxide production. Reduced hydrogen peroxide from the actions of extracellular ferric iron was also reflected in the *L. plantarum* transcriptome. Expression of oxidative stress response genes and redox-associated amino acid metabolism/transport genes induced with DHNA exposure was either unaffected or downregulated when FeAC was also present. Although *sufB* and sufC, genes encoding for iron-sulfur cluster assembly proteins, were found to be upregulated in *L. plantarum* CAUH2 after hydrogen peroxide exposure (Zhai et al., 2020), we measured reduced expression of these genes in mMRS with DHNA or DHNA and FeAC. Thus, we show that extracellular ferric iron, a

terminal electron acceptor for EET, reduces *L. plantarum* quinone-associated oxidative stress by reducing hydrogen peroxide production.

***L. plantarum* EET activity is dependent on quinone structure**

Quinones are a structurally diverse class of electron shuttles with over 1,000 structural forms (Glasser et al., 2017). This diversity expands the potential for EET in environmental niches, such as foods or intestinal environments which *L. plantarum* inhabits (Martino et al., 2016). We found that *L. plantarum* more efficiently performs EET with hydrophilic, naphthoquinone-based quinones with electron-withdrawing substituents compared to long-chain, hydrophobic menaquinones or phylloquinone. Many extracellular electron shuttles are small, hydrophilic molecules (Lin et al., 2021), and the presence of electron-withdrawing groups on quinones can stabilize radicals in the aromatic ring (Mirkhalaf et al., 2004). Our data is also supported by our previous findings where DHNA stimulated ferrihydrite production in several quinone auxotrophic LAB including *Lactiplantibacillus pentosus*, *Lacticaseibacillus casei*, and *Lacticaseibacillus rhamnosus* (Tejedor-Sanz et al., 2021). Additionally, both ACNQ or menadione have been shown to stimulate EET activity in other LAB including *E. faecalis* (Pankratova et al., 2018) and *L. lactis* (Freguia et al., 2009).

Given the role of MK-6 and MK-7 for inducing *L. plantarum* EET, the absence of ferrihydrite reduction with MK-7 was surprising. For example, supplementation of a quinone-null mutant of *S. oneidensis* with MK-4 (as well as ACNQ or DHNA) reconstituted EET through AQDS reduction (Mevers et al., 2019). It is possible that although *L. plantarum* uses membrane-associated MK-6 and MK-7 to facilitate electron transfer, the *L. plantarum* EET system requires a soluble environmental electron carrier be present. The absence of ferrihydrite reduction by *L.*

plantarum with hydroquinone, a hydrophilic menaquinone precursor, poses another question. For example, *Enterobacter cloacae* self-secretes hydroquinone as an electron shuttle for EET (You et al., 2019). However, *L. plantarum* does not secrete different redox mediators, even after growth in DHNA-supplemented medium. Given the structural similarities of EET-stimulatory quinones used by *L. plantarum* for iron reduction, we hypothesize that the *L. plantarum* EET system is specifically adapted for using naphthoquinone-based compounds in the environment for electron transfer.

Quinone cross-feeding to L. plantarum has important ecological and biotechnological implications

Several LAB species including *Enterococcus*, *Lactococcus*, *Leuconostoc*, and *Weissella* are capable of synthesizing menaquinones (Pedersen et al., 2012), but quinone cross-feeding to stimulate EET in LAB has yet to be shown. Existing reports suggest the possibility of this phenomenon. For example, *L. lactis* quinone production could stimulate respiration in Group B *Streptococcus* (GBS) in co-culture, which resulted in enhanced growth and acidification from GBS (Rezaïki et al., 2008). Quinones from *L. lactis* could also reconstitute EET activity in a quinone-null mutant of *S. oneidensis* (Mevers et al., 2019). Our results indicated that quinones cross-fed by *L. lactis*, *L. mesenteroides*, and *L. citreum* were sufficient to simulate ferrihydrite reduction by *L. plantarum*. While both *L. lactis* and *L. mesenteroides* are also capable of producing endogenous flavins as electron shuttles (Thakur et al., 2016), we confirmed the role of quinones for EET stimulation by demonstrating that spent growth medium from *L. lactis* TIL999, a *menC* deletion mutant unable to synthesize menaquinones, could not stimulate *L. plantarum* EET.

L. plantarum is commonly found in food fermentations with other quinone-producing LAB including *L. lactis* and *L. mesenteroides* (Michalak et al., 2018), suggesting that quinone cross-feeding to *L. plantarum* may influence ecological outcomes through EET. In this study, we observed an initial decline in *L. plantarum* cell numbers after 6 h growth with either *L. lactis* TIL46 or TIL999, but a greater abundance of *L. plantarum* after 24 h compared to growth by itself. *L. lactis* can produce bacteriocins inhibitory to *L. plantarum* growth (Settanni et al., 2005) which may have primarily influenced *L. plantarum* growth trends over quinone-cross feeding. *Leuconostoc* spp. are also capable of producing bacteriocins inhibitory to *L. plantarum* (Chang et al., 2007), but instead, we observed significantly greater *L. plantarum* abundance at 8 h versus *L. plantarum* growth by itself. *Leuconstoc* spp. are heterofermentative LAB which can produce CO_2 (Gänzle, 2015) that has been shown to stimulate *L. plantarum* growth (Arsène-Ploetze and Bringel, 2004). In our previous work, we showed that although *L. plantarum* EET occurred during the fermentation of kale juice, there were no differences in viable cell numbers in the kale juice medium (Tejedor-Sanz et al., 2021). Thus, our results highlight the complexity of *L. plantarum* growth in co-culture with *L. lactis* or *L. mesenteroides* which may be influenced by other metabolic compounds produced by these LAB.

The major metabolic action of LAB in food fermentations is the conversion of carbohydrates into lactic acid (Bintsis, 2018). This action allows for LAB to inhibit the growth of competitive (and potentially pathogenic) microorganisms which are less acidophilic (Pessione, 2012). We previously found that EET increased the acidification of kale juice with *L. plantarum* through increased metabolic flux and lactic acid production (Tejedor-Sanz et al., 2021). Thus, we hypothesized quinone-cross feeding in co-culture could yield similar outcomes. We confirmed this hypothesis by showing that *L. plantarum* growth with *L. lactis* TIL46 induced more iron

reduction *in situ* and accelerated environmental acidification more than *L. plantarum* growth with TIL999. Similar EET-induced acidification effects were seen with *L. plantarum* in co-culture with *L. mesenteroides* as well, and are in line with greater lactic acid and acetic acid production measured during the co-fermentation of Chinese sauerkraut with these LAB (Xiong et al., 2014). In summary, our results are the first to highlight a major metabolic and ecological impact of EET induced by quinones cross-fed amongst LAB.

Conclusions

Our work contributes to the growing field of EET research in Gram-positive bacteria by demonstrating how exogenous quinones and their exposure conditions affects *L. plantarum* EET. Furthermore, we show that quinones have a direct effect on *L. plantarum* physiology, along with ecological changes during co-culture with quinone-producing LAB. We previously proposed the use of EET activity by *L. plantarum* during food fermentations to enhance growth and organic acid production, a process akin to electro-fermentation (Moscoviz et al., 2016). With these data, we further suggest screening for other EET-stimulatory LAB to use with *L. plantarum* in starter cultures or co-cultures to further improve the success of food fermentations through EET.

Materials and Methods

Strains and culture conditions

All strains and plasmids used in this study are listed in **Table S1.** Standard laboratory culture medium was used for routine growth of bacteria as follows: *Lactiplantibacillus plantarum* and *Leuconostoc* spp., MRS (BD, Franklin Lakes, NJ, USA), *Lactococcus* lactis, M17 (BD) with 2% w/v glucose (gM17), and *Escherichia coli*, LB (Teknova, Hollister, CA, USA). *L. plantarum*

FLEET deletion mutants of *ndh2* or *pplA* were constructed through double-crossover homologous recombination as previously described (Tejedor-Sanz et al., 2021). Strains were also grown at 30 or 37 °C when indicated. In place of standard laboratory culture medium, strains were grown (when indicated) in modified MRS (De MAN et al., 1960) with no beef extract and with either 110 mM glucose [gMRS] or 110 mM mannitol [mMRS], or a chemically defined minimal medium (Tejedor-Sanz et al., 2021) with 125 mM glucose [gCDM] or 125 mM mannitol [mCDM].

L. plantarum growth rate experiments

After overnight growth in MRS at 37 °C, *L. plantarum* cells were collected via centrifugation (10,000 g / 3 min) and washed twice in phosphate-buffered saline (PBS) at pH 7.2 (http://cshprotocols.cshlp.org). Cells were resuspended in PBS at an optical density at 600 nm (OD_{600nm}) of 1 before inoculation into 96-well culture plates (Thermo Fisher Scientific, Waltham, MA) at a final OD_{600nm} of 0.01 in mMRS. When indicated, the mMRS was supplemented with ferric ammonium citrate (VWR, Radnor, PA, USA) (1.25 mM) or ammonium citrate tribasic (Alfa Aesar, Haverhill, MA, USA) (1.25 mM). The following quinones were also supplemented; 1,4-benzenediol (hydroquinone) (Sigma-Aldrich, St. Louis, MO, USA), 1,4-dihydroxy-2-naphthoic acid (DHNA) (Alfa Aesar), 1,4-naphthoquinone (TCI, Tokyo, Japan), 2-methyl-1,4-naphthoquinone (menadione) (Sigma-Aldrich), 2-amino-3-carboxy-1,4-naphthoquinone (ACNQ) (Mevers et al., 2019), Vitamin K1 (phylloquinone) (TCI), or Vitamin K2 in the form of menaquinone-4 (Sigma-Aldrich) or menaquinone-7 (Sigma-Aldrich). Quinones were supplemented at 2.5, 5, 10, 20, 50, 100, 150, or 200 μg/mL where indicated. The OD_{600nm} was measured over 48 h in a Synergy 2 microplate reader (Biotek, Winooski, VT) set to

37 °C with no aeration. Growth rates were determined by first determining exponential (logarithmic) phase growth and measuring the change in OD_{600nm} per hour.

In experiments where cell-free supernatant (CFS) was used in place of quinone supplementation, overnight cultures of *L. lactis* (gM17) or *Leuconostoc* spp. (gMRS) were grown for 18 h at 30 °C before normalizing the OD_{600nm} of these cultures with carbon-free M17 or MRS, respectively. Cells were then centrifuged (10,000 g / 3 min) and the supernatant was sterile filtered through a 0.22 μm syringe filter. Uninoculated, carbon-free media was also sterile-filtered as a control. Twice-washed *L. plantarum* cells (described above) were resuspended in PBS at an optical density at 600 nm (OD_{600nm}) of 1 before inoculation into 96-well culture plates at a final OD_{600nm} of 0.01 in 1:1 CFS (or carbon-free media) to 2x (twice-concentrated) mMRS. The OD_{600nm} was measured over 48 h as described above.

RNA-seq library construction and transcriptome analysis

The RNA-seq library was constructed and analyzed as previously described (Tejedor-Sanz et al., 2021). In brief, *L. plantarum* NCIMB8826 was grown in mMRS (in triplicate) with or without supplementation of 20 μg/mL DHNA and 1.25 mM ferric ammonium citrate. Cultures were grown at 37 °C to exponential phase (OD_{600} = ~1.0) before collection via centrifugation (10,000 g / 3 min) at 4 °C. After decanting, cells were flash frozen in liquid N_2 and stored at -80 °C until RNA extraction with acidic phenol:chloroform:isoamyl alcohol (pH 4.5) as previously described (Golomb et al., 2016). RNA was quantified on a Nanodrop 2000c (ThermoFisher) before two rounds of DNAse digestion using the Turbo DNA-free Kit (Invitrogen, Waltham, MA, USA) following the manufacturer's protocols. RNA quality was checked using a Bioanalyzer RNA

6000 Nano Kit (Agilent Technologies, Santa Clara, CA, USA) (all RIN values > 9), quantified with the Qubit 2.0 RNA HS Assay (Life Technologies, Carlsbad, CA, USA), and depleted of ribosomal-RNA (rRNA) with the RiboMinus Eukaryote Kit v2 using specific probes for prokaryotic rRNA (ThermoFisher). The remaining RNA was then fragmented to approximately 200 bp, converted to cDNA, and given barcode sequences using the NEBnext Ultra-directional RNA Library Kit for Illumina (New England Biolabs, Ipswitch, MA, USA) with NEBnext Multiplex Oligos for Illumina (Primer Set 1) (New England Biolabs) following the manufacturer's instructions. The barcoded cDNA libraries were pooled and run across two lanes of a HiSeq400 (Illumina, San Diego, CA, USA) on two separate runs for 150 bp paired-end reads (http://dnatech.genomecenter.ucdavis.edu/).

After sequencing and demultiplexing, DNA sequences for all 12 samples were first visualized in FastQC (ver. 0.11.8) (Andrews, 2010) followed by read trimming with Trimmomatic (ver. 0.39) (Bolger et al., 2014). Remaining reads were aligned to the *L. plantarum* NCIMB8826 chromosome and plasmids using Bowtie2 (ver. 2.3.5) in the [-sensitive] mode (Langmead and Salzberg, 2012) and output ".sam" files were converted to ".bam" files with Samtools (ver 1.9) (Li et al., 2009). Aligned reads which corresponded to NCIMB8826 genes, excluding noncoding sequences (e.g., rRNA, tRNA, trRNA, etc.) were enumerated with FeatureCounts in the [--stranded=reverse] mode (ver. 1.6.4) (Liao et al., 2014). DESeq2 (Love et al., 2014) using the Wald test in the R-studio shiny app DEBrowser (ver 1.14.2) (Kucukural et al., 2019) was used to quantify differential gene expression based on culture condition. The significance cutoff for differential expression was set to a False-discovery-rate (FDR)-adjusted p-value ≤ 0.05 and a

Log_2 (fold-change) $\geq$ 0.5. Clusters of Orthologous Groups (COGs) were also assigned to genes based the eggNOG (ver. 5.0) database (Huerta-Cepas et al., 2019).

Hydrogen peroxide production assay

L. plantarum NCIMB8826 was grown in mMRS (in triplicate) with or without supplementation of 20 μg/mL DHNA and 1.25 mM ferric ammonium citrate. Cultures were grown at 37 °C to exponential phase (OD_{600} = ~1.0) before collection via centrifugation (10,000 g / 3 min). Uninoculated cultures (in triplicate) were used for abiotic hydrogen peroxide production and were sampled after 5 h which was when *L. plantarum* cultures reached OD_{600} = 1 in exponential phase. Hydrogen peroxide was measured fluorometrically with the Fluorimetric Hydrogen Peroxide Assay Kit (Sigma-Aldrich) following the manufacturer's instructions.

ACNQ synthesis

The quinone ACNQ (2-amino-3-carboxy-1,4-naphthoquinone) was synthesized and purified as previously described (Mevers et al., 2019). Briefly, 20 g ammonium chloride was dissolved in 2 L of deionized (DI) water. The pH was then adjusted to 9.0 using ~10 mL of ammonium hydroxide solution. Next, 1 g DHNA (1,4-dihydroxy-2-naphthoic acid) was added, and the mixture was stirred for 24 h at RT. The pH was adjusted to 5.0 five and then twice extracted with 2 L ethyl acetate (EtOAc) before concentrating the organic layer under vacuum. The crude material was then resuspended in 10 mL 50% ACN/H2O, syringe filtered (0.2 mm) (Corning Inc, Corning, NY, USA), and purified using prep-HPLC. Pure ACNQ eluted between 33-35 min using a Phenomenex Luna 5 mm C8(2) 100 Å preparative column (250 x 21.2 mm) (Phenomenex, Torrance, CA, USA) with the following method: holding 20% ACN +0.1%

FA/H2O + 0.1% FA for 5 min then gradient to 55% ACN +0.1% FA/H2O + 0.1% FA over 35 min at 10 mL/min flow rate.

Ferrihydrite reduction assays

L. plantarum strains were first incubated in mMRS for 18 h at 37 °C. When indicated, quinones were supplemented at concentrations ranging from 0.01 to 200 μg/mL, and/or ferric ammonium citrate was supplemented at 1.25 mM. Cells were collected via centrifugation (10,000 g, 3 min) and washed twice in PBS. The OD_{600nm} was adjusted to 2 in PBS containing 2.2 mM ferrihydrite (Schwertmann and Fischer, 1973; Stookey, 1970), 2 mM ferrozine (Sigma-Aldrich), and 55 mM mannitol. Quinones were supplemented at the above concentrations when indicated, and uninoculated controls were used to subtract background ferrihydrite reduction by quinones. After 3 h incubation at 37 °C, the cells were collected by centrifugation (10,000 g / 5 min) the supernatant was used to determine iron reduction from absorbance measurements at 562 nm with a Synergy 2 microplate reader. Absorbance was converted to the concentration of reduced iron(II) using a standard curve containing a 2-fold range of $FeSO_4$ (Sigma-Aldrich) (0.25 mM to 0.016 mM) dissolved in 10 mM cysteine-HCL (RPI, Mount Prospect, IL, USA) and supplemented with 2 mM ferrozine.

In experiments where cell-free supernatant (CFS) was used in place of PBS as the assay medium, overnight cultures of *L. lactis* (gM17) or *Leuconostoc* spp. (gCDM) were grown for 18 h at 30 °C before normalizing the OD_{600nm} of these cultures with carbon-free M17 or CDM, respectively. Cells were then centrifuged (10,000 g / 3 min) and the supernatant was sterile filtered through a 0.22 μm syringe filter. Uninoculated, carbon-free media was also sterile-filtered as a control. The

OD_{600nm} of PBS-washed *L. plantarum* cells were then adjusted to 2 in the CFS or uninoculated media which was supplemented with ferrihydrite, ferrozine, and mannitol as described above. Ferrihydrite reduction assays with *L. lactis* or *Leuconostoc* CFS were carried out at 37 °C for 3 h before measuring reduced iron as described above.

Bioelectrochemical measurements

The bioreactors consisted of double-chamber electrochemical cells (Adams & Chittenden, Berkeley, CA) with a cation exchange membrane (CMI-7000, Membranes International, Ringwood, NJ) that separated them. We used a 3-electrode configuration consisting of an Ag/AgCl (sat. KCl) reference electrode (BASI), a titanium wire counter electrode, and a working electrode of either 6.35-mm-thick graphite felt working electrode of 4x4 cm (Alfa Aesar) with a piece of Ti wire threaded as a current collector and connection to the potentiostat. The bioreactors were sterilized by filling them with ddH2O and autoclaving at 121 °C for 30 min. After this, each chamber media was replaced with 150 mL of filter sterilized CDM media (for the working electrode chamber), and 150 mL of M9 media (BD) (for the counter electrode chamber). The medium (before filter-sterilization) was supplemented with a final concentration of 10 g/L of mannitol and with 20 μg/mL of DHNA diluted 1:1 in DMSO: ddH2O, where appropriate. The media in the working electrode chamber was mixed with a magnetic stir bar for the course of the experiment and N_2 gas was continuously purged in the working electrode chamber to maintain anaerobic conditions. Four bioreactors were prepared which differed in the CDM used in the working electrode chamber: two bioreactors contained mCDM supplemented with 20 μg/mL of DHNA (diluted 1:1 in DMSO: ddH2O), and other two bioreactors contained mCDM with no DHNA. All the experiments were tested under 30 °C. After approximately 4 h of

bubbling the working electrode chamber with N_2 gas, the working electrode of each bioreactor was polarized. The applied potential to the working electrodes was of 0.2 V versus the Ag/AgCl (sat. KCl) reference electrode. A Bio-Logic Science Instruments potentiostat model VSP-300 was used for performing electrochemical measurements. Once the current density stabilized overnight, the mCDM+DHNA bioreactors were inoculated to a final OD_{600nm} of ~0.1-0.15 with the cell suspensions of *L. plantarum* prepared in M9 medium. Cell suspensions were prepared from an overnight, statically grown culture (~16-18 h) of *L. plantarum* cultured in MRS medium at 30 °C. After 45 h of operating the bioreactors and observing current density production, we collected cells from each bioreactor by vigorously shaking the bioreactors to detach cells from the electrode and collecting the medium from the bioreactors (~150 mL). Cells were collected from each medium by performing 2 cycles of centrifugation (15,228 g, 7 min) and washing with M9 medium. The resulting cell pellets were suspended in oxygen-free M9 medium, and inoculated in the two DHNA-free bioreactors, previously polarized to 0.2 V and left overnight to achieve a stable current density baseline. Cyclic voltammetry analyses were performed at a scan rate of 5 mV/s and in the potential region of -0.7 to 0.4 V vs Ag/AgCl.

Cell membrane quinone quantification

Strains were grown in laboratory culture medium as follows: *L. plantarum* in mMRS supplemented with 20 µg/mL DHNA and/or 1.25 mM ferric ammonium citrate and *L. mesenteroides* in gMRS. All strains were grown for 18 h at 30 °C before cells were collected via centrifugation (10,000 g / 3 min). Cells were washed twice in PBS before flash freezing with liquid N_2. The cell pellet was placed on a lyophilizer for 18 h and then transferred to a 40 mL glass vial. The cell pellet was then ground and extracted with 3.0 mL of 2:1 dichloromethane

(DCM)/MeOH for 2 h while rocking on gently on a shaker. The organic solvent was filtered using a glass plug containing celite and dried under vacuum. The crude material was then resuspended in 200 µL of 2:1 isopropanol (IPA)/MeOH and 5 µL of this mixture was analyzed on a LCMS (Agilent 1260 HPLC equipped with a LTQ XL Thermo mass spectrometer) where the menaquinone analogs were quantified using the Phenomenex Luna 5 µm C5 100 Å (50 × 4.6 mm) under the following method: hold 100% solvent A for 5 min then quickly gradient to 80% solvent A/20% solvent B over 0.1 min, then gradient to 100% solvent B over 34.9 min with a flow rate of 0.4 mL/min (solvent A: 95% H2O/5% MeOH +0.1% FA with 5 mM ammonium acetate, solvent B: 60% IPA/35% MeOH/5% H2O + 0.1% FA with 5 mM ammonium acetate). Integrated extracted ion chromatograms for two ion adducts, [M + H]+ and [M+NH4]+, for each menaquinone analog were summed and compared to a five-point standard curve of commercially available menaquinone-4 (Sigma Aldrich) in order to obtain the absolute production quantification.

L. plantarum co-culturing experiments

L. plantarum NCIMB8826, *L. lactis* TIL46, *L. lactis* TIL999, and *L. mesenteroides* ATCC8293 were grown overnight in gMRS for 18 h at 30 °C. Cells were collected by centrifugation (10,000 g / 3 min) and washed twice in PBS. Approximately 10^7 CFU/mL of each strain was used to inoculate (in triplicate) 125 mL screw-cap bottles containing gCDM supplemented with 1.25 mM ferric ammonium citrate. Each strain was grown by itself at 30 °C and each *L. plantarum* strain was also grown in co-culture with either TIL46, TIL999, or ATCC8293. At t = 0, 4, 6, 8, and 24 h, cultures were sampled for pH and CFU/mL enumeration on MRS agar (30 °C) for monocultures and mMRS agar (37 °C) for co-cultures to distinguish between *L. plantarum*, *L.*

lactis, and *L. mesenteroides* by colony size. At these times, culture aliquots were also centrifuged (10,000 g / 5 min) and the supernatant was collected for Fe^{2+} analysis by immediately adding 2.2 mM ferrozine and using a Fe^{2+} standard curve as described previously.

Data accession numbers

L. plantarum RNA-seq data are available in the NCBI Sequence Read Archive (SRA) under BioProject accession no. PRJNA717240. DEseq2 analysis of RNA-seq data (Supplementary File 1) is available in the Harvard Dataverse: https://doi.org/10.7910/DVN/SAQ5AT

Acknowledgements

This work was supported by the National Science Foundation grant #1650042.

References

Altwiley, D., Brignoli, T., Edwards, A., Recker, M., Lee, J.C., Massey, R.C.Y. 2021, 2021. A functional menadione biosynthesis pathway is required for capsule production by Staphylococcus aureus. Microbiology 167, 001108. https://doi.org/10.1099/mic.0.001108

Andrews, S., 2010. FastQC: A Quality Control tool for High Throughput Sequence Data [WWW Document]. URL http://www.bioinformatics.babraham.ac.uk/projects/fastqc/ (accessed 2.6.20).

Arsène-Ploetze, F., Bringel, F., 2004. Role of inorganic carbon in lactic acid bacteria metabolism. Le Lait 84, 49–59. https://doi.org/10.1051/lait:2003040

Beulens, J.W.J., van der A, D.L., Grobbee, D.E., Sluijs, I., Spijkerman, A.M.W., van der Schouw, Y.T., 2010. Dietary Phylloquinone and Menaquinones Intakes and Risk of Type 2 Diabetes. Diabetes Care 33, 1699–1705. https://doi.org/10.2337/dc09-2302

Bintsis, T., 2018. Lactic acid bacteria as starter cultures: An update in their metabolism and genetics. AIMS Microbiol. 4, 665–684. https://doi.org/10.3934/microbiol.2018.4.665

Bron, P.A., Wels, M., Bongers, R.S., Veen, H. van B. de, Wiersma, A., Overmars, L., Marco, M.L., Kleerebezem, M., 2012. Transcriptomes Reveal Genetic Signatures Underlying Physiological Variations Imposed by Different Fermentation Conditions in Lactobacillus plantarum. PLOS ONE 7, e38720. https://doi.org/10.1371/journal.pone.0038720

Brooijmans, R.J.W., Vos, W.M. de, Hugenholtz, J., 2009. Lactobacillus plantarum WCFS1 Electron Transport Chains. Appl. Environ. Microbiol. 75, 3580–3585. https://doi.org/10.1128/AEM.00147-09

Chang, J. y., Lee, H. j., Chang, H. c., 2007. Identification of the agent from Lactobacillus plantarum KFRI464 that enhances bacteriocin production by Leuconostoc citreum GJ7. J. Appl. Microbiol. 103, 2504–2515. https://doi.org/10.1111/j.1365-2672.2007.03543.x

Damon, M., Zhang, N.Z., Haytowitz, D.B., Booth, S.L., 2005. Phylloquinone (vitamin K1) content of vegetables. J. Food Compos. Anal. 18, 751–758. https://doi.org/10.1016/j.jfca.2004.07.004

Dantas, J.M., Ferreira, M.R., Catarino, T., Kokhan, O., Pokkuluri, P.R., Salgueiro, C.A., 2018. Molecular interactions between Geobacter sulfurreducens triheme cytochromes and the redox active analogue for humic substances. Biochim. Biophys. Acta BBA - Bioenerg. 1859, 619–630. https://doi.org/10.1016/j.bbabio.2018.05.007

Di Cagno, R., Filannino, P., Gobbetti, M., 2015. Vegetable and Fruit Fermentation by Lactic Acid Bacteria, in: Biotechnology of Lactic Acid Bacteria. John Wiley & Sons, Ltd, pp. 216–230. https://doi.org/10.1002/9781118868386.ch14

Elling, F.J., Becker, K.W., Könneke, M., Schröder, J.M., Kellermann, M.Y., Thomm, M., Hinrichs, K.-U., 2016. Respiratory quinones in Archaea: phylogenetic distribution and application as biomarkers in the marine environment. Environ. Microbiol. 18, 692–707. https://doi.org/10.1111/1462-2920.13086

Eom, J.-E., Kwon, S.-C., Moon, G.-S., 2012. Detection of 1,4-Dihydroxy-2-Naphthoic Acid from Commercial Makgeolli Products. Prev. Nutr. Food Sci. 17, 83–86. https://doi.org/10.3746/pnf.2012.17.1.083

Eom, J.-E., Moon, G.-S., 2015. Construction of a Recombinant Leuconostoc mesenteroides CJNU 0147 Producing 1,4-Dihydroxy-2-Naphthoic Acid, a Bifidogenic Growth Factor. Korean J. Food Sci. Anim. Resour. 35, 867–873. https://doi.org/10.5851/kosfa.2015.35.6.867

Feng, T., Wang, J., 2020. Oxidative stress tolerance and antioxidant capacity of lactic acid bacteria as probiotic: a systematic review. Gut Microbes 12, 1801944. https://doi.org/10.1080/19490976.2020.1801944

Fenn, K., Strandwitz, P., Stewart, E.J., Dimise, E., Rubin, S., Gurubacharya, S., Clardy, J., Lewis, K., 2017. Quinones are growth factors for the human gut microbiota. Microbiome 5, 161. https://doi.org/10.1186/s40168-017-0380-5

Finnegan, M., Linley, E., Denyer, S.P., McDonnell, G., Simons, C., Maillard, J.-Y., 2010. Mode of action of hydrogen peroxide and other oxidizing agents: differences between liquid and gas forms. J. Antimicrob. Chemother. 65, 2108–2115. https://doi.org/10.1093/jac/dkq308

Freguia, S., Masuda, M., Tsujimura, S., Kano, K., 2009. Lactococcus lactis catalyses electricity generation at microbial fuel cell anodes via excretion of a soluble quinone. Bioelectrochemistry, Advanced design of electron-transfer pathways across biomolecular interfaces, Dedicated to Professor Lo Gorton 76, 14–18. https://doi.org/10.1016/j.bioelechem.2009.04.001

Furuichi, K., Hojo, K., Katakura, Y., Ninomiya, K., Shioya, S., 2006. Aerobic culture of Propionibacterium freudenreichii ET-3 can increase production ratio of 1,4-dihydroxy-2-naphthoic acid to menaquinone. J. Biosci. Bioeng. 101, 464–470. https://doi.org/10.1263/jbb.101.464

Futuro, D.O., Ferreira, P.G., Nicoletti, C.D., Borba-Santos, L.P., Silva, F.C.D., Rozental, S., Ferreira, V.F., 2018. The Antifungal Activity of Naphthoquinones: An Integrative Review. An. Acad. Bras. Ciênc. 90, 1187–1214. https://doi.org/10.1590/0001-3765201820170815

Gänzle, M.G., 2015. Lactic metabolism revisited: metabolism of lactic acid bacteria in food fermentations and food spoilage. Curr. Opin. Food Sci., Food Microbiology • Functional Foods and Nutrition 2, 106–117. https://doi.org/10.1016/j.cofs.2015.03.001

Gerstle, K., Klätschke, K., Hahn, U., Piganeau, N., 2012. The small RNA RybA regulates key-genes in the biosynthesis of aromatic amino acids under peroxide stress in E. coli. RNA Biol. 9, 458–468. https://doi.org/10.4161/rna.19065

Glasser, N.R., Saunders, S.H., Newman, D.K., 2017. The Colorful World of Extracellular Electron Shuttles. Annu. Rev. Microbiol. 71, 731–751. https://doi.org/10.1146/annurev-micro-090816-093913

Goel, S., Parihar, P.S., Meshram, V., 2020. Plant-Derived Quinones as a Source of Antibacterial and Anticancer Agents, in: Singh, J., Meshram, V., Gupta, M. (Eds.), Bioactive Natural Products in Drug Discovery. Springer, Singapore, pp. 245–279. https://doi.org/10.1007/978-981-15-1394-7_6

Hansen, E.B., 2018. Redox reactions in food fermentations. Curr. Opin. Food Sci., Food Chemistry and Biochemistry * Food Bioprocessing 19, 98–103. https://doi.org/10.1016/j.cofs.2018.03.004

Hederstedt, L., Gorton, L., Pankratova, G., 2020. Two Routes for Extracellular Electron Transfer in Enterococcus faecalis. J. Bacteriol. 202. https://doi.org/10.1128/JB.00725-19

Isawa, K., Hojo, K., Yoda, N., Kamiyama, T., Makino, S., Saito, M., Sugano, H., Mizoguchi, C., Kurama, S., Shibasaki, M., Endo, N., Sato, Y., 2002. Isolation and identification of a new bifidogenic growth stimulator produced by Propionibacterium freudenreichii ET-3. Biosci. Biotechnol. Biochem. 66, 679–681. https://doi.org/10.1271/bbb.66.679

Janßen, H.J., Steinbüchel, A., 2014. Fatty acid synthesis in Escherichia coli and its applications towards the production of fatty acid based biofuels. Biotechnol. Biofuels 7, 7. https://doi.org/10.1186/1754-6834-7-7

Jiang, C., Garg, S., Waite, T.D., 2015. Hydroquinone-Mediated Redox Cycling of Iron and Concomitant Oxidation of Hydroquinone in Oxic Waters under Acidic Conditions: Comparison with Iron–Natural Organic Matter Interactions. Environ. Sci. Technol. 49, 14076–14084. https://doi.org/10.1021/acs.est.5b03189

Kang, J.-E., Kim, T.-J., Moon, G.-S., 2015. A Novel Lactobacillus casei LP1 Producing 1,4-Dihydroxy-2-Naphthoic Acid, a Bifidogenic Growth Stimulator. Prev. Nutr. Food Sci. 20, 78–81. https://doi.org/10.3746/pnf.2015.20.1.78

Karl, J.P., Meydani, M., Barnett, J.B., Vanegas, S.M., Barger, K., Fu, X., Goldin, B., Kane, A., Rasmussen, H., Vangay, P., Knights, D., Jonnalagadda, S.S., Saltzman, E., Roberts, S.B., Meydani, S.N., Booth, S.L., 2017. Fecal concentrations of bacterially derived vitamin K forms are associated with gut microbiota composition but not plasma or fecal cytokine concentrations in healthy adults. Am. J. Clin. Nutr. 106, 1052–1061. https://doi.org/10.3945/ajcn.117.155424

Kracke, F., Vassilev, I., Krömer, J.O., 2015. Microbial electron transport and energy conservation – the foundation for optimizing bioelectrochemical systems. Front. Microbiol. 6. https://doi.org/10.3389/fmicb.2015.00575

Light, S.H., Su, L., Rivera-Lugo, R., Cornejo, J.A., Louie, A., Iavarone, A.T., Ajo-Franklin, C.M., Portnoy, D.A., 2018. A flavin-based extracellular electron transfer mechanism in diverse Gram-positive bacteria. Nature 562, 140. https://doi.org/10.1038/s41586-018-0498-z

Lin, X., Yang, F., You, L., Wang, H., Zhao, F., 2021. Liposoluble quinone promotes the reduction of hydrophobic mineral and extracellular electron transfer of Shewanella oneidensis MR-1. The Innovation 2, 100104. https://doi.org/10.1016/j.xinn.2021.100104

Lovley, D.R., Holmes, D.E., 2022. Electromicrobiology: the ecophysiology of phylogenetically diverse electroactive microorganisms. Nat. Rev. Microbiol. 20, 5–19. https://doi.org/10.1038/s41579-021-00597-6

Luo, S., Levine, R.L., 2009. Methionine in proteins defends against oxidative stress. FASEB J. 23, 464–472. https://doi.org/10.1096/fj.08-118414

Lyngsie, G., Krumina, L., Tunlid, A., Persson, P., 2018. Generation of hydroxyl radicals from reactions between a dimethoxyhydroquinone and iron oxide nanoparticles. Sci. Rep. 8, 10834. https://doi.org/10.1038/s41598-018-29075-5

Martino, M.E., Bayjanov, J.R., Caffrey, B.E., Wels, M., Joncour, P., Hughes, S., Gillet, B., Kleerebezem, M., Hijum, S.A.F.T. van, Leulier, F., 2016. Nomadic lifestyle of Lactobacillus plantarum revealed by comparative genomics of 54 strains isolated from different habitats. Environ. Microbiol. 18, 4974–4989. https://doi.org/10.1111/1462-2920.13455

Masuda, M., Freguia, S., Wang, Y.-F., Tsujimura, S., Kano, K., 2010. Flavins contained in yeast extract are exploited for anodic electron transfer by Lactococcus lactis. Bioelectrochemistry 78, 173–175. https://doi.org/10.1016/j.bioelechem.2009.08.004

McFeeters, R.F., Chen, K.-H., 1986. Utilization of electron acceptors for anaerobic mannitol metabolism by Lactobacillus plantarum. Compounds which serve as electron acceptors. Food Microbiol. 3, 73–81. https://doi.org/10.1016/S0740-0020(86)80029-6

Meng, Y., Zhao, Z., Burgos, W.D., Li, Y., Zhang, B., Wang, Y., Liu, W., Sun, L., Lin, L., Luan, F., 2018. Iron(III) minerals and anthraquinone-2,6-disulfonate (AQDS) synergistically enhance bioreduction of hexavalent chromium by Shewanella oneidensis MR-1. Sci. Total Environ. 640–641, 591–598. https://doi.org/10.1016/j.scitotenv.2018.05.331

Mevers, E., Su, L., Pishchany, G., Baruch, M., Cornejo, J., Hobert, E., Dimise, E., Ajo-Franklin, C.M., Clardy, J., 2019. An elusive electron shuttle from a facultative anaerobe. eLife 8, e48054. https://doi.org/10.7554/eLife.48054

Michalak, M., Gustaw, K., Waśko, A., Polak-Berecka, M., 2018. Composition of lactic acid bacteria during spontaneous curly kale (Brassica oleracea var. sabellica) fermentation. Microbiol. Res. 206, 121–130. https://doi.org/10.1016/j.micres.2017.09.011

Mirkhalaf, F., Tammeveski, K., Schiffrin, D.J., 2004. Substituent effects on the electrocatalytic reduction of oxygen on quinone-modified glassy carbon electrodes. Phys. Chem. Chem. Phys. 6, 1321–1327. https://doi.org/10.1039/B315963A

Morishita, T., Tamura, N., Makino, T., Kudo, S., 1999. Production of Menaquinones by Lactic Acid Bacteria. J. Dairy Sci. 82, 1897–1903. https://doi.org/10.3168/jds.S0022-0302(99)75424-X

Nagata, K., Inatsu, S., Tanaka, M., Sato, H., Kouya, T., Taniguchi, M., Fukuda, Y., 2010. The Bifidogenic Growth Stimulator Inhibits the Growth and Respiration of Helicobacter pylori. Helicobacter 15, 422–429. https://doi.org/10.1111/j.1523-5378.2010.00789.x

Nitzschke, A., Bettenbrock, K., 2018. All three quinone species play distinct roles in ensuring optimal growth under aerobic and fermentative conditions in E. coli K12. PLoS ONE 13. https://doi.org/10.1371/journal.pone.0194699
Pandey, A., Bringel, F., Meyer, J.-M., 1994. Iron requirement and search for siderophores in lactic acid bacteria. Appl. Microbiol. Biotechnol. 40, 735–739. https://doi.org/10.1007/BF00173337
Pankratova, G., Leech, D., Gorton, L., Hederstedt, L., 2018. Extracellular Electron Transfer by the Gram-Positive Bacterium Enterococcus faecalis. Biochemistry 57, 4597–4603. https://doi.org/10.1021/acs.biochem.8b00600
Papadimitriou, K., Alegría, Á., Bron, P.A., de Angelis, M., Gobbetti, M., Kleerebezem, M., Lemos, J.A., Linares, D.M., Ross, P., Stanton, C., Turroni, F., van Sinderen, D., Varmanen, P., Ventura, M., Zúñiga, M., Tsakalidou, E., Kok, J., 2016. Stress Physiology of Lactic Acid Bacteria. Microbiol. Mol. Biol. Rev. MMBR 80, 837–890. https://doi.org/10.1128/MMBR.00076-15
Paquete, C.M., 2020. Electroactivity across the cell wall of Gram-positive bacteria. Comput. Struct. Biotechnol. J. 18, 3796–3802. https://doi.org/10.1016/j.csbj.2020.11.021
Pedersen, M.B., Gaudu, P., Lechardeur, D., Petit, M.-A., Gruss, A., 2012. Aerobic respiration metabolism in lactic acid bacteria and uses in biotechnology. Annu. Rev. Food Sci. Technol. 3, 37–58. https://doi.org/10.1146/annurev-food-022811-101255
Pessione, E., 2012. Lactic acid bacteria contribution to gut microbiota complexity: lights and shadows. Front. Cell. Infect. Microbiol. 2.
Rezaïki, L., Lamberet, G., Derré, A., Gruss, A., Gaudu, P., 2008. Lactococcus lactis produces short-chain quinones that cross-feed Group B Streptococcus to activate respiration growth. Mol. Microbiol. 67, 947–957. https://doi.org/10.1111/j.1365-2958.2007.06083.x
Ryan, E.M., Duryee, M.J., Hollins, A., Dover, S.K., Pirruccello, S., Sayles, H., Real, K.D., Hunter, C., Thiele, G.M., Mikuls, T.R., 2019. Antioxidant properties of citric acid interfere with the uricase-based measurement of circulating uric acid. J. Pharm. Biomed. Anal. 164, 460–466. https://doi.org/10.1016/j.jpba.2018.11.011
Schlievert, P.M., Merriman, J.A., Salgado-Pabón, W., Mueller, E.A., Spaulding, A.R., Vu, B.G., Chuang-Smith, O.N., Kohler, P.L., Kirby, J.R., 2013. Menaquinone Analogs Inhibit Growth of Bacterial Pathogens. Antimicrob. Agents Chemother. 57, 5432–5437. https://doi.org/10.1128/AAC.01279-13
Settanni, L., Massitti, O., Van Sinderen, D., Corsetti, A., 2005. In situ activity of a bacteriocin-producing Lactococcus lactis strain. Influence on the interactions between lactic acid bacteria during sourdough fermentation. J. Appl. Microbiol. 99, 670–681. https://doi.org/10.1111/j.1365-2672.2005.02647.x
Shi, L., Dong, H., Reguera, G., Beyenal, H., Lu, A., Liu, J., Yu, H.-Q., Fredrickson, J.K., 2016. Extracellular electron transfer mechanisms between microorganisms and minerals. Nat. Rev. Microbiol. 14, 651–662. https://doi.org/10.1038/nrmicro.2016.93
Tachon, S., Brandsma, J.B., Yvon, M., 2010. NoxE NADH Oxidase and the Electron Transport Chain Are Responsible for the Ability of Lactococcus lactis To Decrease the Redox Potential of Milk. Appl. Environ. Microbiol. 76, 1311–1319. https://doi.org/10.1128/AEM.02120-09
Tachon, S., Michelon, D., Chambellon, E., Cantonnet, M., Mezange, C., Henno, L., Cachon, R., Yvon, M., 2009. Experimental conditions affect the site of tetrazolium violet reduction in

the electron transport chain of Lactococcus lactis. Microbiol. Read. Engl. 155, 2941–2948. https://doi.org/10.1099/mic.0.029678-0
Tejedor-Sanz, S., Stevens, E.T., Finnegan, P., Nelson, J., Knoessen, A., Light, S.H., Ajo-Franklin, C.M., Marco, M.L., 2021. Extracellular electron transfer increases fermentation in lactic acid bacteria via a hybrid metabolism. bioRxiv 2021.05.26.445846. https://doi.org/10.1101/2021.05.26.445846
Teusink, B., Enckevort, F.H.J. van, Francke, C., Wiersma, A., Wegkamp, A., Smid, E.J., Siezen, R.J., 2005. In Silico Reconstruction of the Metabolic Pathways of Lactobacillus plantarum: Comparing Predictions of Nutrient Requirements with Those from Growth Experiments. Appl. Environ. Microbiol. 71, 7253–7262. https://doi.org/10.1128/AEM.71.11.7253-7262.2005
Thakur, K., Tomar, S.K., De, S., 2016. Lactic acid bacteria as a cell factory for riboflavin production. Microb. Biotechnol. 9, 441–451. https://doi.org/10.1111/1751-7915.12335
Voordeckers, J.W., Kim, B.-C., Izallalen, M., Lovley, D.R., 2010. Role of Geobacter sulfurreducens Outer Surface c-Type Cytochromes in Reduction of Soil Humic Acid and Anthraquinone-2,6-Disulfonate. Appl. Environ. Microbiol. 76, 2371–2375. https://doi.org/10.1128/AEM.02250-09
Walther, B., Chollet, M., 2017. Menaquinones, Bacteria, and Foods: Vitamin K2 in the Diet, Vitamin K2 - Vital for Health and Wellbeing. IntechOpen. https://doi.org/10.5772/63712
Walther, B., Karl, J.P., Booth, S.L., Boyaval, P., 2013. Menaquinones, Bacteria, and the Food Supply: The Relevance of Dairy and Fermented Food Products to Vitamin K Requirements123. Adv. Nutr. 4, 463–473. https://doi.org/10.3945/an.113.003855
Watthanasakphuban, N., Virginia, L.J., Haltrich, D., Peterbauer, C., 2021. Analysis and Reconstitution of the Menaquinone Biosynthesis Pathway in Lactiplantibacillus plantarum and Lentilactibacillus buchneri. Microorganisms 9, 1476. https://doi.org/10.3390/microorganisms9071476
Wendlandt, A.E., Stahl, S.S., 2016. Quinones in Hydrogen Peroxide Synthesis and Catalytic Aerobic Oxidation Reactions, in: Liquid Phase Aerobic Oxidation Catalysis: Industrial Applications and Academic Perspectives. John Wiley & Sons, Ltd, pp. 219–237. https://doi.org/10.1002/9783527690121.ch14
Widhalm, J.R., Rhodes, D., 2016. Biosynthesis and molecular actions of specialized 1,4-naphthoquinone natural products produced by horticultural plants. Hortic. Res. 3, 1–17. https://doi.org/10.1038/hortres.2016.46
Xiong, T., Peng, F., Liu, Y., Deng, Y., Wang, X., Xie, M., 2014. Fermentation of Chinese sauerkraut in pure culture and binary co-culture with Leuconostoc mesenteroides and Lactobacillus plantarum. LWT - Food Sci. Technol. 59, 713–717. https://doi.org/10.1016/j.lwt.2014.05.059
Yang, L., Mih, N., Anand, A., Park, J.H., Tan, J., Yurkovich, J.T., Monk, J.M., Lloyd, C.J., Sandberg, T.E., Seo, S.W., Kim, D., Sastry, A.V., Phaneuf, P., Gao, Y., Broddrick, J.T., Chen, K., Heckmann, D., Szubin, R., Hefner, Y., Feist, A.M., Palsson, B.O., 2019. Cellular responses to reactive oxygen species are predicted from molecular mechanisms. Proc. Natl. Acad. Sci. 116, 14368–14373. https://doi.org/10.1073/pnas.1905039116
You, L.-X., Pan, D.-M., Chen, N.-J., Lin, W.-F., Chen, Q.-S., Rensing, C., Zhou, S.-G., 2019. Extracellular electron transfer of Enterobacter cloacae SgZ-5T via bi-mediators for the biorecovery of palladium as nanorods. Environ. Int. 123, 1–9. https://doi.org/10.1016/j.envint.2018.11.018

Zerfaß, C., Asally, M., Soyer, O.S., 2019. Interrogating metabolism as an electron flow system. Curr. Opin. Syst. Biol., • Systems biology of model organisms • Systems ecology and evolution 13, 59–67. https://doi.org/10.1016/j.coisb.2018.10.001

Zhai, Z., Yang, Y., Wang, H., Wang, G., Ren, F., Li, Z., Hao, Y., 2020. Global transcriptomic analysis of Lactobacillus plantarum CAUH2 in response to hydrogen peroxide stress. Food Microbiol. 87, 103389. https://doi.org/10.1016/j.fm.2019.103389

Zhang, E., Cai, Y., Luo, Y., Piao, Z., 2014. Riboflavin-shuttled extracellular electron transfer from Enterococcus faecalis to electrodes in microbial fuel cells. Can. J. Microbiol. 60, 753–759. https://doi.org/10.1139/cjm-2014-0389

Zhang, T., Ding, Y., Li, T., Wan, Y., Li, W., Chen, H., Zhou, R., 2012. A Fur-like protein PerR regulates two oxidative stress response related operons dpr and metQIN in Streptococcus suis. BMC Microbiol. 12, 85. https://doi.org/10.1186/1471-2180-12-85

Zotta, T., Parente, E., Ricciardi, A., 2017. Aerobic metabolism in the genus Lactobacillus: impact on stress response and potential applications in the food industry. J. Appl. Microbiol. 122, 857–869. https://doi.org/10.1111/jam.13399

Figures

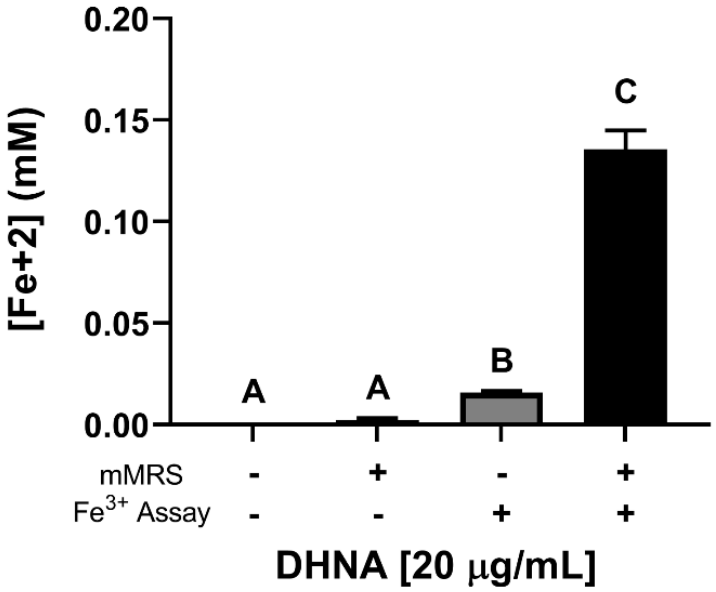

Figure 1. DHNA presence is required for *L. plantarum* at the time of iron reduction. Fe^{3+} (ferrihydrite) reduction assays were performed in PBS with 55 mM mannitol and 20 μg/mL DHNA where indicated. Significant differences between groups were determined by one-way ANOVA with Tukey's post-hoc test (represented by letters, $p \leq 0.05$). The avg $\pm$ stdev of three biological replicates is shown.

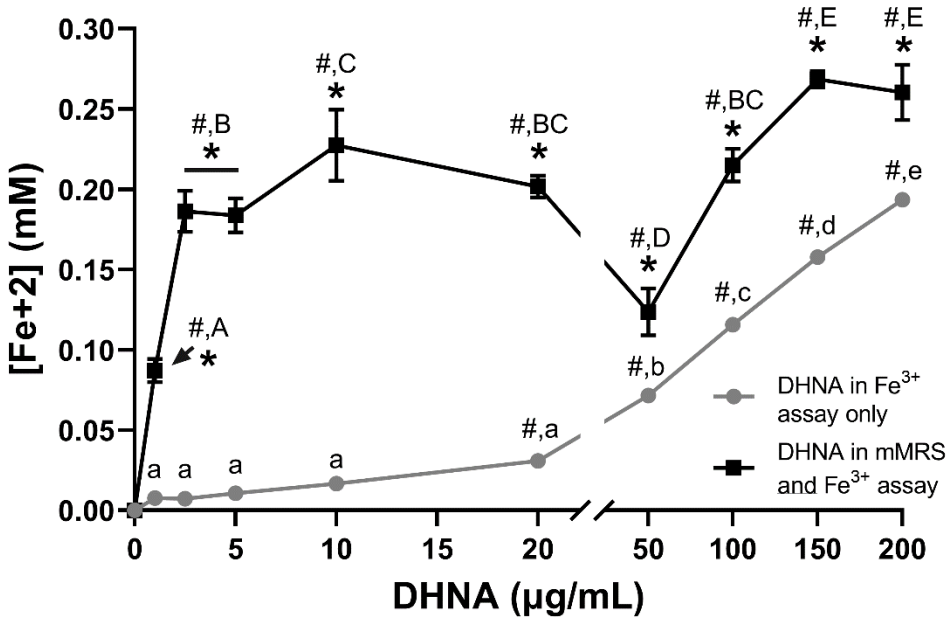

Figure 2. *L. plantarum* reduces more iron when grown with DHNA at high and low concentrations. Reduction of ferrihydrite by *L. plantarum* after growth in mMRS supplemented with 1.25 mM FeAC. DHNA was supplemented in the growth medium and/or the ferrihydrite reduction assay at indicated concentrations. Significant differences between groups were determined by one-way ANOVA with Tukey's post-hoc test ($p \leq 0.05$); # iron reduction was significantly greater after growth in DHNA (compared to cells incubated in DHNA only during the ferrihydrite assay), * iron reduction was significantly greater compared to cells never provided DHNA, letters denote when iron reduction was significantly different between DHNA concentrations within the same growth condition. The avg $\pm$ stdev of three biological replicates is shown.

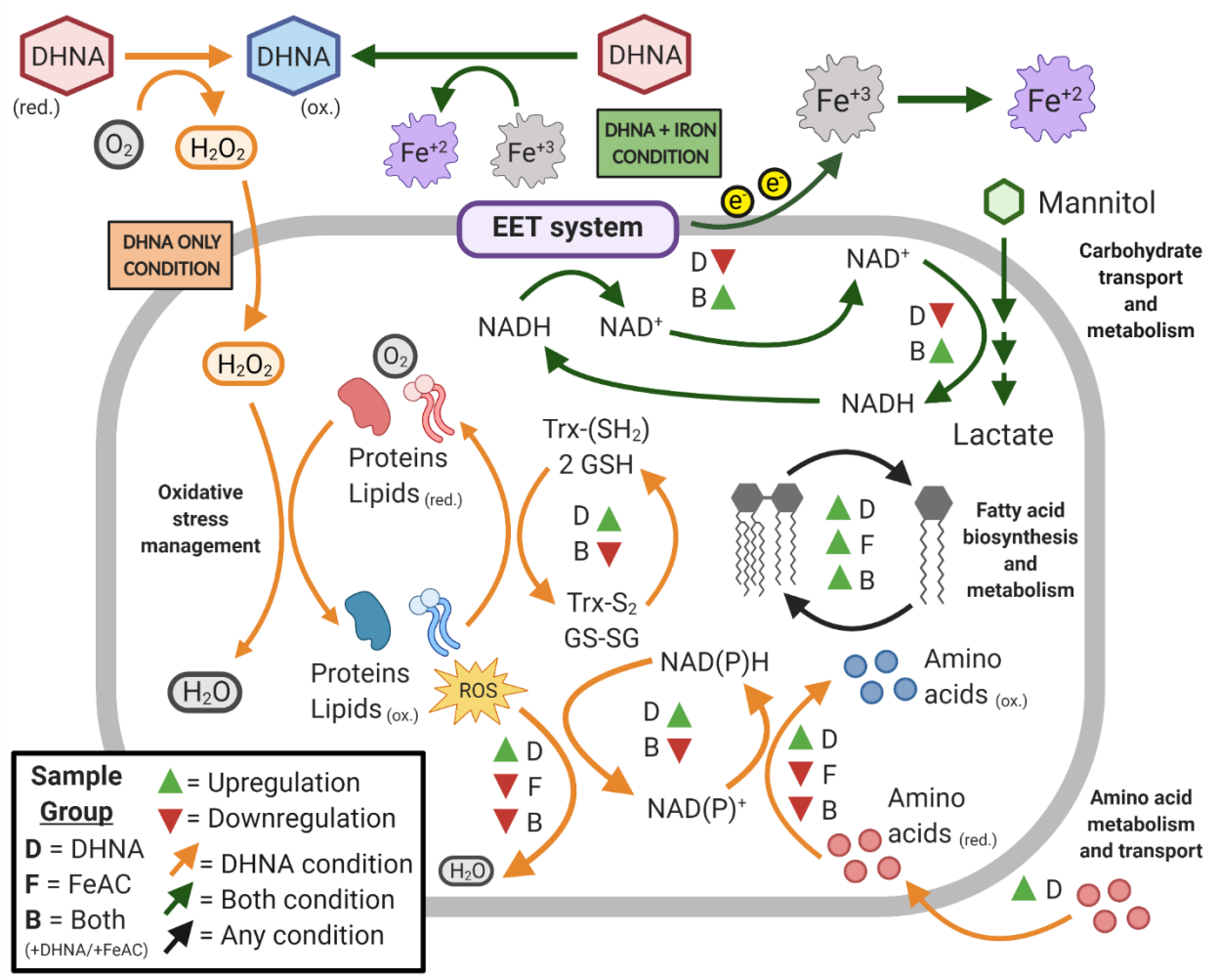

Figure 3. DHNA-caused induction of oxidative stress response in *L. plantarum* is alleviated by FeAC. Summary of *L. plantarum* transcriptome changes in response to DHNA (D = DNHA), FeAC (F = FeAC), or DHNA+FeAC (B = Both) during exponential-phase growth in mMRS. Statistically significant changes in gene expression were determined using DEseq2 with a Log_2 expression fold-change ≥ 0.5 and FDR-adjusted *p*-value ≤ 0.05.

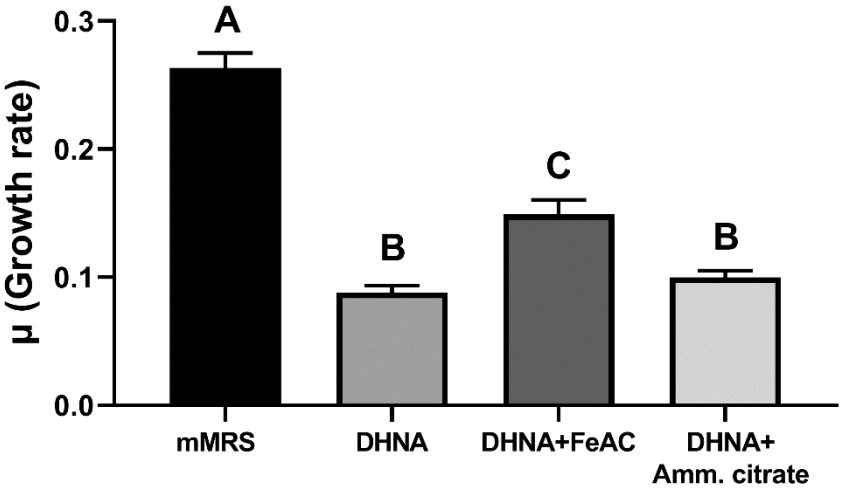

Figure 4. Iron reduces the negative effects of DHNA on *L. plantarum* growth rate in mMRS. Growth rate of *L. plantarum* in mMRS with or without supplementation of 20 μg/mL DHNA and 1.25 mM ferric ammonium citrate (FeAC) or 1.25 mM ammonium citrate. Growth rates were quantified by measuring the change in OD_{600nm} per hour during exponential phase in mMRS. Significant differences represented by letters were determined using one-way ANOVA with Tukey's post-hoc test ($p \leq 0.05$). The average $\pm$ SEM of three biological replicates is shown.

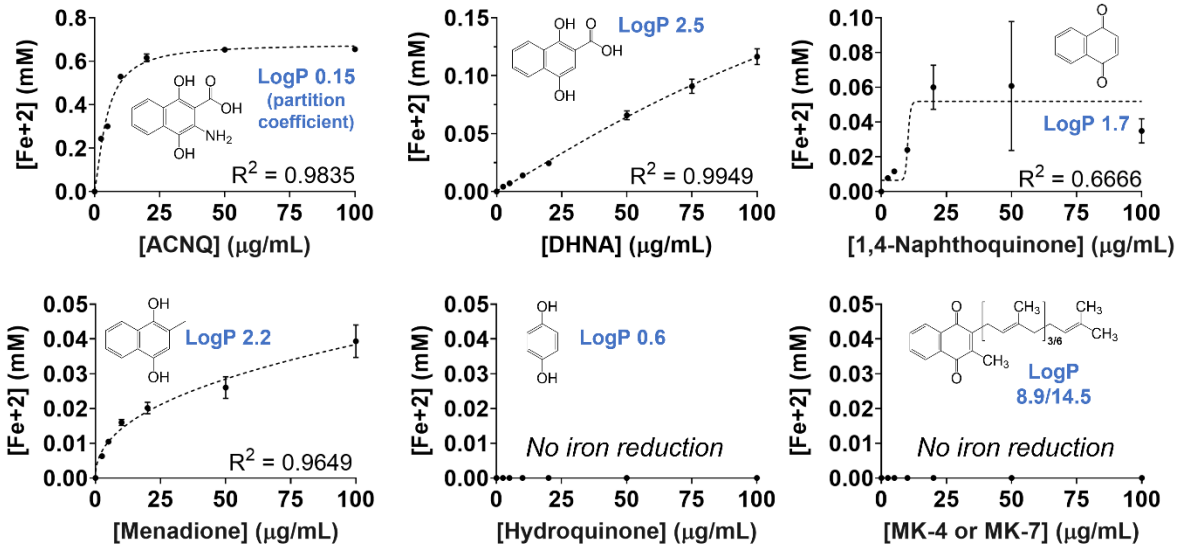

Figure 5. Exogenous quinones catalyze *L. plantarum* iron reduction. Ferrihydrite reduction assays were performed in PBS containing 55 mM mannitol and at specified quinone concentrations. *L. plantarum* cells used in the assay were grown in mMRS without quinone supplementation. The R^2 value corresponds to the sigmoidal dose-response curve fit to the data. The chemical structure of each quinone and its corresponding Log_P (log of partition coefficient) are provided. The avg $\pm$ stdev of three biological replicates is shown.

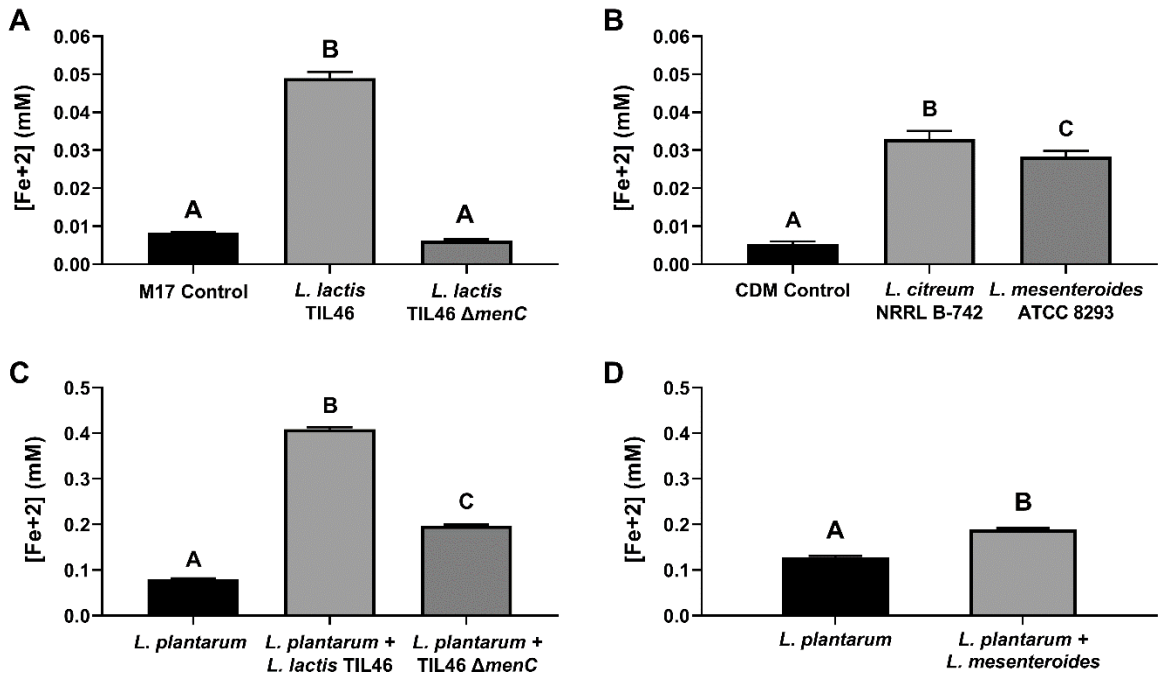

Figure 6. Quinones secreted from other LAB can stimulate *L. plantarum* EET. (A/B) Ferrihydrite reduction by *L. plantarum* in cell-free supernatant (CFS) from **(A)** *Lactococcus lactis* or **(B)** *Leuconostoc* spp. and supplemented with 55 mM mannitol. Uninoculated M17 or CDM lacking glucose was used as a control these experiments. **(C/D)** Iron reduction by *L. plantarum* in gCDM with 1.25 mM ferric ammonium citrate during growth alone or in co-culture with **(C)** *L. lactis* or **(D)** *L. mesenteroides*. Significant differences between groups (represented by letters, $p \leq 0.05$) determined by **(A/B/C)** one-way ANOVA with Tukey's post-hoc test or **(D)** unpaired Student's t-test. The average $\pm$ stdev of three biological replicates is shown.

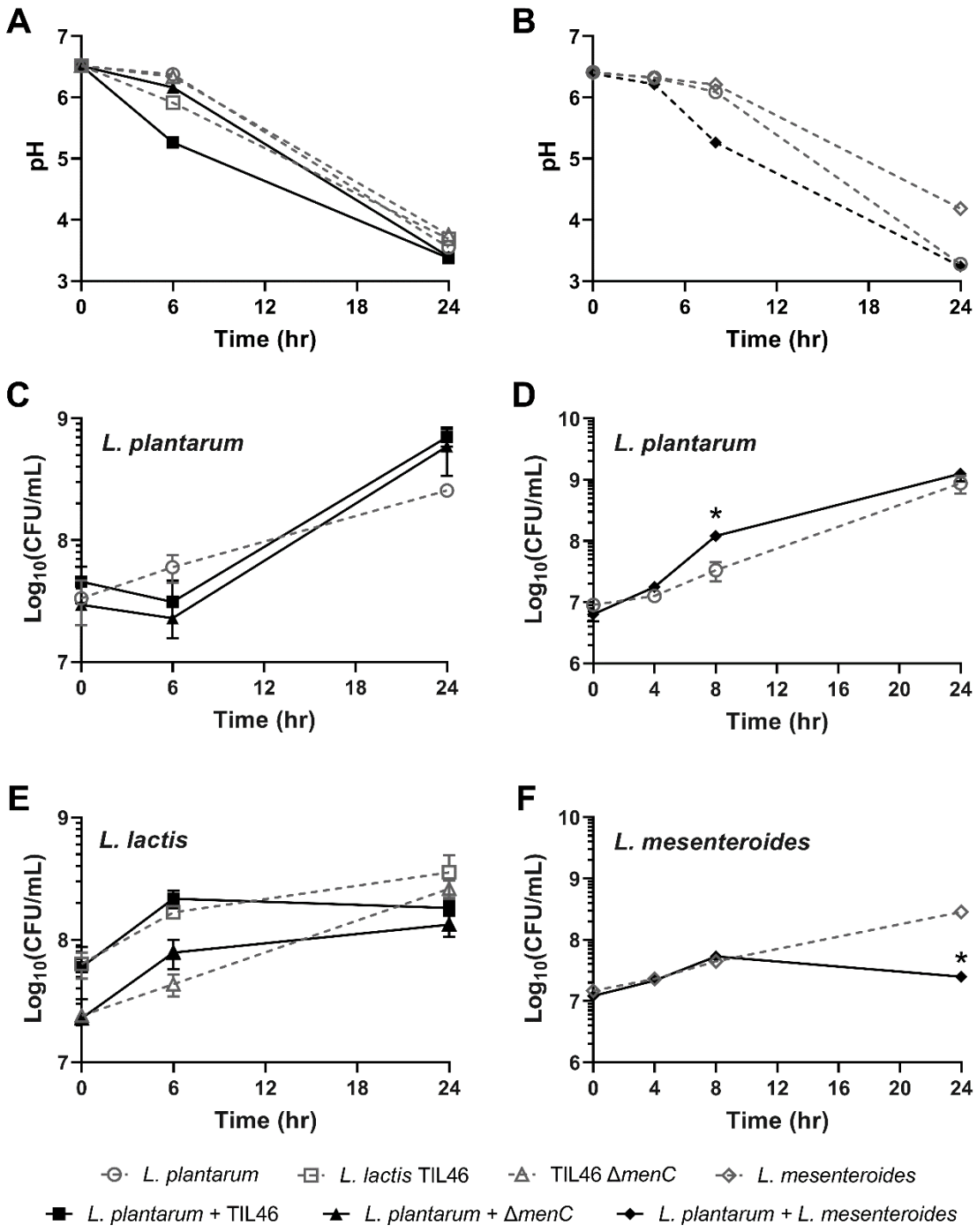

Figure 7. Co-culturing *L. plantarum* with *L. lactis* or *L. mesenteroides* increases acidification and *L. plantarum* growth. (A/B) pH, **(C/D)** *L. plantarum* abundance, and abundance of **(E)** *L. lactis* or **(F)** *L. mesenteroides* in during growth alone or in co-culture with *L plantarum*. Strains were grown in gCDM supplemented with 1.25 mM ferric ammonium citrate. Significant

differences in strain abundance were determined by two-way RM ANOVA with Tukey's post-hoc test (* $p \leq 0.05$). The average $\pm$ stdev of three biological replicates is shown.

Supplemental

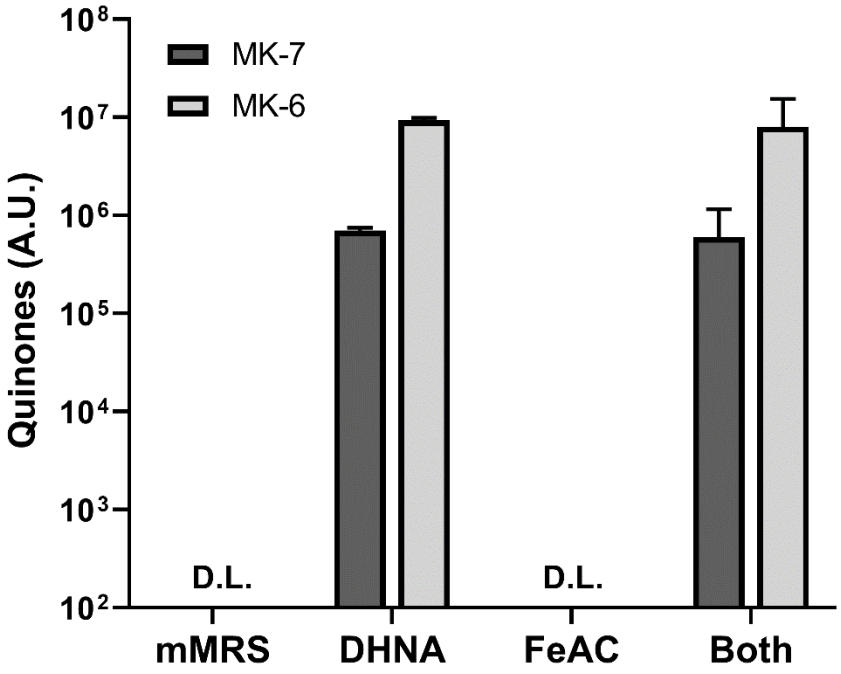

Figure S1. *L. plantarum* makes menaquinone-6 (MK-6) and menaquinone-7 (MK-7) when grown in the presence of DHNA. Relative levels of membrane-bound quinones (measured in absorbance units 'A.U.') in *L. plantarum* after overnight growth in mMRS supplemented with 20 μg/mL DHNA and/or 1.25 mM ferric ammonium cirrate (FeAC). D.L. refers to samples with quinone quantities below detection limit. The avg $\pm$ stdev of three biological replicates is shown.

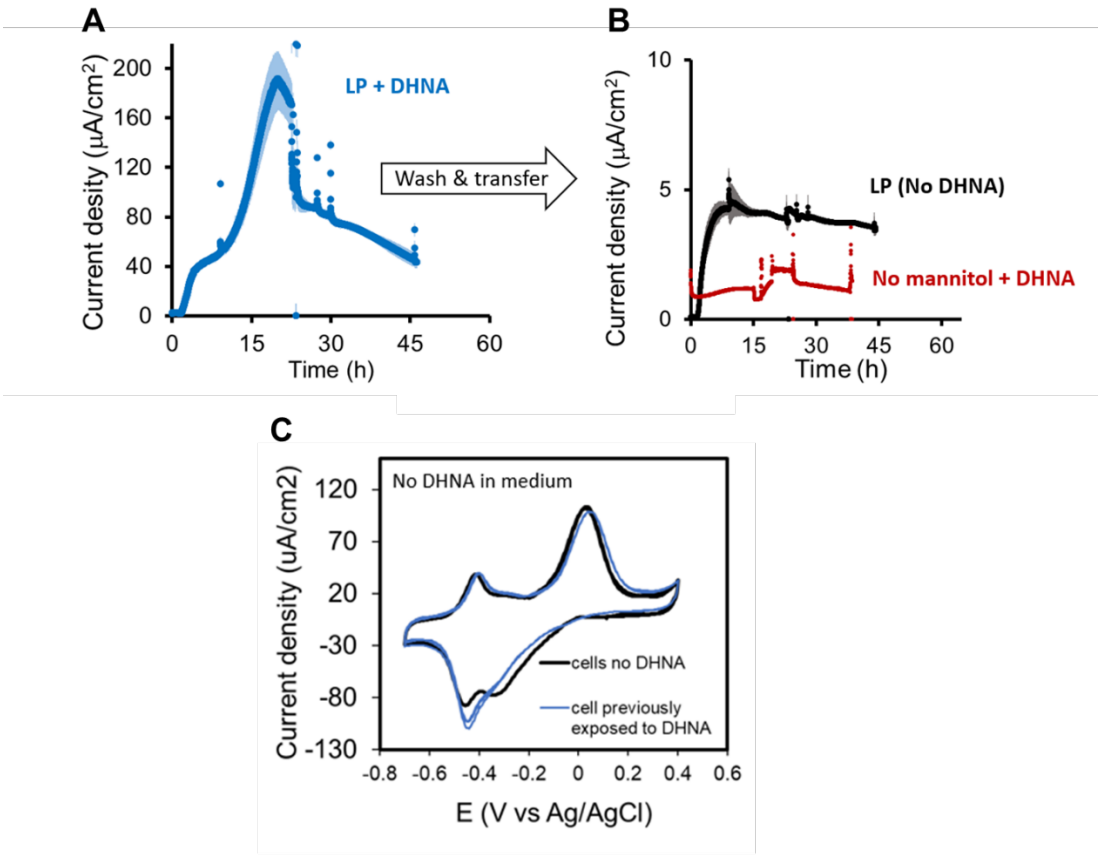

Figure S2. Access to exogenous DHNA is required for *L. plantarum* current production. **(A)** Current density production over time by *L. plantarum* in mCDM supplemented with 20 µg/mL DHNA. The anode was polarized at +0.2V Ag/AgCl. **(B)** Cells from **(A)** were washed and transferred to bioreactors containing mCDM with no DHNA or CDM with no mannitol or DHNA. **(C)** Cyclic voltammetry analysis of *L. plantarum* in mCDM with either prior growth in mCDM with 20 µg/mL DHNA or mCDM alone. The avg + stdev of three biological replicates is shown.

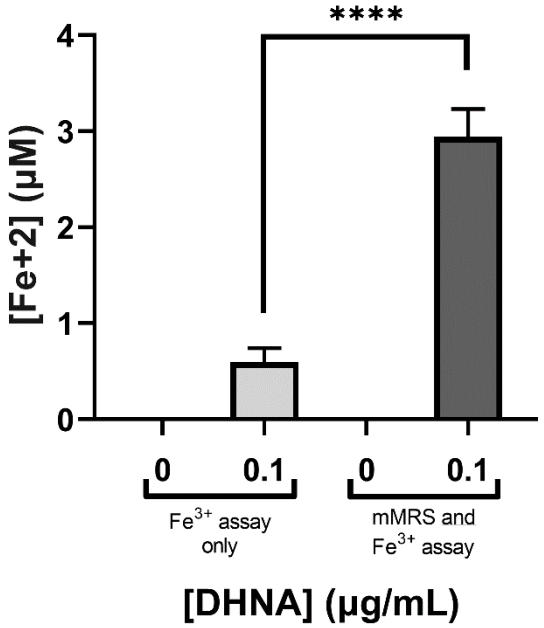

Figure S3. *L. plantarum* incubation in DHNA during growth increases EET activity. Reduction of Fe^{3+} (ferrihydrite) to Fe^{2+} by *L. plantarum* after growth in mMRS supplemented with 1.25 mM ferric ammonium citrate. DHNA was supplemented in the growth medium and/or the iron reduction assay at 0.1 μg/mL. Significant differences were determined by one-way ANOVA with Tukey's post-hoc test; **** $p \leq 0.0001$. The avg ± stdev of three biological replicates is shown.

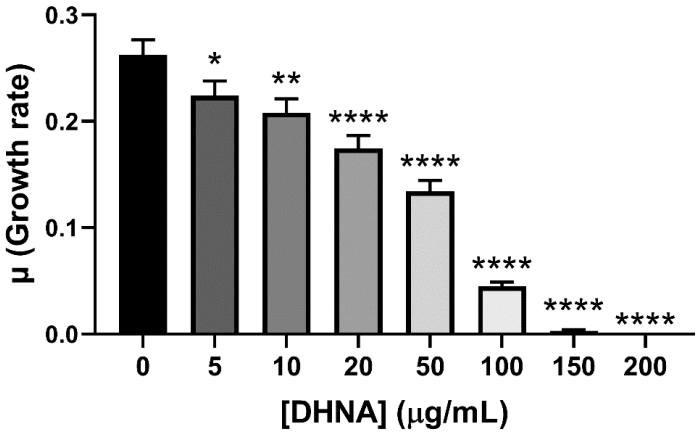

Figure S4. *L. plantarum* growth rate is negatively affected by DHNA. Growth rate of *L. plantarum* in mMRS with or without supplementation DHNA at increasing concentrations. Growth rates were determined by measuring the change in OD_{600nm} per hour during exponential phase. The avg ± SEM of three biological replicates is shown. Significant differences were determined by one-way ANOVA with Dunnett's post-hoc test. * $p \leq 0.05$; ** $p \leq 0.01$; *** $p \leq 0.001$; **** $p \leq 0.0001$.

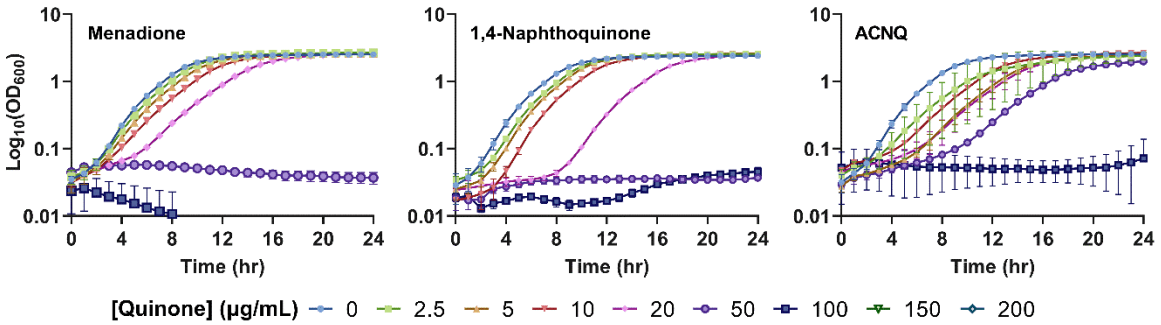

Figure S5. Other exogenous quinones besides DHNA inhibit *L. plantarum* growth. Growth of *L. plantarum* in mMRS supplemented with exogenous quinones at the indicated concentrations. The avg ± stdev of three biological replicates is shown.

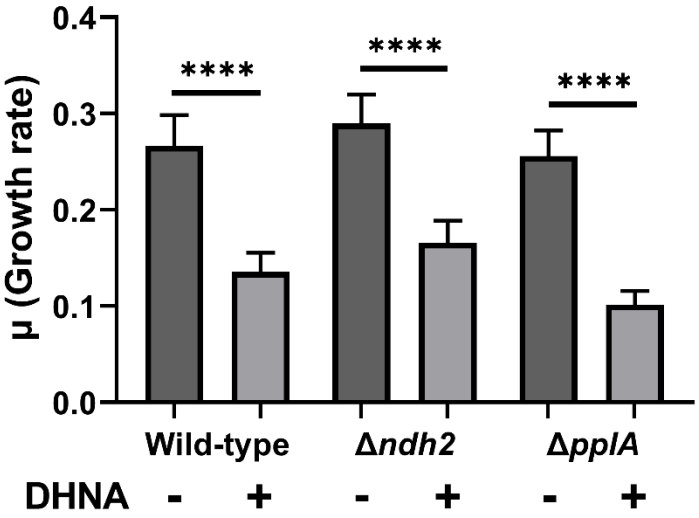

Figure S6. DHNA reduces the growth rate of FLEET deletion mutants in mMRS. Growth rate of wild-type *L. plantarum* NCIMB8826 or deletion mutants of *ndh2*/*pplA* in mMRS with or without supplementation of 20 µg/mL DHNA. Growth rates were quantified by measuring the change in OD_{600nm} per hour during exponential phase. Significant differences were determined using one-way ANOVA with Tukey's post-hoc test (**** $p \leq 0.0001$). The average ± SEM of three biological replicates is shown.

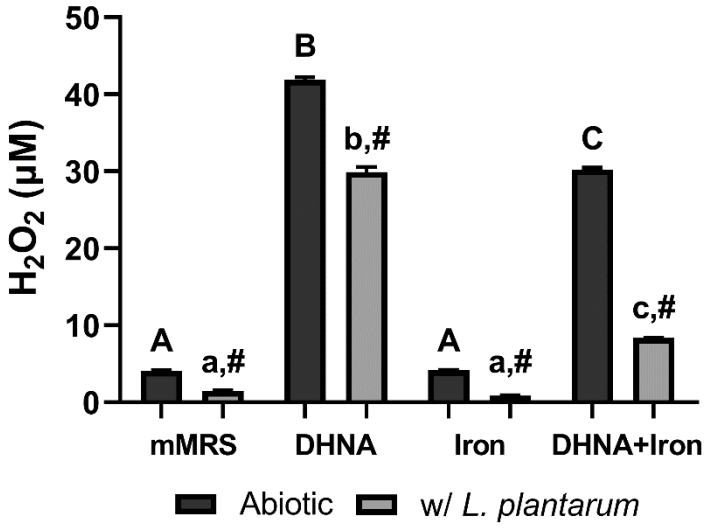

Figure S7. DHNA increases hydrogen peroxide levels in mMRS which are reduced by the presence of FeAC. Hydrogen peroxide produced in mMRS supplemented with 20 μg/mL DHNA and/or 1.25 mM ferric ammonium citrate (FeC) after 5 h at 37 °C. Where indicated, *L. plantarum* was also inoculated at an OD_{600} = 0.1 and culture supernatant was sampled after 5 h at 37 °C corresponding to when *L. plantarum* reached mid-exponential phase growth. Significant differences in H_2O_2 production between culture conditions (represented by letters, $p \leq 0.05$), or H_2O_2 production under abiotic conditions or with *L. plantarum* inoculation (#, $p \leq 0.05$), were determined by one-way ANOVA with Tukey's post-hoc test. The avg ± stdev of three biological replicates is shown.

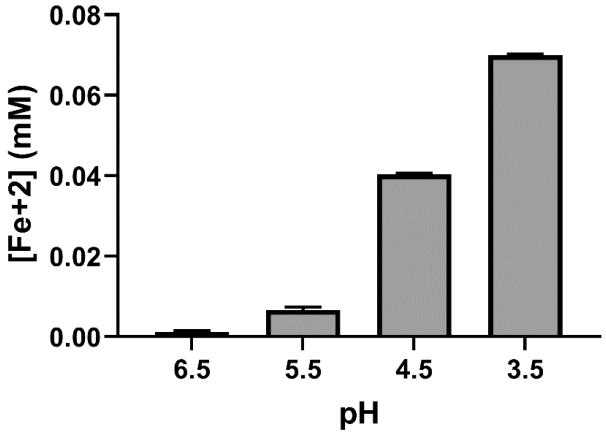

Figure S8. Iron is spontaneously reduced in acidified CDM. Reduction of FeAC in CDM acidified with lactic acid. Iron reduction was detected colorimetrically with 2 mM ferrozine. The avg ± stdev of three replicates is shown.

Table S1. Strains and plasmids used in this study.

Strains	Isolation Source / Description	Reference
L. plantarum NCIMB8826	Human saliva	(Dandekar, 2019)
L. plantarum MLES100	Deletion mutant of NCIMB8826 lacking *ndh2*	(Tejedor-Sanz et al., 2021)
L. plantarum MLES101	Deletion mutant of NCIMB8826 lacking *pplA*	(Tejedor-Sanz et al., 2021)
L. lactis subsp. cremoris TIL46	Strain NCDO763 cured of its 2-kb plasmid	(Wels et al., 2017)
L. lactis subsp. cremoris TIL999	Deletion mutant of TIL46 lacking *menC*	(Tachon et al., 2009)
L. citreum NRRL B-742	Spoiled canned tomatoes	(Passerini et al., 2014)
L. mesenteroides subsp. mesenteroides ATCC 8293	Fermenting olives	(Makarova et al., 2006)

Table S2. Total number of *L. plantarum* genes differentially expressed in DHNA, FeAC, and DHNA+FeAC containing media. Differential expression of all genes in *L. plantarum* during exponential growth in mMRS supplemented with DHNA (20 μg/mL) and/or ferric ammonium citrate (1.25 mM) compared to the mMRS alone control group. Differential expression was considered significant with a FDR-adjusted p-value ≤ 0.05 and $\log_2$ expression fold-change ≥ 0.5.

Growth condition	# Upregulated Genes	# Downregulated Genes	Total # Differentially Expressed Genes
DHNA	452	473	925
FeAC	35	72	107
DHNA+FeAC	123	169	292

Table S3. The presence of DHNA induces redox stress in *L. plantarum*. Differential expression in *L. plantarum* during exponential growth in mMRS supplemented with DHNA (20 μg/mL) and/or ferric ammonium citrate (1.25 mM) compared to the mMRS alone control group. Bold values indicate a $\log_2$ expression fold-change ≥ 0.5 and a FDR-adjusted *p*-value ≤ 0.05.

Locus Tag	Gene	Product	COG ID#	DHNA - Log2 FC	DHNA - p-adjusted	IRON - Log2 FC	IRON - p-adjusted	BOTH - Log2 FC	BOTH - p-adjusted
Oxidation-reduction									
lp_1253	gshR2	glutathione reductase	COG1249	**2.86**	**0.000**	**-1.66**	**0.000**	**-1.95**	**0.000**
lp_1822	gshR3	glutathione reductase	COG1249	**1.04**	**0.000**	0.02	0.978	0.05	0.917
lp_3267	gshR4	glutathione reductase	COG1249	**1.48**	**0.000**	0.00	0.997	0.24	0.221
lp_3578	kat	catalase	COG0753	**1.88**	**0.000**	**-0.88**	**0.000**	**-1.30**	**0.000**
lp_1939	lp_1939	oxidoreductase, medium chain dehydrogenases/reductase (MDR)/zinc-dependent alcohol dehydrogenase-like family	COG0604	**1.73**	**0.000**	-0.30	0.057	**-0.80**	**0.000**
lp_1836	mrsB	protein-methionine-S-oxide reductase	COG0229	**2.32**	**0.000**	**-1.13**	**0.000**	**-1.49**	**0.000**
lp_1835	msrA2	protein-methionine-S-oxide reductase	COG0225	**2.42**	**0.000**	**-1.16**	**0.000**	**-1.38**	**0.000**
lp_3449	nox5	NADH oxidase	COG0446	**0.69**	**0.000**	**-2.40**	**0.000**	**-2.34**	**0.000**
lp_2544	npr2	NADH peroxidase	COG0446	**2.93**	**0.000**	**-0.79**	**0.000**	0.15	0.516
lp_0694	nrdH	glutaredoxin-like protein nrdH	COG0695	-0.05	0.711	0.14	0.515	**-1.05**	**0.000**
lp_2788	panE	2-dehydropantoate 2-reductase	COG1893	**1.23**	**0.000**	-0.60	1.000	0.84	1.000
lp_2629	pox3	pyruvate oxidase	COG0028	**1.70**	**0.000**	**-2.31**	**0.000**	**-2.96**	**0.000**
lp_3589	pox5	pyruvate oxidase	COG0028	0.44	0.001	**-1.18**	**0.000**	**-2.42**	**0.000**
lp_2323	tpx	thiol peroxidase	COG2077	**1.20**	**0.000**	0.15	0.289	0.14	0.578
lp_2270	trxA2	thioredoxin	COG3118	**0.53**	**0.000**	-0.02	0.938	-0.49	0.004
lp_0761	trxB	thioredoxin reductase (NADPH)	COG0492	**0.78**	**0.000**	-0.19	0.075	-0.48	0.000
Amino acid transport and metabolism									
lp_1084	aroD1	shikimate 5-dehydrogenase	COG0169	**2.53**	**0.000**	-0.31	0.751	1.08	1.000
lp_2037	aroF	chorismate synthase	COG0082	**2.21**	**0.000**	-0.39	0.609	0.63	1.000
lp_0861	bcaP	branched-chain amino acid permease	COG0531	**2.12**	**0.000**	0.16	0.357	-0.08	0.603
lp_0981	brnE	branched-chain amino acid transport protein	COG4392	**2.88**	**0.000**	0.29	0.608	0.21	1.000

lp_0982	brnF	branched-chain amino acid transport protein	COG1296	**2.26**	**0.000**	0.01	0.992	0.15	0.830
lp_1245	hicD2	L-2-hydroxyisocaproate dehydrogenase	COG0039	**3.20**	**0.000**	0.17	0.561	0.40	0.062
lp_1297	lp_1297	S-methylmethionine transport protein	COG0833	**2.55**	**0.000**	-0.17	0.715	0.14	0.823
lp_2920	lp_2920	proline-containing amino acid or peptide transport protein	COG0531	**3.23**	**0.000**	-0.26	0.705	0.56	0.546
lp_3214	lp_3214	cystathionine ABC transporter, substrate binding protein	COG0834	**2.14**	**0.000**	-0.01	0.986	0.10	0.808
lp_1375	metE	homocysteine S-methyltransferase (cobalamin-independent)	COG0620	**2.16**	**0.000**	-0.47	0.529	0.88	0.420
lp_1298	metH	homocysteine S-methyltransferase (cobalamin-dependent)	COG2040	**2.35**	**0.000**	-0.16	0.792	0.41	0.515
lp_2536	oahS	O-acetylhomoserine sulfhydrylase	COG2873	**2.20**	**0.000**	-0.56	0.395	0.91	0.462
lp_1261	oppA	oligopeptide ABC transporter, substrate binding protein	COG4166	**6.15**	**0.000**	0.15	0.424	0.09	0.657
lp_1262	oppB	oligopeptide ABC transporter, permease protein	COG0601	**5.00**	**0.000**	0.11	0.696	0.17	0.486
lp_1263	oppC	oligopeptide ABC transporter, permease protein	COG1173	**4.79**	**0.000**	0.06	0.832	0.15	0.508
lp_1264	oppD	oligopeptide ABC transporter, ATP-binding protein	COG0444	**4.79**	**0.000**	0.02	0.960	0.04	0.869
lp_1265	oppF	oligopeptide ABC transporter, ATP-binding protein	COG4608	**4.58**	**0.000**	0.15	0.438	-0.02	0.911
lp_2708	pucR	purine transport regulator	COG2508	**3.56**	**0.000**	-0.17	0.836	0.58	0.483
lp_0203	serA	D-3-phosphoglycerate dehydrogenase	COG0111	**6.41**	**0.000**	-0.20	0.581	-0.34	0.457
lp_0204	serC	phosphoserine aminotransferase	COG1932	**6.04**	**0.000**	-0.18	0.691	-0.11	0.850
lp_1745	lp_1745	D-methionine ABC transporter, permease protein	COG2011	**1.63**	**0.000**	-0.76	1.000	0.72	1.000
Cell membrane biosynthesis									
lp_1680	accA2	acetyl-CoA carboxylase, carboxyl transferase subunit alpha	COG0825	**1.10**	**0.000**	**0.73**	**0.000**	**3.85**	**0.000**
lp_1676	accB2	acetyl-CoA carboxylase, biotin carboxyl carrier protein	COG0511	**1.25**	**0.000**	**0.90**	**0.000**	**3.92**	**0.000**
lp_1678	accC2	acetyl-CoA carboxylase, biotin carboxylase subunit	COG0439	**1.23**	**0.000**	**0.87**	**0.000**	**3.92**	**0.000**

lp_1679	accD2	acetyl-CoA carboxylase, carboxyl transferase subunit beta	COG0777	**1.26**	**0.000**	**0.88**	**0.000**	**3.98**	**0.000**
lp_1672	acpA2	acyl carrier protein	COG0236	**1.33**	**0.000**	**1.11**	**0.000**	**3.90**	**0.000**
lp_1673	fabD	[acyl-carrier protein] S-malonyltransferase	COG0331	**1.35**	**0.000**	**1.05**	**0.000**	**4.00**	**0.000**
lp_1675	fabF	3-oxoacyl-[acyl-carrier protein] synthase II	COG0304	**1.12**	**0.000**	**0.89**	**0.000**	**3.68**	**0.000**
lp_1674	fabG1	3-oxoacyl-[acyl-carrier protein] reductase	COG1028	**1.19**	**0.000**	**0.97**	**0.000**	**3.80**	**0.000**
lp_1671	fabH2	3-oxoacyl-[acyl-carrier protein] synthase III	COG0332	**1.37**	**0.000**	**1.19**	**0.000**	**3.97**	**0.000**
lp_1681	fabI	enoyl-[acyl-carrier protein] reductase (NADH)	COG0623	**1.06**	**0.000**	**0.79**	**0.000**	**3.79**	**0.000**
lp_1670	fabZ1	(3R)-hydroxyacyl-[acyl carrier protein] dehydratase	COG0764	**1.31**	**0.000**	**1.29**	**0.000**	**3.92**	**0.000**
lp_1677	fabZ2	(3R)-hydroxymyristoyl-[acyl carrier protein] dehydratase	COG0764	**1.39**	**0.000**	**0.96**	**0.000**	**4.08**	**0.000**
Iron transport and metabolism									
lp_1467	feoA	ferrous iron transport protein A	COG1918	**-0.71**	**0.002**	-0.36	0.442	-2.56	1.000
lp_1466	feoB	ferrous iron transport protein B	COG0370	**-0.98**	**0.000**	**-0.63**	**0.000**	**-1.97**	**0.000**
lp_0506	sdhA	L-serine dehydratase, alpha subunit	COG1760	**-0.71**	**0.000**	**3.99**	**0.000**	**-1.37**	**0.000**
lp_0505	sdhB	L-serine dehydratase, beta subunit	COG1760	**-0.99**	**0.000**	**4.03**	**0.000**	**-1.72**	**0.000**
lp_0502	sdaC	serine transporter	COG0814	**-1.99**	**0.000**	**4.12**	**0.000**	**-2.20**	**0.000**
lp_1472	sufB	ABC transporter component, iron-sulfur cluster assembly protein	COG0719	**-1.06**	**0.000**	-0.29	0.001	**-1.77**	**0.000**
lp_1468	sufC	ABC transporter, ATP-binding protein, iron-sulfur cluster assembly ATPase protein	COG0396	**-0.71**	**0.000**	-0.32	0.001	**-1.77**	**0.000**
lp_1097	mtsA	manganese/zinc ABC transporter, substrate binding protein	COG0803	**-0.51**	**0.000**	-0.06	0.878	-0.41	0.103
lp_1096	mtsB	manganese ABC transporter, permease protein	COG1108	-0.45	0.003	0.00	0.998	-0.13	0.750
lp_1095	mtsC	manganese ABC transporter, ATP-binding protein	COG1121	**-0.51**	**0.000**	0.10	0.804	-0.30	0.336

FLEET locus									
lp_1066	dmkB	heptaprenyl diphosphate synthase component II	COG0142	**-0.50**	**0.000**	0.06	0.799	0.18	0.426
lp_1067	eetB	heptaprenyl diphosphate synthase component I	COG4769	-0.40	0.000	0.12	0.562	0.39	0.072
lp_1068	eetA	extracellular protein, DUF1312 family	COG5341	-0.42	0.000	0.04	0.890	0.38	0.090
lp_1069	ndh2	NADH dehydrogenase, membrane-anchored	COG1252	-0.24	0.005	0.06	0.719	**0.63**	**0.000**
lp_1070	pplA	lipoprotein precursor, FMN-binding protein	COG4939	**-0.53**	**0.000**	-0.03	0.870	**0.67**	**0.000**
lp_1072	fmnB	thiamin biosynthesis lipoprotein ApbE	COG1477	**-0.52**	**0.000**	0.03	0.895	0.32	0.102
lp_1073	ATPase_2	ABC transporter, ATP-binding protein	COG1122	-0.24	0.005	0.06	0.740	0.15	0.513
lp_1074	ATPase_1	ABC transporter, ATP-binding protein	COG1122	-0.24	0.005	0.03	0.897	-0.01	0.967
lp_1075	fmnA	ABC transporter, permease protein	COG0619	0.05	0.638	0.18	0.188	0.19	0.447
Menaquinone biosynthesis									
lp_1135	lp_1135	1,4-dihydroxy-2-naphthoate octaprenyltransferase	COG1575	0.23	0.012	0.13	0.446	0.17	0.494
lp_1715	lp_1715	1,4-dihydroxy-2-naphthoate octaprenyltransferase, UbiA prenyltransferase family	COG1575	-0.09	0.417	-0.02	0.952	-0.38	0.003
lp_1546	dmkA	1,4-dihydroxy-2-naphthoate octaprenyltransferase, UbiA family	COG1575	-0.34	0.001	0.09	0.649	0.22	0.246
lp_3431	ubiE	menaquinone/ubiquinone biosynthesis methyltransferase	COG2226	0.31	0.031	-0.07	0.886	0.19	0.505